CLRs and their role during *Aspergillus fumigatus* infection

Thesis presented for the degree of Doctor of Philosophy

2018

James S Griffiths

Declaration

This work has not been submitted in substance for any other degree or award at this university or any other university or place of learning, nor is being submitted concurrently in candidate for any degree or other award.

Signed: (candidate) Date:

Statement 1

This thesis is being submitted in partial fulfillment of the requirements for the degree of PhD.

Signed: (candidate) Date:

Statement 2

This thesis is the result of my own independent work, except where otherwise stated, and the thesis has not been edited by a third party beyond what is permitted by Cardiff University's Policy on the use of third party editors by research degree students. Other sources are acknowledged by references. The views expressed are my own.

Signed: (candidate) Date:

Statement 3

I hereby give consent for my thesis, if accepted, to be available online in the university's open access repository and for inter-library loans **after the expiry of a bar on access previously approved by the Academic Standards and Quality Committee.**

Signed: (candidate) Date:

Acknowledgements

First and foremost, I would like to thank my supervisor Selinda Orr for all the guidance, training, support and time I have received over the past three and a half years. I have thoroughly enjoyed beginning my career in science as part of the Orr group. I would like to express my gratitude to Phil Taylor for his regular input and advice throughout my PhD project and Rosemary Barnes for her help setting up, running and analysing the patient study. I would also like to acknowledge Lewis White for giving so much time and effort to help run the patient study and interpret the study results.

I would like to thank all the members of the Orr group and Taylor group for contributing to my research and the enjoyable work environment. I am particularly grateful to have shared my time in the Tenovus building with Rob Pickering, Leah Wallace, Ruth Jones, Chia-Te Liao, Aiysha Thompson and Diogo Fonseca.

When I consider your heavens, the work of your fingers, the moon and the stars, which you have set it place – Psalm 8:3

Contents

Chapter 1: Introduction **6**

1.1: *Aspergillus fumigatus* **7**
1.1.1: The fungi 7
1.1.2: A.*f*. disease in immune-compromised individuals 9
1.1.3: A.*f*. disease in immune-competent individuals 13
1.1.4: Cystic fibrosis and A.*f*. disease 14
1.1.5: A.*f*. clinical relevance 17
1.1.6: Therapeutic insufficiencies 20

1.2: The anti-A.*f*. immune response **23**
1.2.1: A.*f*. Infection 23
1.2.2: A.*f*. cell wall and surface 23
1.2.3: Soluble lung components and respiratory epithelia 24
1.2.4: Alveolar macrophages 25
1.2.4: Neutrophils 27
1.2.5: Secondary metabolites 30
1.2.6: The adaptive response 32
1.2.6: Requirement of A.*f*. immune recognition, signalling and response 34

1.3: A.*f*. recognition and C-type lectin receptors **35**
1.3.1: PRRs 35
1.3.2: CLRs 36
1.3.6: Dectin-1 39
1.3.6: Dectin-2 42
1.3.7: Mincle 43
1.3.8: Mcl 46
1.3.3: CLRs and phagocytosis 48
1.3.4: CLRs and non-phagocytic fungal killing 50
1.3.5: PRR collaboration 52

1.4: Hypothesis **54**

1.5: Aims **54**

Chapter 2: Methods **55**

2.1: Notes **56**
2.1.1: Reagents 56
2.1.2: Animals used in this research 56
2.1.3: Patient samples used in this research 56
2.1.4: DNA sequencing 57

2.2: Cell culture **58**
2.2.1: Cell counting 58
2.2.2: Bone marrow derived macrophages 58
2.2.3: Alveolar macrophages 59
2.2.4: BIOgel elicited cells 59
2.2.5: NIH-3T3 cells 60

2.2.6: Culture and preparation of A.*f*. conidia 61
2.2.7: Preparation of heat-killed A.*f*. 61
2.2.8: Freezing and reviving cells 62

2.3: Generation of cell lines 63
2.3.1: Infusion primer design 63
2.3.2: Restriction endonuclease vector digestion 63
2.3.3: Infusion reaction 63
2.3.4: Transformation 64
2.3.5: Plasmid DNA extraction 64
2.3.6: Retroviral infection 65
2.3.7: Transfected cell selection 65

2.4: *In vitro* assays 67
2.4.1: Flow cytometry 67
2.4.2: ELISA 68
2.4.3: NE treatment 70
2.4.4: NE-induced receptor cleavage 70
2.4.5: NE-induced functional response deficiency 71
2.4.6: NE-induced recognition deficiency 71

2.5: *In vivo* assays 72
2.5.1: Animals used 72
2.5.2: *In vivo* A.*f*. infection 72
2.5.3: Lung extraction 73
2.5.4: Lung homogenisation for fungal burden analysis 74
2.5.5: Lung fungal RNA extraction 74
2.5.6: Fungal RNA standard curve 75
2.5.7: Generation of fungal cDNA 76
2.5.8: Determination of fungal burden by qPCR 77
2.5.9: Extracted lung cytokine and chemokine analysis 78

2.6: Patient study 79
2.6.1: Sample collection 79
2.6.2: Isolation of RNA from whole blood 79
2.6.3: Generation of patient cDNA 81
2.6.4: Patient CLR sequencing 82
2.6.5: Patient CLR expression 83
2.6.6: Extraction of patient PBMCs from whole blood 84
2.6.7: Patient PBMC stimulation 85

Chapter 3: Neutrophil Elastase cleavage of Dectin-1 Isoform A enhances susceptibility to A.*f*. infection 88

3.1: Aims 89

3.2: Introduction 90

3.3: Results 93
3.3.1: Does Neutrophil Elastase cleave Dectin-1? 93
3.3.2: Which Dectin-1 amino acid is required for NE-induced cleavage to occur? 104
3.3.3: Is there a functional consequence resulting from the NE-induced cleavage of Dectin-1? 108

3.4: Discussion 125
3.4.1: Does neutrophil elastase cleave Dectin-1? 126
3.4.2: Which Dectin-1 amino acid is required for NE-induced cleavage to occur? 129
3.4.3: Is there a functional consequence resulting from the NE-induced cleavage of Dectin-1? 130

3.5: Conclusions 133

Chapter 4: Understanding the collective roles of Dectin-1, Dectin-2 and Mincle in anti-*Aspergillus fumigatus* immunity 134

4.1: Aims 135

4.2: Introduction 136

4.3: Results 139
4.3.1: What role do CLRs play in the alveolar macrophage anti-A.*f*. response? 139
4.3.2: Optimising the *in vivo* A.*f*. challenge model 144
4.3.3: What role do CLRs play in the anti-A.*f*. immune response *in vivo*? 151
4.3.4: What impact is the microbiome conferring over experimental results? 161
4.3.5: What impact is gender conferring over experimental results? 165

4.4: Discussion 174
4.4.1: What role do CLRs play in the alveolar macrophage anti-A.*f*. response? 174
4.4.2: What roles do CLRs play in the anti-A.*f*. immune response *in vivo*? 177
4.4.3: What impact was the microbiome conferring over the ability of WT, CLR KO and CLR DKO mice to generate immune responses against A.*f*.? 181
4.4.4: What impact was gender conferring over the ability of WT, CLR KO and CLR DKO mice to generate immune responses against A.*f*.? 183

4.5: Conclusions 184

4.6: Further experiments 185

Chapter 5: Using CLR status and functional response capability to stratify haematology patients according to their A.*f*. disease susceptibility 186

5.1: Aims 187

5.2: Introduction 188

5.3: Results 191
5.3.1: Determination of patient CLR status 191
5.3.2: Determination of patient's functional immune response capabilities 202
5.3.3: Patient stratification system 209

5.4: Discussion 222
5.4.1: Determining patients CLR status. 223
5.4.2: Determining patient's functional response capabilities 225
5.4.3: Patient stratification system 227

5.5: Conclusions 229

5.6: Future experiments 230

Chapter 6: General discussion 231

6.1: Earlier research 232
6.2: CLRs and A.*f*. in the immune-compromised 233
6.3: CLRs and A.*f*. in the immune-competent 235
6.4: CLRs and A.*f*. in the immune-suppressed 238
6.5: Conclusions 241

Chapter 7: Appendix 242

Summary

CLRs are vital for orchestrating anti-fungal immunity. These receptors are expressed on myeloid immune cells and induce robust anti-A.*f*. responses including phagocytosis, cytokine and chemokine release, respiratory burst, and inflammasome activation. The role of Dectin-1 has been thoroughly investigated; however, the CLRs requirement during anti-A.*f*. response is controversial. The impact of Dectin-2, Mcl and Mincle during anti-A.*f*. immunity is not well understood. A.*f*. is complex and poses many challenges for the immune system. PRR collaboration is likely required for A.*f*. clearance. Collaboration between TLRs and CLRs has been identified. Recently, the first CLR:CLR collaboration was demonstrated between Dectin-1 and Dectin-2; however, this was not in response to A.*f*.. The research in this thesis describes many novel interactions between CLRs and A.*f*. and seeks to further the understanding of the complex collaborative anti-A.*f*. immune response.

Firstly, a novel role for NE inducing Dectin-1 Isoform A cleavage was described. This impaired A.*f*. recognition and the anti-A.*f*. response. CF patients possess high airway NE activity and experience a severe A.*f*. disease burden. My research suggests blocking the action of NE in CF patient's airway may restore Dectin-1 expression and improve patient's anti-A.*f*. immune response.

Secondly, *in vivo* CLR KO and DKO models were used to elicit alveolar macrophages reliance on CLRs when generating anti-A.*f*. responses. My research suggests Dectin-1 might exclusively be required during early anti-A.*f*. responses. Unfortunately, discrepancies between the sex and microbiome of mice restricted the conclusions drawn from *in vivo* CLR KO and DKO A.*f*. infection experiments.

Finally, I identified novel risk factors that can be used to stratify patients according to their susceptibility to A.*f*. infection. A.*f*. disease incidence and mortality rates are unacceptably high in immune-suppressed patients. Patients are often prophylactically treated with inadequate anti-fungal therapeutics. Stratifying patients according to their A.*f*. disease susceptibility would allow a personalised medicine approach and reduce unnecessary treatment.

Abbreviations

A.*f*. – *Aspergillus fumigatus*
A.*f*. EG – *Aspergillus fumigatus* early germlings
A.*f*. HY – *Aspergillus fumigatus* hyphae
A.*f*. RC – *Aspergillus fumigatus* resting conidia
A.*f*. SC – *Aspergillus fumigatus* swollen conidia
AAT – Alpha anti-trypsin
ABPA – Allergic bronchopulmonary *Aspergillosis*
ALL – Acute lymphoid leukaemia
AML – Acute myeloid leukaemia
AS – *Aspergillus* sensitisation
Bcl10 – B-cell lymphoma 10
BMDM – Bone marrow derived macrophage
CARD9 – Caspase-associated recruitment domain 9
CF – Cystic fibrosis
CFTR – Cystic fibrosis transmembrane receptor
CGD – Chronic granulomatous disease
CLR – C-type lectin receptor
CTLD – C-type lectin-like domain
CRD – Carbohydrate recognition domain
DC – Dendritic cell
DKO – Double knock out
DMEM – Dulbecco's modified eagle medium
EDTA – Ethylenediaminetetraacetic acid
FITC – Fluorescein isothiocyanate
HSCT – Heamatopoietic stem cell transplant
IA – Invasive *Aspergillosis*
IFI – Invasive fungal infection
IFN – Interferon
IL – Interleukin
IMDM – Iscove's modified Dulbecco's medium
IRF1 – Interferon regulatory factor 1
KO – Knock out
ITAM – Immunoreceptor tyrosine-based activation motif
LPS – Lipopolysaccharide
M-CSF – Macrophage colony stimulating factor
MALT1 – Mucosa-associated lymphoid tissue translocation protein 1
MAPK – Mitogen activated protein kinase
MIP – Macrophage inflammatory protein
MPO – Myeloperoxidase
MyD88 – Myeloid differentiation primary response 88
NADPH – Nicotinamide adenine dinucleotide phosphate

NE – Neutrophil elastase
NET – Neutrophil extracellular trap
NFκB – Nuclear factor kappa-light-chain-enhancer of B-cells
NFAT – Nuclear factor of activated T-cells
NOD – Nucleotide-binding oligomerisation domain-like
PAMP – Pathogen associated molecular pattern
PBMC – Peripheral blood mononuclear cell
PBS – Phosphate buffered saline
PCR – Polymerase chain reaction
PMSF – Phenylmethylsulfonyl fluoride
PRR – Pattern recognition receptor
qPCR – Quantitative polymerase chain reaction
RIG-I – Retinoic acid inducible gene I
ROS – Reactive oxygen species
RPMI 1640 – Roswell park memorial institute medium 1640
RT – Room temperature
Syk – Spleen tyrosine kinase
TDM – Trehalose dimycolate
T_H – Type T helper
TLR – Toll-like receptor
TNF – Tumour necrosis factor

Chapter 1

Introduction

1.1: *Aspergillus fumigatus*

1.1.1: The fungi

Aspergillus fumigatus (A.*f*.) is an ubiquitous fungus with an essential environmental role in recycling carbon and nitrogen. The fungus survives and grows on organic debris found in soil, its natural ecological niche [1, 2]. A.*f*. has a complicated life cycle typically replicating via asexual reproduction and the formation of conidiophores. Three important steps distinguish the A.*f.* life cycle and generate four distinct fungal morphologies as displayed in figure 1.1. Appropriately warm and moist environmental conditions activate resting conidia (RC) and initiate isotropic wall growth. Water and nutrient uptake allows RC to swell and develop in to swollen conidia (SC). The polarised growth of SC results in germ tubes and early germlings (EG). Germ tubes continue polarised growth and develop into hyphae and new mycelium (HY). Fully developed HY provide the structure required for the formation of conidiophores and growth and release of RC [3].

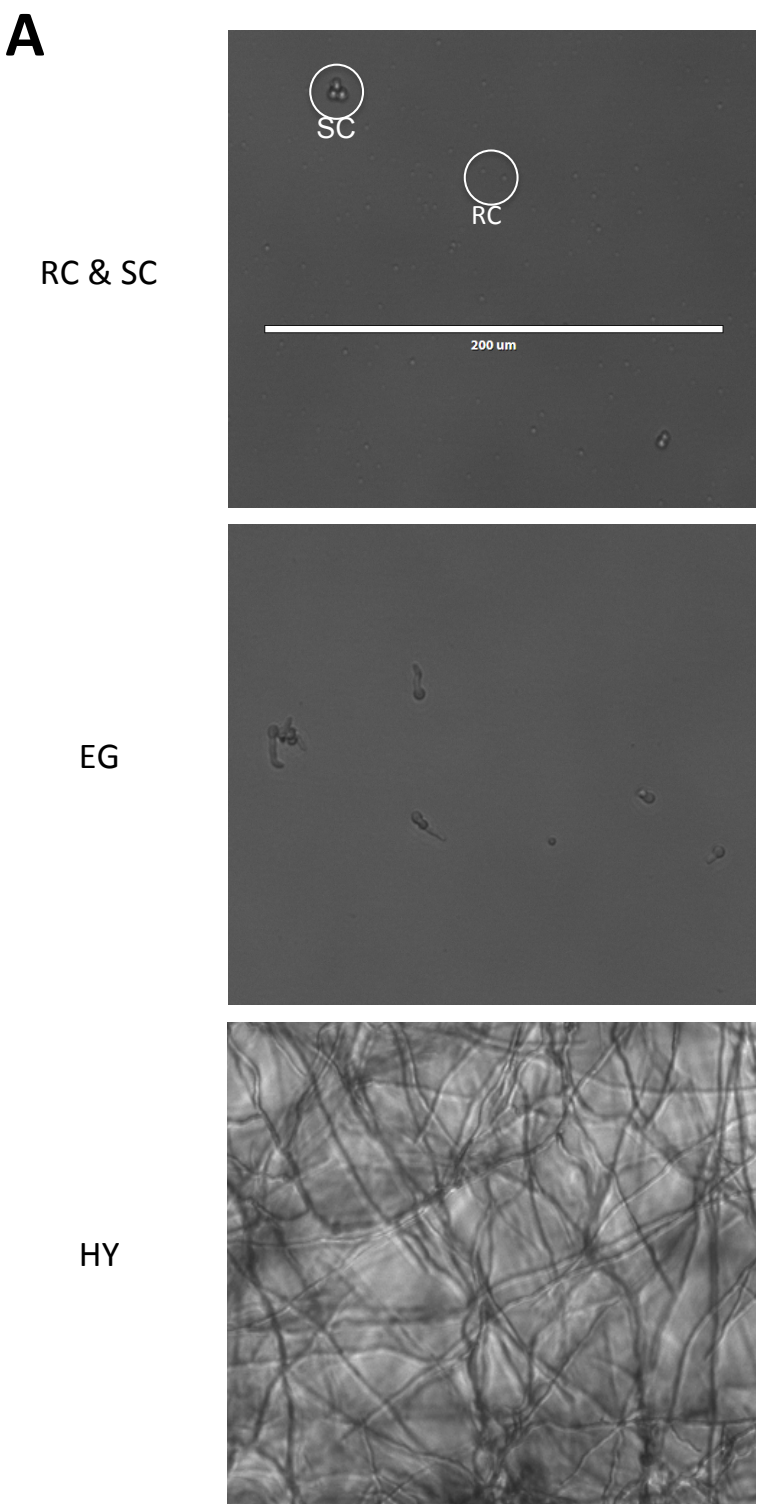

Figure 1.1: A.*f*. life cycle steps and morphologies. (A) 1x10^6/ml A.*f*. RC were grown in RPMI supplemented with Polymixin B at 37^{o}C 5% CO_2. Images were taken of the A.*f*. conidia at 6 hours to display SC, 10 hours to display EG and 24 hours to display HY. All images are the same resolution; therefore, 200µm measurement bar present in the RC & SC image is the correct dimension for all images.

A.*f*. sporulates abundantly with every conidial head producing thousands of RC, 2-3µm in diameter. The produced RC are particularly environmentally resistant withstanding temperature ranges from 0-99^{o}C for prolonged periods whilst maintaining viability. RC can germinate and successfully initiate fungal growth between 20-50^{o}C, temperatures regularly encountered in decaying vegetation [4]. A.*f*. doesn't possess an elaborate mechanism for RC distribution; instead, RC are manually released by disturbances in the air and rely exclusively on air currents for dissemination. Due to their small size RC remain buoyant for long periods of time allowing the fungi to spread extensively. It is estimated humans worldwide will inhale at least several hundred A.*f.* RC each day [1, 5].

Recently a sexual reproduction cycle has been described for A.*f*.. 215 genes implicated in sexual reproduction were detected and isolates of "complimentary mating types" were demonstrated to undergo genetic recombination over a period of 6 months. This allowed for the generation of progeny with increased virulence and resistance to anti-fungal therapeutics. A sexual reproduction cycle may explain the diversity between A.*f.* genotypes despite the predominantly clonal, asexual reproduction cycle [6].

1.1.2: A.*f*. disease in immune-compromised individuals

Until recently, A.*f.* has been described as a weak pathogen responsible primarily for allergic-type disease caused by the repeated inhalation of high quantities of A.*f*. RC. Even in this scenario, A.*f*. could only grow and invade lung tissue in individuals with pre-existing immune-compromised lung cavities resulting from infections such as tuberculosis [1]. Healthy individuals exposed to typical quantities of A.*f.* RC do not experience any disease or symptoms as RC are very efficiently cleared from the lungs, see figure 1.2 (A). Inhaled RC that have escaped mucociliary clearance and been deposited within the bronchioles or alveolar spaces are rapidly recognised and phagocytosed by lung-resident alveolar macrophages. RC that evade both the mucociliary and alveolar macrophage front-line immune response begin to germinate and initiate a robust neutrophil-driven anti-fungal immune response. In healthy

individuals this robust immune response culminates in the efficient pathology-free clearance of all A.*f.* from the lung before RC can germinate into HY [2, 4].

With the extensive use of modern immune-suppressing therapeutics, a very clear pathogenic role for A.*f*. has been identified in patients with compromised immune systems. Two distinct risk factors for A.*f.* disease, termed invasive *Aspergillosis* (IA), linked with immune-suppression have been described, see figure 1.2 (A & B). The first risk factor is prolonged neutropenia, this is often induced by intensive chemotherapy treatment. The second risk factor is the use of corticosteroids to treat graft versus host disease in allogeneic transplant patients. Both these risk factors greatly increase the likelihood of IA [7-9].

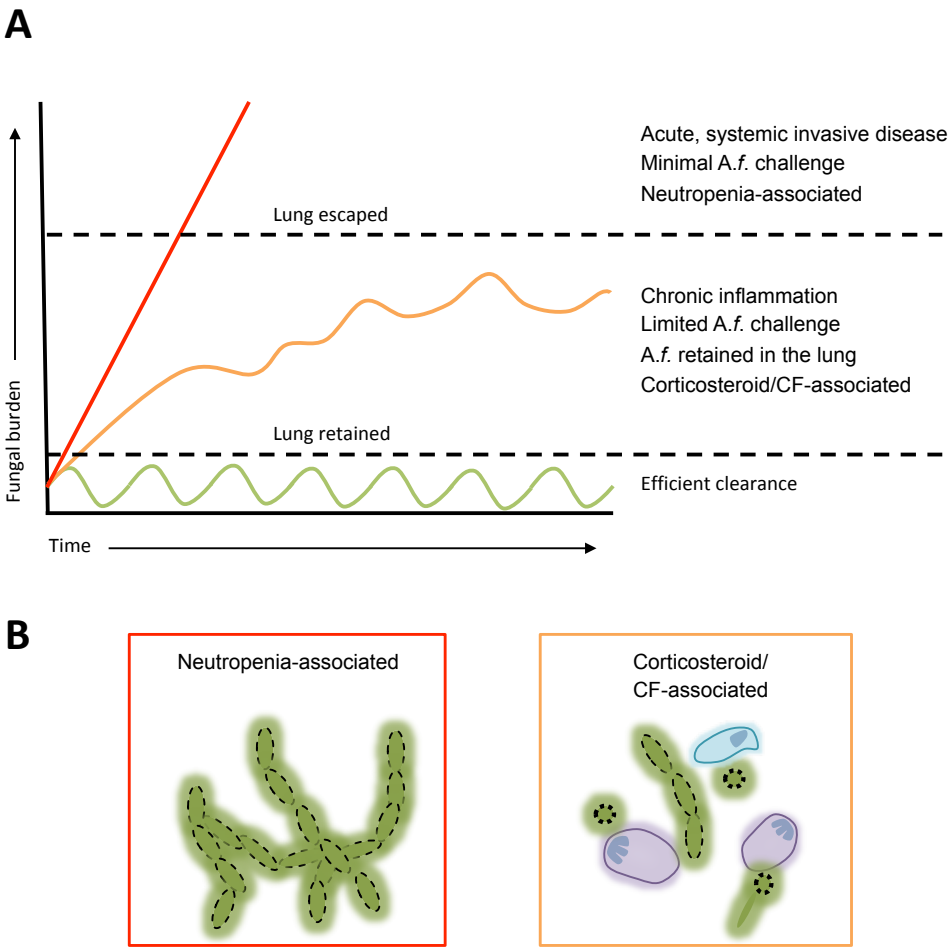

Figure 1.2: A.*f*. disease course is dependent on host immune-capability. (A) Graph describing the different A.*f*. disease courses associated with neutropenia, corticosteroid treatment/cystic fibrosis (CF) disease and a healthy immune system. **(Red line)** Acute disease that typically becomes systemic resulting from a lack of neutrophil recruitment and response. **(Orange line)** Chronic disease resulting from a limited anti-A.*f*. immune response, A.*f*. is retained within the lung but a chronic inflammatory setting is generated. **(Green line)** No A.*f*. disease ensues as inhaled conidia are rapidly and efficiently cleared from the lung. **(B) (Red box)** A.*f*. unchallenged extensive growth in a neutropenia-associated disease course. **(Orange box)** Some A.*f*. germination results from the limited anti-A.*f*. immune response (Purple – neutrophils, Blue - macrophage) but extensive HY growth is perturbed. Figure adapted from [4].

When A.*f.* is not efficiently removed from the lung it is able to germinate and grow into HY. Unperturbed A.*f*. growth disseminates the fungi throughout the lungs with the potential to culminate in a catastrophic invasion of the blood stream. This type of IA typically presents in neutropenic patients. Neutropenia is a common side effect of patients undergoing chemotherapy or radiotherapy for haematological malignancies. A lack of neutrophil recruitment, migration and anti-A.*f*. immune response allows unperturbed A.*f*. growth and minimal fungal killing. In neutropenic patients, large A.*f*. HY structures physically penetrate through lung tissue and result in the formation of a highly inflamed lung setting. If the inflammation is not resolved local tissue infarction and necrosis ensues, further impairing any anti-A.*f*. immune response. As A.*f*. continues to experience unperturbed growth, HY gain access to the host's vasculature by penetrating through the endothelial lining of lung blood vessels. This HY angio-invasion leads to the dispersion of HY fragments into the blood stream. HY fragments are carried around the vasculature of the host regularly invading back through the endothelium at multiple sites of slowed blood flow; therefore, systemically disseminating the A.*f*. infection. HY invasion back out of the blood vessel from the lumen to the abluminal side of the endothelium causes massive local tissue infarction and thrombosis. This localised damage generates multiple enlarging areas of necrosis providing ideal conditions for further A.*f*. growth into the surrounding tissue. At the point of systemic dissemination and growth of A.*f.* in multiple locations the prognosis is bleak for the individual. Multiple enlarging sites of thrombosis, infarction, inflammation and necrosis eventually conclude in multiple organ failure and death [10, 11].

The disease course of A.*f*. infections in patients receiving corticosteroid therapies is very different to the systemic-type disease often encountered in neutropenic patients. Corticosteroid therapies are routinely used in allogeneic transplant patients to prophylactically prevent or treat graft versus host disease. IA presents as the use of corticosteroids significantly impairs the host anti-fungal response. Corticosteroids have a drastic impact on alveolar macrophage function reducing or blocking phagocytosis, oxidative burst, the production of cytokines and chemokines and cellular migration [12]. The inability of alveolar macrophages to phagocytose A.*f.* RC

when treated with corticosteroids has been well described [13]. As RC escape the alveolar-macrophage driven early immune response in patients treated with corticosteroids, A.*f*. germination and the development of HY structures in the lung ensue. Despite the corticosteroid-induced lack of phagocytosis, alveolar macrophages can still recognise pathogens. A weakened cytokine and chemokine response has been described in these patients [14]. A weakened anti-A.*f*. response likely results in limited recruitment of neutrophils and monocytes to the lung. Corticosteroids do not impact the ability of neutrophils to migrate, degranulate and release arachidonic acid metabolites. Therefore limited neutrophil recruitment can still result in perturbation of HY growth and A.*f*. killing, thereby retaining corticosteroid-associated A.*f*. disease in the lung. However, the lack of A.*f*. RC phagocytosis by alveolar macrophages permits regular RC germination, which eventually leads to the robust recruitment of neutrophils creating a chronic neutrophil-driven inflammatory environment [15-17]. A persistent inflammatory lung environment leads to local tissue infarction, thrombosis, necrosis and eventually fibrosis. This concludes in reduced lung function, which is often fatal to the host. Cause of death from corticosteroid-induced A.*f*. infections are generally regarded as a diminished lung function rather than A.*f.* infection itself [4].

1.1.3: A.*f*. disease in immune-competent individuals

A.*f*. can also cause pathology in immune-competent individuals with an underlying airway disease. Allergic bronchopulmonary *Aspergillosis* (ABPA) is a pulmonary disease impacting asthma and cystic fibrosis (CF) patients. Pathology results from hypersensitivity developed against inhaled A.*f*. RC. As previously mentioned, upon RC inhalation and deposition in the lung, conidia are rapidly phagocytosed and cleared by alveolar macrophages. Should RC evade this response a robust neutrophil response is generated and results in RC clearance. It is hypothesised that underlying airway disease dampens and curtails the local lung innate and adaptive immune response; therefore, inefficient RC clearance occurs permitting the germination of RC into HY. As the immune response is still present, although reduced, A.*f*. persists in the lung causing local pathology but is challenged enough so that the infection is retained within the

lung [18]. Angio-invasion and systemic A.*f*. infections are not encountered in immune competent patients even with the presence of underlying airway disease. Long-term persistent A.*f*. infections and their accompanying inflammation culminate in scarring and fibrosis of the airway epithelia and lung, exacerbating underlying airway disease and reducing lung function. Patients with CF have been extensively described to suffer severe morbidity and mortality from A.*f*. infections [19].

1.1.4: Cystic fibrosis and A.*f*. disease

CF is an autosomal recessive disorder caused by mutations in the CFTR gene. Mutation results in the CFTR protein misfolding leading to premature degradation and failure to reach the cell surface [20]. CF disease primarily impacts the airway mucosal glands, as this is where expression of the CFTR is most abundant [21]. The CFTR is responsible for transporting Cl^- across the epithelia; a defective CFTR leads to an absence of Cl^- transport and a lack of proper control over mucus secretion. This concludes in the thick deposition of mucus within the airway that is poorly cleared and retained for much longer than healthy mucus. The long-term presence of thick mucus radically alters airway homeostasis. Importantly the action of the mucociliary escalator, a crucial component of the immune system responsible for trapping and clearing inhaled pathogens, is drastically reduced [20, 22, 23].

CF patients struggle with recurrent and chronic pulmonary infections such as ABPA and *Aspergillus* bronchitis. This is linked to their inability to mount an appropriate, robust immune response in the airway leading to an absence of pathogen clearance and an inability to resolve inflammation in a timely manner. From early childhood onwards bacterial and fungal infections are regularly acquired and associated with a profound, intense neutrophil response [24-26]. Neutrophils represent ~70% of the inflammatory cell population in CF patient's lungs compared to ~1% in healthy lungs [27].

Bacterial and fungal pathogens become trapped in thick mucus, avoid clearance and are retained in the airway providing a constant stimulus for the immune system. A

large neutrophil-driven immune response is generated; however, recruited cells are also retained in mucus further contributing to the inflammatory setting [25]. The CF airway is characterised by prolonged primary inflammation typically associated with an acute infection. This inflammatory response is unable to mature and promote a macrophage-driven more appropriate chronic response. The airway epithelia-pathogen interactions have been suggested to be the key orchestrator in driving the pro-inflammatory response [28]. A.*f*.-associated disease may occur as inhaled RC become trapped in thick mucus avoiding immune clearance and germinate. A robust neutrophil-driven immune response is generated and recruited neutrophils perturb HY growth whilst also becoming stuck in thick mucus. Retained neutrophils persist in a chronically active state driving inflammation in the airway. As A.*f*. and neutrophils are not efficiently cleared and inflammation is not resolved, a state of chronic A.*f*. infection and immune response is created.

Declining lung function in CF patients has been associated with profound neutrophil inflammation and the presence of high quantities of neutrophil-derived serine proteases [27]. Neutrophils, when recruited to the airway or lung are activated and combat pathogens such as A.*f*. using phagocytosis, serine proteases, DNA NETosis and reactive oxygen species. A key facet of the neutrophil anti-microbial response is the ability to release serine proteases [29]. This is particularly of interest during A.*f*. infections. These enzymes degrade microbial polypeptides or amino acids liberated during phagocytosis. When neutrophils are appropriately regulated, serine proteases are an important anti-microbial defence mechanism. However, when poorly regulated, serine proteases can be very damaging to the host. Three main proteases have been implicated in causing pathology in the CF airway: neutrophil elastase (NE), proteinase 3 and cathepsin G. The mature forms of these proteases are stored in granules within the neutrophil cytoplasm, ready for release upon pathogen recognition [27].

High levels of NE have specifically been identified from CF patients struggling with A.*f*. disease. This serine protease is thought to drive inflammation in the CF airway. NE is released following neutrophil activation or necrosis and elevated quantities of NE have

been linked to high neutrophil infiltration within the CF airway [30, 31]. CF patient neutrophils release greater quantities of NE when compared to healthy control patient's neutrophils; this is despite both sets of neutrophils containing similar quantities of NE [31]. The action of CF patient neutrophils to release large quantities of NE is likely due to the highly inflammatory setting their neutrophils are chronically exposed to. A poorly regulated neutrophil-NE response is widely accepted as a key contributor to CF airway pathology [27].

The main impact NE conveys over the CF airway is the degradation and impairment of the host immune response via two distinct mechanisms. Firstly, the cleavage of pathogen PAMPS aids pathogen immune evasion. For example, NE cleaves bacterial flagella, a vital TLR5 ligand, thereby reducing immune recognition and the response against pathogens possessing flagellum [32, 33]. Secondly, NE cleaves host immune receptors. NE-induced cleavage of host-derived antimicrobial peptides and complement opsonising peptides/receptors blocks the action of these proteins and impairs the host immune response. Soluble IL-6R is susceptible to cleavage and inactivation by NE [34, 35]. Elements of the complement immune response such as C3bi, CR1 and C5R are cleaved and rendered obsolete by NE [35, 36]. NE can also cleave cell surface receptors such as TLR4 and CD11b in the CF airway setting [32, 37]. The impact of NE on C-type lectin receptors (CLRs) has not previously been elicited. A role for neutrophils and NE impairing the immune response in the airway of CF patients and enhancing inflammation is clear. However, how this impacts the ability of CF patients to recognise and mount an immune response against A.*f*. has not been described. The ability of A.*f*. to avoid the immune response and germinate when retained in thick mucus is accepted; however, the A.*f*. immune-evasion mechanisms have not been described. Understanding this A.*f*. evasion before a damaging neutrophil response is generated may improve patient's CF disease.

1.1.5: A.*f*. clinical relevance

A.*f*. is a very clinically relevant pathogen with a rapidly increasing disease burden encompassing immune-compromised and immune-competent patients. Within the last two decades the number of patients treated with immune-suppressants has dramatically expanded. This correlates to an equally dramatic rise in the prevalence of invasive fungal infections, specifically IA. In the 2000's IA accounted for 60% of invasive fungal infections identified during autopsy [38]. A.*f*. disease has emerged as a leading cause of infection-related mortality among immune-compromised individuals with mortality rates up to 90% [39]. Figure 1.3 describes the high incidence of A.*f*. infections identified in patients undergoing hematopoietic stem cell transplant, solid organ transplant or receiving cancer immune-suppressing chemotherapy treatments

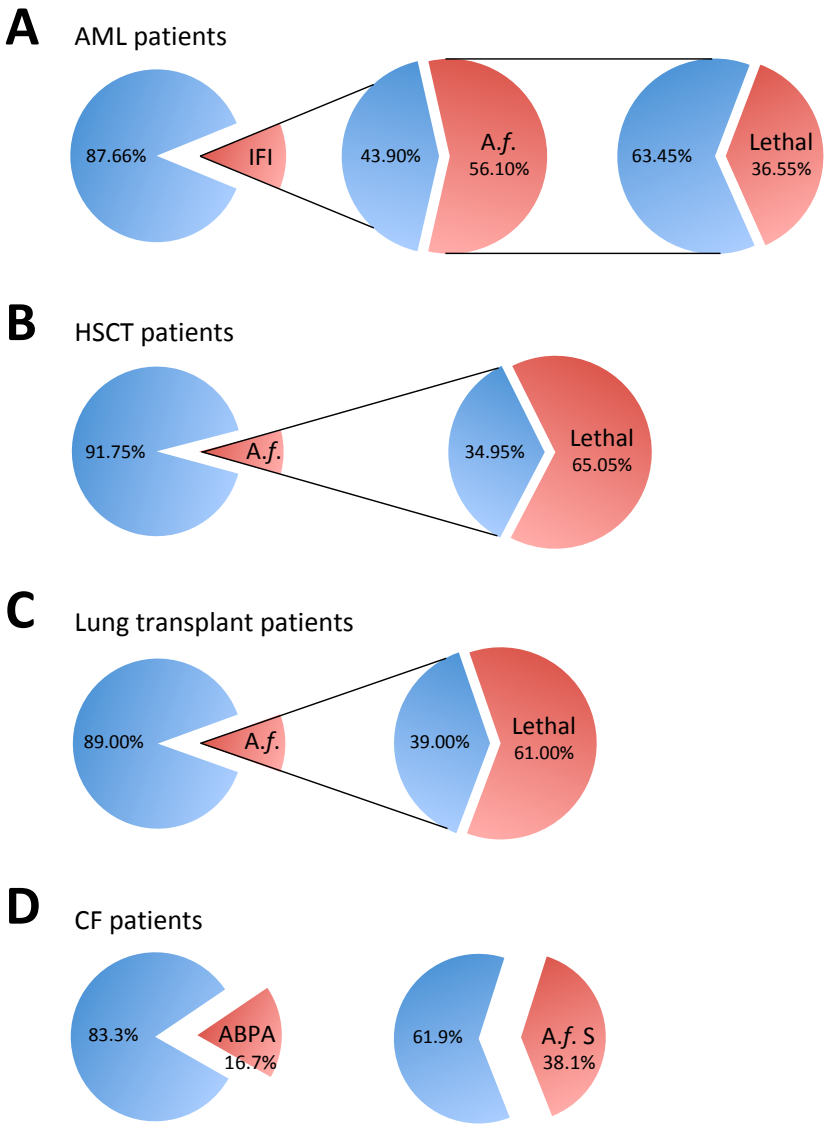

Figure 1.3: A.*f*. incidence and mortality rates in at-risk patient groups. (A) Charts describing the incidence of IFI and A.*f*. infections and their lethality in patient cohorts at-risk of developing invasive fungal infections. **A)** AML patient's IFI incidence and A.*f*. incidence and lethality. **B)** HSCT patient's A.*f*. incidence and lethality. **C)** Lung transplant patient's A.*f*. incidence and lethality. **D)** CF patients ABPA incidence and A.*f*. sensitisation incidence. Figure data derived from [7, 19, 40-48].

The increased prevalence of IA disease in patients with hematologic malignancies is attributed to profound immune-suppression and neutropenia brought about by the extensive therapeutic use of cytotoxic chemotherapies, radiation therapy, HSCT-requirement and the use of corticosteroids and cyclosporine. A large study aiming to describe the incidence and outcome of invasive fungal infections in patients with hematologic malignancies offers some insight into the disease burden associated with A.*f*. infections. A total of 11802 patients diagnosed with acute myeloid leukaemia (AML), acute lymphoid leukaemia (ALL), Hodgkins or non-Hodgkins lymphoma, or multiple myeloma were recruited. As displayed in figure 1.3 (A), an overall incidence of invasive fungal infection of 4.6% was attained across the total patient sample; AML patient's incidence of 12% (373/3021) was the highest. Of the 373 AML patient fungal infections, 213 (69%) were *Aspergillus spp.* of which 80 (37%) were lethal. This study concluded IA was the most prevalent invasive fungal infection recorded. Patients with AML were twice as likely to become infected with *Aspergillus spp.* when compared to the next most IA-likely hematologic malignancy, ALL. Mortality rates after the incidence of IA was confirmed varied between hematologic malignancy groups and ranged from 38% to 80% [40].

Patients receiving allogeneic HSCT are also at high risk of developing an IA infection. These patients typically experience chemotherapy-induced neutropenia and are often treated post-transplant with corticosteroids reducing the impact of graft versus host disease [49-51]. As highlighted in figure 1.3 (B), the incidence of IA in allogeneic HSCT patients ranges from 6-10.5% [7, 41]. More recent studies combining allogeneic and autologous HSCT have found incidence rates ranging from <1-4% depending on the individual hospital and location [42]. Mortality rates following HSCT and confirmed IA vary from 53.8% up to 76.3% [7, 40, 42]. These concerning results led to the generation of a USA-wide survey completed by the CDC with the objective of monitoring trends in the incidence of invasive fungal infections through a nationwide survey of hospitals.

IA has been described as a leading cause of mortality among recipients of solid organ transplants [43]. The profound and prolonged immune-suppression required for successful solid organ transplant has been described as the main risk factor for

developing an A.*f*. infection post-transplant [44]. Figure 1.3 (C), highlights lung transplant patients experience the highest incidence of IA (6-16%) within the total solid organ transplant patient cohort examined [45, 52]. IA has also been identified in patients undergoing heart (~5-14% IA incidence), liver (~1-8% IA incidence) and kidney (~0.7-4% IA incidence) transplants with A.*f*. infections presenting immediately post-transplant up to many years after transplant [42, 53-55].

Immune-competent patients with underlying airway disease such as CF also experience a significant A.*f*. disease burden. A.*f*. has been isolated from 10-57% of airway secretions from CF patients and A.*f*. specific IgG has been detected in 41% of CF patients by the age of 4, rising to 98% by age 10 [19]. These seropositivity rates were much higher than healthy control patients and even asthma patients [46]. *Aspergillus* sensitisation (AS) and ABPA is highly prevalent in the CF population. Figure 1.3 (D), displays results from a meta-analysis review combining 64 studies. This study quantified the incidence of AS and ABPA within the CF population and described a 39.1% prevalence of AS and 8.9% prevalence of APBA [47]. A 2013 study assessing the prevalence of ABPA specifically within the UK CF population described ABPA incidence of 17.7% [48]. Considering the earlier described (1.1.3 & 1.1.4) significant disease pathology associated with ABPA, a CF population ABPA prevalence of 8.9-17.7% is extremely concerning. Due to the high incidence and unacceptable mortality rates of IA across a spectrum of immune competent and immune compromised patients, improvements in diagnosis, treatment and identification of at-risk patients are required.

1.1.6: Therapeutic insufficiencies

Despite the regular introduction of new anti-fungal therapeutics, treatment of IA remains challenging. Amphotericin B has extensively and effectively been used to treat prophylactically or at first suspicion of A.*f*. infection; however, this drug causes serious side effects including nephrotoxicity, electrolyte disturbances and hypersensitivity [56]. Perhaps more concerning is that the patient's primary disease treatment is often

negatively impacted by the use of anti-fungal agents such as Amphotericin B [43, 57]. In the early 1990's the generation of a new anti-fungal class containing azoles was produced. Initially, fluconazole treatment was used prophylactically and upon suspicion of IA. Many fungal species were originally susceptible to fluconazole treatment; however, since the year 2000 a range of resistant fungal strains, including resistant A.*f*. has rendered this therapy almost obsolete. Recently the azole Voriconazole has become the treatment of choice against A.*f*. infections [58]. Voriconazole was compared to Amphotericin B in a large multi centre trial aiming to identify the most effective therapy in the primary treatment of IA. Patients who received Voriconazole had a higher favourable response after 1 week (53% versus 32%) and a higher 12-week survival rate (71% versus 58%) [57]. Voriconazole also has much milder side effects than Amphotericin B; despite this, Voriconazole has a significant number of drug-drug interactions and radically alters patient's primary disease treatment [59, 60]. Although Voriconazole is effective against A.*f*. infections, survival rates post-treatment are still unacceptably low and patient's primary disease treatment can rarely continue whilst the therapeutic is administered [57, 60]. Due to these challenges a targeted personalised medicine approach whereby high-risk IA patients are prophylactically treated should be the aim for future anti-A.*f*. treatment.

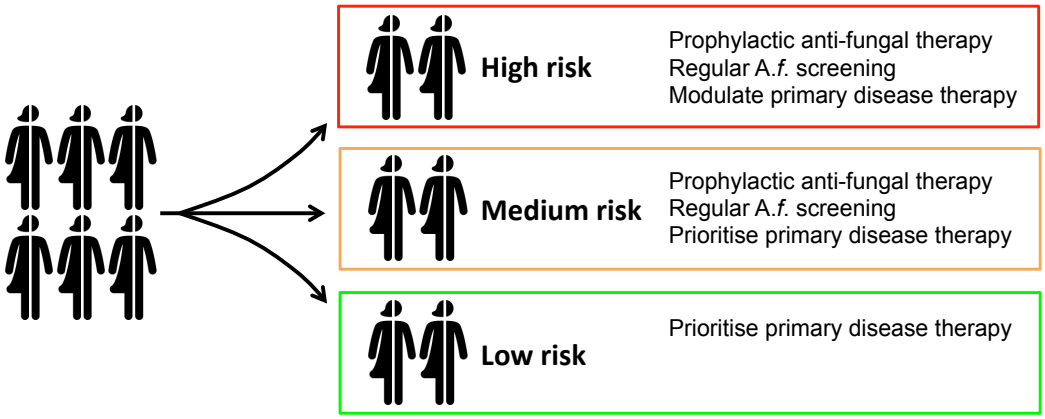

Figure 1.4: Stratification of patients according to their risk of developing IA would allow a personalised medicine approach to treat primary and anti-fungal disease most effectively. Figure developed from [57, 61-63] and consultation with Public Health Wales' microbiology clinical lead Dr Lewis White and Haematology consultants.

Many attempts at identifying risk factors associated with an increased likelihood of developing A.*f*. infections have been unsuccessful. Neutropenia and corticosteroid treatment remain the only widely accepted risk factors increasing the likelihood of an A.*f*. infection [7-9]. Lymphopenia has been described as a risk factor that may increase the likelihood of developing an A.*f*. infection although this data only arises from smaller studies [7, 64]. No significant risk factors associated with patient's age, gender, CMV serology, type of graft versus host disease, and anti-fungal or graft versus host prophylaxis treatment have been identified [64-66]. Recently, mutations in Dectin-1 and DC-SIGN, A.*f*. positive PCR from patient bronchiolar alveolar lavage (BAL), allogeneic stem cell transplantation and infection with a respiratory virus were described as significant risk factors when three or more positive factors were present [67]. Identifying risk factors associated with an increased likelihood of developing IA may aid the implementation of targeted prophylactic anti-fungal therapy in a personalised medicine approach as suggested in figure 1.4.

1.2: The anti-A.*f*. immune response

1.2.1: A.*f*. Infection

A.*f*. is a serious, complicated and potentially lethal human pathogen. The infectious life cycle of A.*f*. begins upon inhalation of RC and their potential deposition in the bronchioles or alveolar spaces. From this point onwards, the immune capability of the infected individual is key to determining whether disease may ensue as discussed in 1.1.2 and 1.1.3. Upon infection A.*f*. must exhibit thermo-tolerant growth utilising specific biosynthetic pathways evolved to promote germination and survival in hostile environments such as the human airway and lung [68]. Once A.*f*. RC have infected the host lung, multiple factors such as the A.*f*. cell wall and surface composition, A.*f*. secondary metabolite production, A.*f*. HY growth rate, HY tissue invasion and A.*f*.'s resistance to host killing mechanisms influence survival and dissemination. However, these factors are secondary to the immune competence of the infected host [69].

1.2.2: A.*f*. cell wall and surface

The surface and cell wall of A.*f*. RC is complex and plays many crucial roles in the successful survival, host-infection and growth of A.*f*. in the host-lung. The outer RC surface contains a hydrophobic, immunologically inert protein rodlet layer that maintains RC survival in challenging environmental conditions. Once RC have infected a host this rodlet layer is shed allowing RC germination thereby unveiling immune activating cell wall components, which consequently results in immune recognition. A.*f*. RC lacking a rodlet layer displayed enhanced susceptibility to alveolar macrophage killing [70]. A.*f*. RC also express sialic acid residues on their surface. These residues are likely involved in RC dispersal and pulmonary deposition as sialic acid blocks RC agglutination. Interestingly, a role for sialic acid binding host-lung fibronectin has also been identified. Lung damage often caused by A.*f*. infection and the ensuing anti-A.*f*.

response results in fibronectin production. A.*f*. may utilise lung fibronectin to bind RC, enhancing infection and disease progression [71, 72]. The cell wall of RC after the rodlet layer has been shed is predominately composed of α-(1-3) glucan, β-(1-3) glucan, β-(1-6) glucan, chitin and galactomannan [73]. Genetic deletion of these cell wall components (when viability is retained) has been demonstrated to generate hyper-virulent A.*f*. strains. Mutated strains possess increased virulence due to their evasion of the host immune response as α-glucans and β-glucans act as PAMPs and are required for A.*f*. recognition and the generation of a robust anti-A.*f*. immune response [74-76].

1.2.3: Soluble lung components and respiratory epithelia

Immediately after inhalation, A.*f*. RC encounter the respiratory tract and airway epithelial mucosa. A key aspect of the epithelial anti-A.*f*. defence involves the mucociliary escalator. This is comprised of epithelial cell secreted mucus, ions, proteins, lipids and fats and contributes to the efficient, pathology-free clearance of inhaled pathogens including A.*f*. [77, 78]. Opsonic PRRs such as collectins are also found in this mucus secretion and opsonise inhaled pathogens increasing pathogen-recognition and bolstering host defence. Other opsonic PRRs such as mannose-binding lectin, surfactant protein A and surfactant protein D have been shown *in vitro* to bind and agglutinate A.*f*. RC leading to their enhanced phagocytosis and killing by alveolar macrophages and neutrophils [79, 80]. Mannose binding lectin, surfactant protein A and surfactant protein D were also recently identified to play a role in the activation of complement [81]. Knocking out these three PRRs *in vivo* enhanced susceptibility to A.*f*. infection, whilst recombinant Mannose binding lectin, surfactant protein A and surfactant protein D have been used to enhance anti-A.*f*. responses *in vivo* [80, 82]. Epithelial-derived collectins and soluble PRRs are crucial during the early A.*f*. response as they enhance A.*f*. RC clearance via opsonising phagocytosis and aggregating A.*f*. RC [4].

Epithelial cells also play a direct role in the anti-A.*f*. response. A.*f*. RC have been demonstrated to bind and be engulfed by epithelial cells. Engulfed RC are retained and

killed in phagolysosomes; however, some evidence suggests A.*f*. growth and escape can occur inside epithelial cells [83, 84]. A.*f*. can secrete factors that modulate and disrupt the airway epithelium, counteracting epithelial anti-A.*f*. immune responses. Culture filtrates from A.*f*. have been demonstrated to alter epithelial cell function and viability by inducing cell shrinkage, actin rearrangement and desquamation [85, 86]. Inhibiting local serine and cysteine proteases can abrogate this anti-epithelial activity; demonstrating that A.*f*. secreted proteases induce this effect [86]. Disruption of the epithelial barrier and epithelial cell immune functions enhances A.*f*. pathogenicity allowing A.*f*. to interfere with mucociliary clearance, bind airway epithelia and establish infection.

1.2.4: Alveolar macrophages

As the primary resident phagocytic cell of the airway and lung, alveolar macrophages are a crucial component of the anti-A.*f*. immune response. Alveolar macrophages act as the front-line response against A.*f*. RC that have inoculated the lung. PRRs located on the surface of alveolar macrophages mediate the recognition of A.*f*.-associated PAMPs and actin-dependent phagocytosis of A.*f*. RC and SC as shown in figure 1.5 [87]. Following phagocytosis, A.*f*. RC and SC are retained in a phagosome that matures and acidifies into a phagolysosome concluding with A.*f*. killing [87]. Alveolar macrophages treated with NADPH oxidase inhibitors *ex vivo* were unable to acidify their phagosomes resulting in significantly impaired A.*f*. phagocytic killing [88]. A.*f*. can resist phagolysosomal killing via the production of the pigment melanin. Melanin's role in ROS scavenging is clear and has been described for many pathogenic fungi. A.*f*. produced melanin greatly increases A.*f*. virulence and survival by blocking acidification of the phagolysosome [89, 90].

A.*f*. engagement of alveolar macrophage associated PRRs initiates a pro-inflammatory response comprising of the production and release of many chemokines and cytokines including TNF, IL-1β, IL-6, IL-8, MIP-1α and KC [1, 91-94]. The initiation of a robust pro-inflammatory response is critical for host defence against A.*f*.. TLR2, TLR4 and Dectin-

1 are the best-described PRRs involved in the alveolar macrophage recognition of A.*f*.. TLR2 and TLR4 have been identified to activate macrophages upon stimulation with A.*f*.. TLR2 has been demonstrated to recognise both conidial and HY morphologies whilst TLR4 only HY [95]. *In vivo* $TLR2^{-/-}$ and $TLR4^{-/-}$ mice display higher A.*f*. fungal burdens when compared to WT mice. This fungal burden difference is exacerbated when KO mice were used in a neutropenia model suggesting a requirement for the expression of these receptors not only on alveolar macrophages but also on neutrophils. Crucially, *in vivo* $TLR2^{-/-}$ and $TLR4^{-/-}$ mice did not exhibit differences in survival when compared to WT mice, despite the increased fungal burden observed [96, 97].

Dectin-1 is a well-characterised PRR which, unlike TLRs, is fundamental for host defence against A.*f*.. Dectin-1 is constitutively expressed on alveolar macrophages and recognises A.*f*. cell surface expressed β1-3 glucans [98]. When RC germinate and shed their immunologically inert rodlet layer, β1-3 glucans located abundantly on the surface of RC and SC are engaged by Dectin-1. Dectin-1 engagement activates alveolar macrophages resulting in A.*f*. RC and SC phagocytosis as well as the robust induction of a pro-inflammatory cytokine and chemokine response [2, 99]. Immune competent individuals who lack functional Dectin-1 expression are at significant risk of developing an invasive fungal infection without any immune-suppression [100]. The ability of Alveolar macrophages to rapidly recognise and kill regularly inhaled A.*f*. RC without pathology preserves host homeostasis. Perhaps more impressive is the capability of alveolar macrophages, when encountering larger quantities of germinated A.*f*., to orchestrate a complex, coordinated and robust anti-A.*f*. response.

1.2.4: Neutrophils

The generation of a successful anti-A.*f*. immune response relies on the recruitment and immune capabilities of neutrophils. This imperative cell requirement is highlighted by the fact that neutropenia is the primary risk factor for the development of A.*f*. infections [7, 8]. The importance of neutrophils when combating the larger EG and HY morphologies of A.*f*. is displayed in figure 1.5. These later A.*f*. morphologies develop after RC successfully evade or resist the alveolar macrophage driven early immune response and germinate. Alongside alveolar macrophages and epithelial cells, neutrophils utilise PRRs such as TLRs and Dectin-1 to mediate A.*f*. interactions and generate appropriate immune responses [97, 101, 102]. An intriguing role for CD11b (also known as Complement Receptor 3) binding fungal β1-3 glucans exclusively in human neutrophils (not murine) has also been described. This may explain the higher than expected incidence of A.*f*. in leukocyte-adhesion deficiency type-1 syndrome patients who lack CD11b expression on neutrophils [103, 104]. *In vivo* and *in vitro* studies have extensively demonstrated the ability of neutrophils to recognise and bind A.*f*. HY before inducing fungal killing via oxidative and non-oxidative killing mechanisms [105, 106].

Neutrophils use NADPH oxidase-generated ROS to mediate efficient A.*f*. HY killing. Neutrophils isolated from chronic granulomatous disease (CGD - characterised by mutations present in NADPH oxidase genes blocking ROS formation) and Myeloperoxidase Deficiency (MPO - Myeloperoxidase catalyses the formation of the ROS produced hypochlorous acid from hydrogen peroxide) have been used to determine the important role of anti-A.*f*. neutrophil ROS. Neutrophils obtained from patients with these diseases lack the ability to kill A.*f*. HY [105, 107]. The lack of A.*f*. HY neutrophil-derived ROS killing activity present in CGD and MPO patient neutrophils could be completely rescued with the addition of hydrogen peroxide or hydrochloric acid. This clear link between A.*f*. HY killing and neutrophil-derived ROS function highlights the importance of ROS in the anti-A.*f*. HY immune response [105, 108].

Neutrophils also possess the ability to perturb and kill A.*f*. using non-oxidative responses. Neutrophils upon activation can de-granulate releasing a range of potent antimicrobial compounds such as proteases, lactoferrins, defensins, pentraxin-3 and lysosymes [109]. Further to this, neutrophils can utilise an elaborate killing mechanism forming neutrophil extracellular traps (NETs). This involves neutrophils, as a final dying act of defence termed NETosis, unravelling chromatin-coiled nuclear DNA, covering this DNA with highly antimicrobial granular proteins and violently forcing this DNA out of the cell rupturing the cell membrane [110]. Neutrophils have been demonstrated *in vitro* to rapidly (within 3 hours of A.*f*.-neutrophil co-incubation) produce NETs against A.*f*. with both conidial and HY morphologies being embedded within the released antimicrobial DNA trap. NETosis was also demonstrated to occur and embed A.*f*. conidia and HY within an *in vivo* A.*f*. lung infection model [111]. Neutrophils isolated from NADPH oxidase deficient mice identified the potential requirement of a functional NADPH oxidase for the successful formation of NETs. Again reiterating the importance of the oxidative capabilities of neutrophils in the anti-A.*f*. response [29].

Recently, neutrophils have been shown to aggregate and surround A.*f*. before saturating the local environment with high concentrations of anti-microbial compounds. This resulted in sequestered A.*f*. being killed. Neutrophil aggregation and anti-microbial compound release was shown to be particularly efficient at killing early A.*f*. morphologies. When larger A.*f*. HY were sequestered, oxidative killing mechanisms were required to kill the fungi [112].

As a result of evolutionary pressure, A.*f*. has developed defence mechanisms against ROS. These mechanisms are relevant during human infection and target neutrophil-mediated ROS production. A.*f*. secreted catalases act as ROS scavengers limiting the potential damage and killing impact associated with neutrophil-derived ROS. Experiments deleting both A.*f*. HY catalyses (CAT1 and CAT2) resulted in an increased HY susceptibility to hydrogen peroxide. *In vivo* this translated to reduced A.*f*. virulence suggesting HY catalases protect against neutrophil-derived ROS-mediated killing; although, the reduced A.*f*. virulence was subtle [113]. A.*f*. HY may possess multiple ROS-scavenger mechanisms that provide redundancy to the underwhelming ROS

scavenger impact CAT1 and CAT2 models displayed [90, 114]. Despite this, the profound immune-suppression and resulting neutropenia common in IA patients likely render the subtle action of A.*f*. ROS scavengers ineffective, as neutrophils are not present. A.*f*. ROS scavengers may play a more fundamental role against neutrophil-derived ROS in corticosteroid or CF-associated A.*f*. infections. Neutrophils are a key facet of the anti-A.*f*. response and are almost exclusively required to combat larger morphologies of the fungi. Due to this, lacking an efficient anti-A.*f*. neutrophil response is the predominant risk factor for the development of IA.

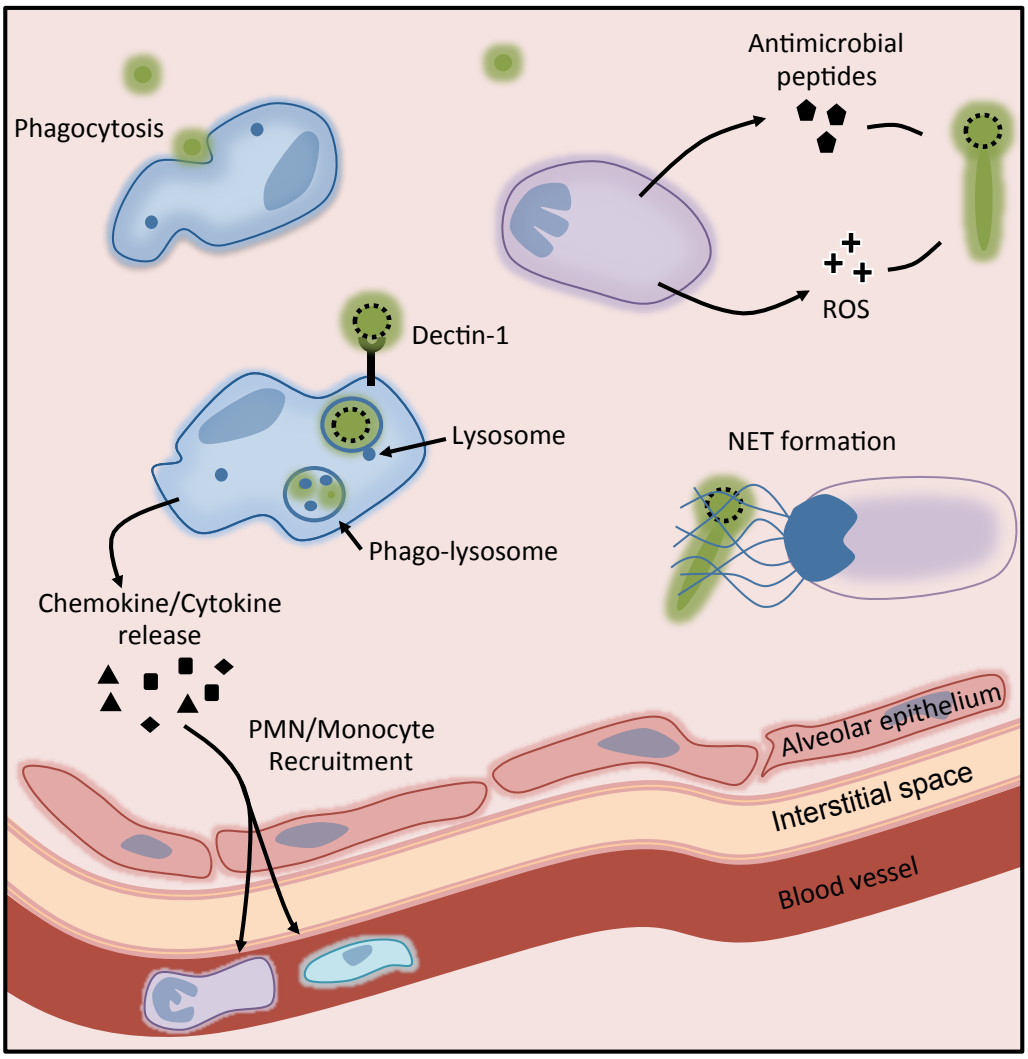

Figure 1.5: Macrophage and Neutrophil driven anti-A.*f*. immune response and killing mechanisms. (Blue) Alveolar macrophage and **(Purple)** neutrophil anti-A.*f*. **(Green)** immune response including phagocytosis, cytokine and chemokine production, ROS production and release, antimicrobial peptide release and NET formation. Figure adapted from [69, 115].

1.2.5: Secondary metabolites

The pathology of A.*f*. infections is strongly influenced by the fungal production of secondary metabolites. These molecules are typically produced during HY formation and exert disease progressive effects. A single A.*f*.-produced secondary metabolite has been isolated *in vivo* and in the serum of IA positive patients. This secondary

metabolite is called epipolythiodioxopiperazine toxin, or gliotoxin and conveys an immune suppressive impact on the host [116, 117]. Gliotoxin, via the formation of a sulphide:thiol exchange donated from gliotoxin's own internal disulphide bridge, disrupts binding and inactivates host immune receptors, proteins and ROS as displayed in figure 1.6 [118]. Almost all A.*f*. clinical isolates (>95%) produce gliotoxin implying this molecule is integral for A.*f*. viability and has been evolutionarily conserved [116]. Research into the *in vitro* effects of gliotoxin have elicited a multitude of immune suppressive actions including the inhibition of alveolar macrophage phagocytosis, mast cell activation, cytotoxic T-cell responses, the induction of epithelial damage and the induction of apoptosis in lymphocytes, alveolar and peripheral macrophages, dendritic cells, fibroblasts and neutrophils. Gliotoxin has also been demonstrated to block antigen presentation by monocytes and DCs to effector T-cells preventing the expansion of antigen-specific T-cells and the formation of an adaptive immune response [119-122]. The repertoire of gliotoxin's immune suppressive actions was described using gliZ (gliotoxin transcriptional regulator) and gliP (glioxin nonribosomal peptide synthase) mutants. Mutating either gene resulted in abrogated gliotoxin production [123, 124]. Interestingly, in a neutrophil depleted *in vivo* model, gliZ and gliP mutant A.*f*. strains were found to be no more or less virulent than non-mutated A.*f*. [124, 125]. In a corticosteroid-treated *in vivo* model, significantly reduced A.*f*. virulence was attained with the gliP mutant strain [126]. The reduced gliP mutant-A.*f*. virulence was attributed to a lack of neutrophil apoptosis at the site of HY growth that was present in WT A.*f*. strains [127]. These *in vivo* models suggest a specific role for gliotoxin inducing apoptosis in neutrophils in the locality of A.*f*. HY thereby suppressing the anti-A.*f*. immune response. Gliotoxin has an immune suppressive impact on a range of innate and adaptive immune cell types; however, the mechanisms and interactions between gliotoxin and these cell types are not well understood.

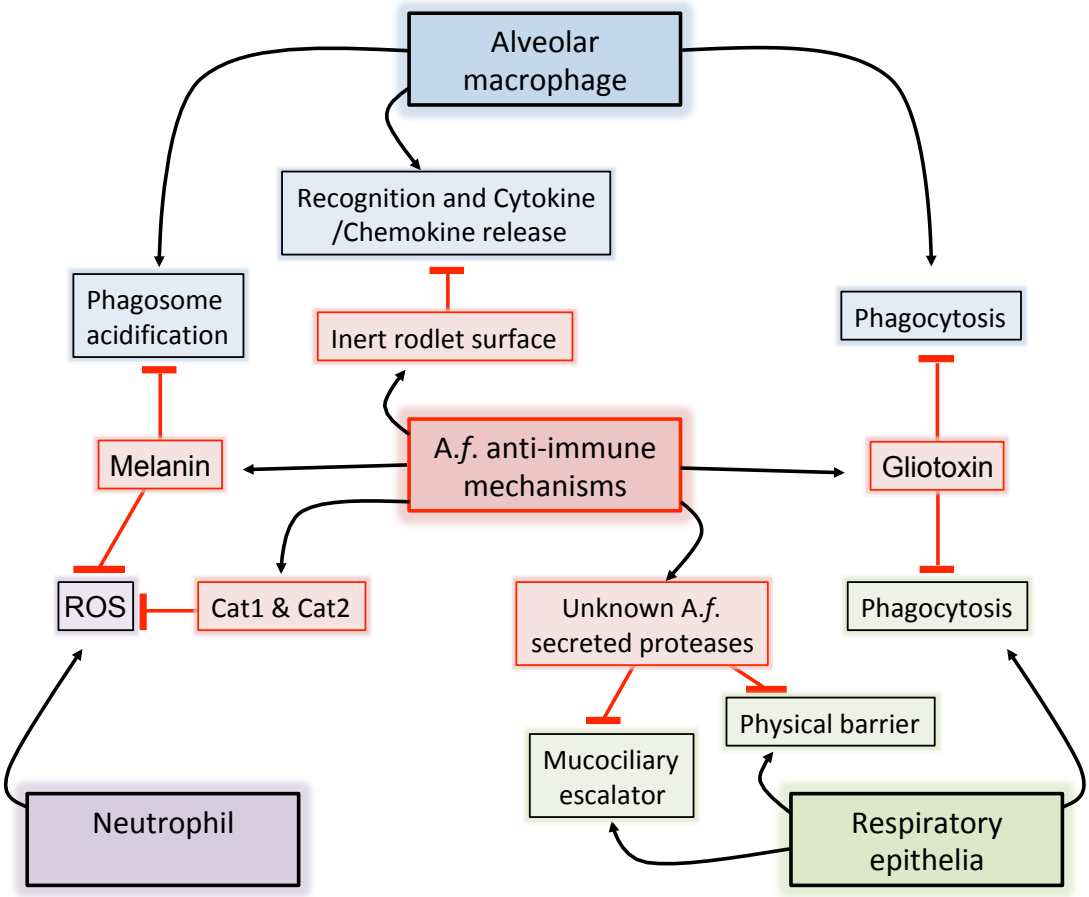

Figure 1.6: A.*f*. mechanisms of resisting the host anti-fungal immune response. (Red) Identifies A.*f*. blocking mechanisms against neutrophil **(Purple)**, respiratory epithelia **(Green)** and alveolar macrophage **(Blue)** anti-fungal actions. Figure adapted from [85, 86, 89, 90, 113, 128].

1.2.6: The adaptive response

As neutropenia is the primary risk factor for the development of A.*f*. disease, the adaptive immune response has not been extensively investigated as a contributor to the anti-A.*f*. response. T-cells are unlikely to be involved in the front-line lung response against inhaled A.*f*. RC as conidia are so efficiently cleared by lung-resident alveolar macrophages without any disease. If RC evade immediate front-line clearance and germinate into HY, any anti-fungal impact T-cells may be able to exert over large HY structures has not been described; although, the formation of a T_H1 anti-A.*f*. response

is thought to be beneficial to the host. A.*f*. HY secrete multiple antigens that promote host-protective T_H1 and T_H17 immunity as well as host-destructive T_H2 immunity. Interestingly, A.*f*. appears to be particularly effective at initiating T_H2 immunity and allergic inflammation via the secretion of several allergen proteins such as Asp F. These proteins promote the generation of an allergic-type response allowing A.*f*. to evade a cytotoxic T_H1 response that may enhance A.*f*. clearance [129].

The adaptive response is initiated as $CD14^+$ inflammatory monocytes recruited to the site of A.*f*. infection in the lung phagocytose A.*f*. and curtail germination [130]. Upon A.*f*. recognition inflammatory monocytes differentiate into monocyte-derived dendritic cells, which migrate and deposit A.*f*. conidia in local lymph nodes. This process culminates in the priming of $CD4^+$ T cells and initiates the adaptive anti-A.*f*. immune response [131]. Successful protection against A.*f*. in humans and mice is benefitted by the generation of an A.*f*.-specific $CD4^+$ T cell population and subsequent T_H1 and T_H17 response [132, 133].

Research into the recruitment of T-cells and generation of T_H1, T_H2 and T_H17 adaptive immune responses during A.*f*. infection has been undertaken. C57BL/6 mice were challenged intranasally with A.*f*. weekly for one, two, four or eight weeks. Leukocyte composition, activation and cytokine production were examined after each repeated challenge was complete. As expected, upon first challenge all A.*f*. was cleared within 24 hours. The second A.*f*. challenge resulted in a small neutrophil and regulatory T-cell influx. From four repeated challenges onwards, A.*f*. induced T-cell recruitment and activation within the lungs. This culminated in the development of T_H1, T_H2 and T_H17 adaptive anti-A.*f*. responses [134].

Recently an intriguing adaptive immune role for Dectin-1 and TLRs has been identified. The initiation of T_H1 and T_H17 immune responses against A.*f*. were found to depend on TLR/MyD88 signalling and Dectin-1 signalling respectively. Dectin-1 signalling following A.*f*. recognition reduced the expression of IFNγ and IL-12p40 in the lung. This in turn reduced T-bet expression in responding $CD4^+$ T-cells and enhanced T_H17 immunity [135].

1.2.6: Requirement of A.*f*. immune recognition, signalling and response

The anti-A.*f*. immune response is complex and requires further study. The required involvement of alveolar macrophages, neutrophils and airway epithelia is well described whilst a role for the adaptive immune system is also emerging. A.*f*. possesses its own unique immune evasion mechanisms producing anti-inflammatory secondary metabolites and hiding many of its PAMPs until nutrient uptake and growth has begun. The initiation of a successful anti-A.*f*. response requires the immediate recognition of A.*f*. and rapid signalling cascade to orchestrate an appropriate immune response. If recognition and signalling does not occur due to A.*f*. evasion, a lack of PRR expression, function or collaboration, a lack of effector cells or the suppression of effector cells, A.*f*. disease can ensue.

1.3: A.*f*. recognition and C-type lectin receptors

1.3.1: PRRs

The innate immune response against pathogens is initiated by PRR-mediated recognition of microbial-specific PAMPs. This activates intracellular pathways that drive an immune response against the pathogen. PRRs also recognise damage-associated molecular patterns, these molecules are frequently released from damaged or necrotic cells and act as danger signals further promoting inflammation [136]. Four families of PRRs: the TLRs, NOD-like receptors, RIG-I like receptors and CLRs have been identified to recognise fungal pathogens [137-139].

A controversial anti-fungal role has been described for the best characterised family of PRRs, the TLRs. *In vivo* experiments using MyD88$^{-/-}$ mice, a key adaptor in the TLR signalling pathway, demonstrated an increased susceptibility to multiple fungal infections including *Candida albicans* and A.*f*.; although, these animals also lacked IL-1R signalling so the fungal susceptibility cannot be directly associated with a lack of TLR signalling. In humans, immune-competent individuals lacking MyD88 do not experience an increased susceptibility to fungal infections [140]. However, multiple TLRs have been implicated in fungal recognition, including TLR1, TLR2, TLR4, TLR6, TLR7 and TLR9 [141-143]. The mechanisms underpinning TLR involvement in anti-fungal immunity are not clear although the impact of some TLRs in the anti-fungal response *in vivo* has been described [144-147]. Interestingly, research suggesting TLRs can collaborate with CLRs to enhance anti-fungal immunity has been described.

CLRs have a well characterised role in driving anti-fungal immunity via the recognition of highly conserved cell wall carbohydrate structures which act as PAMPs. CLRs bind all known human pathogenic fungi and their signalling pathways are essential for the generation of successful anti-fungal responses [148]. The recognition of A.*f*. is mediated predominantly by CLRs.

The impact of NOD-like receptors and RIG-I like receptors in A.*f*. disease is not clear; however, the role of these receptors during anti-fungal immune responses has been researched. NLRs are categorised into two main subsets, NOD1/2 receptors and inflammasome-forming receptors [149]. NLR inflammasome-forming receptors are important for controlling oral *Candida albicans* infection and preventing the systemic dissemination of this fungus [150]. The impact NOD1/2 convey over anti-fungal immunity is not clear. Recently, the role of RIG-I like receptors during anti-fungal immune responses has been investigated. IFIHI, a RIG-I like receptor, was induced by *Candida albicans*. IFIHI deficient macrophages generated impaired IFN-β in response to *Candida albicans* challenge [139].

1.3.2: CLRs

C-type lectin receptors (CLRs) encompass a large and diverse family of proteins exclusively found in the animal kingdom. These proteins have been highly conserved in vertebrates suggesting they play a crucial role within these organisms. CLRs are also prevalent throughout invertebrates; however, these proteins show considerable structural variation between invertebrate species proposing they're less important in this phylum [151]. CLRs are characterised by their possession of a carbohydrate recognition domain (CRD); unfortunately, this led to numerous proteins being inappropriately described as CLRs. Since then, this domain has been identified in over 1000 proteins with a diverse range of functions [151]. Many proteins that contain a CRD are not involved in carbohydrate recognition. Therefore, it is more appropriate to consider the CRD region a characteristic of C-type lectin-like domains to reflect their similarity to CRDs without implying their function. Multiple C-type lectin-like domain structures have been discovered with subtle variation between Ca^{2+} binding regions and oligomerisation domains. This variation is responsible for CLR's different ligands and functions [152, 153].

Vertebrates possess up to 17 groups of CLRs offering a diverse range of functions and responses. Many of these CLRs bind PAMPS and can lead to the mediation of host

immune responses. Soluble CLRs such as the collectin family (CLR group III) bind pathogens and activate host complement. The prototypic collectin, Mannose-binding lectin, binds carbohydrate regions located on bacteria, fungi and viruses and opsonises the pathogens for phagocytosis. This response can provide protection from common pathogens such as *Staphylococcus aureus* and *Streptococcus pneumonia* [151, 154]. Although these soluble proteins can be described as a CLR PRR they are not cell-associated and cannot directly impact gene expression through signalling. In contrast, many CLRs do function as signalling receptors within the innate immune system directly regulating gene expression upon ligand binding and signalling initiation [151].

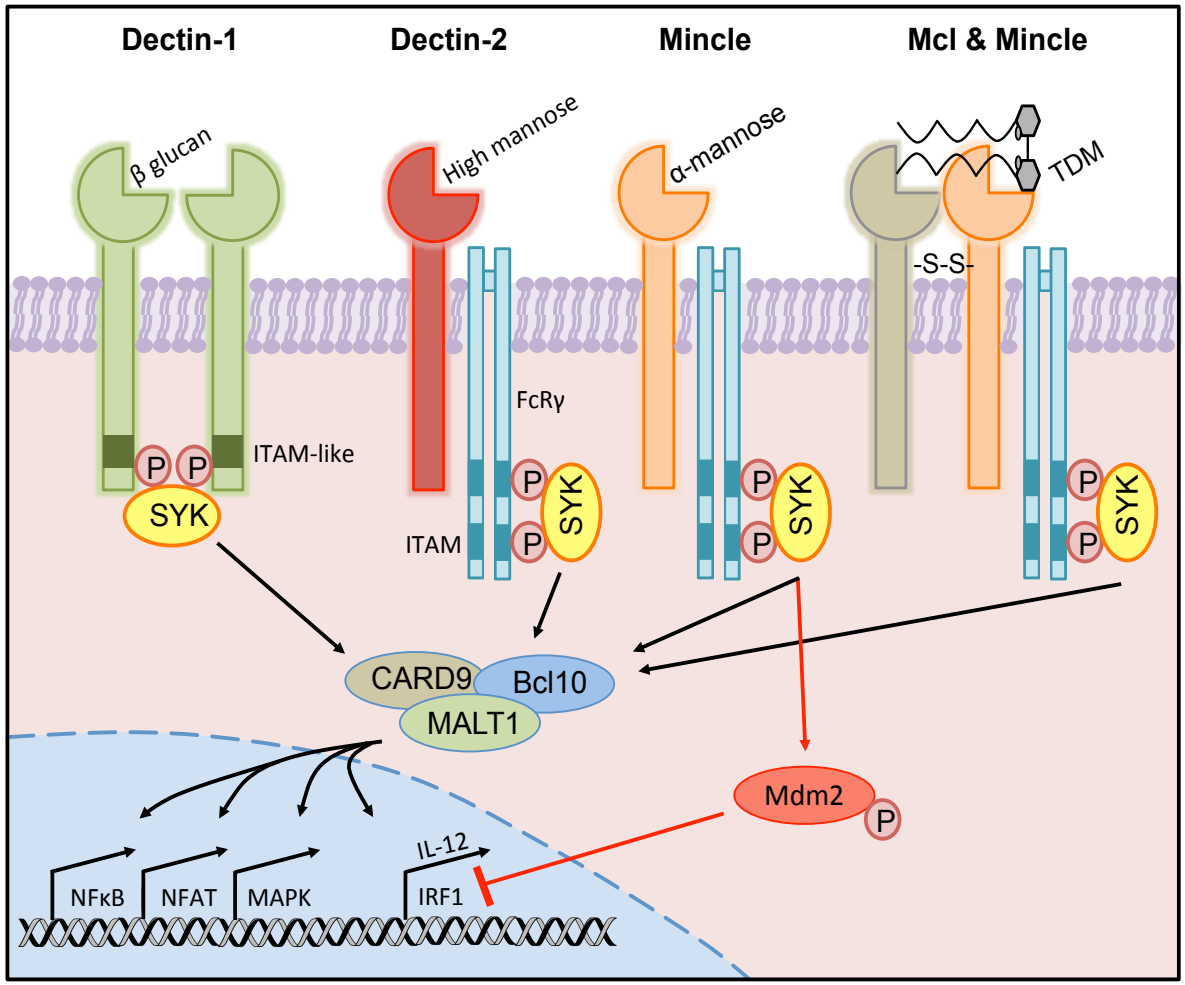

Figure 1.7: Signalling pathways downstream of myeloid CLRs and their transcriptional impact. Dectin-1 likely homodimerises and recruits Syk to initiate downstream signalling through its hemITAM domain. Dectin-2 and Mincle recruit FcRγ and Syk to induce downstream signalling. Mcl has no known signalling motif although can signal through Syk. Recent evidence suggests Mcl can directly couple with FcRγ or Mcl can couple alongside Mincle or another CLR to induce signalling. Syk recruitment and signalling initiate anti-fungal immune gene expression through the CARD9-Bcl10-MALT1 pathway and regulation of NFκB, NFAT, MAPK and IRF1. Mincle engagement can down regulate IRF1 thereby blocking IL-12 expression. Figure adapted from [155-158].

Myeloid cells express many trans-membrane CLRs (often belonging to CLR group II, V and VI). The activation of these CLRs typically induces intracellular signalling utilising one of two distinct signalling pathways. Dectin-1 signals directly through its cytoplasmic tyrosine-based activation motif (hemITAM) whilst Dectin-2 and Mincle require association with an ITAM domain coupled to FcRγ as displayed in figure 1.7. Both the direct and indirect hemITAM/ITAM intracellular signalling pathways require the recruitment of spleen tyrosine kinase (Syk) and coordination of CARD9, Bcl10 and MALT1 complex. Signalling through this complex leads to the activation of NFκβ, MAPK, NFAT and IRF1 eventually culminating in innate immune gene expression and cellular immune responses [155, 156]. Individuals with mutated and defective CARD9 are highly susceptible to fungal infection [159]. CLR signalling pathways lead to the induction of a diverse repertoire of innate functional responses against pathogens including the phagocytosis of non-opsonised bacteria, fungi and viruses, the formation of a robust cytokine and chemokine response driving the pro-inflammatory immune response, respiratory burst and inflammasome activation [156]. Lately, a role for CLRs in the formation of adaptive immune responses has also been identified. The key roles CLRs play driving the multi-faceted innate immune response and coordinating the adaptive response highlights the importance of these proteins. CLRs ability to direct and orchestrate complex anti-fungal immune responses are fundamental to host survival.

1.3.6: Dectin-1

Dectin-1 is a member of the group V CLRs and possesses a single extracellular carbohydrate-recognition domain connected to an intracellular cytoplasmic tail containing a hemITAM domain. Dectin-1 is expressed predominantly on myeloid cells such as macrophages, neutrophils and dendritic cells but is also found on some lymphocyte populations [160]. The CLR is present in two isoforms, a full-length isoform (A) and a shorter isoform (B), which lacks part of the extracellular stalk region. Isoform B lacks exon 3 meaning the extracellular CRD of the receptor sits closer to the membrane. These two isoforms both recognise ligands with the same affinity at 37^{o}C;

although, recognition and signalling through Dectin-1 isoform B led to a greater TNF response [161].

Dectin-1 recognises β1-3 glucans from yeast, fungi, plants and bacteria in a calcium-independent mechanism [162, 163]. Dectin-1 is often found on the cell surface as a homodimer. β-glucan recognition and binding to Dectin-1 homodimers induces Dectin-1 oligomerisation [163]. Dectin-1-mediated recognition of particulate ligand leads to the formation of a phagocytic synapse, while recognition of soluble Dectin-1 ligand does not induce a robust response [164].

Upon ligand binding Dectin-1 mediates intracellular signalling through its hemITAM, which is phosphorylated and recruits Syk. It is proposed this novel signalling pathway requires Syk to bind the cytoplasmic tails of two Dectin-1 monomers in close proximity [165]. The recruitment and phosphorylation of the SH2 region of Syk is necessary for Dectin-1 signalling [165, 166]. Downstream of Syk signalling MAPK, NFκB and NFAT transcriptional responses are reliant on the phosphorylation of Protein Kinase C and formation of the CARD9-Bcl10-MALT1 complex [156, 167]. As briefly mentioned in 1.3.3 a syk-independent role for Dectin-1 signalling has been described. This is thought to occur exclusively in human dendritic cells and use the signalling molecule Raf-1 to induce downstream signalling [157, 168, 169].

Ligand engagement through Dectin-1 has the capability to induce a range of diverse cellular responses coordinated by MAPK, NFκβ and NFAT gene transcription regulators. Dectin-1 can act as a phagocytic receptor and induce ligand uptake by endocytosis. The CLR also plays a key role in the generation of innate immune responses via the production of several chemokines and cytokines including TNF, IL-6, MIP-1, MIP-2 and KC. Dectin-1 can also induce cellular respiratory burst and activate and regulate COX2 and PLA_2. These described cellular responses can occur from Dectin-1 signalling alone; however, aspects of Dectin-1 signalling that lead to the larger formation of an innate response require collaborative signalling likely from TLRs and other CLRs [160]. Dectin-1 has also been demonstrated to induce DC maturation and direct T_H17-cellular responses independently of other TLRs and CLRs. This suggests

Dectin-1 signalling can independently direct and modulate adaptive immune responses [170].

The immune role of Dectin-1 has been well described *in vitro* and *in vivo*. *In vitro* analysis has identified the vast repertoire of fungal pathogens that Dectin-1 can recognise, mediate fungal uptake and killing of, and generate a robust chemokine and cytokine response against. The cell walls of many fungi contain large quantities of carbohydrate sugars, particularly β1-3 glucans allowing for Dectin-1 recognition [160].

The role of the receptor *in vivo* has been investigated for some time; however, the requirement of Dectin-1 during anti-fungal immune responses remains controversial. Experiments blocking Dectin-1 during an intra-tracheal A.*f*. infection generated significantly reduced levels of lung inflammation and significantly higher fungal burden than WT animals [2]. A similar enhanced susceptibility and increased fungal burden was identified in Dectin-1 KO mice. Upon A.*f*. infection, Dectin-1 KO animals had succumbed to infection within 5 days whereas 80% of WT mice survived past day 5. This was mainly thought to be due to a lack of A.*f*. recognition by macrophages, reduced neutrophil recruitment and subsequently impaired anti-A.*f*. immune response [100]. Dectin-1 KO mice possess enhanced susceptibility to *Candida albicans*; this was associated with inflammatory defects and a limited reduction in fungal killing [171]. Mice lacking the downstream signalling component CARD9 were also more susceptible to A.*f*. and *Candida albicans* infection [167]. These data suggest an important role for Dectin-1 in driving the innate cytokine and chemokine responses and controlling fungal killing and fungal burden.

Contradicting these studies, a different Dectin-1 KO strain displayed the same susceptibility as WT controls and no significant difference in chemokine or cytokine response upon challenge with *Candida albicans.* A small discrepancy in macrophage respiratory burst was observed in this Dectin-1 KO model although this had a minor impact on pathogen clearance and fungal burden [172]. This model suggests a lesser role for Dectin-1, or Dectin-1 redundancy *in vivo*. The reasons for the differences observed between these two Dectin-1 KO strains were, until recently, unknown. The

requirement for Dectin-1 during *Candida albicans* infection was found to be fungal strain dependent. Specifically, variation between *Candida albican's* cell wall chitin composition significantly influenced Dectin-1 recognition [173].

An interesting pathologic role has recently been described for Dectin-1 in an allergic-type A.*f*. disease model. In this chronic exposure setting Dectin-1 was demonstrated to induce the expression of multiple pro-allergy and pro-inflammatory mediators that exacerbated underlying airway disease potentially via the Dectin-1-dependent production of IL-22. Removing Dectin-1 and blocking IL-22 in the model reduced pathology associated with chronic A.*f*. exposure and restored lung function [174].

Dectin-1's impact during the anti-A.*f*. immune response is complicated. The CLR's signalling capabilities are likely dependent on the cell type the receptor is expressed on and morphological state of A.*f*. encountered. The ability of Dectin-1 to collaborate with TLRs during A.*f*. challenge has been described; a similar mechanism has not been identified for CLR collaboration. The important role of Dectin-1 during anti-fungal immune responses suggests any CLR-enhancing collaboration could be a very attractive therapeutic target.

1.3.6: Dectin-2

Dectin-2 is a member of the group II CLRs and is a type II transmembrane receptor possessing a highly conserved, single extracellular C-type lectin-like domain (CTLD) [175]. The receptor is expressed on tissue-resident macrophages, neutrophils and DCs [176]. Recent evidence suggests Dectin-2 is also expressed at a low level on peripheral blood monocytes although its expression on these cells can be greatly up regulated by fungal and other inflammatory stimuli [176, 177]. In the lung Dectin-2 mRNA expression is restricted to alveolar macrophages and is significantly up regulated during A.*f*. infection suggesting a role for this receptor in the anti-A.*f*. immune response [178]. Cell surface expression of Dectin-2 on alveolar macrophages has not been confirmed.

Dectin-2 possesses a short cytoplasmic tail that signals indirectly via FcRγ association. Receptor signalling is mediated through Syk and the CARD9-Bcl10-MALT1 complex leading to the induction and formation of an immune response [179]. Dectin-2 signalling results in the production of an extensive range of pro and anti-inflammatory cytokines and chemokines such as TNF, IL-1β, IL-10, IL-6 and IL-12 [156, 180]. Activation of Dectin-2 also induces respiratory burst and inflammasome activation [181]. Dectin-2 has been shown to utilise the MAPK pathway and drive a T_H17 regulatory response via the induction of IL-23 and IL-1β [182].

Dectin-2 predominantly recognises larger, hyphal morphologies of fungi. Binding occurs through its carbohydrate recognition domain containing a cation-dependent mannose-binding EPN motif, which binds high mannose structures. Limited evidence suggests the receptor may recognise conidial morphologies of fungi but with weak affinity [183]. Dectin-2 is proficient in recognising a range of pathogens including A.*f*., *Candida albicans*, *Mycobacterium tuberculosis,* and house dust mite allergens [179, 183, 184]. Dectin-2 has been directly implicated in anti-A.*f*. immunity. In this role the recognition of A.*f*. HY and formation of a cytokine and chemokine response was dependent on the presence of Dectin-2, and not Dectin-1 [185].

A clear role for Dectin-2 has been described in *Candida albicans* infection. During infection Dectin-2 was essential for host protective immune responses and the receptor was shown to drive inflammatory cytokine and chemokine responses and direct an adaptive T_H1 and T_H17 response against *Candida albicans*. Mice lacking Dectin-2 were significantly more susceptible to infection possessing increased fungal burden and decreased survival compared to WT mice [180, 186]. The impact Dectin-2 has on the immune response during the complex stages of A.*f*. infection has yet to be clearly described.

1.3.7: Mincle

Like Dectin-2, Mincle is a member of the group II CLRs and is a type II transmembrane receptor possessing a highly conserved, single extracellular CTLD [175]. The name Mincle stands for Macrophage-inducible C-type lectin and the receptor was identified by its strong induction after inflammatory stimuli on macrophages. Since the initial discovery of Mincle on macrophages, the receptor has been shown to be present on monocytes, neutrophils, DCs and some B-cell subsets [136]. Mincle, like Dectin-2, couples to FcRγ to induce intracellular signalling through Syk and the CARD9-Bcl10-MALT1 complex resulting in the production of many cytokines and chemokines such as TNF, IL-6, MIP2 and KC and inducing cellular respiratory burst [136]. These immune responses represent a solo role for Mincle pathogen-recognition through to cellular response and are generated independently of MyD88.

A role for Mincle synergistically collaborating with TLRs and generating an enhanced inflammatory cytokine and chemokine response has been described, most recently during *Fonsecaea perdrosoi* infection [187]. Infections caused by this pathogen are thought to result from an insufficient host pro-inflammatory response induced by the pathogen. Exogenously administering TLR ligands resolved disease by inducing a synergistic Mincle:TLR collaboration enhancing the pro-inflammatory cytokine response [187]. This data describes the improvement Mincle:TLR collaboration provides the pro-inflammatory host immune response.

Mincle recognises several different types of carbohydrates through its single CTLD. Mincle has a particularly strong binding affinity for α-mannose, a carbohydrate typically found on fungal cell walls [188]. Mycobacterial molecules such as trehalose dimycolate and cellular necrosis markers such as spliceosome-associated protein 130 have also been identified as Mincle ligands suggesting a role for the CLR in bacterial immunity and host-homeostasis [136, 189]. Although, the spliceosome-associated protein 130 binding site on Mincle was not located within the CRD [136]. The evidence that Mincle acts as a fungal PRR results from experiments utilising cell wall components of *Candida albicans*. Mincle was able to recognise cell wall components from this fungus and subsequently induce a robust inflammatory cytokine response and enhance *Candida albicans* phagocytosis [190]. This data describes a role for Mincle

in driving the anti-fungal protective immune response. Mincle's involvement in A.*f*. infections has not been thoroughly explored. Recently, the receptor's up regulation upon A.*f*. infection has been described in a rat A.*f*. keratitis model. Mincle up regulation was significantly associated with the changing expression of TNF, IL-1β, IL-10 and MIP-1α; although, this research only states "Mincle may play a role in the early innate immune response against A.*f*." [191].

Mincle's impact *in vivo* is controversial. A protective role for Mincle has been identified with experiments using *Mycobacterium tuberculosis* strains Erdman or BCG. Knocking out Mincle in these models resulted in modified inflammatory responses and increased bacterial loads in Mincle KO mice. Conversely, Mincle KO mice infected with *Mycobacterium tuberculosis* H37Rv produced a normal inflammatory response and disease burden was not increased [192, 193].

An intriguing role has been described for Mincle *in vitro*. A human *Helicobacter pylori* infection model identified a pathogen immune evasion aspect to Mincle engagement. This model involved *in vitro* cultured human macrophages being stimulated with *Helicobacter pylori*. The pathogen was found to drive an anti-inflammatory response by up regulating Mincle expression independently of host-cell contact. The proposed mechanism involves up-regulated Mincle interacting with the Lewis antigens of *Helicobacter pylori* resulting in an anti-inflammatory response; therefore, aiding the survival of *Helicobacter pylori* due to the evasion of an appropriate pro-inflammatory immune response. A robust pro-inflammatory response could be restored upon siRNA knockdown of Mincle in the stimulated macrophages [194].

Recently a similar Mincle-engagement evasion role for fungal pathogens has been identified. The fungal pathogen *Fonsecaea monophora* (responsible for the chronic skin infection chromoblastomycosis) when engaged by Dectin-1 activates the transcription factor IRF1 and results in the downstream production of pro-inflammatory cytokines such as IL-12 and orchestration of protective anti-fungal immune responses. However, *Fonsecaea monophora* can evade this Dectin-1 driven pro-inflammatory response by engaging Mincle. The engagement of Mincle induces

the E3 ubiquitin ligase Mdm2-dependent degradation pathway that culminates in the loss of IRF1 and lack of pro-inflammatory cytokine production. Therefore the engagement of Mincle by *Fonsecaea monophora* results in the evasion of an appropriate anti-fungal immune response and pathogen survival [157].

There is still much to understand about Mincle's action. The CLR's ability to synergistically collaborate with other PRRs such as TLRs, its ability to recognise bacterial and fungal pathogens driving proinflammatory and protective immune response as well as the CLRs role recognising self-necrotic tissue have begun to be unravelled. Mincle's more recently described implications in pathogen immune evasion via the receptors ability to control immune responses and modulate anti-inflammatory responses highlight an intriguing aspect to Mincle engagement.

1.3.8: Mcl

Mcl is the most recently described CLR within the group II family of CLRs. Mcl is a type II transmembrane receptor with a single extracellular CTLD. This CLR is expressed on macrophages, neutrophils, monocytes and some DC subsets. Mcl's ability to couple and signal through FcRγ is controversial. Research has suggested Mcl does not associate with FcRγ but can initiate intracellular signalling through the Syk and CARD9-Bcl10-MALT1 complex pathway. This signalling leads to the induction of phagocytosis, respiratory burst and production of pro-inflammatory cytokines [158, 195]. Interestingly, Mcl requiring Mincle coupling before FcRγ could be recruited has also been described [196]. Conversely, challenging Mcl-deficient mice with trehalose dimycolate has elicited a direct role for Mcl coupling with FcRγ. Trehalose dimycolate (TDM), is a glycolipid molecule found in the cell wall of bacteria such as *Mycobacterium tuberculosis*. TDM-induced acquired immune responses such as experimental autoimmune encephalomyelitis were almost completely dependent on Mcl, not Mincle. This research also found Mcl was crucial for driving Mincle induction upon TDM challenge [158]. Mcl's ability to directly couple to FcRγ is unclear; the receptor

may directly couple to FcRγ or require heterodimerisation with other CLRs such as Mincle to induce signalling through FcRγ.

Mcl possesses no known signalling motifs in its cytoplasmic region and no charged amino acid residues in its transmembrane domain drawing much investigation into how the CLR signals using Syk. The CTLD of Mcl does not contain an EPN motif or similar conserved amino acid region associated with carbohydrate recognition. Therefore, it is hypothesised Mcl cannot recognise unconjugated sugars but may bind glycolipids. Glycolipid recognition is thought to occur as the receptor possesses a shallow hydrophobic region located in its extracellular CTLD. The ability of Mcl to recognise glycolipids explains the receptors affinity to bind trehalose dimycolate [195, 197].

The ability of Mcl to signal using Syk may rely on the receptor collaborating with other CLRs. The intracellular retention of Mcl has been demonstrated to greatly increase Mincle surface expression suggesting the two CLRs may be linked. Analysing the expression of Mincle and Mcl on peritoneal macrophages after IL-4 or LPS stimulation identified a tight co-linear expression relationship for the two receptors. Immunoprecipitation experiments co-transfecting 293T cells with combinations of Mcl, Mincle and FcRγ revealed a complex of these three molecules was present. This data suggests that Mcl ligand recognition and Syk signalling is Mincle-dependent [198].
A similar collaborative role for Mcl and Dectin-2 has been explored. Mcl and Dectin-2 were co-expressed in RAW264.7 cells before these cells were challenged with *Candida albicans* HY. Cells expressing both receptors produced an enhanced response linked with their increased NFκB activation. No Mcl collaborations with other Dectin-2-CLR family members mimicked this synergistic response. A series of antibody blocking experiments elicited the function of Mcl and Dectin-2 to form hetero, or homodimers; although, the signalling and response implications of this were not explored beyond the increased NFκB expression [199].
A role for Mcl during fungal infection is still unknown; however, the CLR has been demonstrated upon recognition of trehalose dimycolate to drive anti-mycobacterial immunity [158]. *In vivo* experiments challenging Mcl KO mice with *Mycobacterium tuberculosis* resulted in exacerbated pulmonary inflammation, higher mycobacterial

burdens and increased mortality when compared to WT mice [200]. It is thought Mcl plays a similar role in human *Mycobacterium tuberculosis* infection. An Mcl polymorphism in humans is significantly associated with an increased susceptibility to pulmonary mycobacterium infections such as *Mycobacterium tuberculosis* [200]. Recently an *in vivo* anti-fungal role for Mcl has begun to be explored. Mcl KO mice, when infected with a low dose of *Candida albicans* displayed increased mortality compared to WT mice. Around 60% of Mcl KO mice succumbed to infection within 2 weeks whereas no mortality was present in WT mice, this was likely the result of a significantly reduced cytokine and chemokine response present in Mcl KO mice. Contrary to this, when a higher dose of *Candida albicans* was used to infect WT and Mcl KO mice, no difference in survival or cytokine and chemokine response was attained [199].

The anti-fungal capability of Mcl is complicated, as the receptor likely requires collaboration with other CLRs to signal and potentially even recognise ligands. The impact Mcl has on the *Candida albicans* response does suggest this CLR is important in anti-fungal immunity. Due to this receptor's likely ability to collaborate with other CLRs either by physically interacting with or up regulating their expression, this receptor may be an interesting therapeutic target to enhance CLR expression and/or synergistically improve anti-fungal responses.

1.3.3: CLRs and phagocytosis

CLRs coordinate immune responses with multiple anti-fungal immune response outcomes. The alveolar macrophage and neutrophil phagocytic uptake and destruction of fungal pathogens within the phagolysosome is one of the most important mechanisms of host anti-fungal defence. CLRs are exclusively required for fungal uptake and phagocytosis. TLRs play a role as their signalling can regulate phagosomal maturation; however, TLRs themselves are not directly required for phagocytic uptake [201]. A complex role for TLR involvement in the alveolar macrophage and neutrophil uptake of A.*f*. conidia has been described. Alveolar

macrophages require MyD88-independent involvement of TLR2 in A.*f*. phagocytosis. While neutrophils require MyD88-dependent involvement of TLR4 in A.*f*. phagocytosis. The mechanistic role of TLR2 and TLR4 during uptake of A.*f*. is not fully understood [202].

The recognition and phagocytosis of fungal pathogens is dependent on a range of host and fungal components. The variable mechanisms of host-fungal phagocytosis is directed by the host-cell type the CLR is expressed on, the composition of the fungal cell wall, the opsonisation of the fungi and the morphological form of the fungi. For example, the phagocytic mechanism Dectin-1 uses to engulf fungal pathogen varies depending on the host-cell type Dectin-1 is expressed on. Dectin-1, unlike most myeloid cell resident phagocytic CLRs, possesses a distinct hemITAM domain on its cytoplasmic tail. Upon ligand binding and CLR activation this motif promotes the syk-dependent phagocytic internalisation of the CLR:fungi complex leading to the formation of early endosomes [203]. Following this, an additional intracellular tri-acidic motif directs this early endosome to the lysosome. These motifs instruct pathogen phagocytosis and the required signalling cascade necessary for the pathogen to be trafficked to lysosomes and killed [204].

Dectin-1's cell-specific phagocytosis response has been demonstrated using zymosan. The murine dendritic cell-expressed Dectin-1 phagocytosis of zymosan requires the tyrosine-kinase Syk pathway and culminates in actin polymerisation, membrane extension and zymosan phagocytosis. Syk signalling generates the production of ROS within the endocytosed vesicle [165, 205]. The murine macrophage-expressed Dectin-1 phagocytosis of zymosan was demonstrated to also require actin polymerisation and membrane extension phagocytosis but occurred independently of Syk. Although, ROS production within the endocytosed vesicle was still Syk-dependent [206]. The mechanisms by which Dectin-1 and other non-soluble CLRs mediate phagocytosis is not clearly known and varies depending on a range of host and fungal factors [207].

After the CLR-directed phagocytosis of a fungal pathogen has taken place, the internalised vesicle containing the CLR:fungi complex matures through the endosomal

pathway and culminates in the formation of a phagolyosome. This compartment contains potent anti-microbial peptides that lead to fungal killing. CLRs, whilst trafficked through the phagosome maturation pathway, can be recycled and re-positioned back to the cell surface [205]. The role CLRs and TLRs convey over the kinetics of phagosomal maturation is complex and not well described. Some evidence suggests TLRs and CLRs influence phagosomal maturation perhaps linked with their ability to communicate with autophagy pathways [208]. The activation of the group V secretory phospholipase A_2 (a key enzyme involved in the regulation of inflammation and endosome pathway control) by CLRs may lead to phagosome maturation and fungal killing [209].

The mediation of phagocytosis and phagosome maturation by CLRs is key not only for pathogen clearance but also for the generation of antigenic fragments driving adaptive immunity. Antibody mediated targeting to CLRs such as DC-SIGN (which possesses a tri-acidic internalisation motif) has been shown to deliver antigen to lysosomal compartments of antigen-presenting cells and generates a peptide complex with MHC for T-cell presentation [210, 211]. CLRs ability to couple PAMP recognition with the downstream induction of innate immune responses, including A.*f*. phagocytosis is vital for the generation of appropriate anti-fungal immune responses.

1.3.4: CLRs and non-phagocytic fungal killing

CLRs also possess many non-phagocytic anti-fungal immune response capabilities. The receptors through their ability to induce pro-inflammatory gene expression play a critical role in orchestrating the anti-fungal immune response. Signalling cascades initiated by CLR-fungi interaction drive the release of a range of pro-inflammatory cytokines and chemokines such as TNF, IL-1β, IL-6, IL-12, MIP1α, MIP2 and KC. The release of these pro-inflammatory mediators leads to the mobilisation of the innate immune system against fungal pathogens. Consequently, the innate response via antigen-presenting cells generates and presents antigen, mobilising the adaptive immune response. Antigen presenting cells induce naïve $CD4^+$ T cells to differentiate

into T_H1, T_H2 or T_H17 effector cells. CLR-associated cytokines and chemokines co-ordinate and control the complex and multi-faceted anti-fungal response.

A successful host immune response against fungal pathogens requires CLR induced gene expression resulting in the release of cytokines and chemokines. Lacking TNF or IL-6 significantly enhances *in vivo* susceptibility to fungal infection by impairing macrophage and neutrophil function and fungal killing [212, 213]. The necessity of a TNF response against fungal pathogens has been highlighted in humans that possess a TNF mutation that increases the production of this cytokine far beyond normal quantities. These individuals are particularly resistant to A.*f*. infection [214]. CLRs can also induce many oxidative and non-oxidative fungal killing mechanisms in a variety of immune cell types. These responses are largely influenced by the cytokine and chemokine controlled state of cellular activation, which as previously mentioned is itself primarily controlled by CLRs.

The respiratory burst is a crucial anti-fungal killing mechanism triggered by CLRs. The NADPH oxidase complex containing NOX2 assembles at the cell membrane and upon activation transfers electrons from cytoplasmic NADPH to O_2 generating superoxide molecules. Superoxides through the Haber-Weiss reaction produce H_2O_2 and hydroxyl radicals that act as potent fungicidal oxidants [215]. Dectin-1 and Fcγ are capable of directly activating the respiratory burst via the syk-dependent signalling through their ITAM domain [206]. CLR activation has also been described to induce the release of many antimicrobial peptides. These molecules such as α-defensins are small cationic proteins that interfere with the fungal cell wall and lead to fungal killing; however, their exact mechanism of cell wall interference and disruption is unknown [216]. CLRs expressed on many innate immune cells and epithelial cells secrete antimicrobial peptides following activation and intracellular signalling. The extensive repertoire of CLR-associated anti-fungal responses regularly leads to the efficient clearance of fungal pathogens and, when required, can orchestrate and mediate complex anti-fungal immune responses.

1.3.5: PRR collaboration

Fungal pathogens are often morphologically complex organisms and their recognition by the immune system involves multiple PRRs that produce a coordinated response [217]. Receptor collaboration ensures redundancy and reduces the risk of immune evasion by the pathogen despite the pathogen's genetic diversity. Several TLRs have been demonstrated to recognise fungal pathogens and the requirement of CLRs when combating fungal pathogens is clear. Many examples of TLR and CLR anti-fungal receptor collaboration have been described. Due to the challenging nature of fungal pathogens, it is highly likely that multiple receptors recognising multiple PAMPs are required to initiate a successful immune response against the pathogen.

The first TLR CLR collaboration was described when macrophages and DCs were stimulated with β-glucan particulates. An enhanced TNF, IL-10 and IL-23 response was achieved when both TLR2 and Dectin-1 were engaged. This synergistic response relied upon the Dectin-1 collaboration with MyD88-coupled TLR2 [218]. The mechanisms of TLR CLR collaboration are not well understood; they're thought to involve the physical interaction of receptors upon ligand binding and subsequent modification of intracellular signalling cascades [219].

Recent work using the fungal pathogen *Fonsesaea pedrosoi* has provided further evidence highlighting the requirement of TLR CLR collaboration. *Fonsesaea pedrosoi* is recognised by CLRs such as Mincle whilst no recognition was identified with TLRs. Interestingly, CLR-exclusive *Fonsesaea pedrosoi* recognition produced what was found to be a deficient inflammatory response against the pathogen. The *in vivo* engagement of TLRs by the exogenous administration of TLR ligands produced TLR CLR collaboration, enhanced the inflammatory response and led to *Fonsesaea pedrosoi* clearance. The successful initiation of an appropriate inflammatory response able to resolve the infection was dependent on the activation of both the Syk/CARD9-Bcl10-MALT1 signalling pathway and the MyD88 signalling pathway [187].

The requirement for a collaborative response is not limited to *Fonsesaea pedrosoi*; treatment with heat-killed *E. coli* enhances the clearance of chronic *P. carinii* infections *in vivo* [220]. These limited results suggest collaborative PRR signalling is necessary for the generation of an appropriate immune response against the pathogen. Although TLR:CLR immune enhancing collaboration has begun to be investigated, CLR:CLR collaboration has not been extensively explored. Recently, a CLR:CLR collaboration was identified between Dectin-1 and Dectin-2 during *Trichophyton rubrum* infection. Although some IL-1β, TNF, IL-10 and IL-6 was produced when Dectin-1 KO and Dectin-2 KO BMDCs were stimulated with the fungal pathogen, knocking out both CLRs almost completely abrogated cytokine production. *In vivo* Dectin-1 Dectin-2 DKO mice possessed the highest fungal burden when compared to single KO and WT controls. This data suggests collaboration between Dectin-1 and Dectin-2 is required for the successful control of *Trichophyton rubrum* [221].

Pathogenic fungi possess multiple life cycles and complex infectious mechanisms. Hosts likely require extensive CLR collaboration throughout the fungi's life cycle stages and disease progression to generate appropriate immune responses. Understanding CLR receptor collaboration may allow the development of immune-modulating therapeutics that enhance the anti-A.*f*. immune response. Similar to the exogenous administration of TLR ligands improving Mincle-TLR collaboration and response against *Fonsesaea pedrosoi*, the therapeutic engagement of CLRs may enhance collaboration synergistically improving the anti-fungal response.

1.4: Hypothesis

The hypothesis tested in this thesis is that CLRs are important during *Aspergillus fumigatus* infection. CLRs mediate A.*f*. recognition and orchestrate complex immune responses. CLR collaboration is required to successfully clear A.*f*. disease.

1.5: Aims

I. Identify the role of Dectin-1 in immune-compromised cystic fibrosis patients at risk of A.*f*. disease

II. Use *in vivo* CLR KO and CLR DKO models to determine the role of CLRs during immune-competent A.*f*. disease

III. Identify CLR-associated risk factors that stratify immune-suppressed patients according to A.*f*. disease susceptibility

Chapter 2

Methods

2.1: Notes

2.1.1: Reagents

All reagents including cell specific media, experiment specific buffers, PCR primers, qPCR probes, antibodies and ELISA KITS are detailed in chapter 7 appendix. All sequences of CLR genes are detailed in chapter 7 appendix.

2.1.2: Animals used in this research

All *in vivo* animal work was conducted in accordance with UK Home Office and Cardiff University guidelines and regulations. Experiments were completed under Cardiff University's Home Office establishment license, Professor Phil Taylor's Home Office project license (P05D6A456, formerly 30/2938) and my Home Office personal license (Mice A & B). Mice were housed and maintained in Cardiff University's Joint Biological Services Unit.

2.1.3: Patient samples used in this research

The clinical research project was undertaken with sponsorship from Cardiff University and ethical approval from Health and Care Research Wales (NISCHRC CRC 1351-14). REC reference 14/WA/1119 and IRAS project ID 151136. I completed the NISCHRC CRC 'Good Clinical Practice' course before undertaking this clinical research study. Samples were collected from medical staff on the hematology ward (B4) at the University of Wales teaching hospital, Heath Park. Samples were link-anonymised by Dr Lewis White, the microbiology lead for hematology.

2.1.4: DNA sequencing

Sequencing reactions were completed using a Lightrun Sanger sequencing service from GATC Biotech. The sequencing of purified PCR product required 5µl of 20-100ng/µl DNA to be premixed with 5µl 0.5µM gene-specific primer. The sequencing of purified Plasmid DNA required 5µl of 80-100ng/µl DNA to be premixed with 5µl 0.5µM gene-specific primer.

2.2: Cell culture

2.2.1: Cell counting

Cells were counted using a bright line haemocytometer (Neubaur) with a depth of 0.1mm and small square area of 0.0025mm^2. The total cells in the four large squares (made up of 16 smaller squares) were counted and the number divided by 4 to gain the average cell count per 0.001mm^3. This cell number was multiplied by 10^4 to provide the cell count per 1cm^3, or per 1ml of cell solution.

2.2.2: Bone marrow derived macrophages (BMDMs)

Mice were sacrificed by exposure to CO_2 and cervical dislocation. Mice femurs were harvested, cleaned and cut either side of the knee joint. Bone marrow was flushed from the femur with 10ml PBS (Life Technologies) in a syringe and collected. Bone marrow in PBS was centrifuged at 350g for 5 minutes, PBS was aspirated and 5ml fresh PBS added. This wash cycle was repeated three times. Cells were counted and re-suspended at 2x10^5/ml in BMDM media. Occasionally bone marrow was obtained from stocks stored in liquid nitrogen. Bone marrow was retrieved from liquid nitrogen storage and rapidly warmed to 37^{o}C before the immediate addition of 10ml BMDM media. Cells were centrifuged at 350g for 5 minutes and the BMDM media aspirated. Cells were counted and re-suspended at 2x10^5/ml in BMDM media.

On day 0, 7x10^6 bone marrow cells in 35ml BMDM media were added to each 145mm^2 culture dish. M-CSF (Peprotech) was added to each culture dish at a final concentration of 10ng/ml. The plates were then incubated at 37^{o}C 5% CO_2. On day 3, 15ml BMDM media was added to each BMDM culture dish and the concentration of M-CSF brought up to 10ng/ml. On day 6 or 7 BMDMs were fully developed from bone marrow cells. BMDMs were harvested with the removal of BMDM media and addition of 4mg/ml

lidocaine (Sigma) in 5ml PBS or 5ml trypsin (Life Technologies) incubated for 5 minutes at 37°C 5% CO_2. After incubation the addition of 7ml BMDM media neutralised lidocaine or trypsin. BMDMs were collected and centrifuged at 350g for 5 minutes. BMDM media and lidocaine or trypsin was aspirated before BMDMs were counted with a haemocytometer, plated out as each experiment required and rested overnight at 37°C 5% CO_2 before use.

2.2.3: Alveolar macrophages

Mice were anaesthetised with 140mg/kg intra-peritoneal Euthatal (Vet Tech) and sacrificed by exsanguination. Alveolar macrophages were extracted by bronchiolar alveolar lavage. A 0.8mm^3 tube was inserted into the trachea, taking care not to go past the carina and only access one lung. A total of 10ml PBS supplemented with 0.01mM EDTA (Fisher Scientific) was flushed through the lungs in 0.5ml increments. Each increment of PBS supplemented with 0.01mM EDTA was left to dwell in the lungs for 10 seconds before being removed and collected. Two 10ml syringes and a stopcock were used to inject and retrieve PBS supplemented with 0.01mM EDTA so each 0.5ml increment only passed through the lungs once. The recovered alveolar macrophage containing lavage fluid was immediately stored at 4°C. Lavage fluid was pooled per genotype and centrifuged at 350g for 5 minutes at 4°C. PBS supplemented with 0.1mM EDTA was aspirated before cells were re-suspended in 1ml Alveolar macrophage media and counted by haemocytometer. Cells were plated at 1x10^6/ml in a 96 well plate and rested for 2-4 hours at 37°C 5% CO_2 before use in experiments.

2.2.4: BIOgel elicited cells

Mice were intra-peritoneally injected with 0.5ml 2% BIOgel (Bio-Rad). 14-16 hours later mice were sacrificed by exposure to CO_2 and cervical dislocation before peritoneal lavage was performed. 5ml ice cold PBS supplemented with 0.01mM EDTA was injected into the peritoneal cavity and manually washed around for 60 seconds

before being extracted. Recovered lavage fluid was immediately stored at 4^{o}C. When ready for processing recovered lavage fluid was run through a 100µM filter and the pass-through was centrifuged at 350g for 5 minutes at 4^{o}C. PBS supplemented with 0.01mM EDTA was aspirated and recovered cells suspended in Neutrophil/Monocyte media, NE assay buffer or PBS and counted by haemocytometer. Cells were plated out at 1x10^{6}/ml in a 96 well plate and immediately used for experiments.

2.2.5: NIH-3T3 cells

Cells were typically cultured from NIH-3T3 parental stocks stored in liquid nitrogen. Parental NIH-3T3 cells were removed from liquid nitrogen and rapidly warmed to 37^{o}C before the immediate addition of 10ml 3T3 media. Cells were centrifuged at 350g for 5 minutes, 3T3 media aspirated and 10ml fresh 3T3 media added. NIH-3T3 cells were added to a T25 tissue culture flask to be grown and passaged.

NIH-3T3 cells were maintained in 3T3 media and incubated at 37^{o}C 5% CO_2, Geneticin (G418) was added at a concentration of 0.6mg/ml if selection was required. Cells were passaged when necessary by incubation with 5ml trypsin for 5 minutes at 37^{o}C 5% CO_2. After trypsin incubation the addition of 7ml 3T3 media neutralised trypsin. NIH-3T3 cells were collected and centrifuged at 350g for 5 minutes. 3T3 media and tryspin was aspirated before cells were re-suspended in 1ml 3T3 media. From this 1ml, 100µl was removed and used to start a new culture flask. NIH-3T3 cells were progressed through T25 flasks before larger T75 or T175 flasks were used for cell culture.

For experimental use, cells were harvested via incubation with 5 ml PBS supplemented with 10mM EDTA and 4mg/ml lidocaine at 37^{o}C 5% CO_2. After lidocaine incubation the addition of 7ml 3T3 media neutralised lidocaine. NIH-3T3 cells were collected and centrifuged at 350g for 5 minutes. 3T3 media and lidocaine was aspirated before cells were counted with a haemocytometer and used in experiments.

2.2.6: Culture and preparation of A.*f*. conidia

A.*f*. isolate 13073 (stored in endofree dH_2O at -80°C) was cultured on potato dextrose agar for 7 days at 37°C. Conidia were harvested by vigorous washing with 40ml PBS supplemented with 0.1% Tween 20 and passed through a 40µm filter to remove hyphal fragments. The pass-through suspension was centrifuged at 350g for 5 minutes and the A.*f*. pellet re-suspended in 25ml PBS. Conidia were counted by haemocytometer. A final culture concentration of ~$1x10^8$ conidia/ml was typically attained and stored at 4°C. Cultures maintained efficacy for 6-8 weeks and were discarded after this time. To confirm normal, expected A.*f*. culture growth $1x10^5$ resting conidia were incubated with RPMI 1640 (GE Healthcare) supplemented with 0.2mg/ml Polymixin B (Sigma) at 37°C 5% CO_2. Successful development of hyphal fragments at 24 hours indicated a healthy culture; this was confirmed using a light microscope.

A.*f*. has four morphologies; incubating resting conidia in RPMI 1640 supplemented with 0.2mg/ml Polymixin B for specific periods of time attained the different morphologies. Typically, $3x10^6$ A.*f*. resting conidia were incubated in 1ml RPMI 1640 supplemented with 0.2mg/ml Polymixin B at 37°C 5% CO_2. Swollen conidia developed at 6 hours, early germlings developed at 10 hours and hyphae developed at 24 hours. Germination of resting conidia into latter A.*f*. morphologies was confirmed using a light microscope.

2.2.7: Preparation of heat-killed A.*f*.

A.*f*. swollen conidia were used to produce heat-killed A.*f*. required for experiments. A.*f*. resting conidia were grown into swollen conidia, 10mls of $3x10^6$ A.*f*. resting conidia/ml of RPMI 1640 supplemented with 0.2mg/ml Polymixin B were grown in a tissue flask for 6 hours at 37°C 5% CO_2. A.*f*. swollen conidia in solution were transferred to a 50ml falcon, which was then submerged in boiling water for 20 minutes. Heat-killing was confirmed by incubating 100µl of boiled A.*f*. swollen conidia solution on a

potato dextrose agar plate for 37°C for 48 hours. No visible A.*f*. growth (small white colonies) confirmed successful heat killing.

2.2.8: Freezing and reviving cells

Cells to be frozen were centrifuged at 350g for 5 minutes and any media aspirated. Cells were re-suspended in FCS supplemented with 10% DMSO before being aliquoted into 1ml cryogenic vials. A 'Mr Frosty" (Thermo Scientific) was used to prepare cell aliquots for liquid nitrogen storage, this isopropanol filled contained buffered interior container temperature reduction to 1°C per minute. Cells in cryogenic vials were stored in a 'Mr Frosty' for a minimum of two hours at -80°C. Cryogenic vials were then transferred to liquid nitrogen for long-term storage.

Once removed from liquid nitrogen, cells in cryogenic vials were rapidly thawed in a 37°C water bath. When fully thawed the 1ml cell aliquot was added to 10ml of cell-specific complete media and centrifuged at 350g for 5 minutes. All media was aspirated and cells re-suspended in their specific complete media. Cells were then counted before being plated out or added to tissue culture flasks and incubated at 37°C 5% CO_2. Cells were typically rested overnight before being ready for use in experiments.

2.3: Generation of cell lines

2.3.1: Infusion primer design

Primers were designed and ordered (Sigma) with a target gene specific sequence and 15 base pair vector-overhang specific sequence included. These primers were used to amplify target genes for expression vectors by PCR. Designed primers were used with the In-fusion cloning kit (Clontech) to generate new vectors.

2.3.2: Restriction endonuclease vector digestion

Plasmid vectors were cut using restriction endonuclease enzymes in the presence of their appropriate accompanying buffer (New England Biolabs). Digestion reactions were incubated at 37^{o}C for 1 hour before restriction endonuclease enzymes were inactivated at 65^{o}C for 15 minutes. Digested vector product was separated from any undigested vector by gel electrophoresis. Digested vector was cut out of the gel and purified using a gel-excision purification kit (Qiagen).

2.3.3: Infusion reaction

The infusion reaction involved mixing gel-purified, restriction endonuclease digested vector (100ng) with gel-purified target gene insert (50ng) and 2µl 5X In-Fusion HD enzyme premix. The reaction was incubated at 50^{o}C for 15 minutes before being immediately used for cell transformation or stored at -20^{o}C.

2.3.4: Transformation

Stellar competent cells (Clontech) were used for all transformation reactions. A Stellar competent cell 50µl aliquot was thawed on ice for 15 minutes and gently mixed. 2.5µl of completed reaction mixture from the previous Infusion reaction was added to a 50µl aliquot of Stellar competent cells and the mixture incubated at 4°C. After 30 minutes cells were heat-shocked at 42°C for 45 seconds before being placed on ice for 2 minutes to cool. 447.5µl SOC media (Sigma) was pre-warmed to 37°C and added to the cells. The mixture was incubated at 37°C 200 rpm for one hour. After an hour incubation, 1µl cell solution, 50µl cell solution and 100µl cell solution were spread on LB agar plates containing 100µg/ml ampicillin (Sigma) or carbenocillin (Fisher Scientific) and incubated at 37°C overnight. These antibiotics were appropriate for both PFB-Neo and Pmx-IP plasmid vectors used.

2.3.5: Plasmid DNA extraction

Once the LB plate overnight incubation was complete individual isolated bacteria colonies were picked and grown in 5ml LB broth containing 50µg/ml ampicillin or carbenocillin at 37°C 250rpm overnight. After incubation, 0.5ml of this culture was removed and added to 0.5ml sterile glycerol in a cryogenic vial. Each vial was cryogenically frozen as previously described in 2.2.8. Plasmid vector DNA was extracted from the remaining 4.5ml culture using a plasmid mini-prep kit (Invitrogen). Extracted plasmid DNA was quantified using a nanodrop (Thermo Scientific) and sent for sequencing with target gene insert primers. The correct insertion, orientation and nucleotide sequence of target gene in plasmid was confirmed.

Bacterial colonies containing plasmid with the correct target gene insert were grown up from glycerol stocks in 100ml LB broth containing 50µg/ml ampicillin or carbenocillin at 37°C 250rpm overnight. After incubation, plasmid DNA was extracted from the bacterial culture using a plasmid midi-prep kit (Invitrogen). Extracted plasmid DNA was quantified using a nanodrop before being used to transfect cells.

2.3.6: Retroviral infection

Ecopack 2.293 cells (Clontech) were used to generate viral particles containing extracted plasmid DNA. 2.5 x 10^5 Ecopack cells in 2ml Ecopack media were added to each well on a 6 well plate and incubated for 6 hours at 37^{o}C 5% CO_2. After incubation, Ecopack cells were transfected. The following reaction was completed for each plasmid construct added to each well of Ecopack cells. 200µl RPMI 1640 was mixed with 9µl Fugene (Promega) for 5 minutes at RT before 1.5µg extracted plasmid DNA was added. The mixture was incubated for 30 minutes at RT and then added to each well containing Ecopack cells. Transfected Ecopack cells were incubated at 37^{o}C 5% CO_2 for 24 hours before Ecopack media was replaced.

48 Hours after transfection the supernatant from each Ecopack well was collected and filtered through a 0.45µm filter. 5µg/ml polybrene (Sigma) was added to the collected Ecopack supernatant. This filtrate was used to infect parental NIH-3T3 cells that had been cultured as described in 2.2.5. 1x10^5 Parental NIH-3T3 cells in 3ml 3T3 media were added to each well on a 6 well plate and incubated at 37^{o}C 5% CO_2 for 48 hours. After incubation, media was removed from NIH-3T3 cells and replaced with the supernatant from Ecopack cells. The 6-well plate containing NIH-3T3 cells and Ecopack supernatant was centrifuged at 1025g for 90 minutes at RT. Once this was complete cells were incubated overnight at 37^{o}C 5% CO_2.

2.3.7: Transfected cell selection

Infected NIH-3T3 cells media was aspirated and cells removed from the 6 well plate via the addition of 1 ml PBS supplemented with 10mM EDTA and 4mg/ml lidocaine for 5 minutes at 37^{o}C 5% CO_2. After lidocaine incubation the addition of 2ml 3T3 media neutralised lidocaine. NIH-3T3 cells were collected and centrifuged at 350g for 5 minutes. 3T3 media and lidocaine was aspirated before 10ml 3T3 media was added

and cells placed in a T25 tissue culture flask at 37^{o}C 5% CO_2. G418 (Life Technologies) was used to select NIH-3T3 successfully infected with plasmid. 600µg/ml of G418 was added to each T25 tissue culture flask. Cells were maintained as described in 2.2.5. Once cells had been passaged a minimum of 5 times, expression of transfected plasmid was confirmed by flow cytometry before cells expressing target genes were used in experiments.

2.4: *In vitro* assays

2.4.1: Flow cytometry

Flow cytometry was performed on a minimum of $2x10^4$ and maximum of $5x10^5$ cells per individual sample. Cells to be analysed by flow cytometry were added to wells on a 96 well plate and centrifuged at 350g for 5 minutes at 4°C. Cells were washed twice with 150µl FACS buffer. All aspirations were completed carefully to avoid dislodging cells from each well. Cell non-specific binding was blocked with the addition of 4mg/ml rat 2.4G2 (Life Technologies) in FACS Buffer supplemented with 5% rabbit serum (Sigma) for 15 minutes at 4°C.

If purified antibodies were used, these were added on top of block and each well made up to 50µl with FACS buffer. Cells were incubated at 4°C for 30 minutes before being thoroughly washed three times with 150µl FACS buffer. Anti-Biotin secondary antibodies were added to required wells in 50µl FACS buffer for 20 minutes at 4°C. Cells were again thoroughly washed three times with FACS buffer. After this, all other conjugated-antibodies were added to the required wells and cells incubated for 30 minutes at 4°C. Cells were washed for a final three times with FACS buffer before samples were immediately analysed by flow cytometry or fixed with ¼ cytofix (BD) and analysed by flow cytometry within 5 days.

If purified antibodies were not required, conjugated-antibodies were added on top of block and each well made up to 50µl with FACS buffer. After 30 minutes incubation at 4°C cells were washed three times with FACS buffer before cells were immediately analysed by flow cytometry or fixed with ¼ cytofix and analysed by flow cytometry within 5 days.

Flow cytometry samples were run through a benchtop flow cytometer (Beckman Coulter) using SUMMIT (Cryomation) software. Flow cytometry sample data was analysed with FlowJo (BD, formerly FlowJo LLC) software.

2.4.2: ELISA

Two ELISA kits were used to quantify protein concentrations. ELISA DuoSet (R&D) and ELISA KIT (Thermo Scientific, formerly ebioscience) have slightly different experimental methods. Each method will be described in this section and each kit will be referred to as R&D ELISA or ebioscience ELISA respectively.

Half-well 96-well plates were coated with 50µl capture antibody. For R&D ELISA this involved diluting capture antibody in PBS supplemented with 1% BSA. For ebioscience ELISA 250X capture antibody was diluted in PBS supplemented with 10% capture coating solution. Capture-coated ELISA plates were incubated overnight at 4^{o}C. After incubation plates were washed three times. Each wash step was completed using a Bio-Plex Washstation (BIO-RAD), plates were washed with PBS supplemented with 0.05% Tween 20 (Sigma). ELISA plates were then blocked with reagent diluent for 1 hour at RT. R&D reagent diluent was typically PBS supplemented with 1% BSA, specifically for human IFNγ reagent diluent was PBS supplemented with 1% BSA and 10% goat serum. Reagent diluent concentrate was provided with ebioscience ELISA kits and was diluted with dH_2O.

Blocked plates were washed three times and carefully dried by gentle tapping on absorbent paper. Standards were prepared for each ELISA plate. R&D standards were provided lyophilised and were re-suspended following individual kit specifications with R&D reagent diluent before being stored at -80^{o}C. For each ELISA experiment the kit recommended top-standard was produced in reagent diluent before six serial dilutions were performed producing the seven required standards. Standards from ebioscience ELISA kits were either already made-up or lyophilised. If required, standards were made up in reagent diluent. For each ELISA experiment the kit

recommended top-standard was produced in reagent diluent before six serial dilutions were performed producing the seven required standards. 50µl of each standard sample was then added to the required wells on the blocked 96-well plate; following this, experimental samples were added. If necessary, samples were diluted in each kit's appropriate reagent diluent; 50µl sample was required per well. A reagent diluent only control was added to each plate to act as blank. This allowed the removal of optical imperfections when reading absorbance through the plate. Plates containing standard and sample were incubated overnight at 4^{o}C.

After overnight incubation, standards and samples were removed from the plate and the plate washed three times as previously described. If samples were infectious the aspiration of the plate and first wash were manually completed in appropriate safety category conditions. A Plate washer was used to wash plates a further three times. Gentle tapping onto absorbent paper carefully dried plates before detection antibody was added. R&D ELISA detection antibody was diluted according to kit instructions in reagent diluent, 50µl was added to each well. Detection antibody from ebioscience was provided at 250X and diluted in reagent diluent before 50µl was added to each well. Plates with detection antibody added were incubated at RT for a minimum of 2 hours or overnight at 4^{o}C.

Once detection antibody incubation was complete, plates were washed three times. Plates were gently dried and HRP-streptavidin antibody added. This was provided 250X for ebioscience and diluted in reagent diluent. Either 40X or 200X HRP-streptavidin was provided with R&D ELISA and diluted in reagent diluent. 50µl HRP-streptavidin was added to each well and the plate was incubated at RT away from direct light. For R&D ELISA 1 hour incubation was required, for ebioscience ELISA 30 minute incubation was required. After HRP-streptavidin incubation, plates were washed five times before being dried. TMB substrate was then added to each well. TMB substrate reagent kit (BD) was used with R&D ELISA kits; ebioscience ELISA provided their own TMB substrate. 50µl TMB substrate was added to each well, the reaction was stopped with H_2SO_4 when standards colour change was appropriate to generate a standard curve.

ELISA plates light absorbance was read at λ 450nm – 570nm using a Multiscan Spectrum (Thermo Scientific). Standard curve absorbance values, minus blank value were used to generate a standard curve. The standard curve allowed the determination of experimental sample protein concentrations.

2.4.3: NE treatment

NE, purified from human neutrophils (Athens research technology) was used in NE-induced cleavage assays. For typical cleavage assays $1x10^6$ cells/ml were re-suspended in NE Assay buffer. Macrophages or NIH-3T3 cells were rested by incubation at 37°C 5% CO_2 overnight prior to re-suspension in NE assay buffer. BIOgel elicited neutrophils or monocytes were used immediately. 50µl cells in assay buffer ($5x10^4$ cells) were added to a 96-well plate. 50µl NE diluted to the required concentration in NE assay buffer was added on top of the cells in each well.

NE was inactivated using two methods; firstly, heat inactivation was completed by incubation at 95°C for 10 minutes. Secondly, inhibition inactivation was completed by incubation at 37°C with AAT (or other small molecule inhibitor) for 10 minutes before addition to cells. These were also added on top of cells.

2.4.4: NE-induced receptor cleavage

The impact NE had on cell's receptor expression was often examined. After incubation with NE, cells were centrifuged at 350g for 5 minutes and washed with NE assay buffer. Cells were analysed by flow cytometry.

2.4.5: NE-induced functional response deficiency

The impact NE has on cell's ability to produce TNF was examined. After incubation with NE, cells were stimulated with zymosan (Sigma), Pam(3)CSK(4) (Invivogen) or A.*f*. SC on top of NE treatment for up to 4 hours at 37^{o}C 5% CO_2. After incubation cells were centrifuged at 350g for 5 minutes and supernatant aspirated and stored. ELISA was used to determine TNF concentration in cell supernatant.

2.4.6: NE-induced recognition deficiency

Typically, FITC-labeled zymosan was used in recognition assays. Fluorophore-labelled A.*f*. was also generated and used in recognition assays. A.*f*. RC were grown into SC as described in 2.2.6 before being stained with a fluorophore.

Cell's ability to recognise ligands after NE treatment was examined. After incubation with NE, cells were stimulated with flurophore-labeled ligand such as FITC-labeled zymosan on top of cells and NE treatment for up to 4 hours at 37^{o}C 5% CO_2. After incubation cells were centrifuged at 350g for 5 minutes and washed three times with NE assay buffer. Cells ability to recognise ligands was analysed by flow cytometry.

2.5: *In vivo* assays

2.5.1: Animals used

BALB/C male and female mice were bought from Charles River Services. C57BL/6 male and female mice were either bred from in-house colonies or bought from Charles River Services. C57BL/6 Dectin-1$^{-/-}$, C57BL/6 Mincle$^{-/-}$, C57BL/6 Dectin-1$^{-/-}$ Mincle$^{-/-}$ and C57BL/6 Dectin-2$^{-/-}$ Mincle$^{-/-}$ were bred from in-house colonies. All *in vivo* experiments were age and sex matched, unless otherwise stated.

2.5.2: *In vivo* A.*f*. infection

A.*f*. challenge experiments were completed in mice aged 8-12 weeks. Male and female mice underwent the same infection process; each experiment describes whether males or females were used.

Prior to A.*f*. infection, mice were weighed and caged. Males were not co-housed, only littermate males were caged together. Females were co-housed placing one mouse of each genotype per cage. Males used in microbiome-controlled experiments were housed only with littermates; bedding was swapped around experiment cages every 48 hours for a minimum of 14 days before A.*f*. infection experiments.

In vivo A.*f*. challenge was completed using A.*f*. RC prepared in PBS at concentrations clearly stated in each experiment. The A.*f*. solution was thoroughly mixed before being used to inoculate each mouse as the solution settled rapidly. The following inoculation protocol was completed per mouse.

Individually, mice were lightly anesthetised with 5% Isoflurane (Vet Tech) and oxygen from a tube controlled by an anaesthetic rig. A mouse was positioned to inhale

isoflurane for 15 seconds whilst the A.*f*. solution was mixed and 50µl drawn into a pipette. Quickly, the mouse was removed from the anaesthetic-delivering tube and the mouse's front teeth exposed by gently pulling back on the jaw. The exposed front teeth were used to hang the mouse onto a thin wire held in place on a stand. The mouse was secured to the stand with tape placed over its tail. Tweezers were used to gently pull the tongue out of the mouth whilst a pipette containing 50µl A.*f*. solution was inserted and ejected into the trachea of the mouse. Care was taken not to go too far down the trachea past the carina, ensuring both lungs were inoculated with A.*f*. solution.

Immediately after A.*f*. inoculation, whilst the mouse's tongue was held out of the mouth, the nose was plugged with a finger for 15 seconds (1 second per 5µl ejected + 5 seconds). When inoculation was successful the mouse was heard gulping the A.*f*. solution into their lungs and not swallowing the solution. Mice came round rapidly from the anaesthetic effects and so after A.*f*. inoculation was complete mice were placed gently in a recovery cage (layered towel without wood-chip). Once the animal had fully regained consciousness and recovered it was placed back in its holding cage. Mice were weighed once and examined and scored twice daily according to Home Office guidelines, the scoring sheet used can be found in 7.6.

2.5.3: Lung extraction

Mice were anaesthetised with 140mg/kg intra-peritoneal Euthatal and sacrificed by exsanguination. This method preserved the integrity of lung tissue and reduced bleeding within the cardio-respiratory cavity. Left and right lung were extracted. For fungal burden analysis, left-lung was stored in 1ml PBS at 4^{o}C or 1ml RNAlater (Thermo Scientific) at 4^{o}C, this is made clear for each experiment. For cytokine and chemokine analysis, right-lung was stored in 1ml PBS at 4^{o}C. Both lungs were processed immediately.

2.5.4: Lung homogenisation for fungal burden analysis

Fungal burden was determined from left lungs using two different protocols. The protocol used for each experiment is clearly stated in results.

2.5.4i: Method A

Left-lung stored in 1 ml PBS was manually homogenised for 30 seconds using a tissue homogeniser. RNA was extracted from 0.1ml of homogenised lung using the MasterPure yeast RNA extraction kit (Illumina).

2.5.4ii: Method B

Left-lung stored in 1ml RNAlater was manually cut using scissors into 1mm^3 sections before being placed into a bead-beater eppendorf (BioSpec). This eppendorf was topped up with 1ml PBS and 0.5mm^3 glass beads (BioSpec). The lung tissue was homogenised at 4200rpm (middle speed setting for this machine) for four 30-second periods using a Mini-beadbeater 1 (BioSpec). To avoid heat damage to samples, between each homogenisation round eppendorfs were stored at 4^oC for 5 minutes. After bead beating was complete, RNA was extracted from 0.1ml homogenate using the MasterPure yeast RNA extraction kit.

2.5.5: Lung fungal RNA extraction

Fungal RNA was extracted from 100µl of left lung homogenate using the MasterPure yeast RNA extraction kit.

The following was completed per lung sample. 100µl of lung homogenate was centrifuged at 17000g for 60 seconds and supernatant aspirated. Contaminating protein, DNA nucleases and RNA nucleases were digested by incubation with 50µg Proteinase K diluted in 300µl extraction reagent at 70^oC for 15 minutes. After

digestion, samples were cooled to 4°C before 175µl MPC protein precipitation reagent was added to each sample. Samples were centrifuged at 4°C, 17000g for 10 minutes to remove precipitated debris and contaminants. Supernatant was transferred to a new eppendorf and 500µl isopropanol added to precipitate RNA out of the sample solution. Each sample was thoroughly inverted 40 times to allow complete RNA precipitation. Samples were centrifuged at 4°C, 17000g for 10 minutes to pellet precipitated RNA, supernatant and isopropanol were carefully aspirated without disrupting the RNA pellet.

Contaminating DNA was removed with DNAse I treatment at 37°C for 30 minutes. After DNAse I treatment, 200µl tissue and cell lysis solution was added and the solution incubated at 4°C for 10 minutes to remove any final cell or protein traces. Finally, 200µl MPC protein precipitation reagent was added at 4°C for a further 10 minutes. Any remaining precipitated contaminants or debris were removed from solution by centrifugation at 4°C, 17000g for 10 minutes. Supernatant was transferred to a new eppendorf and 500µl Isopropanol added. The sample was thoroughly inverted 40 times before precipitated RNA was pelleted by centrifugation at 4°C, 17000g for 10 minutes. Isopropanol was carefully aspirated from the RNA pellet before two washes with 70% EtOH were completed. All EtOH was apirated from the RNA pellet and the eppendorf left open to dry. The RNA pellet was re-suspended in 35µl TE buffer and stored at -80°C.

2.5.6: Fungal RNA standard curve

A standard curve of fungal RNA was generated; fungal RNA was extracted from concentrations of A.*f*. conidia. This was required to determine experimental sample fungal burden. A.*f*. RC concentrations of 10^9, 10^8, 10^7, 10^6, 10^5, 10^4, 10^3 and 10^2 were produced in 1ml PBS. Fungal RNA was extracted from each 1ml A.*f*. RC sample using the same lung homogenisation method (manual homogenisation or bead-beating) that was used for each *in vivo* experiment.

For experiments where lung samples were tissue homogenised, the A.*f*. standard curve was produced by tissue homogenising each 1ml A.*f*. concentration in PBS and extracting RNA from 100µl homogenate using the MasterPure yeast RNA extraction kit. For experiments where lung samples were subject to bead beating, the A.*f*. standard curve was produced following the same bead beating protocols as described above. After bead beating fungal RNA was extracted from 100µl homogenate using the MasterPure yeast RNA extraction kit.

Appropriately produced standard curves were run alongside every experiment. Each standard curve was stored at -80^{o}C and used for a maximum of 8-weeks before efficacy was lost.

2.5.7: Generation of fungal cDNA

A.*f*. fungal burden was determined by the qPCR quantification of the 18S rRNA subunit of A.*f*. Therefore, cDNA was generated from lung extracted fungal RNA samples and standard curve fungal RNA samples. From each lung extracted fungal RNA sample or standard curve fungal RNA sample, 2µl RNA in TE solution was used to produce cDNA using the Quantitect Reverse Transcription Kit (Qiagen). The quantity of kit reagents is described in table 2.1.

Reagents	Quantity required
RT 20X Mastermix	1µl
RT 5X Buffer	4µl
RT Primer mix	1µl
dH_2O	12µl
Fungal RNA	2µl
Reaction total volume	20µl

Table 2.1: Quantitect Reverse Transcription (Qiagen) reaction mixture. Table describing the quantities of Quantitect Reverse Transcription (Qiagen) reagents used when generating cDNA from extracted fungal RNA.

The cDNA reaction was incubated at 42°C for 30 minutes, followed by 95°C for 3 minutes. Generated cDNA was purified using the PCR purification Kit (Qiagen) and used immediately to determine lung fungal burden by qPCR or stored at -80°C.

2.5.8: Determination of fungal burden by qPCR

The quantification of A.*f*. in lung extracted fungal RNA samples and standard curve fungal RNA samples was determined by the qPCR quantification of the single copy 18S rRNA gene of A.*f*.. 5µl of experimental sample or standard curve sample cDNA was used in each qPCR reaction to determine the copy number of the 18S rRNA gene of A.*f*.. Each standard curve or experimental sample was assayed in technical duplicate. Taqman reagents were used for the qPCR assay as described in table 2.2. A 42-cycle comparative Ct Taqman protocol was selected on a Quant Studio 12K Flex Real-Time PCR system (Thermo Scientific).

Reagents	Quantity required
Taqman 60X qPCR Probe	0.33µl
Taqman 2X Mastermix	10µl
dH_2O	4.7µl
Fungal cDNA	5µl
Reaction total volume	20µl

Table 2.2: Taqman qPCR reaction mixture. Table describing the quantities of Taqman qPCR used when quantifying the 18S rRNA gene of A.*f*. in cDNA generated from extracted fungal RNA.

After the qPCR was completed, a graph was created plotting Ct value against the standard curve sample A.*f*. concentrations. This allowed experimental sample's Ct to be compared to this standard curve graph; therefore, the quantity of A.*f*. each experimental sample Ct value corresponds to was determined.

2.5.9: Extracted lung cytokine and chemokine analysis

Whole right lung was extracted and stored in PBS at 4^{o}C. Right lung was manually homogenised for 30 seconds using a tissue homogeniser. After homogenisation, right lung sample in PBS was centrifuged at 17000g for 3 minutes and the supernatant removed and stored at -80^{o}C. ELISA was used to quantify cytokine and chemokines present in the homogenised lung sample supernatant.

2.6: Patient study

2.6.1: Sample collection

From each patient, 17.5ml whole blood was collected into EDTA tubes and 2ml whole blood was collected into PAXgene blood RNA tubes (Preanalytix). Upon receipt of the patient sample, 17.5ml whole blood was removed from the EDTA tubes and mixed with an equal volume of sterile PBS before being immediately processed or stored for a maximum of 24 hours at 4^{o}C. Whole blood in PAXgene blood RNA tubes were sequentially cooled for long term storage and processing in batches. PAXgene blood RNA tubes were incubated at RT for 48 hours (away from direct light), +4^{o}C for 48 hours, -20^{o}C for 48 hours and finally -80^{o}C for a maximum of 6 months. PAXgene blood RNA samples were processed in batches of 6-8.

2.6.2: Isolation of RNA from whole blood

2ml whole blood was collected into a PAXgene RNA tube and stored at -80^{o}C. Samples were equilibrated at RT for a minimum of 2 hours before completing RNA extraction. PAXgene tubes containing 2ml whole blood and the PAXgene RNA stabilising solution were centrifuged at 3000g for 10 minutes, supernatant was aspirated and the pellet re-suspended in 4ml dH_2O. Samples were again centrifuged at 3000g for 10 minutes, supernatant aspirated and pellet re-suspended in 350µl re-suspension buffer. Protein was digested from each sample with the addition of 40µl Proteinase K in 300µl binding buffer. Incubation at 55^{o}C for 10 minutes with 800rpm shaking ensured complete protein digestion. Increasing the temperature to 65^{o}C for 10 minutes then inactivated proteinase K.

Protein digested sample was added to a PAXgene shredder spin column and centrifuged at 17000g for 3 minutes. Cellular protein and debris did not pass through

the column. 350µl of 100% ethanol was added to the column flow-through sample to optimise RNA binding conditions. This sample solution was then added to a PAXgene RNA spin column and centrifuged at 17000g for 3 minutes. RNA was bound to the column whilst DNA, impurities and cellular debris were removed through a series of washes.

Contaminated DNA was removed from the column with DNAse I solution treatment. 10µl DNAse I in 70µl DNA digestion buffer was added to each column and incubated at RT for 15 minutes. The column membrane was thoroughly washed with wash buffer and centrifuged at 17000g to remove any remaining debris and contaminants.

RNA was eluted from the column with the addition of 40µl elution buffer. This was carefully added to the column membrane and incubated for 5 minutes at RT before the column was centrifuged at 17000g for 5 minutes. Eluted RNA was heat-denatured by incubation at 65^{o}C for 10 minutes. A nanodrop was used to quantify extracted RNA. Typically, ≥3µg RNA per 40µl sample was obtained. RNA was extracted with high purity, A_{260}/A_{280} values were consistently measured between 1.8 and 2.2. RNA was stored at -80^{o}C.

The integrity of extracted RNA was determined for the first 8 patient samples. This confirmed the kit and protocols used were successfully extracting and isolating high quality RNA. 100ng of extracted RNA from each of the first 8 patient samples was run on a 1% agarose gel at 100V for 30 minutes alongside a 100bp ladder (Promega). Clearly visible and correctly sized 28S and 18S rRNA bands indicated successful RNA extraction and high RNA integrity.

2.6.3: Generation of patient cDNA

Patient extracted RNA was used to generate cDNA. In batches of 8, 600ng of patient extracted RNA was used to produce 600ng of cDNA using a RT-PCR kit (Life Technologies). Assay reagents used are described in table 2.3 below.

Reagents	Quantity required
RT 10X Taqman Buffer	2.5µl
RT 25mM $MgCl_2$	5.5µl
RT dNTPs	5µl
RT Hexamers	0.625µl
RT Oligos	0.625µl
RT RNAse inhibitor	0.5µl
RT Multi-Scribe reverse transcriptase	0.625µl
Patient RNA	600ng RNA, make up to 9.6µl with dH_2O
dH_2O	
Reaction total volume	25µl

Table 2.3: Reverse Transcription Kit (Life Technologies) reaction mixture. Table describing the quantities of Reverse Transcription Kit (Life Technologies) reagents used when generating cDNA from extracted patient RNA.

This reaction was incubated at 25°C for 10 minutes, 48°C for 30 minutes and 95°C for 5 minutes. Generated cDNA was purified using a PCR purification Kit. For the first 8 patient samples, the successful generation of cDNA from extracted RNA was examined. 100ng of cDNA from each of the first patient 8 samples was run on a 1% agarose gel at 100V for 30 minutes alongside a 100bp ladder. The absence of clear 28S

and 18S rRNA bands and presence of a smear of cDNA confirmed successful cDNA generation.

2.6.4: Patient CLR sequencing

Patient cDNA was used to identify the presence of any mutations within patient's CLR gene sequences. 50ng cDNA was used in each PCR reaction to amplify Dectin-1, Dectin-2, Mcl and Mincle DNA. The reaction mixture for each PCR reaction is described below in table 2.4, Platinum High Fidelity PCR Supermix (Invitrogen) was used.

Reagents	Quantity required
Gene specific Forward Primer 10mM	1µl
Gene specific Reverse Primer 10mM	1µl
Platinum High Fidelity PCR Supermix	21µl
Patient cDNA	2µl
Reaction total volume	25µl

Table 2.4: PCR reaction mixture using Platinum High Fidelity PCR Supermix (Invitrogen). Table describing the quantities of PCR reagents used when generating CLR DNA from patient cDNA.

Each PCR reaction was incubated at 95^{o}C for 2 minutes before 30 cycles of 95^{o}C for 30 seconds, 56^{o}C for 30 seconds and 68^{o}C for 1 minute were completed. After the PCR reaction, samples were purified using a PCR purification Kit and stored at 4^{o}C for up to 48 hours or -20^{o}C for 6 months. For the first 8 patients, the successful amplification of CLR gene DNA was examined. 5µl of purified CLR gene PCR product was run on a 1%

agarose gel at 100V for 30 minutes alongside a 100bp ladder. A Band for each PCR amplified CLR gene around 600bp confirmed successful PCR amplification. Two bands were attained for patient Dectin-1 amplification samples around 100bp difference in size. These two bands were separately excised from the gel and the DNA purified using a Gel Purification Kit (Qiagen). Both patient Dectin-1 samples were sent for sequencing alongside the other amplified patient CLR DNA. Each CLR sequence was examined using four primers, one forward and reverse at each end of the gene and one forward and reverse in the middle of the gene, this provided thorough sequencing coverage.

2.6.5: Patient CLR expression

The expression of patient's CLRs at RNA transcript level was determined. A qPCR reaction was completed using patient's cDNA with qPCR probes specific for each CLR gene. 25ng patient cDNA was used for each CLR reaction and HPRT was used as a patient control.

The qPCR reaction was completed using Taqman PCR Mastermix (Thermo Scientific) and CLR gene-specific qPCR probes (Thermo Scientific), details in 7.4. The reaction mixture for each qPCR reaction is displayed below in table 2.5. The qPCR experiment was run for 40 cycles under standard qPCR Taqman incubation durations and temperatures. A Quant Studio 12K Flex Real-Time PCR system (Thermo Scientific) completed the qPCR reaction.

Reagents	Quantity required
2X Taqman PCR Mastermix	10µl
20X CLR probe	1µl
cDNA	25ng cDNA, make up to 9µl with dH_2O
dH_2O	
Reaction total volume	20µl

Table 2.5: Taqman qPCR reaction mixture. Table describing the quantities of Taqman qPCR used when quantifying the patient CLR genes from cDNA generated from extracted blood RNA.

Every patient's experimental CLR samples were normalised against their HPRT control. The expression of each patient's CLRs was determined against a control patient's CLR expression using ΔΔCt analysis. This allowed the comparison of all patient's CLR expression at RNA transcript level.

2.6.6: Extraction of patient PBMCs from whole blood

17.5ml whole blood was collected into EDTA collection tubes. Upon receipt of the sample, whole blood was removed from the EDTA tubes and mixed with 17.5ml PBS in a 50ml falcon tube. FicollPLUS (Sigma) was warmed to RT and thoroughly mixed before 17.5ml was added to two 50ml Falcon tubes. 17.5ml Whole blood PBS solution was layered on top of FicollPLUS in each Falcon tube. Whole blood PBS solution was added very slowly being careful not to disturb the liquid separation between the FicollPLUS and whole blood PBS solution. Once layering was complete, falcon tubes were centrifuged at 400g for 30 minutes with the centrifuge brake turned off.

After centrifugation, PBMCs (a thin white layer of cells below the plasma fraction) were collected using a Pasteur pipette and pooled. Collected PBMCs were washed once with PBS^{Mg+Ca+} (Life Technologies) and washed three times with RPMI 1640.

Between each wash PBMC solution was centrifuged at 350g for 5 minutes and supernatant aspirated and discarded. During the final RPMI 1640 wash, cells were counted using a haemocytometer and re-suspended at $2x10^7$ PBMCs/ml in PBMC media.

For flow cytometry analysis experiments, 100µl per well of $2x10^7$ PBMCs/ml were plated out on a 96-well plate. For stimulation and ELISA analysis experiments, 100µl per well of $5x10^6$ PBMCs/ml were plated out on a 96-well plate.

2.6.7: Patient PBMC stimulation

Patient PBMCs were plated out on a 96-well plate at the required concentration and rested for 4 hours by incubation at 37°C 5% CO_2. A.*f*. SC were grown following the protocol described in 2.2.6, a culture of live A.*f*. SC and a quantity of heat-killed A.*f*. SC were produced. Once PBMCs had been rested and A.*f*. SC and HKSC were prepared, the PBMCs were stimulated according to figure 2.1. All stimulation reactions were incubated at 37°C 5% CO_2 for the duration of the experiment.

A Initial experiments

24 Hours				7 Days		
Media				Media		
LPS				LPS		
Curdlan				Curdlan		
Live A.*f*. SC				Live A.*f*. SC		
HK A.*f*. SC				HK A.*f*. SC		

B Later experiments

24 Hours					
Media					
LPS					
Curdlan					
Live A.*f*. SC					
HK A.*f*. SC					

Figure 2.1: Protocol for patient PBMC stimulation. 100µl per well of $5x10^6$ PBMCs/ml were plated out on a 96-well plate, rested and stimulated. PBMCs were stimulated with 100µl 1µg/ml LPS, 100µl 2µg/ml Curdlan, 100µl of $5x10^6$ A.*f*. SC/ml and 100µl of $5x10^6$ HK A.*f*. SC/ml. 100µl PBMC media was added as an un-stimulated control. Stimulation experiments were completed for 24 hours and 7 days or 24 hours only before 96-well plates were centrifuged at 350g for 5 minutes and the supernatant collected. **A** Initially stimulation experiments were completed for 24 hours and 7 days with three replicates for each condition. After ELISA examination of these samples, the longer 7-day stimulation was stopped. **B** The 24-hour stimulation was continued and the sample replicates increased to six. This was the protocol layout used for the majority of samples.

Once stimulations were complete, 96-well plates were centrifuged at 350g for 5 minutes and the supernatant removed and immediately used or stored at -80^{o}C. ELISA was used to determine quantity of cytokines and chemokines in PBMC stimulation supernatant.

Chapter 3

Neutrophil Elastase cleavage of Dectin-1 Isoform A enhances susceptibility to A.*f*. infection

3.1: Aims

I. Determine whether Neutrophil Elastase can cleave Dectin-1 on immune cells

II. Identify the NE cleavage location within Dectin-1

III. Determine any functional consequence resulting from Dectin-1 NE-induced cleavage

3.2: Introduction

A.*f*. is a well-described invasive pathogen causing serious disease in immune-compromised individuals. Before the use of modern immune-suppressing therapeutics A.*f*. infections were rare and usually resulted from the repeated inhalation of high quantities of A.*f*. conidia. Even then, conidia were rapidly cleared and only mild allergic-type disease would present [4]. Complications arose if pre-existing immune-privileged lung cavities were present allowing A.*f*. growth; however, this growth would be limited within the immune-privileged cavity [1]. More recently, A.*f*. has been recognised as an important pathogen in immune-competent patients with pre-existing airway disease such as cystic fibrosis (CF). A.*f*. infections in these patients can cause allergic-hypersensitivity and invasive disease resulting in further deterioration of the underlying airway disease [222]. Patients are often caught in a cycle of recurrent A.*f*. infection exacerbating their underlying airway disease, reducing the local-airway immune response, and further inhibiting A.*f*. clearance.

It is estimated worldwide that ~10 million patients with pre-existing airway disease are impacted by A.*f*. infections. A.*f*. has been identified in 10-57% of airway secretions from CF patients and anti-A.*f*. IgG has been detected in 41% of CF patients at age 4, rising to 98% of patients by age 10 [19]. This incidence is much higher than that detected in asthmatic and healthy patient cohorts [46]. Furthermore, allergic bronchopulmonary A*spergillosis* (ABPA), a serious A.*f*. allergic-type disease culminating in airway narrowing and obstruction affects 17.7% of the adult CF population. A.*f*.-induced bronchitis affects 30% of CF patients [48]. Research is required to understand why patients with pre-existing lung disease such as CF but otherwise healthy immune systems are highly susceptible to A.*f*. infection.

The anti-A.*f*. immune response is complicated and poorly understood. As previously mentioned, TLRs and CLRs form a crucial component of the anti-A.*f*. response [1, 137]. The role these receptors exhibit has typically been studied in invasive disease and

immune-suppressed *in vivo* models. Although many of the deductions from these studies are relevant to the overall anti-A.*f*. immune response, the anti-A.*f*. response in the setting of underlying airway disease has not been extensively investigated. In this setting the response may differ greatly from invasive, immune-suppression induced disease. The CLR Dectin-1 has previously been thoroughly discussed. The vital role this receptor plays in the anti-A.*f*. immune response is well described and the increased susceptibility of Dectin-1 KO mice to A.*f*. infection highlights this crucial role [100]. Whilst defects in CLRs such as Dectin-1 increase susceptibility to A.*f*. infection, little is known about their functional status in patients with pre-existing airway disease such as CF. These patients possess a very complex airway inflammatory and structural setting. The presence, expression and function of CLRs in this setting may be markedly different when compared to healthy individuals [223]. Understanding the behavior of CLRs in the CF airway is of critical importance when aiming to identify why CF patients possess increased susceptibility to A.*f*. infection.

CF is a genetic disorder affecting the cystic fibrosis transmembrane conductance regulator (CFTR). A mutated CFTR gene reduces Cl^- transport subsequently reducing hydration of the epithelial surface. This culminates in reduced action of the mucociliary escalator and deposition of thick mucus in the airway [20, 23]. The long-term presence of thick mucus dramatically alters airway homeostasis and results in regular airway infection [26]. Bacteria and fungi are not rapidly cleared from the airway and a chronic inflammatory state is produced. Recruited immune cells are retained in thick mucus further contributing to the inflammatory setting [25, 26]. Eventually the chronic inflammatory environment generated in the airway of CF patients leads to fibrosis of the airway epithelia and lung. Fibrosis results in narrowing of the airway and reduced lung function. Declining lung function in CF patients is associated with profound neutrophilic inflammation and the presence of high quantities of poorly regulated, neutrophil-derived serine proteases such as neutrophil elastase (NE) [27, 224]. These proteases form an important part of the anti-microbial immune response but when poorly regulated can cause local tissue damage and reduce the capabilities of the local immune response [225, 226]. A poorly regulated neutrophil-driven chronic protease response is widely recognised as a contributor to

CF airway pathology [27]. Many facets of the immune response such as complement receptors and signalling, soluble IL-6R and TLRs are susceptible to functional inactivation by serine proteases in the CF airway [32, 34, 35]. Here we investigate the possibility that high quantities of NE present in the CF airway contribute to a reduced anti-A.*f*. response by disrupting Dectin-1's ability to recognise and clear A.*f*.. Reduced A.*f*. clearance may enhance the local inflammatory setting and exacerbate the underlying CF airway disease.

3.3: Results

3.3.1: Does Neutrophil Elastase cleave Dectin-1?

As neutrophil-derived serine proteases have been shown to cleave various immune receptors and Dectin-1 is susceptible to trypsin cleavage, I wanted to determine whether NE cleaves Dectin-1 [227]. NIH-3T3 cells expressing human Dectin-1 were incubated with NE or bronchiolar alveolar lavage fluid (BALF) from CF patients. The ability of NE or CF BALF to reduce Dectin-1 expression was examined along with correlation analysis of CF BALF neutrophil infiltration, CF BALF NE activity and loss of Dectin-1 expression on NIH-3T3 cells.

The experiments and results displayed in this chapter were undertaken for my thesis after an initial series of experiments, shown in figure 3.1, were completed and analysed by Dr Eamon McGreal.

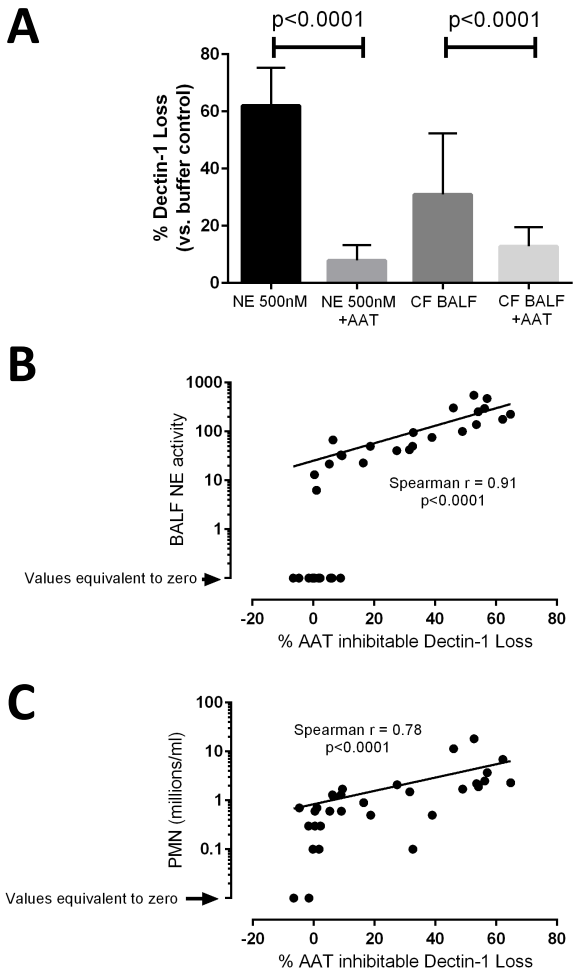

Figure 3.1: Cystic Fibrosis patient's bronchiolar alveolar lavage fluid induces cleavage of Dectin-1. (A) NIH-3T3 cells expressing human HA-tagged Dectin-1 Isoform A were exposed to 0.5µM NE or 50µl CF BALF in the presence or absence of AAT (a small molecule NE inhibitor) for 30 minutes at 37°C 5% CO_2. Cells were stained with anti-HA and analysed by flow cytometry. Graph displays mean +/- s.d.. Student's t-test was used to determine statistical significance. **(B-C)** NIH-3T3 cells expressing human HA-tagged Dectin-1 Isoform A were exposed to CF BALF for 30 minutes at 37°C 5% CO_2. Cells were stained with anti-HA and analysed by flow. **(B)** NE activity in CF BALF samples was measured. Correlation analysis between NE activity and % Dectin-1 loss was performed. **(C)** Neutrophil numbers in CF BALF were counted and correlation analysis between neutrophil numbers in CF BALF and % Dectin-1 loss performed. **(A, B & C)** Data are cumulative results of 7 independent experiments. **(B & C)** Each symbol represents data from a single patient.

Eamon incubated NIH-3T3 cells expressing Dectin-1 with NE and he demonstrated that NE cleaves Dectin-1 (figure 3.1). The loss of Dectin-1 expression in this experiment can be attributed to NE activity as alpha-antitrypsin (AAT) an NE inhibitor, prevents Dectin-1 loss. This identified cleaving capability of NE is also present when NIH-3T3 cells expressing Dectin-1 are incubated with CF BALF. This suggests that CF patient BALF has the capability to cleave Dectin-1, likely due to its high neutrophil infiltration and high NE activity. Although these overexpression experiments were completed *in vitro*, an interesting role for NE cleaving Dectin-1 in the airway of CF patients potentially impairing the anti-fungal immune response required further investigation.

The experiments displayed in figure 3.1 were completed using NIH-3T3 cells expressing hDectin-1 Isoform A. hDectin-1 Isoform B is also highly prevalent on many immune cells relevant to the anti-fungal immune response [228]. hDectin-1 Isoform B is functionally similar to hDectin-1 Isoform A but lacks the stalk region of the receptor, meaning isoform B sits closer to the membrane and does not contain a glycosylation region [229, 230]. The ability of NE to cleave hDectin-1 Isoform B must also be examined. Therefore, NIH-3T3 cells expressing hDectin-1 isoform B were incubated with NE alongside NIH-3T3 cells expressing hDectin-1 Isoform A.

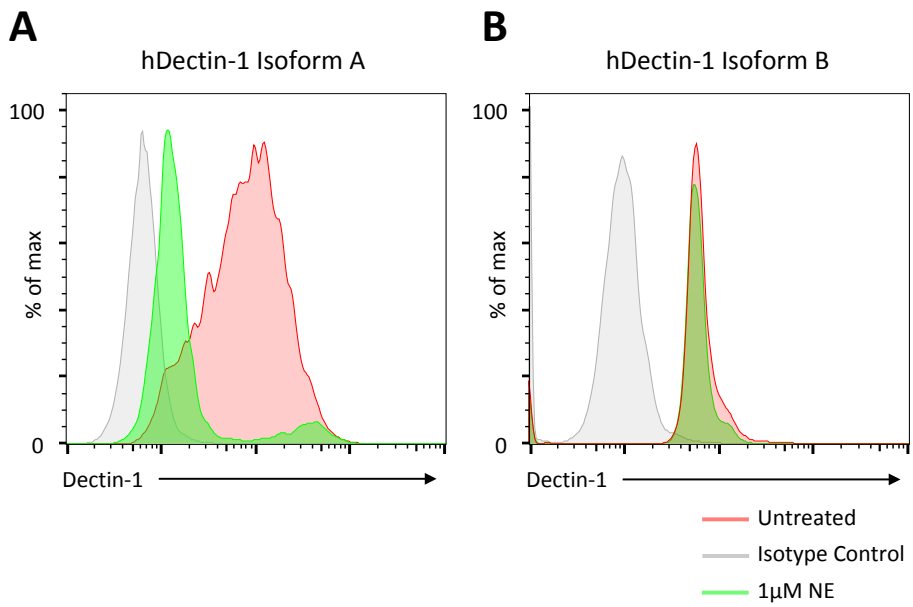

Figure 3.2: NE cleaves hDectin-1 Isoform A but not hDectin-1 Isoform B. NIH-3T3 cells expressing human Dectin-1 isoform A **(A)** or B **(B)** were exposed to 1µM NE for 15 minutes at 37°C 5% CO_2. Cells were stained with anti-hDectin-1 (an antibody that recognises both isoforms of the receptor) and the expression of hDectin-1 Isoform A or B was analysed by flow cytometry. Data displayed are representative of 4 independent experiments.

Interestingly, figure 3.2 shows that NE specifically cleaves hDectin-1 Isoform A but not hDectin-1 Isoform B. This suggests that NE requires the isoform A-exclusive extracellular stalk region of hDectin-1 in order to cleave the receptor.

The experiments displayed in figure 3.1 and 3.2 identify a role for NE cleaving hDectin-1 isoform A on NIH-3T3 cells. It was next important to determine whether the Dectin-1 cleaving action of NE is present on immune cell types resident or recruited to the CF airway that naturally express Dectin-1. Both hDectin-1 Isoform A and B are structurally and functionally similar to their mouse homologues [161, 231]. Therefore, mouse cells would be appropriate to examine NE's ability to cleave Dectin-1 on primary cells. However, before primary mouse cells could be used, the ability of NE to cleave

mDectin-1 Isoform A was confirmed by incubating NIH-3T3 cells expressing mDectin-1 isoform A with NE.

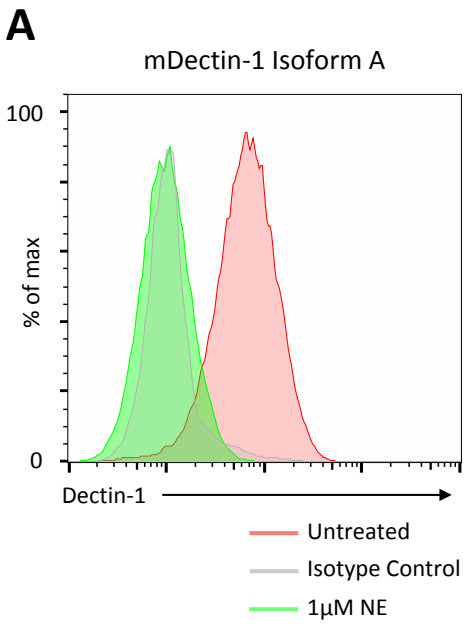

Figure 3.3: NE cleaves mDectin-1 Isoform A. NIH-3T3 cells expressing murine Dectin-1 isoform A **(A)** were exposed to 1µM NE for 15 minutes at 37°C 5% CO_2. Cells were stained with anti-mDectin-1 and the expression of mDectin-1 Isoform A analysed by flow cytometry. Data displayed are representative of 3 independent experiments.

The NE-induced cleavage of hDectin-1 isoform A is conserved for mDectin-1 Isoform A. Figure 3.3 permits the use of mDectin-1 isoform A as a model for the human receptor. Having demonstrated that NE cleaves mDectin-1 isoform A, I next examined the ability of NE to cleave mDectin-1 Isoform A on primary myeloid immune cells. Dectin-1 is expressed on many immune cells types; those relevant to the CF airway include macrophages, neutrophils and monocytes [227, 231-233].

In order to retain as much similarity to the human CF airway as possible, all future experiments (unless otherwise mentioned) were performed in primary cells isolated from BALB/c mice. BALB/c mice express mDectin-1 isoform A and B in a ~1:1 ratio. Humans highly express both Dectin-1 isoform A and B. Therefore, BALB/c mice represent a more relevant model than, for example, C57 BL6 mice that express ~97% isoform B and ~3% isoform A [161].

I first examined the ability of NE to cleave Dectin-1 expressed on cultured BMDMs; therefore, BMDMs were incubated with NE in the presence or absence of the NE inhibitor, AAT.

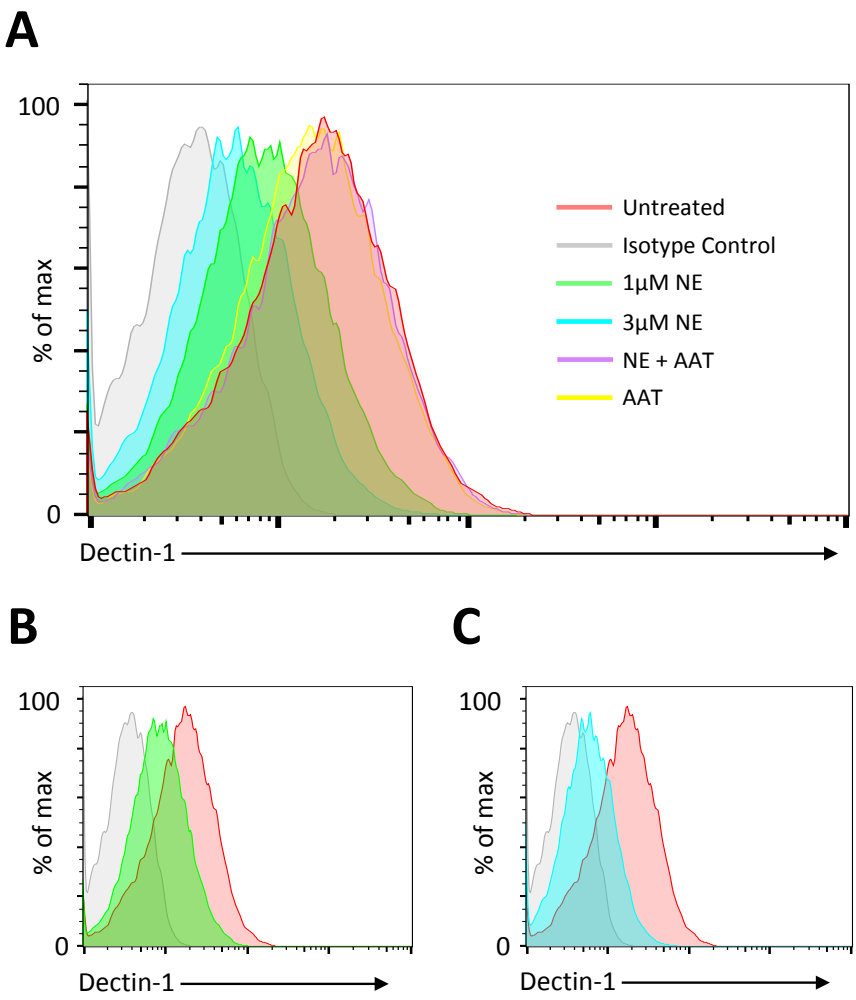

Figure 3.4: NE cleaves mDectin-1 Isoform A on BALB/c derived BMDMs. (A, B & C) Bone marrow derived from BALB/c mice was used to culture BMDMs. Cultured BMDMs were exposed to 1µM NE or 3µM NE with and without the NE inhibitor AAT present for 15 minutes at 37°C 5% CO_2. Cells were stained with anti-mDectin-1 and the expression of mDectin-1 analysed by flow cytometry. Representative flow plot displays **(A)** the total overlay of BMDM cells exposed to 1µM NE, 3µM NE, 3µM NE AAT and AAT alone, **(B)** 1µM NE treatment, **(C)** 3µM NE treatment. Data displayed are representative of 3 independent experiments.

Figure 3.4 demonstrates the susceptibility of BMDM-expressed Dectin-1 to NE cleavage. Having identified that mDectin-1 on macrophages was cleaved by NE, it was next important to determine whether NE cleaves Dectin-1 on neutrophils. Neutrophils represent the majority immune cell present in the CF airway and a cell type responsible for much CF pathology [25]. Low activation state neutrophils were obtained via intra-peritoneal BIOgel injection. In order to determine whether NE cleaves Dectin-1 on neutrophils, total BIOgel recovered cells were incubated with NE or NE and inhibitor. Following NE treatment, total BIOgel-recovered cells were stained with antibodies allowing the identification of specific cell populations within the total BIOgel-recovered population by flow cytometry.

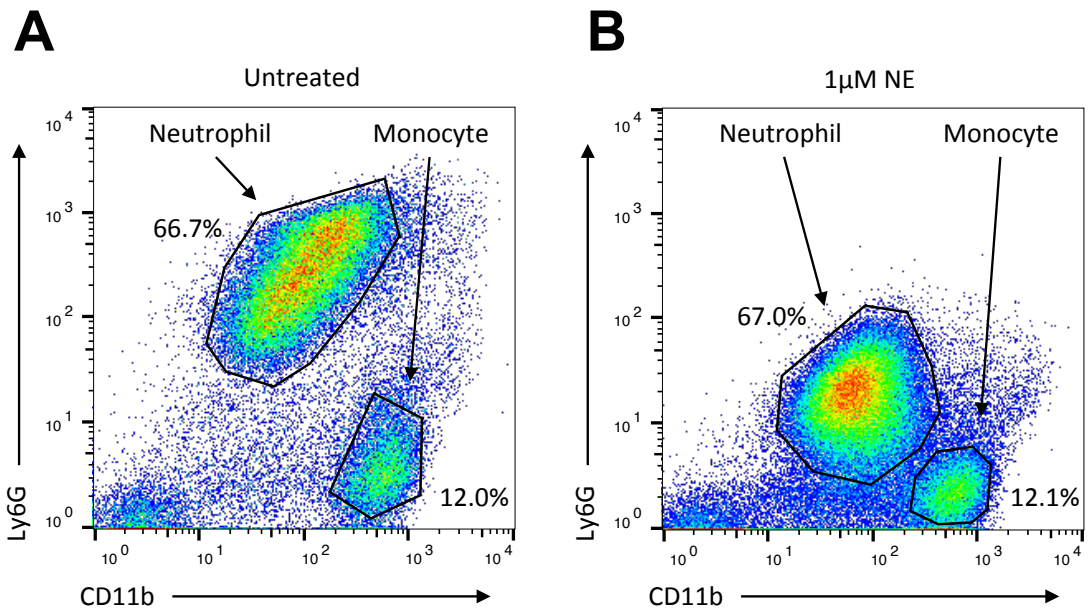

Figure 3.5: NE cleaves Ly6G on BIOgel recovered cells. BIOgel recovered cells were stained with anti-Ly6G and anti-CD11b before being analysed by flow cytometry to identify neutrophils and monocytes within the recovered total cell population. **(A)** Without NE treatment, clear separation of neutrophils and monocytes by anti-Ly6G staining is achieved. **(B)** After 15 minute exposure to 1µM NE at 37°C 5% CO_2 the clear $Ly6G^+$ population had reduced Ly6G expression. As displayed in gating percentages the neutrophil and monocyte populations were still distinguishable and were gated on as such for future experiments. Data displayed are representative of 4 independent experiments.

Figure 3.5 identifies an intriguing and novel role for NE cleaving Ly6G on BIOgel-recovered cells. Although this made the identification of BIOgel-recovered cells more challenging post-NE treatment, neutrophils and monocytes could still be identified and gated on. Figure 3.5 demonstrates the flow cytometry gating required to identify neutrophils and monocytes in total BIOgel-recovered cells. This gating allowed the NE cleaving capability for Dectin-1 to be determined on both these monocyte and neutrophil populations.

In order to examine the ability of NE to cleave Dectin-1 expressed on neutrophils and monocytes, total BIOgel-recovered cells were incubated with NE or NE and inhibitor before cells were stained with antibodies allowing their cell type identification and Dectin-1 expression.

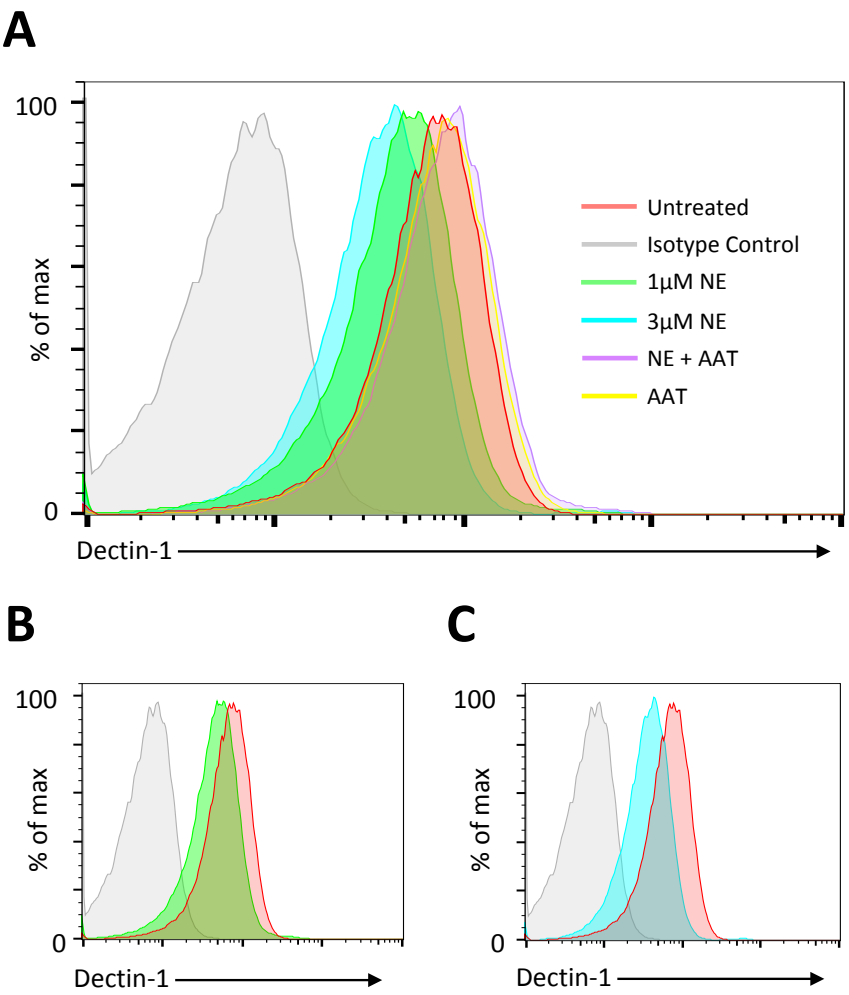

Figure 3.6: NE cleaves mDectin-1 Isoform A on BALB/c BIOgel derived neutrophils. (A, B & C) BIOgel derived neutrophils from BALB/c mice were isolated as previously identified in figure 5.5. Neutrophils were exposed to 1µM NE or 3µM NE with and without the NE inhibitor AAT present for 15 minutes at 37°C 5% CO_2. Cells were stained with anti-mDectin-1 and the expression of mDectin-1 analysed by flow cytometry. Representative flow plot displays **(A)** the total overlay of neutrophils exposed to 1µM NE, 3µM NE, 3µM NE AAT and AAT alone, **(B)** 1µM NE treatment, **(C)** 3µM NE treatment. Data displayed are representative of 3 independent experiments.

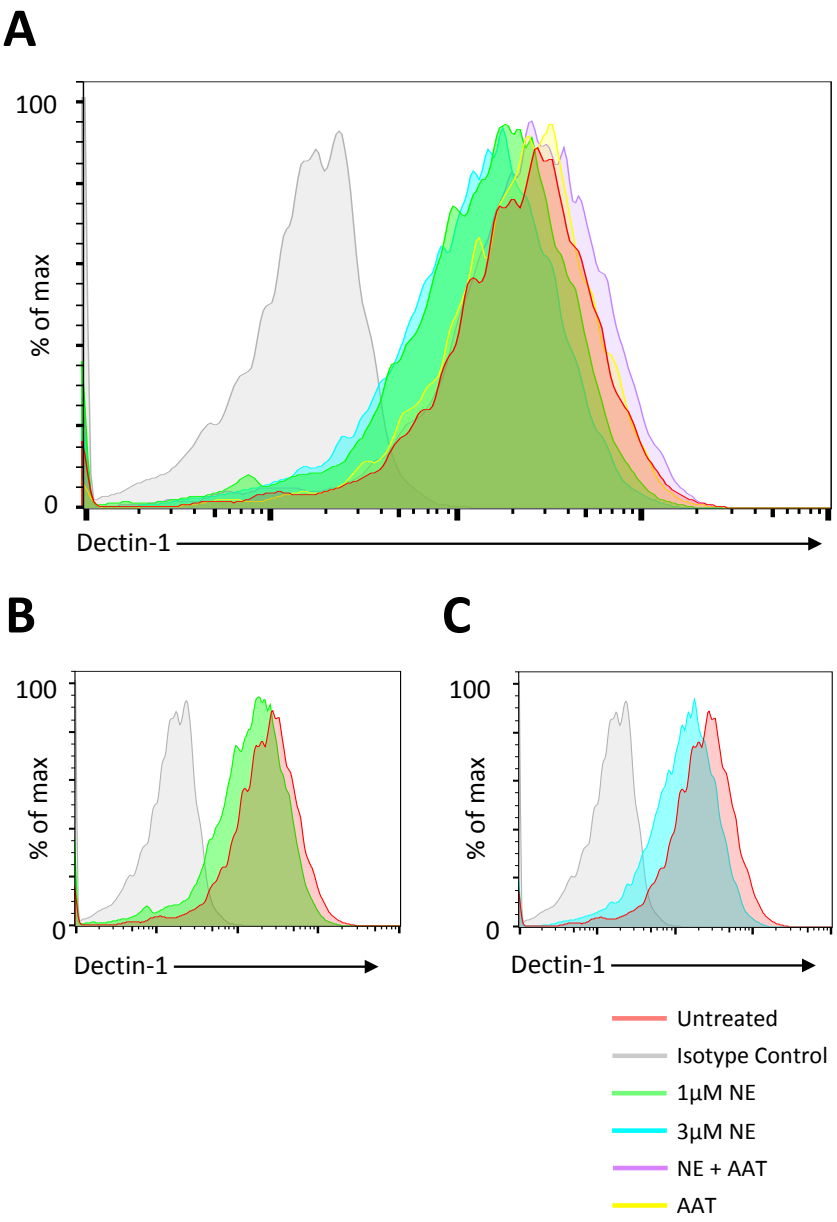

Figure 3.7: NE cleaves mDectin-1 Isoform A on BALB/c BIOgel derived monocytes. (A, B & C) BIOgel derived monocytes from BALB/c mice were isolated as previously identified in figure 5.5. Monocytes were exposed to 1µM NE or 3µM NE with and without the NE inhibitor AAT present for 15 minutes at 37°C 5% CO_2. Cells were stained with anti-mDectin-1 and the expression of mDectin-1 analysed by flow cytometry. Representative flow plot displays **(A)** the total overlay of monocytes exposed to 1µM NE, 3µM NE, 3µM NE AAT and AAT alone, **(B)** 1µM NE treatment, **(C)** 3µM NE treatment. Data displayed are representative of 3 independent experiments.

I have demonstrated the NE-specific cleavage of mDectin-1 occurred on BALB/c derived macrophages (figure 3.4), neutrophils (figure 3.6) and monocytes (figure 3.7). These myeloid cell types are readily recruited to the CF airway and contribute to the local inflammatory setting as well as playing a key role in the host immune response against pathogens in the CF airway [25, 232, 233]. Loss of Dectin-1 Isoform A expression from these cells likely reduces their ability to recognise and respond to pathogens such as A.*f*..

Here we have identified that NE cleaves hDectin-1 Isoform A not Isoform B. I have also demonstrated that NE cleaves the structurally and functionally similar mDectin-1 Isoform A on myeloid immune cells relevant to the CF airway and A.*f*. disease. These immune cells are required for the generation of an appropriate immune response against pathogens.

3.3.2: Which Dectin-1 amino acid is required for NE-induced cleavage to occur?

As previously described in figure 3.2, NE cleaves Dectin-1 Isoform A and not Isoform B. This suggests NE cleaves Dectin-1 at a location within the stalk region of Dectin-1. This region is exclusively found in Isoform A, the longest Dectin-1 isoform. Dectin-1 Isoform B is identical to Isoform A aside from the lack of stalk region. [229]. The nucleotide sequence of hDectin-1 stalk region was identified and the corresponding protein sequence was examined using two protease databases that predict the cleavage site residues of known enzymes [163]. The stalk region protein sequence was analysed for NE cleavage sites by brenda-enzymes.org and merops.sanger.ac.uk databases. Both databases returned the same predicted NE cleavage sites within the protein stalk region of hDectin-1.

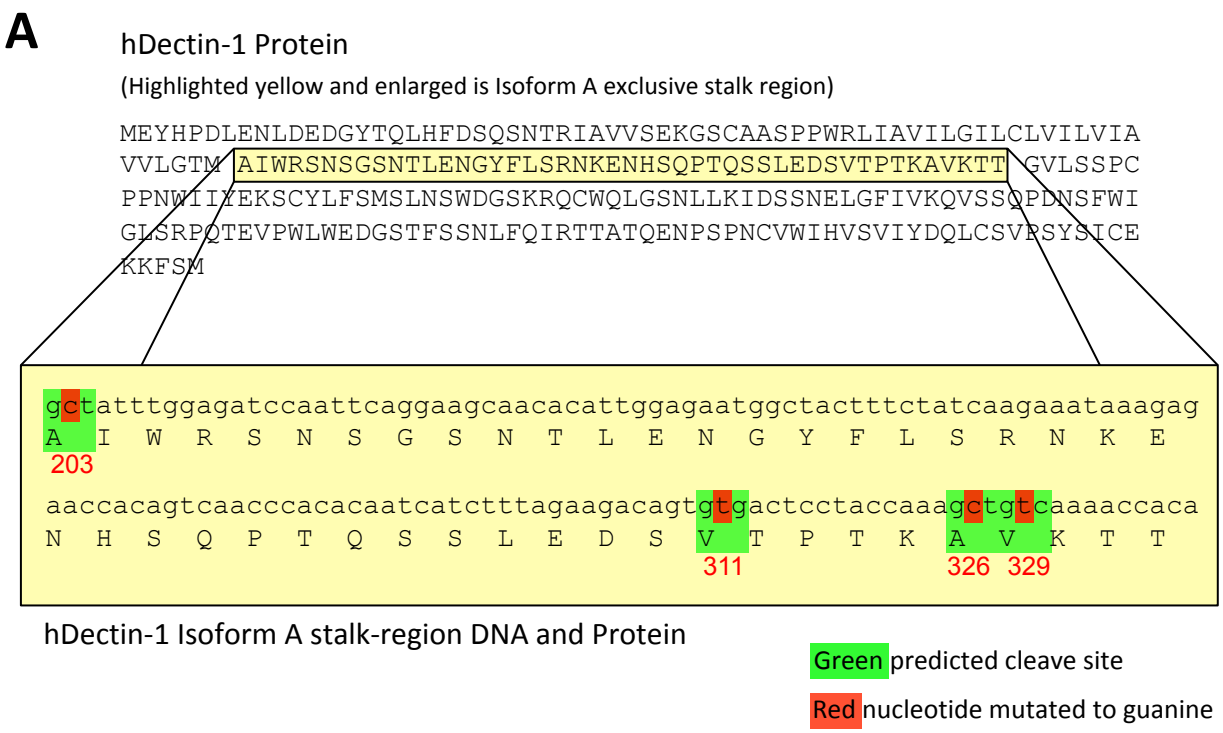

Figure 3.8: NE was predicted to cleave hDectin-1 at four amino acid residue sites located within the CLR's stalk-region. These residues were mutated to glycine. (A) Potential NE cleave sites were identified using the protease databases brenda-enzymes.org and merops.sanger.ac.uk. hDectin-1 stalk-region protein sequence was submitted and NE selected as the enzyme. Residues highlighted in green represent amino acids and their corresponding nucleotide sequence that were predicted cleave sites of NE. Nucleotides highlighted in red represent nucleotides that were mutated to guanine resulting in a corresponding amino acid substitution to glycine.

As displayed in figure 3.8 the four residues identified as potential NE cleavage sites located in hDectin-1 Isoform A stalk region were mutated so the corresponding amino acid was altered to glycine. Glycine was chosen, as it is the simplest amino acid with no side chain. Altering each NE-cleave predicted residue to a glycine does not introduce any new charges across the molecule and although Dectin-1 function may be impacted, tertiary structure and assembly should not change [234]. Unfortunately, the 329 mutant could not be generated.

Each hDectin-1 Isoform A mutant retroviral construct was used to infect NIH-3T3 cells. Wild-type hDectin-1 Isoform A and empty vector controls were also used to infect 3T3 cells. These cell lines were used to determine at which amino acid residue NE cleaves hDectin-1 Isoform A. Each cell line was incubated with NE and the expression of Dectin-1 determined.

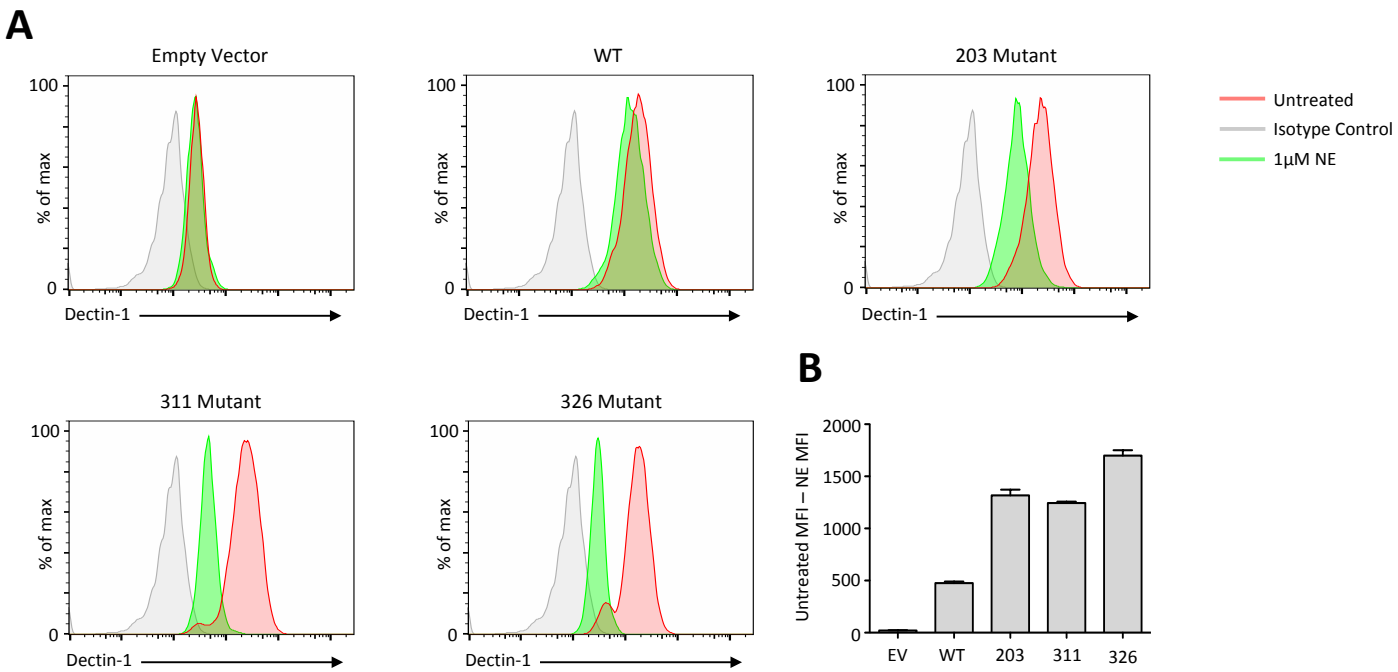

Figure 3.9: Mutating predicted hDectin-1 NE cleave sites to glycine residues increased the NE-induced loss of hDectin-1 when compared to WT. (A) Previously identified NE cleave sites located in hDectin-1 were mutated from their WT amino acid residue to glycine and inserted (in parallel with empty vector and WT hDectin-1) into NIH-3T3 cell lines. These cells were exposed to 1µm NE for 15 minutes at 37°C 5% CO_2 before being stained with anti-hDectin-1 and analysed by flow cytometry. **(B)** Geometic mean of untreated and NE-treated cells anti-hDectin-1 PE was calculated for each EV, WT and mutant hDectin-1 and used to determine NE-induced geometric mean shift. Graph displays mean +/- s.e.m.. **(A)** Displays one experiment, data representative of 4 independent experiments. **(B)** Geometric mean from 3 independent experiments averaged and used to determine NE-induced geometric mean shift.

The results displayed in figure 3.9 were not expected, (B) indicates that Dectin-1 expression of each mutant after NE treatment was lower than the WT Dectin-1 expression after NE treatment. This suggests mutating the predicted NE cleave site residues increased Dectin-1 susceptibility to NE treatment. Mutating a WT Dectin-1 amino acid to glycine may have straightened the tertiary structure of Dectin-1 and increased the ability of NE to access and cleave Dectin-1 Isoform A [235]. Further experiments mutating cleave sites to a different amino acid or mutating multiple cleave sites in tandem may lead to the identification of NE's multiple cleave site residues present in the stalk region of Dectin-1 Isoform A.

3.3.3: Is there a functional consequence resulting from the NE-induced cleavage of Dectin-1?

In order to ascertain whether the NE-induced loss of Dectin-1 impacts the functional immune response against A.*f*., BMDMs from BALB/c mice were cultured, incubated with NE or NE + AAT under various media and treatment conditions before stimulation with Curdlan or A.*f*. SC. TNF production was determined. The Dectin-1 blocking antibody 2A11 was included in experiments to highlight the Dectin-1 specific effect on TNF responses.

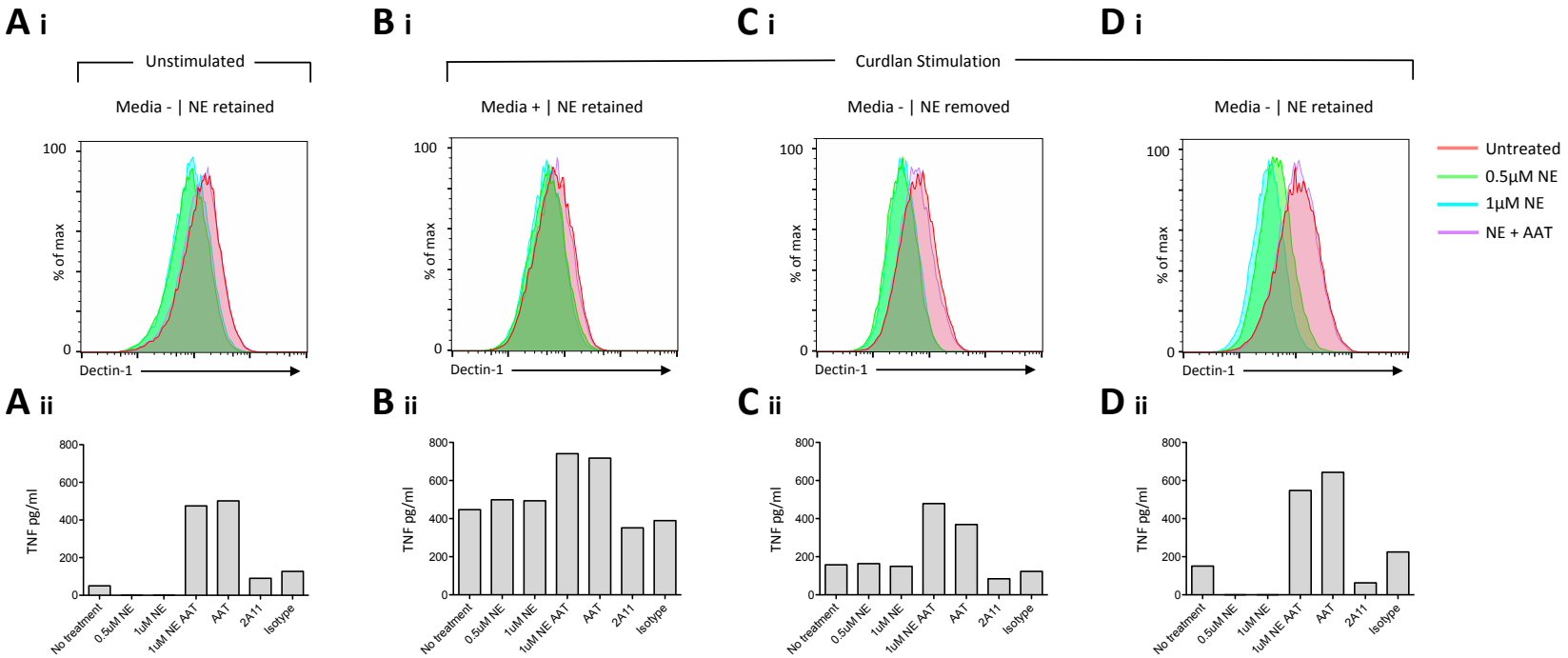

Figure 3.10: BMDM cells must be constantly treated with NE in the absence of serum-containing media to retain Dectin-1 expression loss. The small molecule inhibitor of NE, AAT results in TNF release. (A - D) BALB/c derived BMDMs were treated for 1 hour at 37°C 5% CO_2 with 0.5µM, 1µM NE, 1µM NE AAT or 4µg/ml 2A11 antibody. BMDMs were then simulated for 3 hours at 37°C 5% CO_2 with 25µg curdlan in serum-containing media or serum-lacking assay buffer in the presence of continued NE treatment or with the NE treatment removed. **(Ai - Di)** After stimulation BMDMs were stained with anti-F4/80, anti-CD11b and anti-mDectin-1. Dectin-1 expression for each media or treatment condition was determined by flow cytometry. **(Aii - Dii)** After stimulation ELISA determined TNF concentration for each media or treatment condition. Results displayed are representative of **(Ai - Di)** 3 and **(Aii – Dii)** 2 independent experiments.

The results displayed in figure 3.10 highlight the challenges encountered when aiming to isolate a functional response deficiency specifically resulting from the NE-induced cleavage of Dectin-1. Alongside results shown, experiments were also completed using A.*f*. SC as a stimulant instead of curdlan. No TNF response was detected when using live A.*f*. SC. A.*f*. may not provide a fast or robust enough stimulus to lead to the release of TNF after 3 hours. Live A.*f*. may also kill the cells resulting in no TNF release.

Figure 3.10 (Bi) identifies the requirement for completing the 3-hour stimulation without using serum-containing media. These experimental conditions recovered the expression of Dectin-1 and blocked the cleaving impact of NE. Figure 3.10 (Ai, Ci & Di) stimulations were completed in serum-free buffer and the NE-induced cleavage of Dectin-1 was present. Figure 3.10 (Ci) displays the limited impact removing NE after the initial 1-hour treatment has on maintaining Dectin-1 expression loss. Dectin-1 expression was reduced; although, when NE was removed, expression recovered. Figure 3.10 (Di) proposes the most effective way of maintaining the NE-induced loss of Dectin-1 requires NE-treating cells for 1 hour before stimulating with curdlan in serum-free buffer on top of existing NE treatment. Unfortunately, although the loss of Dectin-1 was maintained through this method, BMDMs likely die or lack nourishment as these cells only produced ~50% the curdlan TNF response that cells in serum-containing media produced.

Figure 3.10 (Aii – Dii) highlights the difficulties encountered when trying to block NE's cleaving impact on cells whilst measuring TNF responses. AAT appears to stimulate cells and result in TNF release independently of Dectin-1. This blocked the association of the NE-induced cleavage of Dectin-1 resulting in a reduced TNF response.

Taking the above-mentioned points from figure 3.10, a refined approach was used attempting to elicit the functional impact the NE-induced cleavage of Dectin-1 may have. Therefore, BMDMs were treated with NE for the entirety of the stimulation experiment and no serum-containing media was added to the cells. BMDMs were stimulated with curdlan or curdlan and Pam(3)CSK(4). This TLR2 ligand was used to greatly enhance the TNF response [236]. Multiple small molecule NE inhibitors were trialed, along with heat-killed NE, to allow the NE-cleavage of Dectin-1 to be directly associated with a TNF response deficiency.

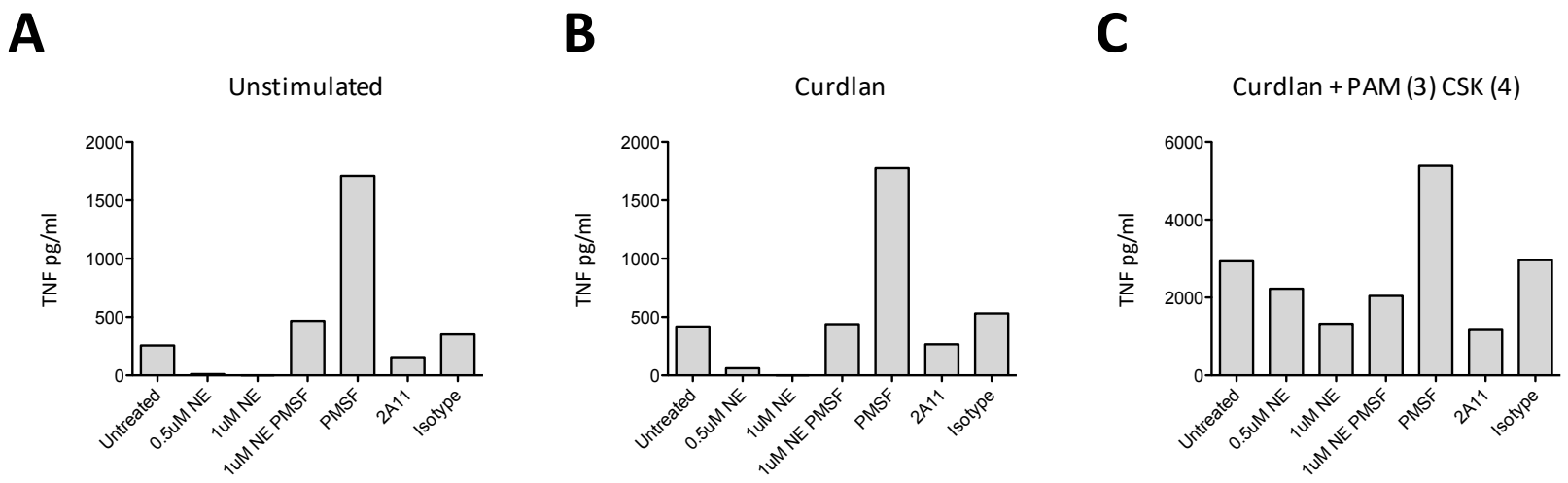

Figure 3.11: NE-induced cleavage of Dectin-1 cannot be directly associated with an impaired TNF response. (A, B & C) BMDM cells derived from BALB/c mice were treated for 1 hour at 37°C 5% CO_2 with 0.5µM or 1µM NE, 1µM NE PMSF or 4µg/ml 2A11 antibody. BMDMs were then stimulated with **(B)** 25µg Curdlan or **(C)** 25µg Curdlan + 10ng PAM (3) CSK (4) in serum lacking assay buffer in the presence of continued NE treatment for 3 hours at 37°C 5% CO_2. After stimulation supernatant was collected and TNF concentration of each stimulation condition determined by ELISA. Results displayed are representative of 2 independent experiments.

The results displayed in figure 3.11 further highlight the challenges encountered when aiming to attribute the NE-induced loss of Dectin-1 to a reduced functional TNF response.

Figure 3.11 identifies un-stimulated BMDMs consistently released a large quantity of TNF against small-molecule NE inhibitors such as PMSF. A range of different small-molecule NE inhibitors and heat-killed NE also elicited TNF responses (data not shown). Therefore, the NE-induced loss of Dectin-1 and subsequent reduced TNF response could not be directly associated. A much larger TNF release was achieved when stimulating BMDMs with Curdlan and the TLR2 ligand Pam(3)CSK(4). This co-stimulation was attempted to enhance the subtle TNF response differences identified in figure 3.10 between NE-treated and NE-inhibited or untreated samples. Although this has been achieved and an NE dose-response reduction in TNF release was attained, the PMSF inhibition of NE has still resulted in a large TNF response.

Due to the challenges faced attempting to treat BMDMs with NE and elicit a functional response deficit by stimulating cells through Dectin-1 and quantifying TNF production, a different approach was required. Identifying whether the NE-cleavage of Dectin-1 compromises the ability of cells to recognise zymosan or A.*f*. SC may provide a functional response outcome directly linked to the NE-cleavage of Dectin-1.

Neutrophils from C57BL/6 WT and Dectin-1 KO mice were obtained from intra-peritoneal BIOgel. These cells were used to determine zymosan and A.*f*. SC recognition and elicit the maximal impact losing Dectin-1 had on the recognition of these two Dectin-1 ligands. Zymosan is derived from fungal cell walls and is well recognised as a Dectin-1 ligand and appropriate sterile model for fungal recognition and phagocytosis [237].

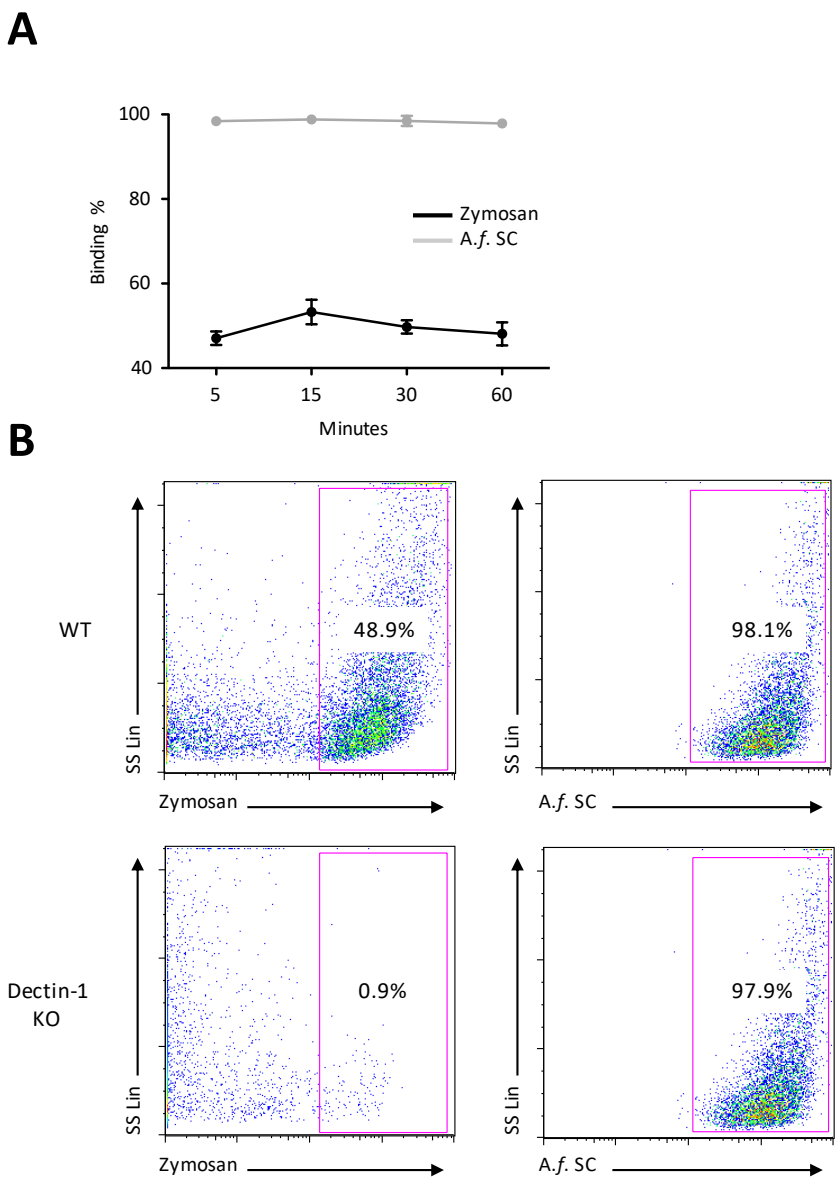

Figure 3.12: Dectin-1 KO neutrophils possess impaired zymosan recognition but retain high binding affinity for A.*f*. SC. (A & B) 2.5µg FITC-zymosan or 1x10^6 PE-A.*f*. SC was incubated with BIOgel-obtained cells. Cells were stained with anti-Ly6G, anti-CD11b and anti-Dectin-1. Flow cytometry was used to identify Ly6G$^+$ and CD11b$^+$ neutrophils; Zymosan or A.*f*. SC binding was determined on these cells. **(A)** FITC-labeled zymosan or far-red labelled A.*f*. SC was incubated with BIOgel-obtained cells from 5-60 minutes at 37^{o}C 5% CO_2. Zymosan or A.*f*. SC binding by neutrophils was determined at each time point by flow cytometry. Graph displays mean +/- s.e.m.. **(B)** Zymosan or A.*f*. SC were incubated with BIOgel-derived cells for 15 minutes at 37^{o}C 5% CO_2 before binding by neutrophils was determined by flow cytometry. **(A)** Mean data displayed from two independent experiments. **(B)** Data displayed representative of two independent experiments.

Figure 3.12 (A) suggests the Dectin-1 recognition of zymosan and A.*f*. SC occurs rapidly. Zymosan recognition peaks at 15 minutes. The quantity of zymosan used (2.5µg) resulted in ~50% binding at 15 minutes. This binding percentage is optimal for the identification of NE-induced binding deficiencies. The cells are not saturated with zymosan but sufficient binding is present for a NE-induced binding reduction to be discernable.

The binding efficiencies identified at 15 minutes in figure 3.12 (A) were used at this time point for the experiments displayed in figure 3.12 (B). These data suggest neutrophils can recognise A.*f*. SC completely independently of Dectin-1; however, zymosan recognition relies heavily on Dectin-1. The redundant role of Dectin-1 in the recognition of A.*f*. SC meant future experiments were carried out using zymosan. Neutrophils are difficult to maintain in a low activation state for use in recognition experiments; therefore, this experiment was completed in BMDMs in order to ascertain a similar zymosan recognition trend between WT and Dectin-1 KO was present in this cell type.

The zymosan used in the experiments displayed in figure 3.12 was a purchased FITC-labeled zymosan (Thermofisher). This FITC-labeled zymosan was very bright. The cell population lacking zymosan recognition could not be contained in the same flow cytometry gate as the positive zymosan-recognition population. Therefore, zymosan (Sigma) was conjugated with a FITC-fluorophore generating a less bright FITC-labeled zymosan ligand that could be used in future recognition experiments. This homemade FITC-labeled zymosan allowed the determination of cells that have and have not recognised zymosan to be viewed in the same flow-cytometry gate.

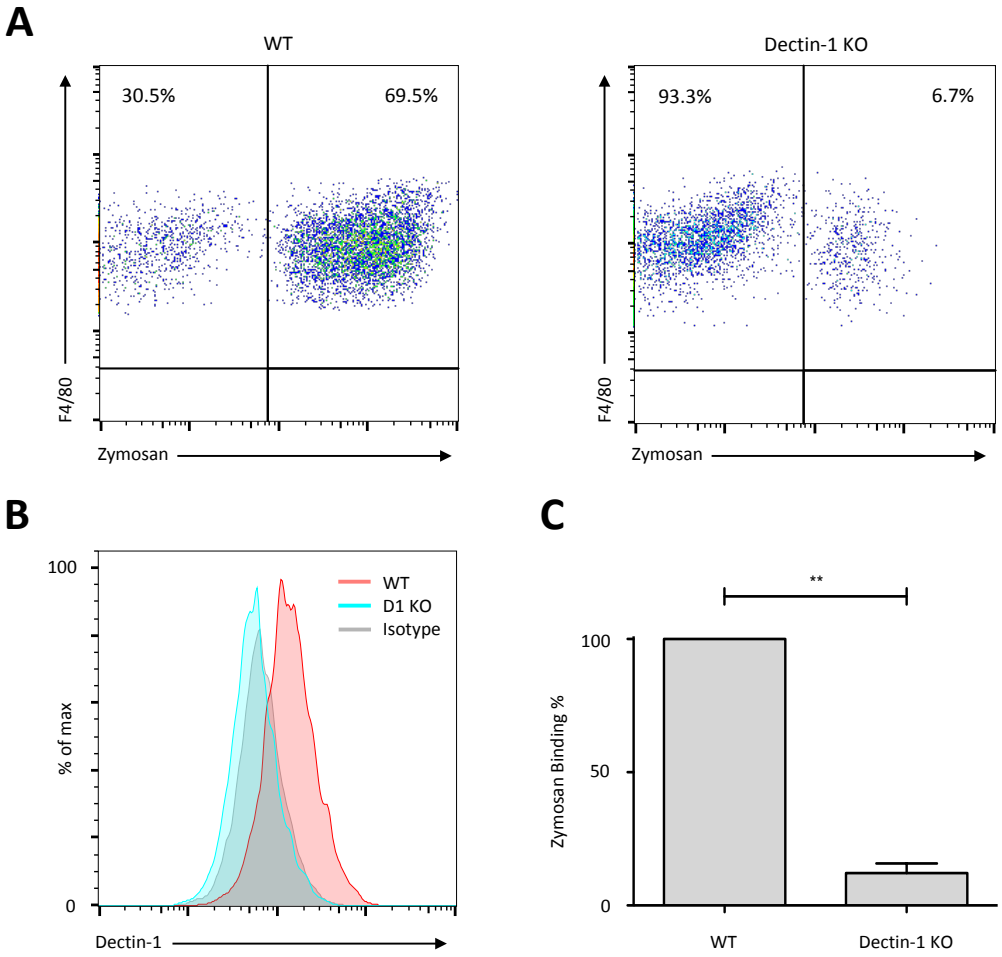

Figure 3.13: Dectin-1 KO BMDMs possess significantly impaired zymosan recognition. (A) 2.5µg FITC-labeled zymosan was incubated with C57BL/6 WT or Dectin-1 KO derived BMDMs for 15 minutes at 37°C 5% CO_2. Cells were stained with anti-F4/80, anti-CD11b and anti-mDectin-1. Flow cytometry was used to identify $CD11b^+$ and $F4/80^+$ macrophages; zymosan recognition was determined on these cells. **(B)** Dectin-1 expression on WT or Dectin-1 KO BMDMs was determined by flow cytometry. **(C)** Data as displayed in **(A)** was used to elicit zymosan binding of WT and Dectin-1 KO BMDMs. WT zymosan binding was set at 100% per independent experiment and corresponding Dectin-1 KO zymosan recognition result calculated against each experiments WT recognition result. Graph displays mean +/- s.e.m.. **(A & B)** Data displayed are representative of three independent experiments. **(C)** Data shown are the mean collated from three independent experiments. Student's t-test was used to determine statistical significance, **p<0.005.

Figure 3.13 shows that Dectin-1 expression on BMDMs is required in order for cells to recognise zymosan. This experiment confirms the Dectin-1 dependency trend identified in neutrophils (figure 3.12) is conserved in BMDMs. The experimental protocol could now be used to identify whether NE-treatment reduces zymosan recognition. These experiments were completed using C57BL/6 WT and C57BL/6 Dectin-1 KO BMDMs. In order to elicit the impact the NE-induced cleavage of Dectin-1 has on the ability of BMDMs to recognise zymosan, BALB/c -derived BMDMs were treated with NE before being incubated with FITC-labeled zymosan.

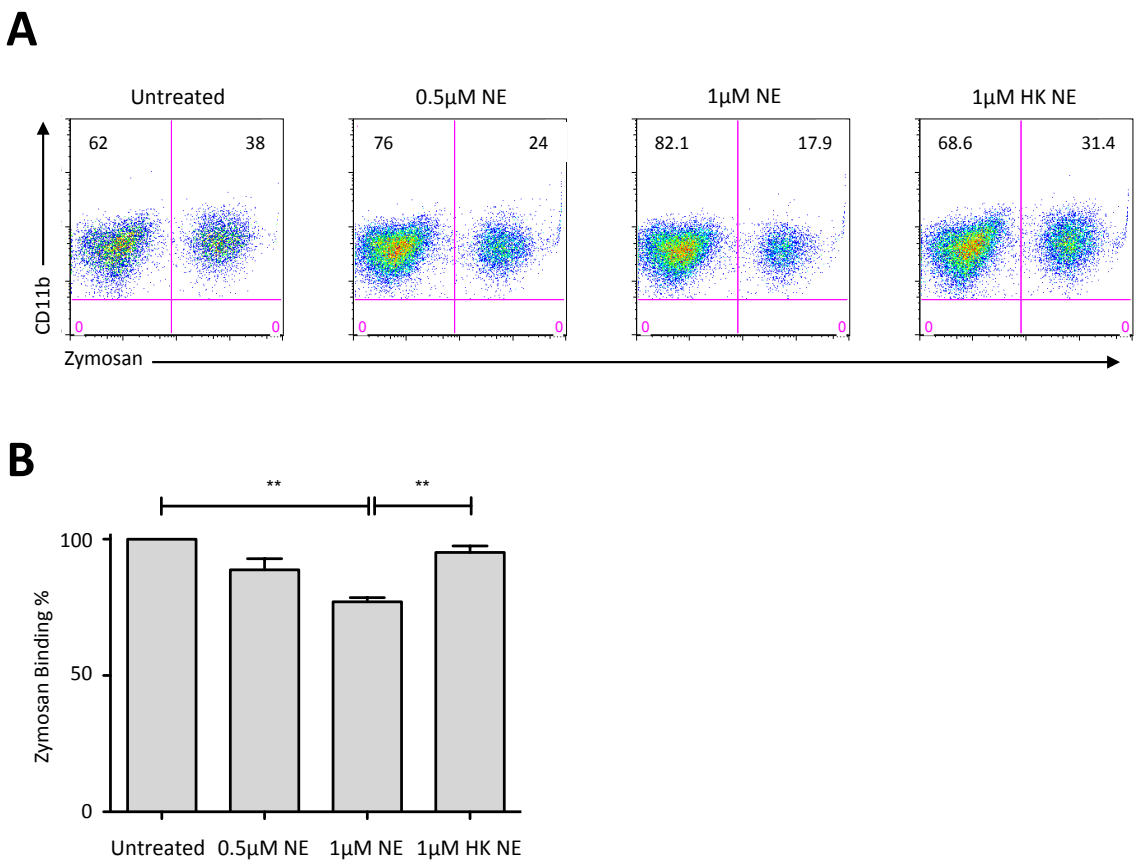

Figure 3.14: NE cleavage of mDectin-1 on BALB/c **derived BMDMs significantly impairs zymosan recognition. (A)** BALB/c derived BMDMs were treated with 0.5µM NE, 1µM NE or 1µM HK NE for 1 hour at 37°C 5% CO_2 before 2.5µg FITC-zymosan was incubated with the cells for 15 minutes. Cells were stained with anti-CD11b, anti-F4/80 and anti-mDectin-1. Flow cytometry was used to identify $CD11b^+$ $F4/80^+$ macrophages; zymosan recognition was determined on these cells. **(B)** Untreated BMDM zymosan binding was set at 100% per independent experiment and corresponding treated BMDM zymosan recognition result calculated against each experiment's untreated recognition result. Graph displays mean +/- s.e.m.. **(A)** Data displayed are representative of three independent experiments. **(B)** Data shown are mean collated from three independent experiments. A one-way analysis of variance with Bonferroni's post-test was used to determine statistical significance. ** $p<0.005$.

Figure 3.14 describes the significant reduction in BMDM's ability to recognise zymosan following the NE- induced cleavage of Dectin-1. These results allow the NE-induced loss of Dectin-1 expression to be associated with a reduced ability to recognise fungal ligands. Here, for the first time a potential role describing the NE cleavage of Dectin-1 reducing airway anti-fungal immune response is described.

The isoform-specific Dectin-1 cleavage impact of NE was examined. Zymosan recognition by NIH-3T3 cells expressing either hDectin-1 isoform A or hDectin-1 isoform B was determined after NE-treatment. This experiment also identified whether the significant reduction in zymosan recognition after NE-treatment described in mDectin-1 (figure 3.14) was conserved in hDectin-1.

The expression of hDectin-1 Isoform A and Isoform B on NIH-3T3 cells was not identical; therefore, optimal zymosan dose was determined to attain ~25-50% recognition for both isoforms. This allowed the same zymosan dose to be used for both isoforms (as untreated zymosan recognition was set at 100%) and for the impact of NE reducing zymosan recognition to be discernable.

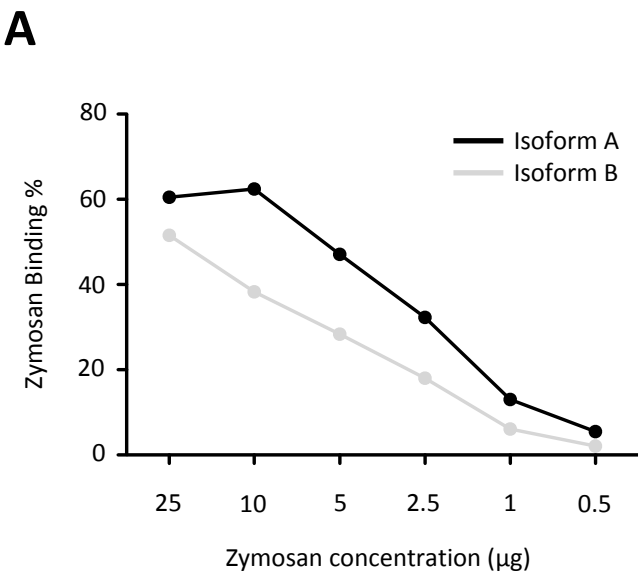

Figure 3.15: hDectin-1 isoform A and isoform B possess enough zymosan recognition affinity that 4µg zymosan provides ~25-50% binding, the optimal requirement for determining the impact NE cleavage has on hDectin-1 in recognition assays. (A) NIH-3T3 cells expressing either hDectin-1 Isoform A or Isoform B were incubated with varying concentrations of FITC-labeled zymosan for 15 minutes at 37^{o}C 5% CO_2 before zymosan recognition was determined using flow cytometry. The expression of hDectin-1 Isoform A and Isoform B was not identical on each cell line, see figure 3.2 for hDectin-1 Isoform expression on each cell line. Data shown are from one pilot experiment.

A dose of 4µg zymosan provided ~25-50% recognition in both hDectin-1 Isoform A and Isoform B. NIH-3T3 cells expressing either hDectin-1 Isoform A or Isoform B were treated with NE before being incubated with 4µg FITC-labeled zymosan. NE's impact on zymosan recognition for each hDectin-1 isoform was determined by flow cytometry.

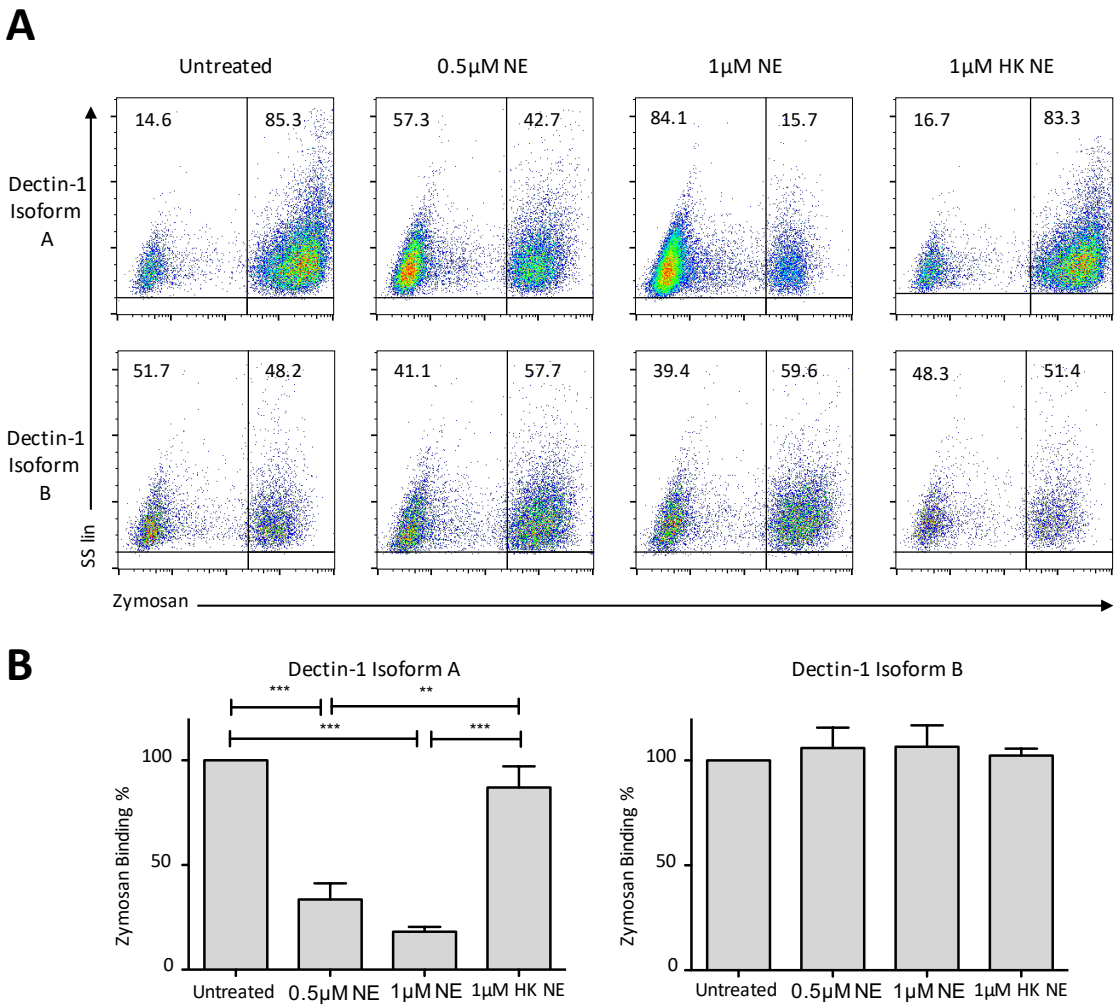

Figure 3.16: NE cleavage of hDectin-1 Isoform A significantly impairs zymosan recognition. **(A)** NIH-3T3 cells expressing either hDectin-1 Isoform A or Isoform B were exposed to 0.5µM NE, 1µM NE or 1µM HK NE for 1 hour at 37°C 5% CO_2 before 4µg FITC-labeled zymosan was incubated with the cells for 15 minutes. Zymosan recognition was determined by flow cytometry. **(B)** Untreated zymosan binding was set at 100% per independent experiment and corresponding treated zymosan recognition result calculated against each experiment's untreated recognition result. Graph displays mean +/- s.e.m.. **(A)** Data displayed are representative of three independent experiments. **(B)** Data shown are mean collated from three independent experiments. A one-way analysis of variance with Bonferroni's post-test was used to determine statistical significance. ** $p<0.005$, *** $p<0.0005$.

Figure 3.16 highlights a significant, isoform-specific role for NE-cleaving hDectin-1 Isoform A and reducing zymosan recognition. No reduction in zymosan recognition was attained when hDectin-1 Isoform B cells were treated with NE. This experiment confirmed the significant trend seen in figure 3.13 and 3.14 using mDectin-1 was conserved in hDectin-1. The greater loss of zymosan binding identified in NIH-3T3 cells (figure 3.16) when compared to BALB/c BMDMs (figure 3.14) is likely due to the exclusive expression of isoform A in the NIH-3T3 cell line but equal expression of Isoform A and B in BALB/c BMDMs.

Finally, although a significant zymosan recognition deficiency has been associated with NE treatment, no impact of NE has been identified to directly impair A.*f*. recognition or the anti-A.*f*. immune response. An A.*f*. specific recognition deficiency could not be described, as immune cells possess A.*f*. recognition redundancy through a range of CLRs and TLRs; therefore, experiments were undertaken to identify an anti-A.*f*. cytokine response deficiency resulting from NE-treatment. The recognition of A.*f*. may not exclusively require Dectin-1; however, the generation of a robust immune response against A.*f*. does require the A.*f*. engagement of Dectin-1 [2, 99].

The data and experiments displayed in figure 3.17 were completed and analysed by Dr Selinda Orr. The protocol used for this experiment was formulated from preliminary experiments I had previously completed, some of which are displayed in figure 3.10 and figure 3.11. In order to identify a functional cytokine impact resulting from the NE-induced cleavage of Dectin-1, purified monocytes (enriched from BIOgel-elicited cells) were treated with NE or HK NE before being stimulated with A.*f*. SC or zymosan. TNF was quantified for each stimulant and treatment condition.

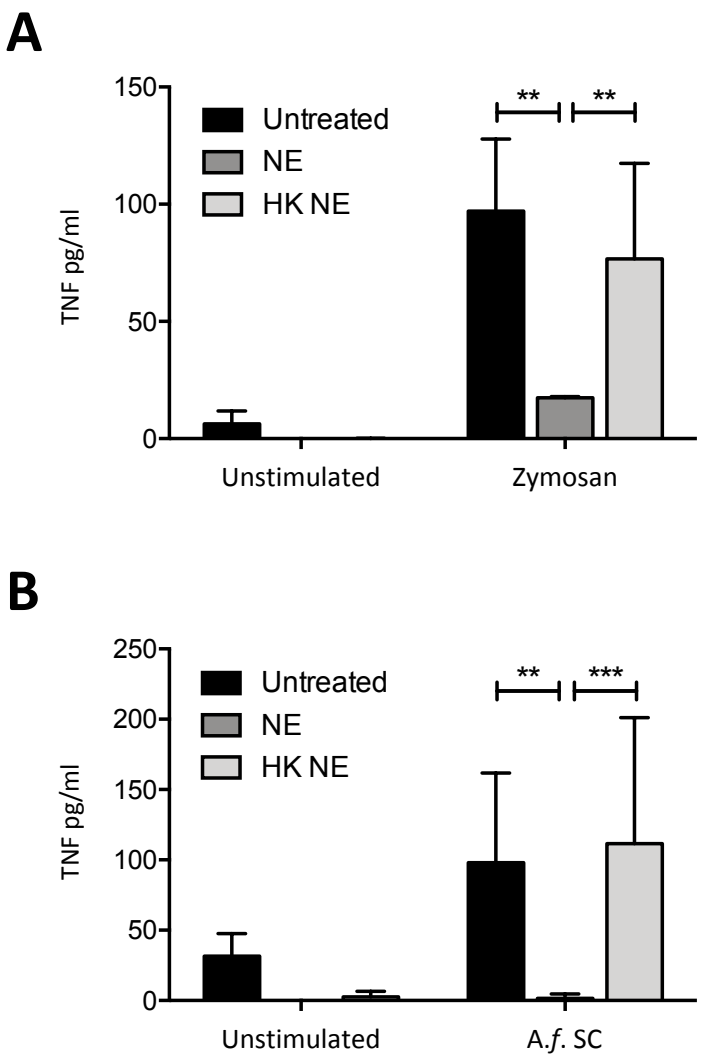

Figure 3.17: NE-treated monocytes produce significantly impaired TNF responses against zymosan and A.*f*. SC. (A & B) BIOgel-elicited cells were washed with MACS buffer (PBS 0.5% BSA 2mM EDTA) and stained with anti-Ly6G-Biotin before cells were incubated with anti-Biotin microbeads. Inflammatory monocytes were enriched by MACS separation according to manufacturer's protocol. 2-4x10^5 Cells were suspended in serum-free assay buffer and treated with 4µM NE or 4µM HK NE for 1 hour at 37°C 5% CO_2. Cells were stimulated on top of existing NE or HK NE treatment for 4 hours at 37°C 5% CO_2 with **(A)** 2.5µg zymosan or **(B)** 0.6-1.2x10^5 A.*f*. SC in a ratio of 3:1 with cells. ELISA was used to determine TNF concentration from each treatment and stimulant condition. Graph displays mean +/- s.e.m.. **(A)** Data shown are mean collated from three independent experiments. **(B)** Data shown are mean collated from five independent experiments. **(A & B)** A one-way analysis of variance with Bonferroni's post-test was used to determine statistical significance. ** $p<0.005$, *** $p<0.0005$.

The data displayed in figure 3.17 describes the significant impairment of monocytes anti-A.*f*. TNF response after treatment with NE. These data associate the NE-induced loss of Dectin-1 on immune cell types recruited to the CF airway with the increased susceptibility to A.*f*. infection CF patient's experience.

Figure 3.17 suggests the mechanism by which CF patients, already with high neutrophil infiltration and high NE airway activity, generate impaired anti-A.*f*. responses. An NE-induced loss of Dectin-1 expression results in reduced A.*f*. recognition and signalling likely culminating in reduced A.*f*. clearance. Recurrent, chronic and poorly challenged A.*f*. infections may enhance airway inflammation and exacerbate underlying airway disease.

3.4: Discussion

CF affects ~1 in every 2500 births in the UK causing progressive airway disease due to recurrent, poorly challenged chronic infections. Recurrent bacterial and fungal infections lead to the generation of a chronic inflammatory setting in the airway. CF patient's increased susceptibility to chronic infections such as A.*f*. is not well understood. Immune cells recruited to combat pathogens become immobilised in mucus not appropriately trafficked by the defective mucociliary escalator and contribute to chronic inflammation [26, 222]. Neutrophils are the predominant cell recruited and retained in the CF airway. A high airway infiltration of neutrophils is directly associated with worsening disease progression and declining lung function [27, 224]. Once recruited and trapped in the airway, neutrophils exacerbate airway pathology by releasing serine proteases into the local tissue environment. Serine proteases are an important facet of neutrophil's anti-microbial response; however, when poorly regulated, proteases damage local tissue and further disrupt the mucociliary escalator. Neutrophil-derived serine proteases also interfere with many integral components of the immune response, weakening the already CF-dampened immune response to pathogens in CF lungs. Currently, neutrophil-derived serine proteases have been described to inactivate elements of the complement system, cleave TLRs and cleave soluble IL-6R rendering these host defence mechanisms obsolete in the CF airway [27, 226].

Similar to NE-induced cleavage of TLRs and IL-6R, the research in this chapter demonstrates the susceptibility of Dectin-1 Isoform A to NE-induced cleavage and investigates the functional consequences this may convey. Cleavage of Dectin-1 Isoform A in the CF airway would likely impair A.*f*. recognition and inhibit A.*f*. immune challenge. This may permit the persistence of A.*f*. infection in the CF airway further enhancing inflammation. Persistent A.*f*. infection and increased inflammation would only worsen CF patient morbidity and mortality. Understanding the immune debilitating action of neutrophil-derived serine proteases such as NE may enhance the

already commenced development of therapeutics that block their action. Blocking the ability of serine proteases to cleave components of the host immune system may increase the effectiveness of the local immune response. This would hopefully contribute to the clearance of chronic infections, resolution of inflammation and improvement of underlying CF disease.

3.4.1: Does neutrophil elastase cleave Dectin-1?

Here, a novel role for NE-induced cleavage of the CLR Dectin-1 has been demonstrated. I demonstrate that NE cleaves Dectin-1 in an isoform specific manner, only cleaving Isoform A that contains the stalk-region. We have also shown that BALF from CF patients induces Dectin-1 cleavage. The percentage loss of Dectin-1 expression *in vitro* correlates with increased NE activity and greater neutrophil numbers in the BALF. This suggests that the cleavage of Dectin-1 may occur in the CF airway where high neutrophil infiltration and NE activity are commonplace. Crucially, this research adds the first CLR, Dectin-1, to the growing repertoire of human immune components including IL-6R, complement receptors and TLRs, susceptible to cleavage and inactivation by the neutrophil serine protease NE [32, 34, 35].

The role of Dectin-1 during invasive A.*f*. infections has been well investigated; the role this CLR conveys in the CF airway, especially when cleaved by NE, has not been explored. Dectin-1 is vital for anti-fungal responses to *A.f.* and multiple other fungal species. A.*f*. utilises an immunologically inert rodlet layer present on resting conidia to mask cell wall components such as β-glucans and α-mannans that act as PAMPs. Upon A.*f*. germination this rodlet layer is shed allowing host immune PRRs to recognise A.*f*. cell wall components and induce an immune response. Dectin-1 is required for the recognition of A.*f*. β-glucans and generation of an anti-A.*f*. immune response [99, 171].

The isoform specific susceptibility of Dectin-1 to NE-induced cleavage is intriguing. The important role Dectin-1 plays during the A.*f*. immune response is clear. Lacking this receptor impairs the anti-A.*f*. response and significantly enhances susceptibility to A.*f*.

infection. The importance of the individual isoforms of Dectin-1 has not yet been studied in depth; although, location-specific expression of isoforms A and B on different myeloid cell subsets is starting to be unraveled. While both isoforms were thought to be functionally similar, recent evidence suggests distinct inflammatory responses result from the engagement of each isoform [161, 228]. This requires further study in different myeloid cell populations. The resistance Dectin-1 Isoform B possesses against NE-induced cleavage suggests this isoform may play a vital role in anti-fungal immunity in the CF airway, specifically during periods of intense neutrophil inflammation producing high concentrations of NE.

I have demonstrated that the NE-induced cleavage of Dectin-1 Isoform A takes place on cell types relevant to the CF airway and recruited during A.*f*. infection. Macrophages act as the front-line immune response against A.*f*. and possess a range of anti-fungal capabilities including A.*f*. phagocytosis and anti-A.*f*. cytokine and chemokine production [69]. Crucial for macrophage fungal-immunity is their expression of Dectin-1. Possessing this CLR is necessary for the orchestration of appropriate anti-A.*f*. immune responses [2]. The NE-induced cleavage of Dectin-1 Isoform A on macrophages likely reduces the ability of these cells to recognise early A.*f*. morphologies and generate robust immune responses that clear A.*f*.. The already impaired immune capabilities of CF patient macrophages are well known [238]. Here, the newly identified role for NE in cleaving Dectin-1 Isoform A and further curtailing the immune capabilities of macrophages, may enhance fungal disease and inflammation, exacerbating underlying disease pathology.

Neutrophils are the best-described contributors to inflammation in the CF airway, mainly due to their release of serine proteases such as NE. Serine proteases have potent anti-microbial properties but when poorly regulated, as is often the case in CF patients, they can be very damaging to local tissue and immune responses. A high infiltration of neutrophils in the CF airway is associated with regular bacterial and fungal infection, a highly inflammatory setting and declining lung function [27, 224]. The role of Dectin-1 expressed on neutrophils during the anti-A.*f*. immune response has not been thoroughly investigated; although, the anti-fungal capabilities of

neutrophil-expressed Dectin-1 has been identified. Experiments blocking Dectin-1 on human neutrophils resulted in the reduced phagocytosis of zymosan and *Candida albicans* and also blocked ROS production [102]. It is likely that neutrophils have a similar impact against A.*f*., phagocytosing conidia and producing ROS against hyphae. More recently, Dectin-1 deficiency has been shown to disrupt NETosis, a crucial A.*f*. hyphae-killing mechanism [29, 239]. The demonstrated NE-induced cleavage of Dectin-1 expressed on neutrophils would suggest these cells lose some capability to recognise fungal pathogens such as A.*f*. and to respond with phagocytosis, ROS production or NETosis.

In addition, the NE-induced cleavage of Dectin-1 is conserved in inflammatory monocytes/macrophages. Monocytes have a complicated role during the anti-A.*f*. immune response dependent on their maturation stage and expression of CD16. $CD14^{+}CD16^{-}$monocytes were particularly effective at phagocytosing A.*f*. conidia but generated little cytokine response. $CD14^{+}CD16^{+}$ monocytes were poor at perturbing A.*f*. germination and phagocytosing conidia but generated robust cytokine responses. Although monocyte's role varies and probably depends on multiple factors, many of which are not understood, the ability of monocytes to block A.*f*. growth is widely accepted [130]. Monocyte-expressed Dectin-1 is required to control the fungal pathogen *Paracoccidioides brasiliensis*; however, the impact monocytes have against A.*f*. exclusively through Dectin-1 is not clear [240]. The pro-inflammatory role of monocytes in the CF airway is interesting. Monocytes have been shown, when recruited to the CF airway during inflammation, to become locked in a tolerant state unable to act upon bacterial or fungal challenge [241]. This tolerant state was thought to be the result of deficient cytokine signalling; however, a role for NE cleaving crucial PRRs such as Dectin-1, may contribute to the lack of monocyte mediated anti-fungal immune responses in CF lungs.

Here, I clearly demonstrate the capability of NE to induce Dectin-1 Isoform A cleavage on macrophages, neutrophils and monocytes. These cell types are readily recruited to the CF airway and are key components of anti-fungal immunity. The requirement of Dectin-1 expression on these cells when mounting anti-A.*f*. immune responses is

partially described. The lack of Dectin-1-A.*f*. engagement on these cells would likely impair the anti-A.*f*. immune response allowing pathogen persistence, enhancing chronic inflammation and worsening underlying CF disease.

3.4.2: Which Dectin-1 amino acid is required for NE-induced cleavage to occur?

Unfortunately, the research undertaken aiming to identify the Dectin-1 amino acid residue required for NE cleavage was unsuccessful. Having identified the isoform-specific cleavage action of NE, two enzyme databases were used to predict cleave locations within the Dectin-1 Isoform A specific stalk region. These databases compiled enzyme activity data from over 137 000 literature references and are regularly used to predict how a range of enzymes may cut sequences [242]. This database request provided four likely NE-cleavage sites located within the Dectin-1 Isoform A stalk region. All these residues were either alanine or valine, consistent with the NE-cleave sites identified in other proteins [243]. For my experiments, these residues were mutated to glycine which shouldn't have altered Dectin-1's tertiary structure; although, it may have impacted protein function [234]. However, as the mutation of predicted cleavage sites to glycine increased the NE-induced cleavage of Dectin-1, I predict that inserted glycine residues have straightened the tertiary structure of Dectin-1 thus increasing the accessibility of the stalk region and enhancing NE cleavage. A similar mechanism of glycine straightening protein tertiary structures has been previously identified [235].

The NE cleavage location of many immune components susceptible to NE inactivation has not been identified. NE's cleavage of complement C3bi, CR1 and C5aR, epithelial cadherins, IL-6R and TLR4 do not have described cleavage sites [32, 34-36, 244]. Here, although I was unsuccessful at abrogating NE activity by mutating single potential NE cleavage sites, it is likely that NE cleavage can occur at all four predicted residues. The fact that NE cannot cleave Dectin-1 Isoform B, at least places the NE-cleavage required amino acid residues within the Isoform A exclusive stalk region. Further experiments

mutating multiple predicted cleavage sites in tandem, or mutating to a different amino acid residue may lead to the abrogation of NE-induced cleavage of Dectin-1 Isoform A.

3.4.3: Is there a functional consequence resulting from the NE-induced cleavage of Dectin-1?

As previously mentioned, Dectin-1 is crucial for the recognition and generation of successful anti-A.*f*. immune responses. Lacking Dectin-1, or Dectin-1 signalling components significantly enhances susceptibility to A.*f*. infection [69, 171]. We have extensively demonstrated human and mouse Dectin-1 Isoform A's susceptibility to NE-induced cleavage in cell types resident or recruited to the CF airway during A.*f*. infections. Here I explore the functional consequences lacking Dectin-1 A.*f*. recognition conveys over the anti-A.*f*. immune response.

Initially experiments were undertaken to identify the importance of Decitn-1 expression on myeloid immune cells for A.*f*. recognition. I show that neutrophils possess high Dectin-1 redundancy when recognising A.*f*., this has been previously identified [99, 245]. Crucially, although many immune cells possess Dectin-1 redundancy when recognising A.*f*., the generation of robust inflammatory responses are dependent on Dectin-1 engagement [2].

In order to investigate a functional consequence resulting from the reduced expression of Dectin-1, zymosan was used for Dectin-1 recognition experiments. Zymosan is routinely used as a sterile model of fungal infection. As a pure β-(1-3) glucan extracted from fungal cell walls, the immunogenic-carbohydrate is recognised almost entirely by Dectin-1 [171, 205, 246]. The experiments completed using zymosan to identify the dependency of myeloid cells on Dectin-1 to recognise β-(1-3) glucans aligns with previous work suggesting this recognition is Dectin-1 dependent [2, 100, 205]. Here, I demonstrate myeloid cells reduced capacity to recognise common fungal cell wall components such as β-(1-3) glucan after NE-induced cleavage of Dectin-1.

Finally, we also demonstrate that the NE-induced cleavage of Dectin-1, along with reducing zymoson recognition, functionally impairs the immune response against A.*f*. and zymosan. Monocytes treated with NE before being stimulated with live A.*f*. or zymosan generated reduced TNF responses. This concurs with research suggesting Dectin-1 KO monocytes exhibit impaired TNF responses [161]. Our results add to the increasing repertoire of research already describing the immune-impairing impact of NE, including the functional inactivation of complement components and soluble IL-6R.

However, our results differ from a recently described role for NE, whereby NE induces TLR4 cleavage and subsequently promotes cytokine production. This result variation may be due to different experimental protocols being used. The study linking TLR4 NE-cleavage with an increased cytokine response removed NE treatment before stimulating cells [32]. In contrast, we stimulated cells in the presence of NE and identified a reduced TNF response. Interestingly, our data highlights the rapid recovery of Dectin-1 expression when serum-containing media is added to cells and/or when NE treatment is removed. It may be the case that Dectin-1 recovered beyond 100% of basal expression in the TLR4 experiments in which NE increased cytokine responses. The CF airway setting exposes immune cells to consistent, high levels of NE. Therefore, our experiments completed in the constant presence of NE are likely more similar to the physiological setting. It is worth mentioning that the reduced TNF response resulting from Dectin-1 NE treatment cannot be completely attributed to Dectin-1. Other CLRs and immune components susceptible to NE-induced cleavage likely contribute to the reduced TNF response.

The NE-induced cleavage of Dectin-1 and ensuing lack of A.*f*. recognition and response may have far reaching consequences for the host's overall anti-fungal response capabilities. CLRs and TLRs are not only involved in fungal killing and inflammatory cell recruitment, but also provide a link to the adaptive immune response [245, 247]. Recent evidence implicating the importance of adaptive immune responses against fungal pathogens such as A.*f*. has emerged [115, 248]. Successful clearance of A.*f*., especially during chronic infections, was associated with the formation of robust T_H1

and T_H17 responses [249]. Dectin-1 and TLRs promote T_H1 and T_H17 responses through their ability to modulate cytokines such as IL-12 and IFNγ. Specifically a robust Dectin-1 IL-12 response reduces T-Bet expression in A.*f*. specific $CD4^+$ T cells and facilitates T_H17 differentiation [135].

A.*f*. appears to be particularly effective at initiating T_H2 immune responses via the release of allergen proteins exclusively recognised by $CD4^+$ T_H2-cells or IgE. The fungal engagement of these immune components likely aids T_H1 response evasion promoting pathogen survival [129]. Our research is specifically relevant here as monocytes and monocyte derived cells link the innate and adaptive immune systems. Recruited monocytes phagocytose A.*f*. using CLRs such as Dectin-1 before migrating to lymph nodes and priming $CD4^+$ T-cells [131]. Monocyte A.*f*. recognition, phagocytosis, migration and antigen presentation culminates in a host-protective T_H1 response. I have demonstrated Dectin-1 expressed on monocytes is susceptible to NE-induced cleavage. As Dectin-1 is the principal A.*f*. phagocytic receptor, NE may block monocyte A.*f*. phagocytosis and antigen presentation abrogating the generation of an anti-A.*f*. T_H1 response.

3.5: Conclusions

The CF airway is a very complicated setting with various immunological and structural abnormalities. A dysfunctional mucociliary escalator resulting from a faulty CFTR protein leads to the accumulation and reduced clearance of thick mucus. Subsequently recurrent and chronic bacterial and fungal infections ensue and large influxes of immune cells, specifically neutrophils are recruited to combat pathogens. A highly inflammatory setting is generated as pathogens and immune cells are retained in thick mucus. Here, neutrophils release serine proteases as a defence mechanism; however, this release is poorly regulated due to the local environment and lack of neutrophil clearance. Released serine proteases such as NE drastically impact the local setting and damage pathogens and host tissues as well as impairing the immune response. Here we describe a role for the NE-induced cleavage of Dectin-1 in the CF airway reducing the ability of resident and recruited immune cells such as macrophages, neutrophils and monocytes to recognise and respond to pathogens such as A.*f*.. Reduced pathogen recognition and an impaired immune response would result in the insufficient killing and clearance of the pathogen. Overall this would lead to increase inflammation in the CF airway driving further tissue damage, fibrosis and culminating in diminished lung function.

Therapeutically blocking the action of serine proteases in the CF airway may halt the damaging impact NE has on Dectin-1. Retaining immune cells ability to recognise pathogens would permit the more successful killing and clearance of pathogens. This may curtail the chronic inflammation resulting from recurrent and ineffectively challenged airway infections such as A.*f*..

Chapter 4

Understanding the collective roles of Dectin-1, Dectin-2 and Mincle in anti-*Aspergillus fumigatus* immunity

4.1: Aims

i. Identify the role of Dectin-1, Dectin-2 and Mincle in anti-A.*f*. immunity

ii. Determine any redundancy/collaboration between these CLRs

iii. Identify whether CLR collaboration enhances the anti-A.*f*. immune response

4.2: Introduction

Invasive A*spergillosis* is a major cause of infection-related mortality in severely immune-compromised patients. The disease often caused by A.*f*. is becoming an increasingly serious, worldwide healthcare problem. The anti-A.*f*. immune response is complex and not well understood. A.*f*. RC are protected from environmental stress by an inert outer protein rodlet layer, this provides very little immune stimulation upon conidial inhalation. As conidia begin to germinate multiple carbohydrate molecules are revealed and act as PAMPs. Immune recognition and response is driven by the exposure of PAMPS to PRRs [2, 99]. The best-described PRR involved in A.*f*. recognition is the CLR Dectin-1. This CLR is crucial in the early anti-A.*f*. immune response and leads to the phagocytosis of inhaled conidia and recruitment of non-resident immune cells such as neutrophils via the release of cytokines and chemokines [2]. Dectin-1 has been thoroughly investigated and a clear anti-fungal and anti-A.*f*. role for this CLR has been identified. I am particularly interested in the CLRs Dectin-1, Dectin-2 and Mincle. I hypothesise that these CLRs are crucial in the recognition, initiation and driving of the complex anti-A.*f*. immune response.

Alveolar macrophages act as the first responders in the anti-A.*f*. immune response. These resident phagocytic cells of the respiratory tract and lung express many PRRs [1]. Alveolar macrophages deficient in Dectin-1 possess a significantly reduced ability to generate appropriate pro-inflammatory responses against A.*f*.. When alveolar macrophages were stimulated with early morphologies of A.*f*. a robust TNF, MIP-1, MIP-2 and IL-1β response was attained [92-94]. When the same experiments were completed with Dectin-1 blockade a significant reduction in the pro-inflammatory response occurred highlighting the key role Dectin-1 plays in early A.*f*. recognition on alveolar macrophages [2, 98]. The presence of, and a role for, Dectin-2 and Mincle on alveolar macrophages have yet to be fully described. Mincle expression on lung-resident alveolar macrophages was described after infection with *Mycobacterium*

bovis bacillus Calmette-Guérin [192]. Suggesting the CLR is at least inducible on alveolar macrophages.

Although alveolar macrophages are the resident lung immune cell and first responder against A.*f*., it is important to determine the role CLRs play in the whole organism's anti-A.*f*. response and not just in *ex vivo* cells. *In vivo* A.*f*. challenge experiments have previously described the enhanced susceptibility of Dectin-1 KO mice when challenged with A.*f*.. Significantly reduced cytokine and chemokine profiles at 24 hours, increased fungal burden at 24 and 48 hours, and reduced survival at 5 days highlight the requirement of Dectin-1 expression when challenged with A.*f*. [100]. Interestingly, a collaborative role for Dectin-1 and Dectin-2 during *Trichophyton rubrum* infection has recently been identified. Mice lacking Dectin-1 and Dectin-2 produced significantly impaired anti-fungal cytokine and chemokine responses when compared to WT or Single CLR KO mice. This resulted in a significantly increased fungal burden [221]. A collaborative role for Dectin-1 with other CLRs during A.*f*. infection has not been described. The impact of Dectin-2 and Mincle engagement individually and collaboratively on the *in vivo* anti-A.*f*. immune response also requires investigation.

Limited data suggests the expression of Dectin-2 is up regulated during fungal challenge and the receptor has been demonstrated to recognise predominantly larger morphologies of A.*f*. [179, 183]. Dectin-2 is thought to possess a range of possible responses when encountering A.*f*.. The receptor can induce cytokines and chemokines such as TNF, IL-6 and Mip-1, producing a pro-inflammatory anti-fungal response. Dectin-2 signalling through the MAPK pathway drives the generation of a T_H17 regulatory response via the induction of IL-1β and IL-23. Dectin-2 can also activate the inflammasome resulting in respiratory burst [181, 182]. Dectin-2's impact during the anti-A.*f*. response has not been extensively investigated. An *in vivo* role for this receptor within the CLR-mediated anti-A.*f*. response has not been described.

The role Mincle plays within the anti-A.*f*. response is complicated and poorly defined. Mincle associates with FcγR upon *Candida albicans* stimulation leading to the production of pro-inflammatory cytokines and chemokines [190]. A role for Mincle

synergistically collaborating with TLRs whilst binding α-mannan has been described. This collaboration enhanced bacterial challenge response [187]. A similar role for Mincle collaborating with other CLRs is unknown. A controversial role for Mincle has been described *in vivo* during *Heliobactor pylori* infection. Mincle was up regulated and engaged by *H. pylori*, which consequently skewed the immune response in an anti-inflammatory direction and increased disease burden [194]. The impact A.*f*. engagement has on Mincle and the subsequent Mincle-driven and anti-A.*f*. response is unknown.

Understanding the role CLRs play within the anti-A.*f*. immune response will provide valuable insights into the complex challenge the immune system faces when coordinating appropriate responses to A.*f*.. This challenge is often made more difficult with the complex immune-suppression therapies susceptible patients are often receiving. Determining which CLRs are involved in the early and later immune response, their expression profile and their role in the collaborative response may identify crucial cellular and receptor requirements to successfully challenge A.*f*.. Ultimately, describing the role of CLRs in orchestrating the immune response, and identifying any collaboration or redundancy within the system could lead to the generation of new therapeutics with the potential to enhance the anti-A.*f*. response in patients struggling to control disease.

4.3: Results

4.3.1: What role do CLRs play in the alveolar macrophage anti-A.*f*. response?

Alveolar macrophages are a crucial facet of the anti-A.*f*. immune response required for the host's control of the pathogen. The ability of alveolar macrophages to challenge A.*f*. is likely dependent on CLR-mediated responses. Here I examine the impact CLRs convey over alveolar macrophages anti-A.*f*. cytokine and chemokine response. The requirement of Dectin-1 on alveolar macrophages has been well described [2, 99, 250]. This permitted our Dectin-1 KO model results to be aligned with published research before all other CLR KO and CLR DKO models were examined.

Alveolar macrophages were extracted by performing BAL on naïve mice. In order to determine whether alveolar macrophages needed to be enriched from BAL, the purity of alveolar macrophages within recovered BAL was examined. Total recovered BAL cells were stained with alveolar macrophage markers and analysed by flow cytometry.

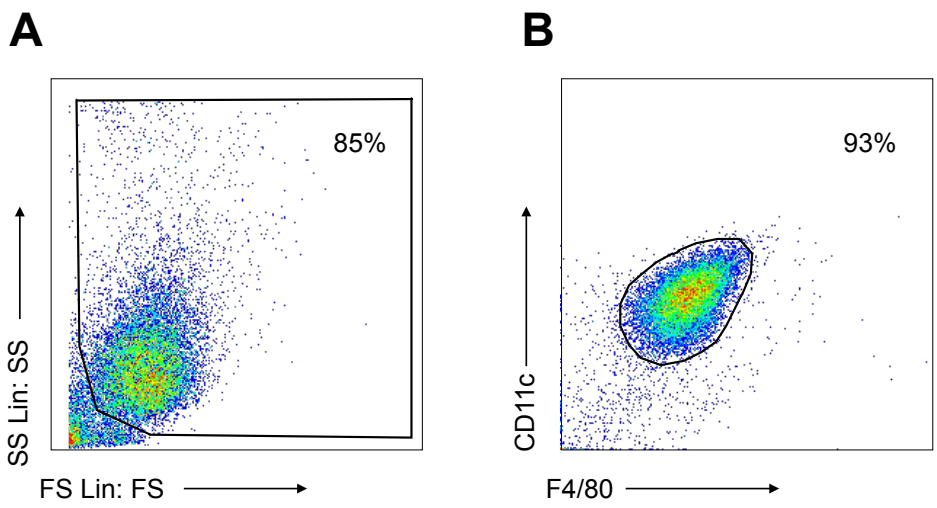

Figure 4.1: BAL recovered cells are ~90-95% alveolar macrophage. BAL was performed on C57BL/6 mice; BAL-recovered cells were stained with anti-CD11c and anti-F4/80 and analysed by flow cytometry. **A)** Cells were separated by SS Lin: SS and FS Lin: FS, dead cells and debris were gated out and live cells were carried through to a new gate. **B)** Alveolar macrophages were identified by $CD11c^+$ and $F4/80^+$ expression. Similar flow cytometry profiles were observed for all WT, CLR KO and CLR DKO BAL-recovered cells. Data displayed are representative of 4 independent experiments each with at least 5 mice per WT, CLR KO or CLR DKO genotype.

BAL-recovered cells consist predominantly of alveolar macrophages; therefore, in all following experiments BAL-recovered cells were used as a pure alveolar macrophage population.

To identify the impact CLRs convey over the alveolar macrophage anti-A.*f*. response the expression of CLRs on each CLR knock out (KO) or CLR double knock out (DKO) model was confirmed. BAL was performed on WT mice and mice from each CLR KO or CLR DKO model. Total BAL-recovered cells were stained with anti-CD11c and anti-F4/80 to identify alveolar macrophages. Antibodies against each CLR were used to elicit the expression of CLRs on each CLR KO or CLR DKO model; this was determined by flow cytometry.

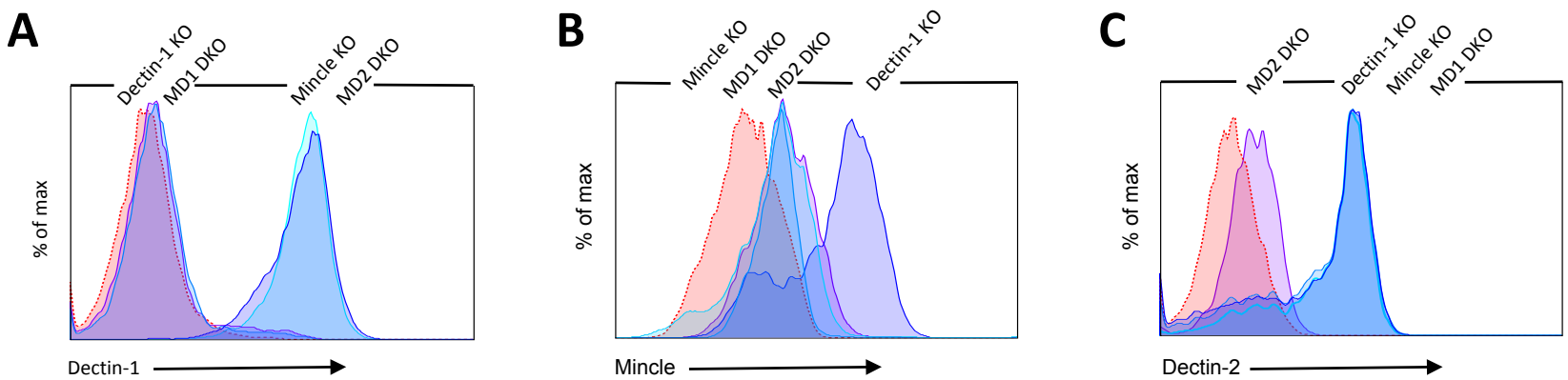

Figure 4.2: All CLR KO models express their expected CLRs. BAL was performed on C57BL/6, CLR KO and CLR DKO mice. In order to determine Mincle and Dectin-2 expression, BAL-recovered cells were stimulated with 2µg/ml LPS for 4 hours at 37°C 5% CO_2 prior to antibody staining. BAL-recovered cells were stained with anti-CD11c, anti-F4/80 and anti-CLR before being analysed by flow cytometry. CLR expression was determined on alveolar macrophages that were gated on as described in figure 4.1. **A)** Dectin-1 expression on WT, CLR KO and CLR DKO mice **B)** Mincle expression on WT, CLR KO and CLR DKO mice **C)** Dectin-2 expression on WT, CLR KO and CLR DKO mice. CLR Isotype antibody staining is displayed as red-dotted histograms. Data displayed are representative of 3 independent experiments.

The WT, CLR KO and CLR DKO *in vivo* models used for experiments possess the expected CLR expression profiles. This permits the use of alveolar macrophages from these *in vivo* models to elicit the impact CLRs have on the alveolar macrophage anti-A.*f*. response. BAL was performed on WT mice and mice from each CLR KO or CLR DKO model. Obtained alveolar macrophages were stimulated with live A.*f*. and ELISA used to quantify cytokine and chemokine response.

A.*f*. possess an immunologically inert protein rodlet layer that is shed within 4-6 hours of germination. This rodlet layer masks PAMPS and helps A.*f*. resist immune recognition during early infection. Consequently, alveolar macrophages respond particularly well to germinated, SC and EG A.*f*. morphologies [2, 98]. 24 hours post-germination A.*f*. has developed HY structures that are much larger than alveolar macrophages rendering their immune response capabilities mostly obsolete. Due to this A.*f*. morphology-specific recognition and response, alveolar macrophages were stimulated for 24 hours with live A.*f*. RC allowing the immune cells to experience, recognise and respond to the full life cycle of A.*f*..

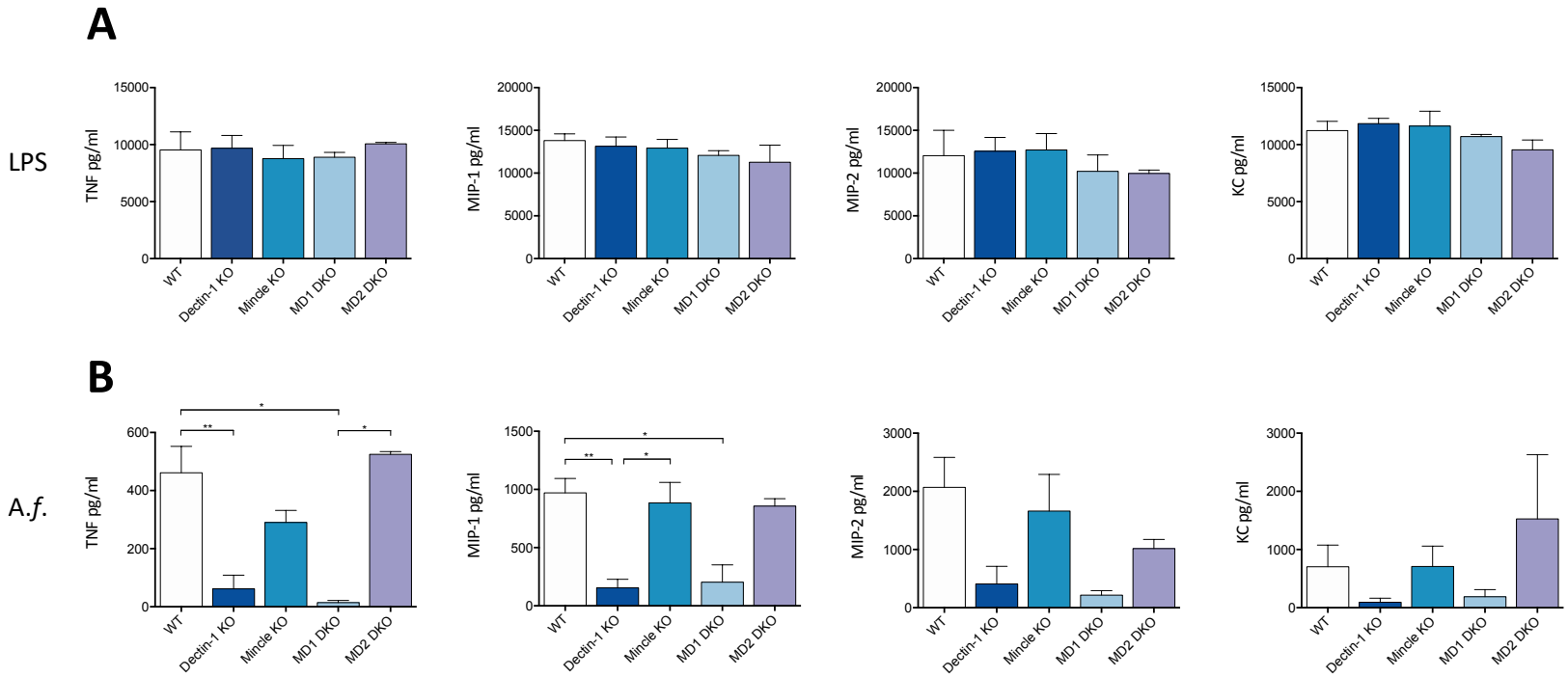

Figure 4.3: Dectin-1 KO and MD1 DKO alveolar macrophages produce a significantly impaired anti-A.*f*. chemokine and cytokine response. BAL-recovered cells from WT, CLR KO and CLR DKO mice were stimulated with **A)** 2µg/ml LPS or **B)** $1x10^5$ A.*f*. RC for 24 hours at 37°C 5% CO_2. After stimulation, ELISA was used to identify cytokine and chemokine quantities in supernatant. Graph displays mean +/- s.e.m.. WT data displayed are collated from 7 experiments, Dectin-1 KO and Mincle KO data displayed are collated from 4 experiments and MD1 DKO and MD2 DKO data displayed collated from 3 experiments. A one-way analysis of variance with Bonferonni's post-test was used to determine statistical significance. *p<0.05, **p<0.005.

Figure 4.3 indicates all CLR KO alveolar macrophages have the ability to produce TNF, KC, MIP-1 and MIP-2 upon LPS stimulation. No significant difference between WT, CLR KO or CLR DKO's LPS response was attained. Alveolar macrophages extracted from Dectin-1 KO and MD1 DKO mice produced a significantly impaired anti-A.*f*. TNF and MIP-1 response when compared to WT and Mincle extracted alveolar macrophages. The quantity of cytokines and chemokines produced from Dectin-1 and MD1 DKO alveolar macrophages is similar. This suggests Dectin-1 expression is required for alveolar macrophages to generate robust anti-A.*f*. cytokine and chemokine responses.

Figure 4.3 confirms the previously described Dectin-1-KO phenotype was preserved in the Dectin-1 KO alveolar macrophage model used for these experiments [2, 99, 250]. This provides validity to the impact described herein that other CLR KO and CLR DKOs have on alveolar macrophage's ability to respond to A.*f*..

It was next important to determine how each CLR KO impacts the whole organism's ability to generate an appropriate anti-A.*f*. response and control fungal burden.

4.3.2: Optimising the *in vivo* A.*f*. challenge model

An *in vivo* A.*f*. infection protocol was established and optimised for use in our facility. The protocol used as a starting point was taken from a well-described model of A.*f*. *in vivo* challenge [100]. These experiments identified the most accurate and least variable method of quantifying A.*f*. fungal burden following *in vivo* A.*f*. challenge. This method required the extraction of fungal genetic material from lung homogenate and A.*f*. 18S rRNA quantification using qPCR. Fungal burden was calculated by comparing experimental samples against a standard curve. This protocol was confirmed as the most sensitive method of quantifying fungal burden after comparing multiple techniques against actual fungal burden identified by histological analyses [251]. The histological determination of fungal burden is costly and time consuming rendering this technique unusable for large sample numbers.

The above-mentioned protocol for quantifying A.*f*. fungal burden *in vivo* requires two main components; firstly, the generation of an accurate A.*f*. standard curve; and secondly, the sensitive extraction of fungal genetic material from lung tissue. Typically for A.*f*. *in vivo* challenge experiments, the extraction of fungal RNA from known concentrations of A.*f*. RC is used to generate an A.*f*. standard curve. Extracted fungal RNA is used to produce cDNA, which is analysed by qPCR alongside experimental samples [100, 174, 252]. The clinical method of diagnosing an A.*f*. infection from BAL also involves the extraction of fungal genetic material; however, fungal DNA is extracted and used for qPCR quantification [253]. In order to determine most sensitive method of generating an A.*f*. standard curve, the extraction of fungal RNA and fungal DNA was compared.

The extraction of fungal genetic material from an infected-lung requires lung tissue and fungal cell walls to be vigorously disrupted. Lung A.*f*. fungal burden has been identified in fungal genetic material extracted via the blunt-crush method (manually grinding tissue with a pestle) and the homogenising method (using a tissue homogeniser for ~10 seconds at ~1200rpm). From this comparison, homogenising lung tissue resulted in a more sensitive RNA extraction. However, a noted drop in fungal burden at 24 hours was associated with the incomplete homogenisation of large hyphae [254]. This suggests both these methods do not fully disrupt tissue. Recently, 0.5mm^3 glass beads (Biospec) have been used to disrupt lung tissue and fungal cell walls increasing the yield of extracted fungal genetic material in clinical samples [255] and *in vivo* [256, 257]. In order to achieve high fungal burden assay sensitivity a comparison of homogenising A.*f*. against bead-beating A.*f*. to obtain fungal genetic material was completed.

A.*f*. RC PBS solutions were generated at concentrations from 10^9 A.*f*. RC/ml to 10^2 A.*f*. RC/ml. To compare the extraction sensitivity of fungal RNA against fungal DNA, A.*f*. PBS solutions were homogenised (10 seconds at 1200rpm) and either fungal RNA or DNA extracted. Fungal RNA was used to generate cDNA before the A.*f*. 18S rRNA was quantified by qPCR. The A.*f*. 18S rRNA was quantified by qPCR directly in extracted fungal DNA samples. To compare whether tissue homogenisation or bead beating

yielded the most fungal genetic material, A.*f*. PBS solutions were homogenised (10 seconds at 1200 rpm) or bead beat (4.5m/s for 4 x 30 seconds with 5 minutes at 4°C between cycles) before fungal RNA was extracted and the A.*f*. 18S rRNA quantified by qPCR.

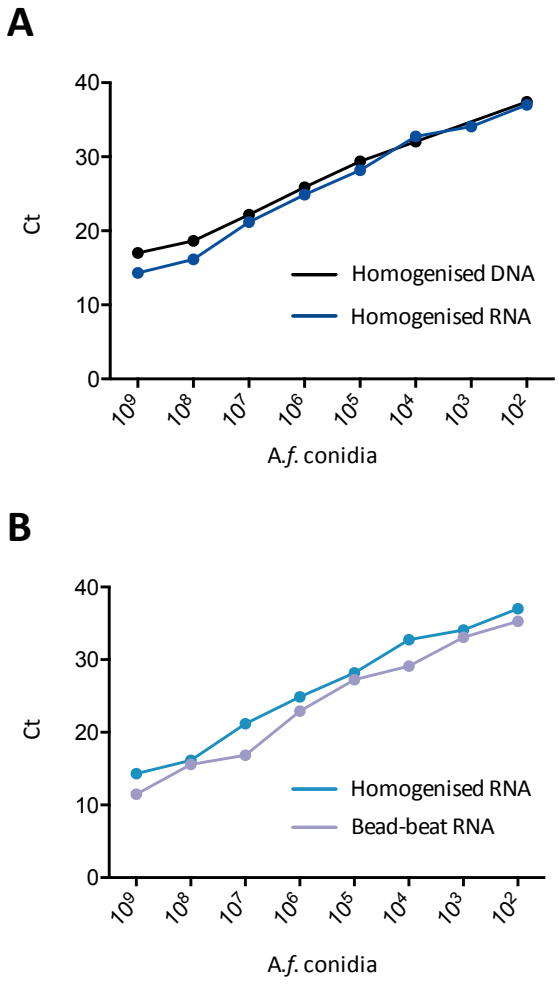

Figure 4.4: Extracting fungal RNA by bead beating is the optimum method of obtained fungal genetic material. A) A.*f*. fungal RNA and DNA were extracted from homogenised 10^9 to 10^2 A.*f*. RC in 1ml PBS using MasterPure RNA Purification Kit (Epicentre). Extracted fungal RNA was used to generate cDNA. The quantity of A.*f*. 18S rRNA was determined within extracted fungal DNA and generated cDNA samples by qPCR using a Taqman probe (Thermofisher). **B)** A.*f*. fungal RNA was extracted after homogenisation or bead beating with 0.5mm^3 glass beads. Extracted fungal RNA was used to generate cDNA. The quantity of A.*f*. 18S rRNA was determined within generated cDNA samples by qPCR using a Taqman probe. This experiment was undertaken as part of the optimisation protocol. Data is representative of two independent experiments.

Figure 4.4 identifies extracting fungal RNA after bead beating tissue samples as the most sensitive method of obtaining fungal genetic material. Therefore, all standard curve samples and experimental samples were processed following this protocol.

Ideally, the same A.*f*. standard curve would be used to analyse all *in vivo* experimental samples; however, A.*f*. standard curves are often produced alongside each experiment [258]. To address the long-term stability of A.*f*. extracted RNA a standard curve was produced and cDNA generated. The quantity of A.*f*. 18S rRNA was determined from this cDNA immediately by qPCR. The RNA sample was then stored for 12 weeks at -80^{o}C before being used to generate new cDNA and the A.*f*. 18S rRNA qPCR reaction was repeated. A HPRT control was used as a reference gene to calculate ΔΔCt for both qPCR experiments and allow the comparison of A.*f*. standard curve quantification values.

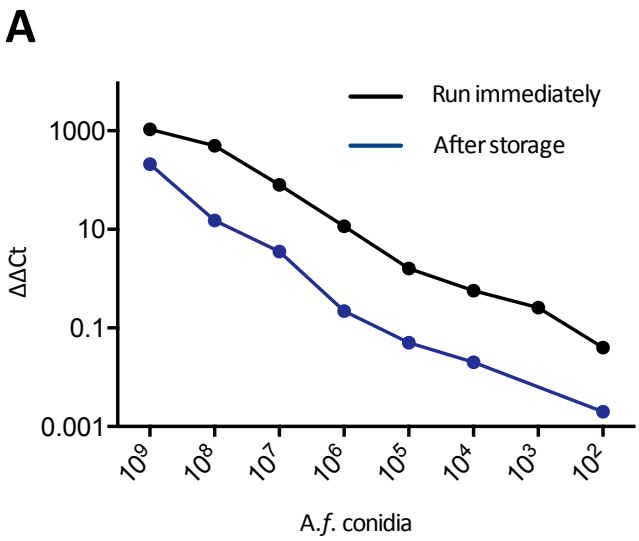

Figure 4.5: The A.*f*. standard curve degrades and loses sensitivity over time and through freeze-thaw cycles. A.*f*. fungal RNA was extracted from bead beat 10^9 to 10^2 A.*f*. RC in 1ml PBS using MasterPure RNA Purification Kit (Epicentre). Extracted fungal RNA was used to generate cDNA. **(Black line)** The quantity of A.*f*. 18S rRNA was determined immediately within extracted fungal RNA samples by qPCR using a Taqman probe (Thermofisher). **(Blue line)** After the first, immediate qPCR reaction, fungal RNA was stored at -80^{o}C for 12 weeks before fresh cDNA was generated and the quantity of A.*f*. 18S rRNA again determined by qPCR. A HPRT control was included on both qPCR plates to permit the ΔΔCt comparison of A.*f*. 18S rRNA Ct values. This experiment was undertaken as part of the optimisation protocol. Data is representative of one independent experiment.

Figure 4.5 indicates A.*f*. extracted RNA degrades over time. Therefore, standard curves were newly generated alongside each experiment. Having identified the most sensitive method of extracting fungal genetic material, generating A.*f*. standard curves and quantifying fungal burden *in vivo*, the A.*f*. infection protocol was next optimised. The well described A.*f*. infection protocol as previously mentioned was again used as a starting point for our A.*f*. infection experiments [100].

The A.*f*. intra-tracheal infection procedure required the A.*f*. PBS solution being pipetted in to the upper trachea of each mouse. If the pipette was placed too far down

the trachea, past the carina and accessing the bronchi, the A.*f*. solution may only inoculate one lung. In order to verify both lungs were being inoculated with A.*f*., mice were infected for 24 hours with $5x10^7$ A.*f*. RC in PBS before both lungs were harvested and fungal burden quantified independently from each lung.

Usually between 12-20 mice were used for A.*f*. infection experiments. Infected-lung samples were harvested sequentially but only processed once all samples had been obtained. The protocols that were optimised for our facility incubated extracted lung samples on ice until all samples were harvested and processed together [100, 174]. This often meant the first extracted lung sample would not be processed for 4-6 hours as the remaining lung samples were obtained. The duration samples remained unprocessed may impact the integrity of fungal RNA. Therefore, a comparison of sample collection in PBS or RNAlater was completed. RNAlater (Thermo Fisher Scientific, Massachusetts, USA) rapidly penetrates tissues and stabilises RNA in an intermediary solution preserving the integrity of RNA within tissues. Mice were infected for 24 hours with $5x10^7$ A.*f*. RC in PBS before both lungs were harvested. Left lung was stored in PBS at 4^oC for 24 hours before fungal RNA was extracted. Right lung was stored in RNAlater at RT for 24 hours before fungal RNA was extracted. Fungal burden was quantified from each lung in PBS and RNAlater.

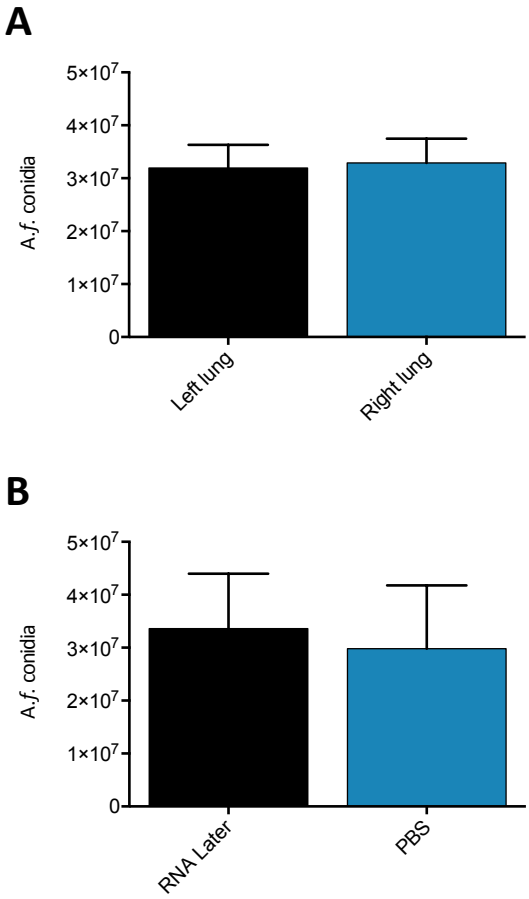

Figure 4.6: A.*f*. fungal RNA can be extracted from right or left lung and stored in PBS or RNALater. (A) Animals were infected with 5x10^7 A.*f*. RC for 24 hours before left and right lungs were harvested. A.*f*. fungal RNA was extracted from bead beat lung tissue using the MasterPure RNA Purification Kit (Epicentre). Extracted fungal RNA was used to generate cDNA and the quantity of A.*f*. 18S rRNA determined by qPCR. No significant difference was attained when quantifying fungal burden from left or right lung. (**B)** Animals were infected with 5x10^7 A.*f*. RC for 24 hours before left and right lungs were harvested. Right lung was collected in RNA later and stored for 24 hours at RT before A.*f*. fungal RNA was extracted. Left lung was collected in PBS at 4^{o}C and stored for 24 hours before A.*f*. fungal RNA was extracted. After incubation fungal RNA was extracted from bead beat lung tissue using the MasterPure RNA Purification Kit (Epicentre). Extracted fungal RNA was used to generate cDNA and the quantity of A.*f*. 18S rRNA determined by qPCR. No significant difference was attained when quantifying fungal burden from RNAlater stored left lung or PBS stored right lung. 6 mice were used for this experiment. This experiment was undertaken as part of the optimisation protocol. Graph displays mean +/- s.e.m.. **(A)** Data collated from 5 mice. **(B)** Data collated from 6 mice. These experiments were completed once.

No significant difference was attained in figure 4.6 comparing the fungal burden quantified from left and right lung. This suggests the protocol technique was successfully inoculating both lungs with an equal dose of A.*f*.. For consistency, left lung was used in all future experiments to quantify fungal burden. No significant difference was attained in figure 4.6 when comparing the impact storing lungs in RNAlater or PBS had on the quantification of fungal burden. This implies fungal RNA is stable within lung tissue when stored in RNAlater at RT or PBS at 4^{o}C for up to 24 hours. RNAlater was used for the temporary storage of left lung lobes in all future experiments quantifying A.*f*. fungal burden.

4.3.3: What role do CLRs play in the anti-A.*f*. immune response *in vivo*?

Having optimised the *in vivo* assay protocols, the role CLRs play in the anti-A.*f*. response *in vivo* could be investigated.

Experiments were first designed to elicit the impact A.*f*. dose had on fungal burden and survival of WT, Dectin-1 KO and Mincle KO mice. Current literature describes a range of A.*f*. doses used to intra-tracheally infect and challenge *in vivo*. Doses as low as $5x10^6$ and as high as $2x10^8$ have been used [2, 259, 260]. The majority of experiments investigating the impact CLR KO or TLR KO have on the anti-A.*f*. immune response used doses in the region of $5x10^7$ through to $9x10^7$ [99, 100]. Therefore, initial experiments were completed using A.*f*. at a low dose $5x10^7$, intermediate dose $7x10^7$ and high dose $9x10^7$. WT, Dectin-1 KO and Mincle KO mice were infected with low, intermediate or high dose A.*f*. RC in PBS for 10 days. After 10 days (or before if mice reached humane end point, see scoring sheet in chapter 7.6) left lungs were harvested and fungal burden determined.

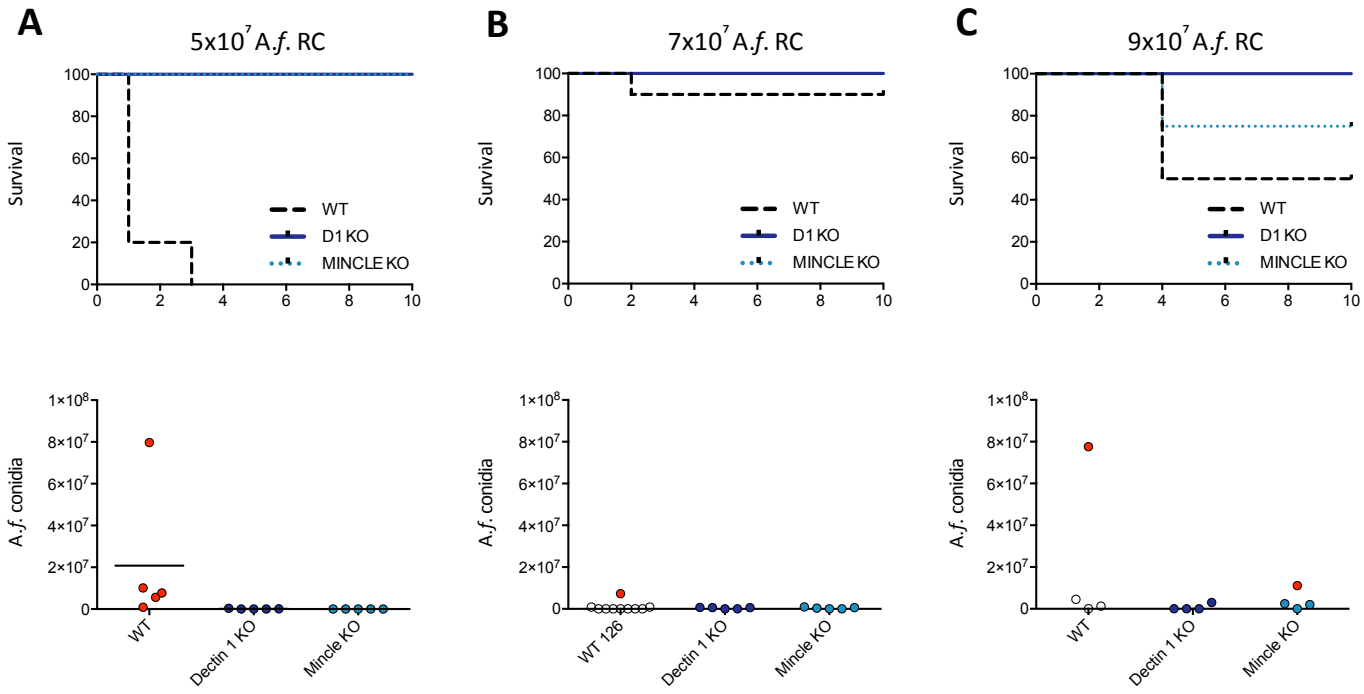

Figure 4.7: Increasing the dose of A.*f*. did not increase CLR KO mortality or fungal burden. WT, Dectin-1 KO and Mincle KO mice were infected with **A)** 5x10^7, **B)** 7x10^7 or **C)** 9x10^7 A.*f*. RC in PBS for 10 days before left lungs were harvested. A.*f*. fungal RNA was extracted from bead beat lung tissue using the MasterPure RNA Purification Kit (Epicentre). Extracted fungal RNA was used to generate cDNA and the quantity of A.*f*. 18S rRNA determined by qPCR. Each data point represents one mouse. Each column bar represents mean of results. Red data points indicate mice taken before the experiment end point. This experiment was undertaken as part of the optimisation protocol. **A)** Comprises of 5 WT, 5 Dectin-1 KO and54 Mincle KO mice. **B)** Comprises of 10 WT, 5 Dectin-1 KO and 5 Mincle KO mice. **C)** Comprises of 4 WT, 4 Dectin-1 KO and 4 Mincle KO mice. Each dose experiment was completed once.

Figure 4.7 demonstrates that increasing the infection dose of A.*f*. from $5x10^7$ through to $9x10^7$ decreased mortality and had no impact on fungal burden at 10-days. Independent of the A.*f*. dose used for infection, WT mice consistently displayed higher mortality than the Dectin-1 KO and Mincle KO mice. No Dectin-1 KO mouse succumbed to infection and only one Mincle KO mouse succumbed to infection whereas 7 WT mice succumbed to the infection. Here, the CLR KO models may be protective due to their impaired inflammatory response reducing the development of cytokine storm/sepsis disease, this is further discussed in 4.4.2. Fungal burden quantification indicated the A.*f*. infection had been cleared after 10 days irrespective of CLR status. Therefore, in order to ascertain the impact the A.*f*. dose has on fungal burden and the anti-A.*f*. chemokine and cytokine response, high $9x10^5$ and low $5x10^5$ dose 2-day experiments were completed.

WT, Dectin-1 KO and Mincle KO mice were infected with low or high dose A.*f*. RC in PBS for 2 days. After 2 days (or before if the mice reached a humane end point, see scoring sheet in chapter 7.6) both lungs were harvested. Fungal burden was determined from the left lung and the anti-A.*f*. cytokine and chemokine response determined from the right lung.

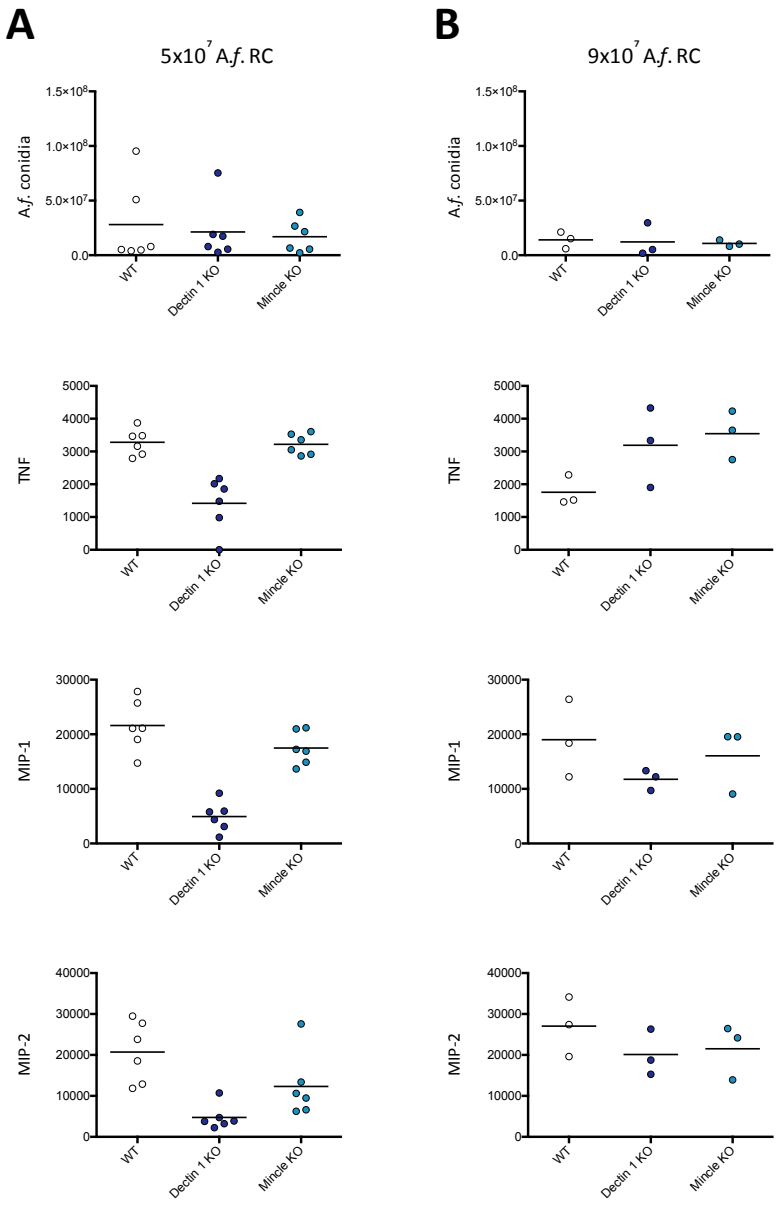

Figure 4.8: The lower dose 5x10^7 A.*f*. infection model yields greater differences in chemokine and cytokine response between WT, Dectin-1 KO and Mincle KO mice without impacting fungal burden. WT, Dectin-1 KO and Mincle KO mice were infected with **A)** 5x10^7 or **B)** 9x10^7 A.*f*. RC in PBS for 2 days before both lungs were harvested. A.*f*. fungal RNA was extracted from bead beat left lung tissue using the MasterPure RNA Purification Kit (Epicentre). Extracted fungal RNA was used to generate cDNA and the quantity of A.*f*. 18S rRNA determined by qPCR. Anti-A.*f*. cytokine and chemokine response was determined from homogenised right lung by ELISA. All cytokine/chemokine results are pg/ml. Each data point represents one mouse. Each column bar represents mean of results. Red data points indicate mice taken before the experiment end point. This experiment was undertaken as part of the optimisation protocol. **A)** Comprises of 6 WT, 6 Dectin-1 KO and 6 Mincle KO mice. **B)** Comprises of 3 WT, 3 Dectin-1 KO and 3 Mincle KO mice. Each dose experiment was completed once.

The results displayed in figure 4.8 compare the high and low A.*f*. dose 2-day infection experiment. These data describe an increased fungal burden and greater cytokine and chemokine response difference between WT and CLR KO mice when the lower, $5x10^5$ A.*f*. dose was used.

Having determined the optimal dose required to elicit differences between fungal burden and anti-A.*f*. cytokine and chemokine response in WT and CLR KO mice, experiments were completed using this protocol. Figure 4.8 displays preliminary results suggesting there are differences in the anti-A.*f*. response and fungal burden between WT and CLR KO mice at 48 hours. Therefore, initial experiments were completed at this time point.

WT, Dectin-1 KO, Mincle KO, MD1 DKO and MD2 DKO mice were infected with $5x10^7$ A.*f*. RC in PBS for 2 days. After 2 days (or before if mice reached a humane end point, see scoring sheet in chapter 7.6) both lungs were harvested. Fungal burden was determined from the left lung and the anti-A.*f*. cytokine and chemokine response determined from the right lung.

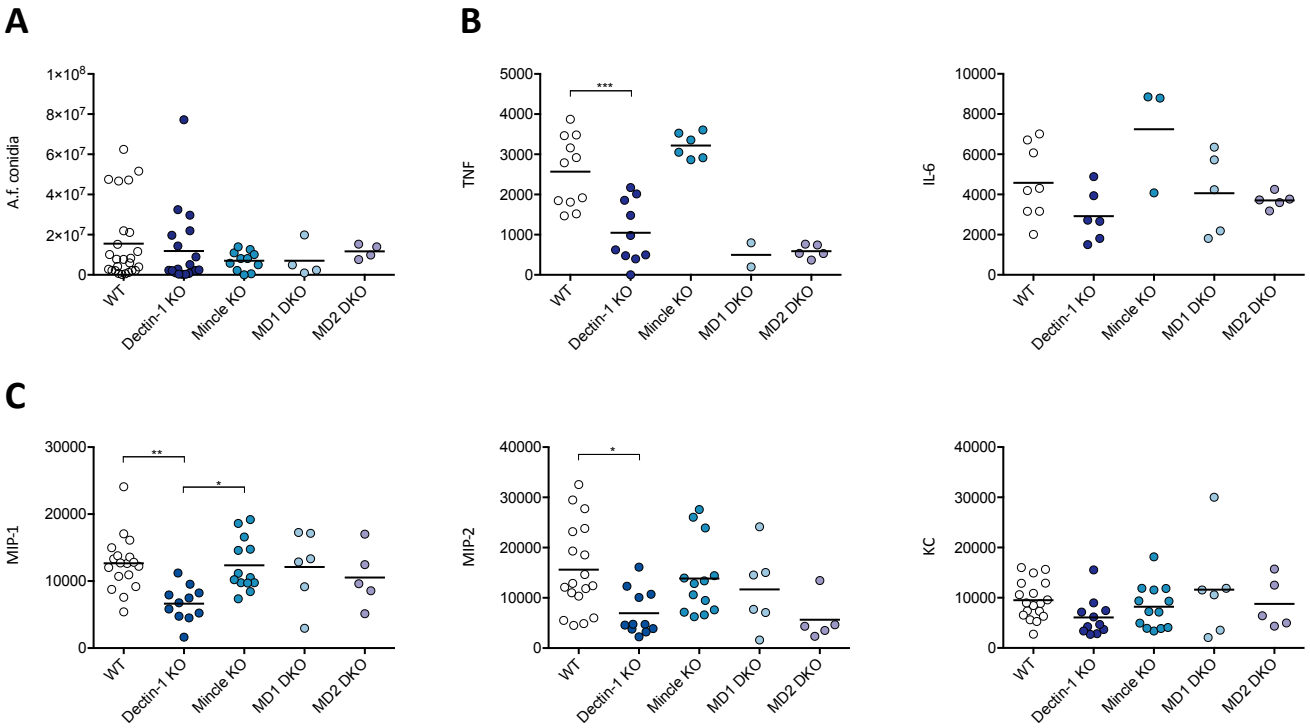

Figure 4.9: Dectin-1 KO mice lack a robust anti-A.*f*. cytokine and chemokine response although this does not impair their A.*f*. clearance up to 48 hours. WT, Dectin-1 KO, Mincle KO, MD1 DKO and MD2 DKO mice were infected with $5x10^7$ A.*f*. RC in PBS for 2 days before both lungs were harvested. **A)** A.*f*. fungal RNA was extracted from bead beat left lung tissue using the MasterPure RNA Purification Kit (Epicentre). Extracted fungal RNA was used to generate cDNA and the quantity of A.*f*. 18S rRNA determined by qPCR. **B & C)** Anti-A.*f*. cytokine and chemokine response was determined from homogenised right lung by ELISA. All cytokine/chemokine results are pg/ml. Each data point represents one mouse. Each column bar represents mean of results. Data is from 7 independent experiments containing different numbers of WT, CLR KO and CLR DKO mice. A one-way analysis of variance with Bonferonni's post-test was used to determine statistical significance. *p<0.05, **p<0.005, ***p<0.0005.

The results displayed in figure 4.9 align with previously published work describing Dectin-1 KO's impaired anti-A.*f*. cytokine and chemokine response *in vivo* [2, 100]. Dectin-1 KO mice significantly lack a robust cytokine and chemokine anti-A.*f*. response; however, in these experiments no significant difference was attained when quantifying fungal burden. Results from the other CLR KO or CLR DKO mice were not expected. Fungal burden between WT, CLR KO and CLR DKO was similar, suggesting all these mice irrespective of their CLR status cleared A.*f*. from the lung. This was not what we expected. The differences between CLR KO and CLR DKO are subtle; due to the low mice numbers it is difficult to draw firm conclusions from these experiments.

As differences in the anti-A.*f*. cytokine and chemokine response had been attained at 48 hours, an earlier 24-hour experiment was completed. At 24 hours the mice may not have cleared the A.*f*. infection, but due to their varying cytokine and chemokine response, differences in fungal burden may be present.

WT, Dectin-1 KO, Mincle KO, MD1 DKO and MD2 DKO mice were infected with $5x10^7$ A.*f*. RC in PBS for 24 hours. After 24 hours (or before if mice reached a humane end point, see scoring sheet in chapter 7.6) both lungs were harvested. Fungal burden was determined from the left lung and the anti-A.*f*. cytokine and chemokine response determined from the right lung.

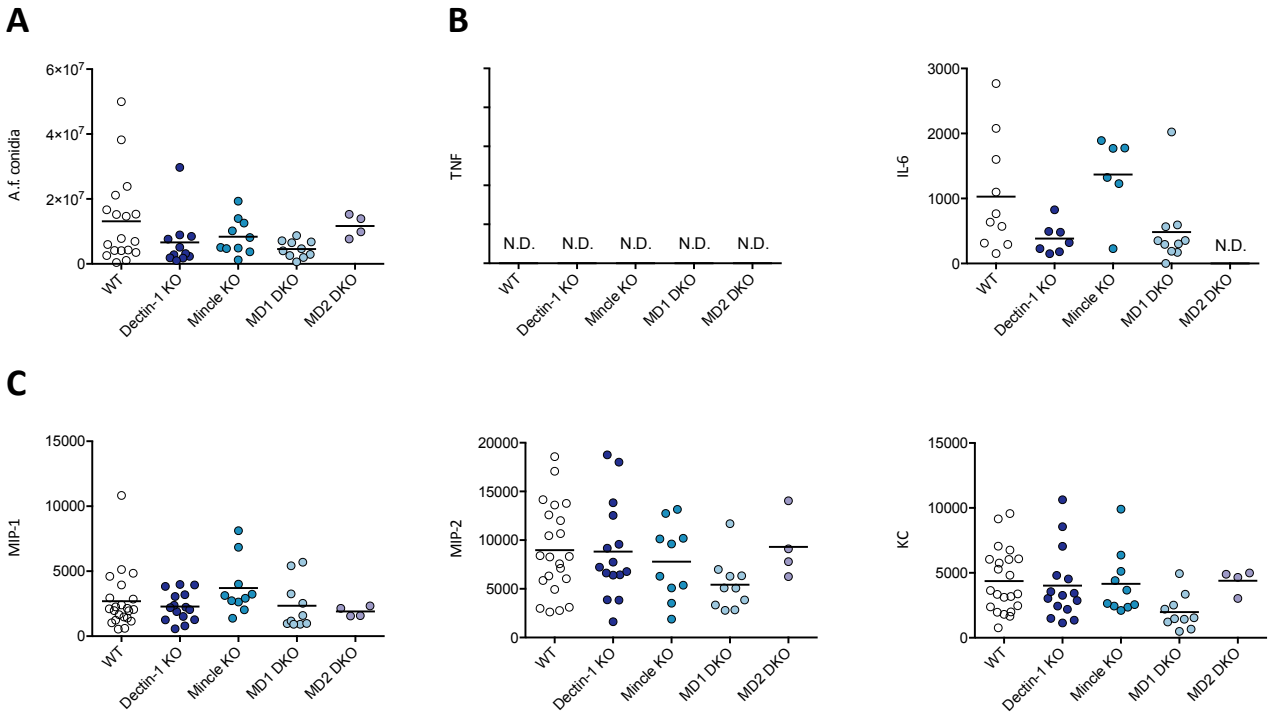

Figure 4.10: WT, CLR KO and CLR DKO mice all generate a robust anti-A.*f*. response and have partially cleared A.*f*. from the lung at 24 hours. WT, Dectin-1 KO, Mincle KO, MD1 DKO and MD2 DKO mice were infected with $5x10^7$ A.*f*. RC in PBS for 24 hours before both lungs were harvested. **A)** A.*f*. fungal RNA was extracted from bead beat left lung tissue using the MasterPure RNA Purification Kit (Epicentre). Extracted fungal RNA was used to generate cDNA and the quantity of A.*f*. 18S rRNA determined by qPCR. **B & C)** Anti-A.*f*. cytokine and chemokine response was determined from homogenised right lung by ELISA. All cytokine/chemokine results are pg/ml. Each data point represents one mouse. Each column bar represents mean of results. N.D. represents no result detected. Data is from 6 independent experiments containing different numbers of WT, CLR KO and CLR DKO mice. A one-way analysis of variance with Bonferonni's post-test was used to determine statistical significance.

Figure 4.10 displays no significant difference between the ability of WT, CLR KO and CLR DKO mice to generate an anti-A.*f*. cytokine and chemokine response. There is also no significant difference when comparing fungal burden between the WT, CLR KO and CLR DKO mice. Fungal burden at this time-point is low indicating these animals are clearing the infection rapidly.

The Dectin-1 KO deficient response trend identified in figure 4.9 is present without significance in the 24-hour IL-6 response but is not conserved in the 24-hour chemokine response. The quantities of cytokine and chemokine produced from all WT, CLR KO and CLR DKO mice are reduced when compared to the later 48-hour results. Chemokine production is very tightly controlled and resolved abruptly upon completion of the immune response [261]. This, along with the fact fungal burden may increase from 24 to 48 hours suggests these mice are still actively responding to A.*f*..

Although the significant differences between WT, CLR KO and CLR DKO mice anti-A.*f*. cytokine and chemokine response was not present at 24 hours, fungal burden was increased at this time point. In order to identify whether any fungal burden difference was at all present between WT, CLR KO and CLR DKO groups a 12-hour experiment was completed.

WT, Dectin-1 KO and Mincle KO mice were infected with $5x10^7$ A.*f*. RC in PBS for 12 hours. After 12 hours (or before if mice reached a humane end point, see scoring sheet in chapter 7.6) both lungs were harvested. Fungal burden was determined from the left lung and the anti-A.*f*. cytokine and chemokine response determined from the right lung.

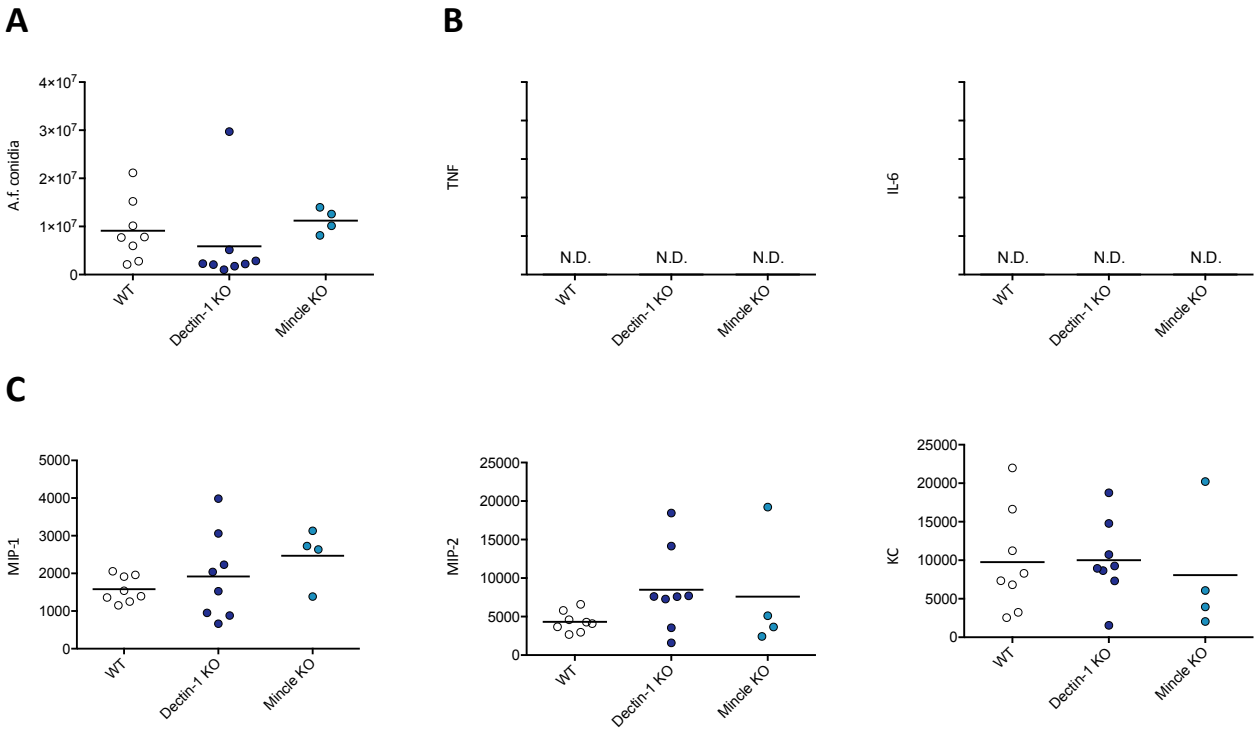

Figure 4.11: WT and CLR KO mice all generate a robust anti-A.*f*. response and have partially cleared A.*f*. from the lung at 12 hours. WT, Dectin-1 KO and Mincle KO mice were infected with 5x10^7 A.*f*. RC in PBS for 12 hours before both lungs were harvested. **A)** A.*f*. fungal RNA was extracted from bead beat left lung tissue using the MasterPure RNA Purification Kit (Epicentre). Extracted fungal RNA was used to generate cDNA and the quantity of A.*f*. 18S rRNA determined by qPCR. **B & C)** Anti-A.*f*. cytokine and chemokine response was determined from homogenised right lung by ELISA. All cytokine/chemokine results are pg/ml. Each data point represents one mouse. Each column bar represents mean of results. N.D. represents no result detected. Data is from 2 independent experiments containing different numbers of WT and CLR KO mice. A one-way analysis of variance with Bonferonni's post-test was used to determine statistical significance.

Figure 4.11 displays no significant difference between the ability of WT and CLR KO mice to generate an anti-A.*f*. cytokine and chemokine response. There is also no significant difference when comparing fungal burden between the WT and CLR KO mice. Fungal burden at this time-point is lower than the fungal burden results attained for 24 hours and 48 hours infection. This indicates these animals rapidly clear a large quantity of A.*f*. before A.*f*. begins to germinate and replicate within the lung, increasing in number over a 48-hour period. Earlier experiments displayed in figure 4.7 suggest A.*f*., after increasing in quantity up to 48 hours is cleared by 10 days.

No significant difference in WT, CLR KO or CLR DKO mice fungal burden has been obtained at multiple time points. Although a significant Dectin-1 KO reduction of anti-A.*f*. cytokine and chemokine response was identified at 48 hours, this had no bearing over the ability of mice to clear A.*f*.. This was not what we expected and not what published research suggests. The lack of impact Mincle KO has individually or alongside Dectin-1 was also not hypothesised. The reason underlining the differences between our *in vivo* A.*f*. model and other published research was not clear. Therefore, a different approach was taken aiming to align our model with that described in published research. Initially, the differences between WT, CLR KO and CLR DKO microbiomes were investigated as possibly being responsible for our unexpected results.

4.3.4: What impact is the microbiome conferring over experimental results?

Recently the impact of the microbiome on the development, maintenance and function of the immune response has begun to be understood [262, 263]. The homeostatic role the microbiome plays within the pulmonary immune system has also been investigated. In this setting the microbiome has been implicated to direct immune development and function and set the threshold for immune responses. A key role for the microbiome maintaining the balance between immune tolerance, acute lung inflammation and chronic lung inflammation was highlighted [264].

Controlling and minimising the impact the microbiome has on WT and KO mice can reduce, or even nullify, a previously observed disease phenotype [265].

The mice used in the previous 48-hour, 24-hour and 12-hour experiments were males derived from separate genetic lineages. Males were not co-housed prior to, or throughout, experiments. Therefore, the impact each genotype's microbiome may be bearing over their immune response was investigated. Addressing and rectifying any microbiome irregularities may restore the previously described Dectin-1 KO increased fungal burden. This would allow investigation into anti-A.*f*. response between WT, CLR KO and CLR DKO and may uncover novel fungal burden and anti-A.*f*. response differences.

To address any microbiome discrepancies, male mice underwent a minimum of 2 weeks of cage bedding swapping between the ages of 4-8 weeks when their microbiome retained plasticity [266]. This process involved moving mice between cages containing a WT, CLR KO or CLR DKO genotype without changing the bedding in that cage. This protocol is used routinely to address microbiome differences between groups of mice that are not co-housed. The transfer of microbiome from one genotype to another using this protocol has a profound impact on disease pathogenesis, in some cases resulting in the loss of a KO phenotype [265, 266].

In order to examine the impact the microbiome confers over the previously displayed A.*f*. infection results, mice from each genotype were cohoused as described above before being used in A.*f*. infection experiments.

After the co-housing protocol was completed for a minimum of 2 weeks, WT, Dectin-1 KO, MD1 DKO and MD2 DKO mice were infected with $5x10^7$ A.*f*. RC in PBS for 24 or 48 hours. Mincle mice were not available for use in these experiments. After 24 or 48 hours (or before if mice reached a humane end point, see scoring sheet in chapter 7.6) both lungs were harvested. Fungal burden was determined from the left lung and the anti-A.*f*. cytokine and chemokine response determined from the right lung.

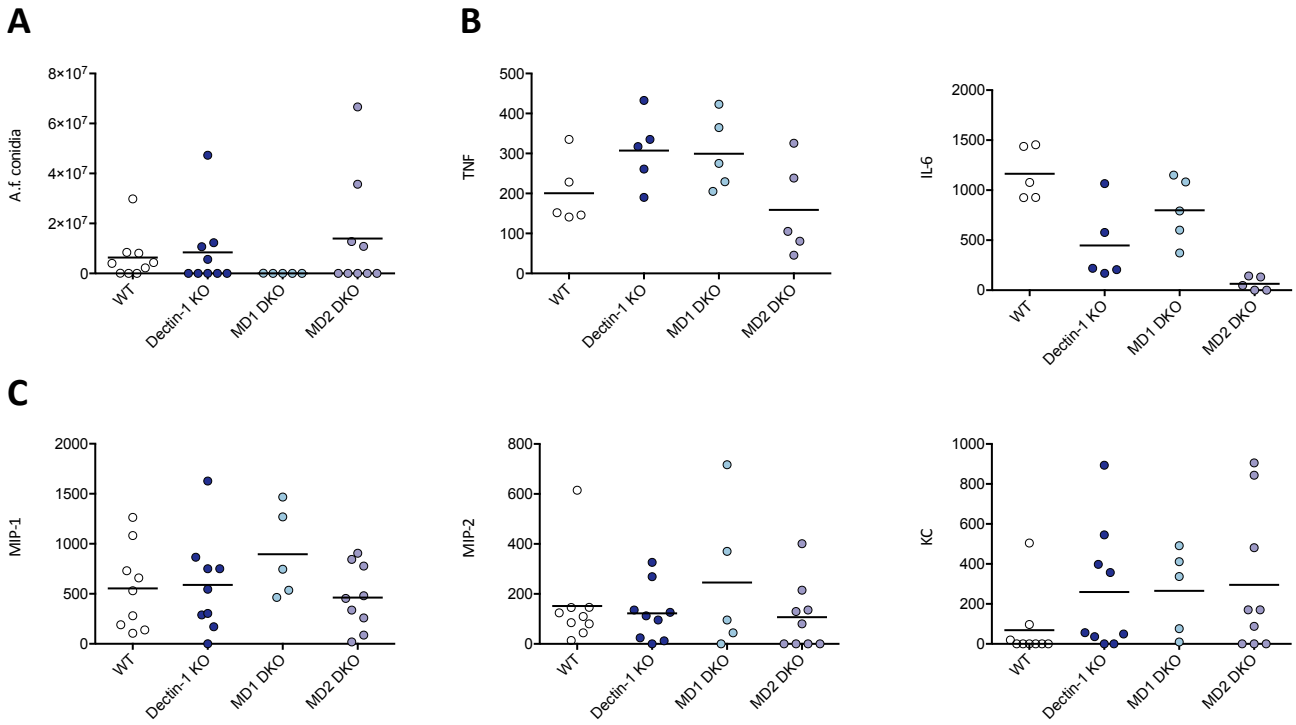

Figure 4.12: Microbiome-controlled WT, CLR KO and CLR DKO mice all generate a robust anti-A.*f*. response and have partially cleared A.*f*. from the lung at 48 hours. WT, Dectin-1 KO, MD1 DKO and MD2 DKO mice were infected with 5x10^7 A.*f*. RC in PBS for 48 hours before both lungs were harvested. **A)** A.*f*. fungal RNA was extracted from bead beat left lung tissue using the MasterPure RNA Purification Kit (Epicentre). Extracted fungal RNA was used to generate cDNA and the quantity of A.*f*. 18S rRNA determined by qPCR. **B & C)** Anti-A.*f*. cytokine and chemokine response was determined from homogenised right lung by ELISA. All cytokine/chemokine results are pg/ml. Each data point represents one mouse. Each column bar represents mean of results. Data is from 2 independent experiments containing different numbers of WT, CLR KO and CLR DKO mice. A one-way analysis of variance with Bonferonni's post-test was used to determine statistical significance.

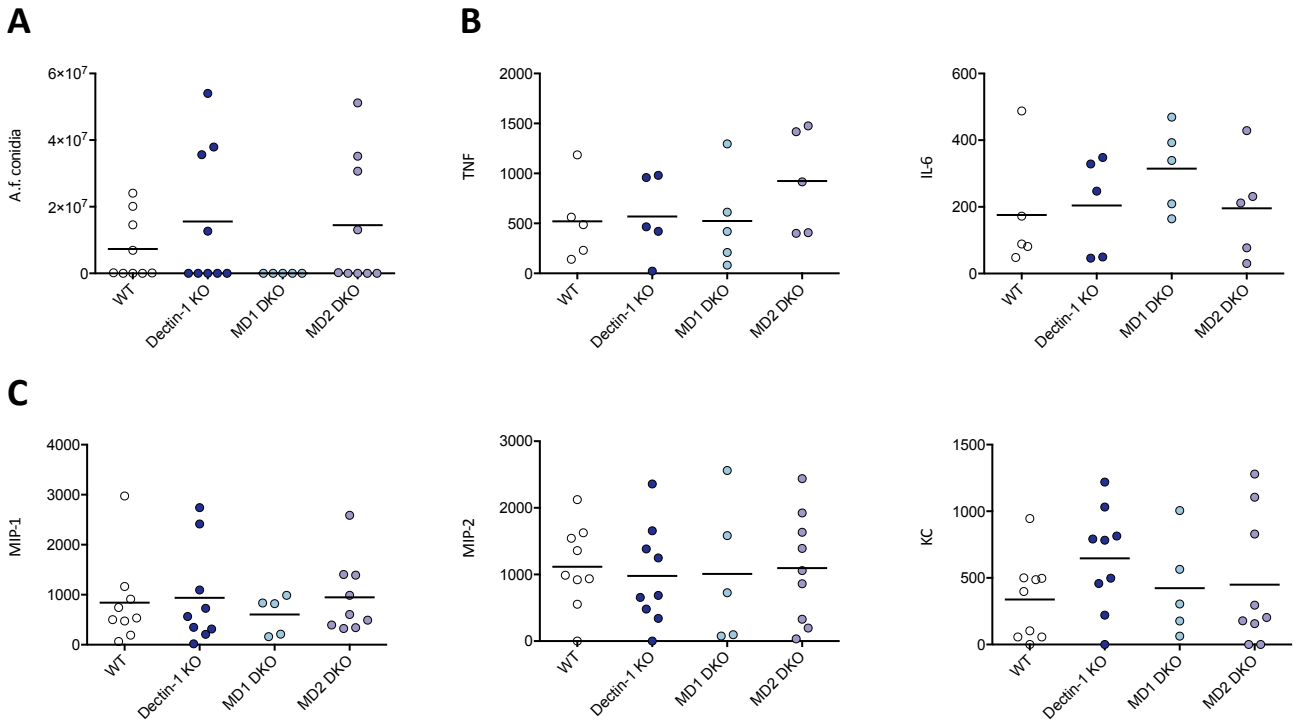

Figure 4.13: Microbiome-controlled WT, CLR KO and CLR DKO mice all generate a robust anti-A.*f*. response and have partially cleared A.*f*. from the lung at 24 hours. WT, Dectin-1 KO, MD1 DKO and MD2 DKO mice were infected with $5x10^7$ A.*f*. RC in PBS for 24 hours before both lungs were harvested. **A)** A.*f*. fungal RNA was extracted from bead beat left lung tissue using the MasterPure RNA Purification Kit (Epicentre). Extracted fungal RNA was used to generate cDNA and the quantity of A.*f*. 18S rRNA determined by qPCR. **B & C)** Anti-A.*f*. cytokine and chemokine response was determined from homogenised right lung by ELISA. All cytokine/chemokine results are pg/ml. Each data point represents one mouse. Each column bar represents mean of results. Data is from 2 independent experiments containing different numbers of WT, CLR KO and CLR DKO mice. A one-way analysis of variance with Bonferonni's post-test was used to determine statistical significance.

Figure 4.12 and 4.13 display the results from microbiome controlled A.*f*. infection experiments. These two figures were compared with their respective non-microbiome-controlled experiments described in figures 4.9 and 4.10. The quantity of cytokines and chemokines produced in the microbiome-controlled experiments were reduced when compared to non-microbiome-controlled experiments. Interestingly, the quantity of cytokines and chemokines produced in the non-microbiome-controlled experiments increased from 24 to 48 hours, suggesting the A.*f*. infection and immune response were active and increasing in magnitude. This trend was not present in the microbiome-controlled experiments, suggesting the infection and immune response were being rapidly cleared and resolved.

Comparing fungal burden results from the microbiome and non-microbiome-controlled experiments indicates that controlling the microbiome improves the ability of WT, CLR KO and CLR DKO to clear A.*f*. infection. Fungal burden results were consistently increased when the microbiome was not controlled. The previously identified Dectin-1 KO and MD1 DKO impaired cytokine and chemokine anti-A.*f*. responses were not conserved in the microbiome-controlled experiments.

The microbiome-controlled experiment results displayed in figure 4.12 and 4.13 were not hypothesised. Furthermore, these results have not been previously identified in published research using similar A.*f*. infection models. Therefore, a different approach was again taken aiming to align our model with that described in published research. Finally, the differences between the gender of WT, CLR KO and CLR DKO mice was investigated as possibly being responsible for our unexpected results.

4.3.5: What impact is gender conferring over experimental results?

The genetic and hormonal difference between males and females of the same species and the subsequent impact this has on their immune response is well described [267-269]. The immune response between males and females of the same species has been established to significantly differ when animals are challenged with LPS, self-antigen,

or foreign-antigen from fungi, bacteria and viruses [270]. In order to determine whether the sex of the mice was impacting our WT, CLR KO and CLR DKO A.*f*. infection results, 48-hour and 24-hour A.*f*. infection experiments were completed in females. To address any microbiome discrepancies within these experiments female mice were co-housed as previously described.

After the co-housing protocol was completed for a minimum of 2 weeks, WT, Dectin-1 KO, Mincle KO, MD1 DKO and MD2 DKO female mice were infected with $5x10^7$ A.*f*. RC in PBS for 24 or 48 hours. After 24 or 48 hours (or before if mice reached a humane end point, see scoring sheet in chapter 7.6) both lungs were harvested. Fungal burden was determined from the left lung and the anti-A.*f*. cytokine and chemokine response determined from the right lung.

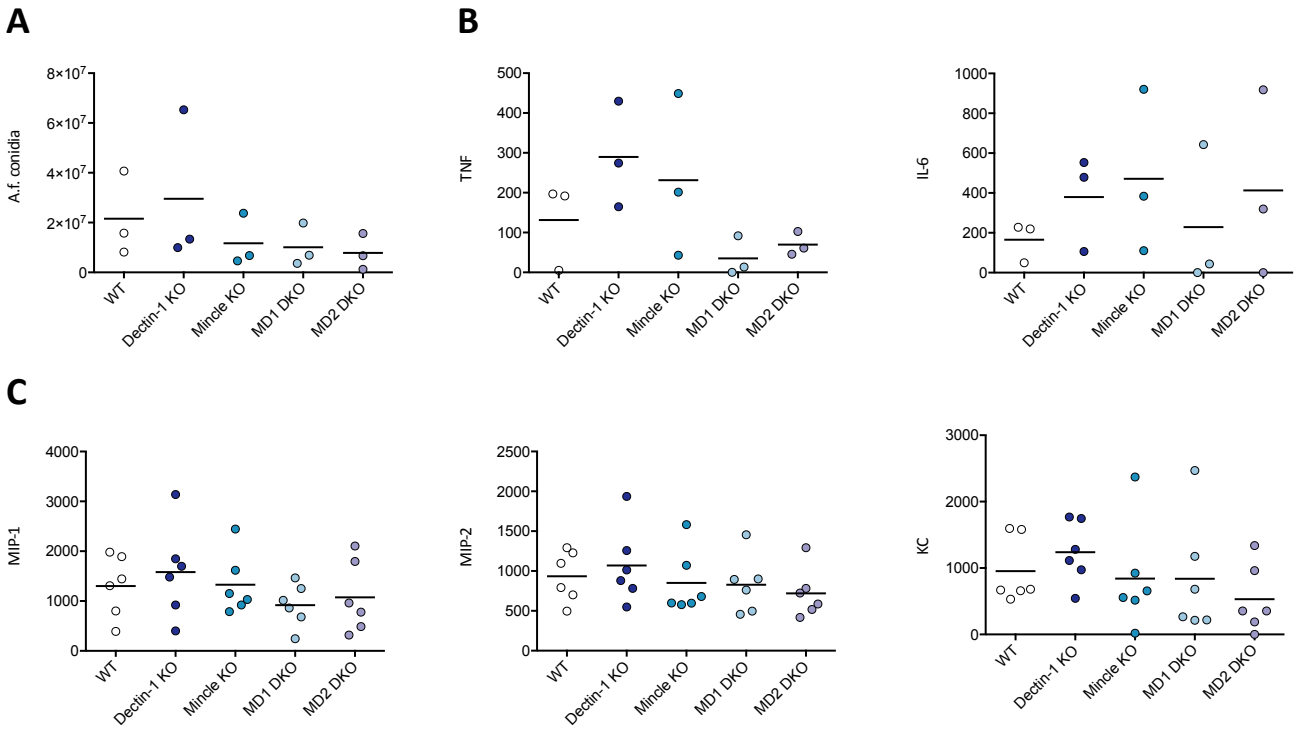

Figure 4.14: Microbiome-controlled female WT, CLR KO and CLR DKO mice all generate a robust anti-A.*f*. response and have partially cleared A.*f*. from the lung at 48 hours. WT, Dectin-1 KO, Mincle KO, MD1 DKO and MD2 DKO mice were infected with $5x10^7$ A.*f*. RC in PBS for 48 hours before both lungs were harvested. **A)** A.*f*. fungal RNA was extracted from bead beat left lung tissue using the MasterPure RNA Purification Kit (Epicentre). Extracted fungal RNA was used to generate cDNA and the quantity of A.*f*. 18S rRNA determined by qPCR. **B & C)** Anti-A.*f*. cytokine and chemokine response was determined from homogenised right lung by ELISA. All cytokine/chemokine results are pg/ml. Each data point represents one mouse. Each column bar represents mean of results. Data is from 1 independent experiment containing different numbers of WT, CLR KO and CLR DKO mice. A one-way analysis of variance with Bonferonni's post-test was used to determine statistical significance.

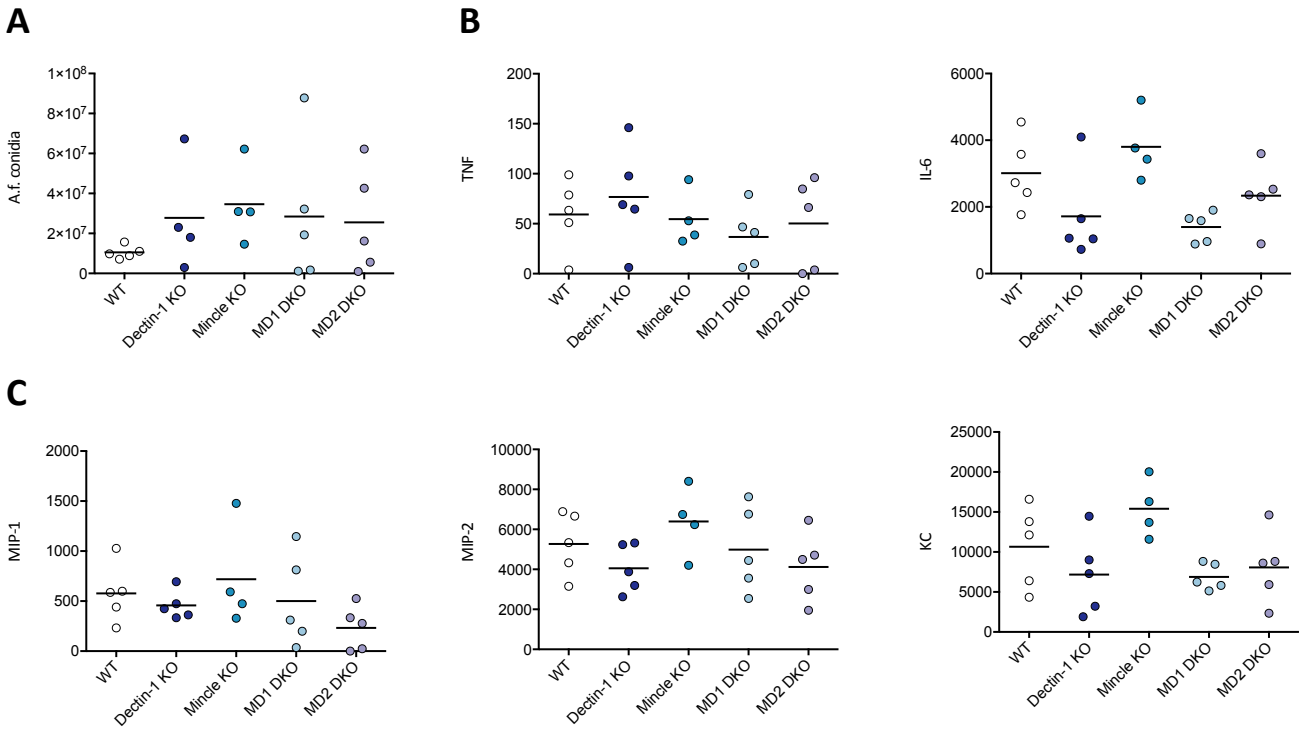

Figure 4.15: Microbiome-controlled female WT, CLR KO and CLR DKO mice all generate a robust anti-A.*f*. response but have not cleared A.*f*. from the lung at 24 hours. WT, Dectin-1 KO, Mincle KO, MD1 DKO and MD2 DKO mice were infected with $5x10^7$ A.*f*. RC in PBS for 24 hours before both lungs were harvested. **A)** A.*f*. fungal RNA was extracted from bead beat left lung tissue using the MasterPure RNA Purification Kit (Epicentre). Extracted fungal RNA was used to generate cDNA and the quantity of A.*f*. 18S rRNA determined by qPCR. **B & C)** Anti-A.*f*. cytokine and chemokine response was determined from homogenised right lung by ELISA. All cytokine/chemokine results are pg/ml. Each data point represents one mouse. Each column bar represents mean of results. Data is from 1 independent experiment containing different numbers of WT, CLR KO and CLR DKO mice. A one-way analysis of variance with Bonferonni's post-test was used to determine statistical significance.

Figure 4.15 displays our initially hypothesised fungal burden results; as CLRs are knocked-out fungal burden increases. However, this data is derived from a limited number of mice and is not significant. Figure 4.14 shows fungal burden decreasing from 24 to 48 hours suggesting these mice, independent of their CLR expression can clear the A.*f*. infection rapidly.

The quantity of anti-A.*f*. cytokine and chemokines produced from female mice is similar to that obtained from male microbiome-controlled male experiments. The previously described Dectin-1 KO impaired cytokine and chemokine response was not conserved in the 48 hour female mice experiment displayed in figure 4.14. Female Dectin-1 KO mice may have a subtly reduced anti-A.*f*. cytokine and chemokine response at 24 hours, as displayed in figure 4.15, but this is not significant.

It is clear the microbiome and gender of mice used in A.*f*. infection experiments has a key role controlling these mice anti-A.*f*. immune response. In order to clarify the impact gender and the microbiome conferred over our CLR KO and CLR DKO A.*f*. infection model, results from figures 4.9, 4.10, 4.12, 4.13, 4.14 and 4.15 were collated and analysed.

Increased at 48 hours		24 hours						48 hours					
Decreased at 48 hours		**TNF**	**IL-6**	**MIP-1**	**MIP-2**	**KC**	**Fungal burden**	**TNF**	**IL-6**	**MIP-1**	**MIP-2**	**KC**	**Fungal burden**
Male	**WT**	N.D.	1028	2688	8966	4374	$1.31x10^7$	2568	4579	12660	15603	9500	$1.55x10^7$
	Dectin-1 KO	N.D.	383	2278	8830	4022	$0.66x10^7$	1049	2921	6649	6947	6079	$1.18x10^7$
	Mincle KO	N.D.	1369	3702	7799	4158	$0.83x10^7$	3220	7244	12357	13835	8207	$0.75x10^7$
	MD1 DKO	N.D.	484	2343	5431	1987	$0.49x10^7$	498	4062	12118	11693	11617	$0.70x10^7$
	MD2 DKO	N.D.	N.D.	1901	9303	4392	$1.16x10^7$	587	3707	10549	5655	8796	$1.16x10^7$
Male microbiome-controlled	**WT**	175	521	840	1117	338	$0.73x10^7$	200	1164	588	151	69	$0.63x10^7$
	Dectin-1 KO	204	569	936	978	646	$1.55x10^7$	307	447	555	122	259	$0.84x10^7$
	MD1 DKO	314	524	604	1008	422	N.D.	299	799	753	254	265	N.D.
	MD2 DKO	195	923	947	1096	449	$1.48x10^7$	159	64	464	106	295	$1.39x10^7$
Female co-housed	**WT**	59	3010	577	5274	10661	$1.05x10^7$	131	165	1303	934	953	$2.15x10^7$
	Dectin-1 KO	79	1716	457	4051	7182	$2.78x10^7$	289	379	1582	1069	1238	$2.95x10^7$
	Mincle KO	54	3802	718	6399	15407	$3.46x10^7$	231	471	1326	851	840	$1.17x10^7$
	MD1 DKO	36	1398	500	4988	6894	$2.84x10^7$	35	228	919	827	837	$1.01x10^7$
	MD2 DKO	50	2338	232	4122	8066	$2.55x10^7$	69	412	1074	719	532	$0.78x10^7$

Figure 4.16: Co-housing mice prior to A.*f*. infection radically alters the anti-A.*f*. cytokine and chemokine response and fungal burden. The data in this figure is collated from the experiments displayed in figure 4.9, 4.10, 4.12, 4.13, 4.14 and 4.15. The cytokine, chemokine and fungal burden values from each WT, CLR KO and CLR DKO experiment were averaged and added to this figure. All cytokine/chemokine results are pg/ml. Results highlighted in green indicate this value increased from 24 to 48 hours. Results highlighted in red indicate this value decreased from 24 to 48 hours. N.D. represents no result detected. See individual experiment figures for the number of independent experiments completed and mice used.

Figure 4.16 displays the large influence gender and the microbiome have on the capability of mice to generate robust anti-A.*f*. immune responses.

Male mice that were not co-housed generated large anti-A.*f*. cytokine and chemokine responses that increased from 24 to 48 hours. This suggests these animals were actively responding against A.*f*. through to the 48-hour experiment end point. Fungal burden had not decreased at 48 hours indicating the infection was ongoing and not completely cleared.

Results from the microbiome controlled male and female experiments were very different to the previously described male experiments. Co-housing mice resulted in much smaller anti-A.*f*. cytokine and chemokine responses at 24 hours; this response had typically decreased by 48 hours. Fungal burden in both co-housed males and co-housed females mainly reduced from 24 to 48 hours. This suggests these mice generated an appropriate immune response that led to A.*f*. clearance. At 48 hours A.*f*. fungal burden was similar or reduced and the anti-A.*f*. cytokine and chemokine response had begun to resolve.

In order to highlight the stark difference co-housing mice and using male and female mice had the anti-A.*f*. cytokine and chemokine response, data collated in figure 4.16 was graphically displayed. The anti-A.*f*. MIP-1 response at 24 hours and 48 hours was displayed for male, male microbiome-controlled and co-housed female mice of each WT, CLR KO and CLR DKO genotype.

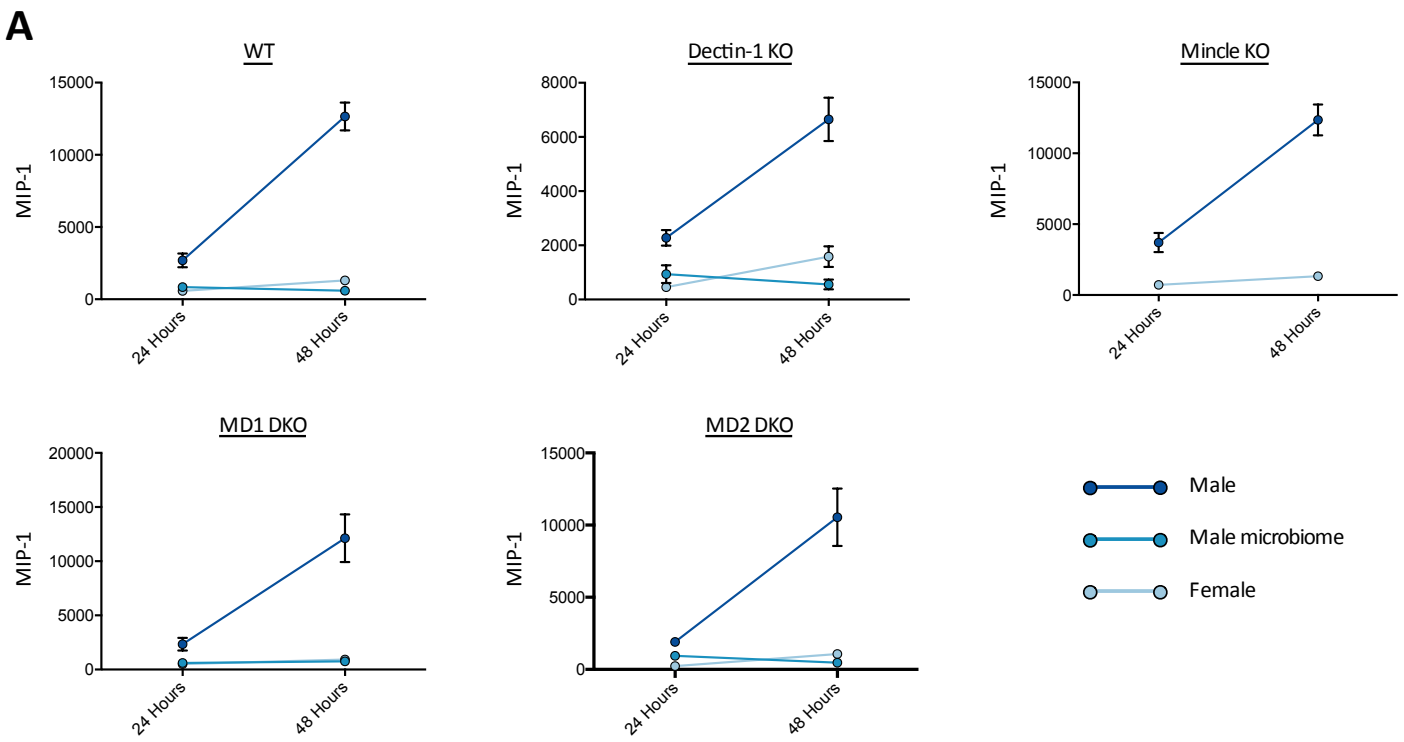

Figure 4.17: Co-housing animals to control the microbiome prior to A.*f*. infection drastically alters anti-A.*f*. MIP-1 response. A) The data in this figure is collated from the experiments displayed in figure 4.9, 4.10, 4.12, 4.13, 4.14 and 4.15. The MIP-1 pg/ml response values from each WT, CLR KO and CLR DKO experiment were added to this figure. Graph displays mean +/- s.e.m. See individual experiment figures for the number of independent experiments completed and mice used.

172

Figure 4.17 highlights the challenges identified aiming to determine the impact CLR KO and CLR DKO has on the anti-A.*f*. immune response. Although initial experiments were promising, the results obtained in figures 4.9 and 4.10 were not expected. When examining the influence each genotype's microbiome may confer over the anti-A.*f*. immune response a drastic alteration of results was attained. When examining the gender of mice used for CLR KO and CLR DKO A.*f*. infection experiments, a similarly drastic alteration of results was attained. This role the microbiome and gender of mice has on their ability to respond against A.*f*. has not been published. Here, we show both these factors have a crucial role influencing the anti-A.*f*. response. Unfortunately, the requirement for Dectin-1, Dectin-2 and Mincle expression and signalling was not determined. Before these experiments could be accurately and appropriately completed, a better understanding of microbiome and gender influence is required. Here, I describe the ability of immune-competent mice to clear A.*f*. infection irrespective of CLR status. In order to identify the true role of CLRs during A.*f*. infection mice may have to be immune-suppressed.

4.4: Discussion

The aims of this chapter were centered on identifying the importance of CLRs when generating anti-A.*f*. immune responses. Initially, I aimed to elicit the impact CLR expression had on the ability of alveolar macrophages to respond against A.*f*.. Once these experiments were completed, a well-described *in vivo* model of A.*f*. infection was optimised for our facility before being used to infect WT, CLR KO and CLR DKO mice. Only Dectin-1 has a defined role during alveolar macrophage anti-A.*f*. responses and during *in vivo* A.*f*. challenge. The role of Dectin-2 and Mincle during the anti-A.*f*. alveolar macrophage and *in vivo* response are unknown.

I was particularly interested in identifying CLR collaboration within this model. I hypothesised that CLRs collaboratively recognise and respond to A.*f*. enhancing the immune response. This project aims to describe anti-A.*f*. immune-enhancing CLR collaboration that could be therapeutically boosted to improve the anti-A.*f*. response resulting in clearance of A.*f*. disease.

4.4.1: What role do CLRs play in the alveolar macrophage anti-A.*f*. response?

Alveolar macrophages act as the first responder during A.*f*. infection. A.*f*. RC are regularly inhaled and rapidly cleared without pathology by alveolar macrophages. The efficient recognition and phagocytosis of inhaled A.*f*. RC is exclusively undertaken by lung-resident alveolar macrophages [1, 87, 250].

Dectin-1 has a clearly described role on macrophages during the anti-A.*f*. immune response. Research has demonstrated the murine peritoneal macrophage phagocytosis of A.*f*. SC and EG required Dectin-1. Blocking Dectin-1 using antibody significantly reduced A.*f*. phagocytosis in these experiments [98]. RAW 264.7 macrophages over-expressing Dectin-1 generated a significantly increased cytokine

and chemokine response when stimulated for 24 hours with A.*f*. This increased response from over-expressed Dectin-1 could be completely abrogated with the addition of 2A11 blocking antibody [2]. The requirement for Dectin-1 expression on alveolar macrophages during anti-A.*f*. responses is also well described. When A.*f*. was incubated with alveolar macrophages from WT and Dectin-1 KO mice for 24 hours an 80% decrease in cytokine and chemokine response was attained from Dectin-1 KO alveolar macrophages [2]. Here, the Dectin-1 KO A.*f*. cytokine and chemokine response (displayed in figure 4.3) aligns with published research highlighting the importance of Dectin-1 expression on alveolar macrophages. Lacking Dectin-1 expression significantly impairs the early anti-A.*f*. inflammatory response. The impact Mincle and Dectin-2 convey on the alveolar macrophage anti-A.*f*. response is not well described.

The expression of Mincle on alveolar macrophages is poorly defined. However, Mincle expression is well described on macrophages and neutrophils in response to several inflammatory stimuli including LPS, TNF and IFN-γ [271, 272]. Mincle expression on alveolar macrophages has been induced after stimulation with *Mycobacterium bovis bacillus Calmette-Guérin*. The induction of Mincle in these experiments was very delayed and often required >24 hours of alveolar macrophage stimulation [192]. Here, I have shown, in figure 4.2, that Mincle expression is induced on alveolar macrophages by stimulating with 2µg/ml LPS for 4 hours.

The role of Mincle during the alveolar macrophage anti-A.*f*. response has not been identified. The receptor binds fungal pathogens and induces intracellular signalling culminating in the production of cytokines and chemokines including TNF, IL-6, MIP-1, MIP-2 and KC [136]. Some research has elicited a pro-inflammatory role for Mincle on alveolar macrophages; stimulating Mincle KO alveolar macrophages with TDM resulted in a significantly impaired TNF, MIP-2 and KC response [192]. Here a similar pro-inflammatory role for Mincle expressed on alveolar macrophages during the anti-A.*f*. response was not identified. My experiments show the Mincle KO anti-A.*f*. cytokine and chemokine response was not significantly different to the response from WT mice. These experiments also included a Mincle Dectin-1 DKO model. The Dectin-1 KO impaired anti-A.*f*. cytokine and chemokine response is conserved within the MD1

DKO. This further suggests Mincle KO has a limited impact on the ability of alveolar macrophages to recognise and produce anti-A.*f*. responses during early A.*f*. infection.

An immune evasion role for pathogens engaging Mincle has been described. The fungal pathogen *Fonsecaea monophora* engages Mincle to avoid interaction with Dectin-1 and a subsequent pro-inflammatory response. Engaging Mincle results in the induction of the E3 ubiquitin ligase Mdm2-dependent degradation pathway. This culminates in the loss of IRF1 impairing the pro-inflammatory immune response [157]. An evasion role for A.*f*. engaging Mincle is not present in my alveolar macrophage response results. Mincle KO does not increase the anti-A.*f*. cytokine and chemokine response. Mincle KO does not alter the Dectin-1 KO impaired cytokine and chemokine response when both receptors are knocked-out together.

The expression of Dectin-2 on alveolar macrophages has not been clearly described. Dectin-2 expression was identified on large, scattered lung cells but these cells were $CD11c^{low}$. The majority of $CD11c^{high}$ lung cells did not express Dectin-2 [176]. Murine alveolar macrophages are typically defined by $CD11c^{high}$ expression [273]. Dectin-2 expression at mRNA level in alveolar macrophages has been described although the presence of the receptor at the cell surface was not confirmed [178]. Here, (as shown in figure 4.2) I show that Dectin-2 expression is induced on alveolar macrophages stimulated with 2µg/ml LPS for 4 hours.

The role of Dectin-2 during the early, alveolar macrophage driven anti-A.*f*. response is not described. However, the receptor has been implicated in the neutrophil and monocyte derived, later anti-A.*f*. response. Dectin-2 recognises hyphal morphologies of A.*f*. and is essential when producing robust cytokine and chemokine responses against A.*f*. HY [185]. Therefore, it is possible that the impact that Dectin-2 has in the alveolar macrophage-driven early A.*f*. response may be minimal [183].

A role for Dectin-2 expression on alveolar macrophages has been described in a house dust mite *ex vivo* model. The release of cysteinyl leukotrienes (potent inflammatory lipid mediators associated with allergic inflammation) following house dust mite

challenge was dependent on alveolar macrophage Dectin-2 expression. Interestingly, stimulating alveolar macrophages with house dust mite also resulted in the production of TNF and KC but this was independent of Dectin-2 [274]. Here, while I did not have access to alveolar macrophages from Dectin-2 KO, I show that Mincle Dectin-2 DKO do not display any defects in cytokine and chemokine production. This suggests Dectin-2 is not required for the early anti-A.*f*. immune response and may only be important if A.*f*. persists and germinates into HY.

Here I clearly demonstrate our Dectin-1 KO alveolar macrophage A.*f*. experiments align with published research. My results describing the limited impact Dectin-2 expression has on the alveolar macrophage anti-A.*f*. response was expected. Dectin-2 likely plays a role during the later anti-A.*f*. response against extensively developed A.*f*. infections. The role of Mincle during alveolar macrophage anti-A.*f*. responses appears to be minimal.

4.4.2: What roles do CLRs play in the anti-A.*f*. immune response *in vivo*?

The role of CLRs during the complicated and multi-faceted *in vivo* anti-A.*f*. response is not well described. The experiments completed and results displayed in figures 4.9, 4.10 and 4.11 were based on similar experiments used to identify the importance of Dectin-1 during *in vivo* A.*f*. infection. This protocol challenged mice with the same dose as my experiments, $5x10^7$ A.*f*. RC, for 5 days, 48 hours and 24 hours. In these experiments Dectin-1 KO mice experienced significantly decreased survival, significantly impaired anti-A.*f*. cytokine and chemokine responses and significantly increased lung fungal burden [100]. The impact Mincle and Dectin-2 have during A.*f*. *in vivo* challenge has not been identified.

An anti-fungal *in vivo* role for Mincle has been described. Mincle enhances *in vivo* *Candida albicans* infection clearence. When Mincle KO mice were intravenously challenged with *Candida albicans* a significant increase in kidney fungal burden was obtained; however, this did not result in decreased survival at 5 days. Increased fungal

burden was thought to arise from an impaired TNF inflammatory response produced by Mincle KO mice [190]. The role Dectin-2 plays during *in vivo* fungal challenge has also been described. Dectin-2 KO mice were more susceptible to systemic *Candida albicans* infection, generating an impaired pro-inflammatory immune response and possessing an elevated fungal burden in the kidney [180]. Dectin-2 KO mice also produced an impaired pro-inflammatory response when challenged with *Pneumocystis* lung infection [275].

Here, the anti-A.*f*. cytokine and chemokine results shown in figure 4.9 align with previous research clarifying the importance of Dectin-1 during *in vivo* A.*f*. challenge. A significant reduction in TNF, MIP-1 and MIP-2 response was observed at 48 hours from Dectin-1 KO mice. However, no significant difference was attained between WT and Dectin-1 KO fungal burden. Contrary to published research, our model suggests high Dectin-1 redundancy *in vivo* in this immune-competent model. Although Dectin-1 KO mice lack a robust cytokine and chemokine response, they still efficiently clear A.*f*..

Figure 4.10 displays the 24-hour A.*f*. infection results in which the Dectin-1 KO impaired cytokine and chemokine response is not present. This was not expected and may arise from the large, single dose of A.*f*. masking early, subtle CLR-dependent differences. At 24 hours Dectin-1 KO fungal burden appears to be lower than WT fungal burden. A very robust anti-A.*f*. response in WT mice may impair their early fungal clearance. The reduced cytokine and chemokine response exhibited by Dectin-1 KO mice is potentially, in this model at least, protective.

Further to WT mice possessing increased 24-hour fungal burden, WT mice also experienced decreased survival in figure 4.7. The robust cytokine and chemokine response of WT mice may lead to systemic inflammatory response syndrome or sepsis culminating in mice succumbing to the resulting pathology [276, 277]. A recent publication suggests infection with higher doses of A.*f*. results in efficient fungal killing; lower A.*f*. doses increase the likelihood of developing persistent, invasive disease [278]. This may explain the reduced survival elicited from mice infected with lower doses of A.*f*. shown in figure 4.7.

Here, in figures 4.9, 4.10 and 4.11 I describe the ability of Mincle KO mice to successfully respond to and clear A.*f*. infection. Unlike Mincle's pro-inflammatory role during *Candida albicans* infection, Mincle KO mice did not possess significantly increased or decreased anti-A.*f*. cytokine or chemokine response at 12, 24 or 48 hours. However, the earlier mentioned Mincle KO reduced TNF response against *Candida albicans* was attained from BMDMs and not *in vivo* experiments. Mincle does not appear to have a role in controlling A.*f*. fungal burden, as was found in the *Candida albicans in vivo* experiments [190].

I can also speculate Dectin-2 has a limited role during *in vivo* A.*f*. infection. The Dectin-2 KO model was not available so all Dectin-2 results are extrapolated from MD2 DKO mice. As mentioned, Mincle does not play a significant role during A.*f. in vivo* infection. The results from MD2 DKO suggest Dectin-2 also does not contribute to the anti-A.*f*. cytokine and chemokine response and has limited impact controlling A.*f*. fungal burden. No significant change in results was obtained with MD2 DKO mice. Either Dectin-2 does not play a crucial role, or Mincle KO when alongside Dectin-2 KO restores the immune response back to WT levels. The subtle or lack of CLR importance may be due to the immune-competent model used here. Immune-suppressing mice may identify much clearer CLR roles.

CLRs likely collaborate during the anti-A.*f*. response, I hypothesised this collaboration enhances the immune response and promotes A.*f*. clearance. Many examples of CLR TLR collaboration have been described. Dectin-1 collaborates with TLR2 and TLR4 to enhance LPS and Pam3CSK4 cytokine responses [279], Dectin-1, mannose receptor and TLR2 collaborate to enhance inflammatory responses and drive T_H17 immunity against *Paracoccidioides brasiliensis* [280] and Mincle and TLR collaborative signalling results in clearance of *Fonsecaea perdrosi* infection [187]. These examples of CLR TLR signalling highlight the importance of receptor collaboration during immune responses. Recently, a similar collaboration involving multiple CLRs was identified. Dectin-1 and Dectin-2 collaboratively promote control of *Trichophyton rubrum*. Both CLRs were demonstrated to recognise the fungal pathogen and were required for robust TNF, IL-1β, IL-10 and IL-6 responses. Dectin-1 and Dectin-2 DKO impaired fungal

clearance to a greater extent than the sum of individually lacking both CLRs [221]. CLR collaboration when recognising and responding to A.*f*. infection has not been described; although, the complex anti-A.*f*. response likely requires CLR collaboration.

Interestingly, the significantly impaired anti-A.*f*. cytokine and chemokine response identified in Dectin-1 KO and MD1 DKO alveolar macrophages was not conserved within the *in vivo* A.*f*. infection. Only the Dectin-1 KO impaired response was maintained in the *in vivo* infection results. This suggests a pro-inflammatory role for Mincle during the anti-A.*f*. cytokine and chemokine response *in vivo*. However, this role may be complicated, Mincle KO alone does not alter the anti-A.*f*. response. Here, I describe a protective role for Mincle KO recovering the Dectin-1 KO impaired anti-A.*f*. cytokine and chemokine response in MD1 DKO mice.

Mincle may act as an A.*f*. immune evasion target in a similar mechanism to *Fonsecaea monophora* [157]. The A.*f*. engagement of Mincle may aid the evasion of pro-inflammatory responses. When Mincle is knocked out, A.*f*.-Mincle evasion cannot occur and the pro-inflammatory response is restored. This may be the mechanism by which Mincle KO recovers the Dectin-1 KO impaired anti-A.*f*. pro-inflammatory responses. However, an enhanced anti-A.*f*. response is not present in Mincle KO suggesting the reason MD1 DKO responds robustly to A.*f*. when Dectin-1 KO does not, may be more complicated than this.

The results displayed in figures 4.9 through 4.11 begin to describe the complex role each CLR plays in the collaborative and complex anti-A.*f*. response. However, the A.*f*. fungal burden results and anti-A.*f*. cytokine and chemokine results from these experiments were not expected. Dectin-1 KO mice only produced an impaired cytokine and chemokine response after 48 hours and this did not impact their ability to clear A.*f*. infection. No other CLR KO or CLR DKO produced an enhanced or impaired anti-A.*f*. response. The fact WT mice experienced the highest mortality was also not expected. Therefore, the impact the microbiome may be conferring over WT, CLR KO and CLR DKO mice ability to mount an immune response was examined.

4.4.3: What impact was the microbiome conferring over the ability of WT, CLR KO and CLR DKO mice to generate immune responses against A.*f*.?

The role the microbiome controls over the development, function and threshold of immune response is starting to be understood [262, 263]. The microbiome directs immune development and function and sets the threshold for immune responses. An important homeostatic role for the microbiome maintaining the balance between immune tolerance, acute lung inflammation and chronic lung inflammation has been described [264]. Controlling and minimising microbiome variation between mice can reduce, or even nullify, a previously observed disease phenotype [265]. The experiment results displayed in figures 4.12 and 4.13 suggest controlling the WT, CLR KO and CLR DKO microbiome through co-housing mice dramatically alters the anti-A.*f*. response in these animals.

The results from figure 4.12 and 4.13 are summarised alongside non-microbiome controlled experiments in figure 4.16 and 4.17. These figures describe the decreased fungal burden and reduced anti-A.*f*. cytokine and chemokine response attained from microbiome-controlled experiments. Controlling the microbiome appears to impact the duration of the anti-A.*f*. response. Non-microbiome-controlled WT, CLR KO and CLR DKO mice possessed higher fungal burden and produced greater quantities of cytokines and chemokines at 48 hours. Controlling the microbiome appears to enhance A.*f*. clearance as WT, CLR KO and CLR DKO mice fungal burden was reduced at 48 hours and their inflammation was resolving.

Here, in the experiments displayed in figures 4.12 and 4.13, I demonstrate the profound impact altering the microbiome can have on the host immune system and disease susceptibility. The results attained from controlling the microbiome align with other research highlighting the dramatic implications the microbiome can convey during immune responses. An example of this was described within a *Clostridium difficile* infection model. Mice lacking one single gut bacteria (often destroyed by the therapeutic administration of a specific antibiotic class) were highly susceptible to a

resistant strain of *C. difficile*. When this bacterium was added back into the microbiome a dramatic reduction in susceptibility to *C. difficile* infection was attained [281]. A similar mechanism may be present in my experiments. Upon switching the bedding from WT, CLR KO and CLR DKO mice around each cage, I may have introduced new bacteria into the gut of mice that resulted in an enhanced anti-A.*f*. response and promotion of A.*f*. clearance.

Furthermore, CLRs play a role within gut immunity contributing to the maintenance and homeostasis of the microbiome. The CLRs I am investigating are present on many gut-resident cells [282]. Many of these cells are responsible for controlling intestinal infections [283]. Therefore, although forcibly controlling the microbiome radically alters the anti-A.*f*. immune response, the microbiome differences between WT, CLR KO and CLR DKO may naturally result from their CLR expression impacting their gut immunity.

Controlling the microbiome did drastically alter the anti-A.*f*. immune response; however, not in the way I expected or hypothesised. This moved the Dectin-1 KO results further away from published research. Therefore, the impact the gender of WT, CLR KO and CLR DKO mice had on the anti-A.*f*. response was examined.

4.4.4: What impact was gender conferring over the ability of WT, CLR KO and CLR DKO mice to generate immune responses against A.*f*.?

Gender has a significant influence on the generation of anti-fungal immune responses [270]. This is thought to be associated with the genetic and hormonal differences between males and females [267]. Here, the experiments displayed in figure 4.14 and 4.15 align with this research, as the female anti-A.*f*. response is very different to the male and male microbiome-controlled experiments.

Interestingly, the fungal burden results obtained from female mice at 24 hours agree with our initial hypothesis that as more CLRs are knocked out fungal burden increases. At 48 hours, inflammation had started to resolve and aside from WT mice, fungal burden was similar or had decreased. This suggests female mice may clear A.*f*. more efficiently than males. Research examining the influence of age and gender when mice were challenged with *Crytococcus neoformans* concluded female mice produce more robust immune responses and experience increased survival when compared to male mice. Interestingly, young male mice (6-8 weeks) possessed the shortest survival and highest infection burden [284]. The mice used for my *in vivo* A.*f*. challenge experiments were 8-12 weeks of age.

The Dectin-1 KO impaired chemokine response may be subtly present at 24 hours, however; the low number of mice used reduces the female experiment results power. At 48 hours the chemokine response was similar across all WT, CLR KO and CLR DKO mice. The significant Dectin-1 impaired 48-hour chemokine response attained in males was not present in females. As previously described in males, WT mice possessed the highest fungal burden at 48 hours. This is potentially due to their robust response inhibiting A.*f*. clearance. Female mice were co-housed before being used in experiments. As with the male microbiome-controlled experiments, this may have radically altered their anti-A.*f*. response.

4.5: Conclusions

The results displayed in these experiments highlight the complex and poorly understood anti-A.*f*. immune response. Alveolar macrophages require Dectin-1 to appropriately recognise and respond to A.*f*.. Dectin-2 and Mincle may not be involved in the early, alveolar macrophage driven anti-A.*f*. response. The response *in vivo* is much more difficult to interpret. The microbiome may have an important role defining the capability of each animal's anti-A.*f*. response. The microbiome appears to modulate the anti-A.*f*. cytokine and chemokine response irrespective of CLR status or gender; ultimately impacting how efficiently A.*f*. infections are cleared.

My experiments identified no significant difference in fungal burden between WT, CLR KO and CLR DKO mice. This suggests high levels of CLR redundancy during the anti-A.*f*. response in an immune-competent model. However, an interesting role for Mincle recovering the Dectin-1 impaired anti-A.*f*. cytokine and chemokine response has been identified. This recovery does not involve Mincle's alveolar macrophage action but likely requires Mincle's presence and anti-A.*f*. impact on other cell types. Here, alongside the microbiome, I also show the gender of the animal has an impact on the anti-A.*f*. response. Female mice cleared the A.*f*. infection faster than male mice; however, initially hypothesised differences between WT, CLR KO and CLR DKO fungal burden were identified in females at 24 hours.

4.6: Further experiments

The clinical course of A.*f*. infection typically involves a high level of immune-suppression, low dose inoculation and A.*f*. growth resulting from an impaired immune response. This is very different to the single, high-dose A.*f*. infection model used for the experiments described in this chapter. Switching to an immune-suppression A.*f*. infection *in vivo* model involving a low-dose A.*f*. infection and extensive A.*f*. growth within the lung may more closely reflect clinical disease course. An immune-suppression model may also exacerbate the subtle differences I have identified between WT, CLR KO and CLR DKO mice anti-A.*f*. response. The course of infection during an immune suppression model would permit longer experiments and A.*f*. growth, not simply a robust A.*f*. immune response leading to rapid clearance. This may help attain differences between WT, CLR KO and CLR DKO fungal burden.

In order to identify the mechanism by which MD1 DKO recovers the Dectin-1 KO deficient anti-A.*f*. cytokine and chemokine response, the influx of cells into the lung could be examined alongside the ability of those cells to respond against A.*f*.. Determining the Mincle-expressing cell-type with the ability to recover the Dectin-1 deficient response may be very interesting. This cell-type may provide a therapeutic target enhancing the anti-A.*f*. response.

Here, I begin to describe the important impact the microbiome has in controlling host immunity in the lung, but only in males. In order to identify the role of the microbiome in females, experiments without co-housing females could be completed.

Chapter 5

Using CLR status and functional response capability to stratify haematology patients according to their A.*f*. disease susceptibility

5.1: Aims

I. Determine patient's CLR status

II. Determine patient's functional immune response capability

III. Identify novel risk factors that can be used to stratify patients according to their A.*f*. disease susceptibility

5.2: Introduction

Before the clinical use of immune suppressing therapeutics, A.*f*. infections were uncommon and rarely serious. Typically, a mild allergic-type disease would present after the repeated and regular inhalation of A.*f*. spores. Only individuals with pre-existing lung cavities that were exposed to high doses of A.*f*. would experience A.*f*. growth within the lung; however, even in this scenario A.*f*. could not grow outside of the cavity and cause serious disease. As the use of immune suppressing therapeutics has become more prevalent, the incidence of serious and invasive A.*f*. infections has increased [1].

The immune response against A.*f*. is rapid and robust; however, when the anti-A.*f*. immune response is impaired, A.*f*. growth and disease may ensue. Two different types of immune suppression give rise to two different A.*f*. disease courses. Patients with cancers including AML often become neutropenic during chemotherapy and radiotherapy treatments. Neutropenia is a significant risk factor for developing A.*f*. infections [7]. Neutropenic patients with A.*f*. infections are subject to systemic, invasive A.*f*. disease [285].

Patients undergoing corticosteroid therapy for graft versus host disease experience a different A.*f*. disease course. These patients do not lack immune cells but their anti-A.*f*. immune response is impaired. For example, macrophages treated with corticosteroids display significantly reduced A.*f*. RC phagocytosis [14]. Corticosteroid therapy patients contain A.*f*. infections within the lung but suffer from chronic lung inflammation. This often results in scarring, lung fibrosis and a reduced lung capacity.

Current diagnostic and therapeutic clinical tools used for A.*f*. infections are insufficient. Patients are diagnosed with a proven A.*f*. infection only when histological evidence is available, probable disease relies on radiological changes and biomarkers. The diagnostic procedure is often a slow process with inaccurate results and many

patient's A.*f*. infections are only confirmed post-mortem [286]. Poor A.*f*. infection diagnosis culminates in the widespread empirical use of anti-fungal therapies at the first suspicion of infection. Therefore, many patients are inappropriately treated with anti-fungal therapies. PCR and galactomannan ELISA can be used to screen patients at high risk where negative tests can be used to rule out A.*f*. infection and multiple positive results can suggest A.*f*. infection [287-289].

Currently used anti-fungal therapeutics are inadequate to deal with complex patient's fungal disease. Voriconazole and liposomal amphotericin B are the most frequently used therapeutics for A.*f*. infection. These drugs are toxic to the liver and kidneys, adversely interact with other drugs and acquisition costs are high [59]. Furthermore, some A.*f*. strains have become resistant to azole treatment [290]. The widespread use of prophylactic and empirical anti-fungal treatment and the complex issues this causes, suggest a better approach to diagnosis and treatment is required.

Stratifying patients according to their risk of developing A.*f*. infections would reduce unnecessary treatment, limit further fungal resistance and allow low risk patient's primary disease treatment to be prioritised. Currently, neutropenia is the only widely accepted risk factor for the development of A.*f*. infections. Identifying more risk factors may further aid patient stratification. I aim to investigate associations between the incidence of IA and patient's CLR status and patient's functional immune response capability.

Many CLRs integral to anti-fungal immunity signal using the CARD9 complex, individuals possessing mutated CARD9 are at significantly greater risk of developing invasive fungal infections [159]. Individuals with mutated Dectin-1 are at risk of developing invasive fungal infections even without immune suppression [291]. The Dectin-1 mutation Y238X, leading to an early stop codon and truncated Dectin-1, has been associated with an increased susceptibility to A.*f*. infection in hematopoietic transplant patients [292]. Y238X Dectin-1 resulted in an impaired peripheral mononuclear cell IFN-γ, IL-10, IL-1β, IL-6 and IL-17A response [293]. Recently, mutations in Dectin-1 and DC-SIGN, respiratory viral infection, allogeneic stem cell

translation and A.*f*. PCR positivity were used to stratify patients in a predictive disease model. Patients with no risk factors had a 2.4% probability of developing an A.*f*. infection whilst patients with four or more risk factors had a 79% probability of developing an A.*f*. infection. This study begins to identify patient stratification risk factors permitting the implementation of a personalised medicine approach [67].

Here, I aim to examine the expression levels of Dectin-1, Dectin-2, Mincle and Mcl and determine the prevalence of mutations in these CLRs. Identifying correlation between CLR expression or mutation and the incidence of A.*f*. disease may identify novel risk factors. Currently, CLR status has not been linked to an increased susceptibility to A.*f*. disease beyond the previously described Dectin-1 and DC-SIGN mutations. It may also be possible to identify patient's CLR co-expression and determine whether this impacts A.*f*. disease susceptibility.

I also aim to determine the ability of patient's PBMCs to respond to inflammatory stimuli; this has not been used to stratify patients before. If successful, these CLR expression and functional assays may be used in healthcare centers to stratify patients according to their A.*f*. disease susceptibility. This would permit a personalised medicine approach to treating A.*f*. disease in complex haematology patients.

5.3: Results

A prospective cohort of 43 patients with haematological malignancies admitted for stem cell transplantation (23 patients) or remission-induction therapy for AML (19 patients) were studied. Of the 23 SCT patients included in this study, 5 developed proven IA and 1 developed probable IA. Of the 19 AML patients included in this study 4 developed proven IA.

Blood samples collected in PAXgene blood RNA tubes and EDTA tubes were transferred to the laboratory within 24 hours. Patients were screened throughout their hospital stay for IA using *Aspergillus* PCR and galactomannan Platelia assay [288]. IA was diagnosed using EORTC/MSG criteria [294]. See 2.1.3 for ethical approval statement.

The results throughout this chapter include varying numbers of patients. Due to limited sample for some patients, not all CLR status and functional results were determined for each patient. Patient 18's blood samples were not processed. CLR expression results were not attained from five patients; four of these were SCT and one AML. Functional results were not attained from two patients; these were both AML.

5.3.1: Determination of patient CLR status

CLRs are crucial for anti-fungal immune responses. The requirement for CARD9 complex signalling and Dectin-1 signalling during A.*f*. infection has been well described. Similar roles for Dectin-2, Mincle and Mcl during A.*f*. infection have not been described.

Here, the expression and genetic sequence of Dectin-1, Dectin-2, Mincle and Mcl was examined, I also investigated CLR co-expression. Identifying CLR expression deficiencies, mutations and receptor collaboration may provide novel risk factors aiding patient stratification according to A.*f*. infection risk.

Patient RNA was obtained from 2ml whole blood using the PAXgene Blood RNA equipment and standard protocol (PreanalytiX). The integrity of extracted RNA was examined. Patient's CLR status could only be determined from highly intact RNA. RNA was extracted from Patients 1, 2 and 3, and was separated by gel electrophoresis.

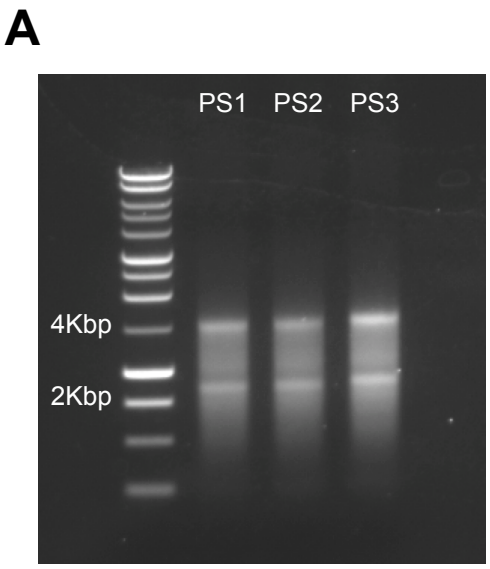

Figure 5.1: Whole blood extracted RNA is intact and suitable for further analysis. RNA was extracted from whole blood collected in PAXgene RNA blood tubes. Patient 1, 2 and 3 blood-extracted RNA samples were separated by gel electrophoresis. A 1kb ladder was included. This experiment was undertaken as part of the optimisation protocol. Data is representative of one independent experiment.

Figure 5.1 displays clear 28S ribosomal bands at 4kb and 18S ribosomal bands at 2kb in each patient sample. This indicates intact RNA was extracted from blood and this RNA is suitable for further experimental analysis [295]. In order to identify the

presence of mutations in the coding region of patients' CLRs, Dectin-1, Dectin-2, Mincle and Mcl genes were amplified by PCR. The product of each PCR reaction was examined; the presence of a single, correctly sized band for each CLR gene was confirmed.

cDNA was generated from Patient 1, 2 and 3's extracted RNA and PCR was used to amplify each CLR gene. After PCR amplification, CLR samples were purified and separated by gel electrophoresis.

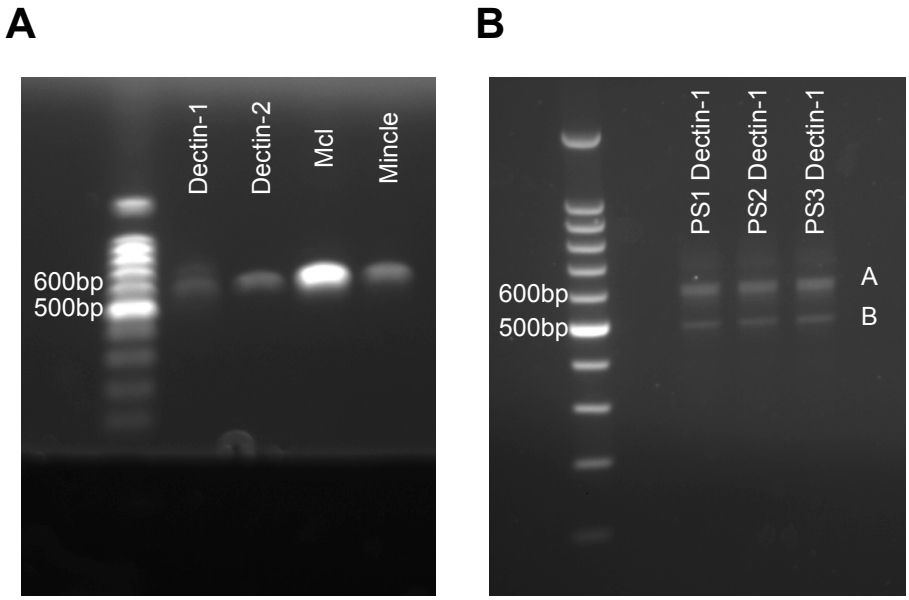

Figure 5.2: Dectin-1 Isoform A and Isoform B, Dectin-2, Mincle and Mcl were successfully amplified from patient cDNA. A) Amplification of Patient 1's CLR genes produced correctly sized (~600bp) PCR product. Two bands were attained from Dectin-1 amplification **B)** Patient 1, 2 and 3's Dectin-1 PCR amplification samples were separated by 3% gel electrophoresis. Dectin-1 Isoform A is ~600bp in size, Dectin-1 Isoform B is ~500bp in size, both CLR isoforms were amplified. A 100bp ladder was included. This experiment was undertaken as part of the optimisation protocol. Data is representative of one independent experiment.

Figure 5.2 (A) displays the successful amplification of Dectin-2, Mincle and Mcl genes from patient cDNA. This permitted the sequencing of these genes for each patient. Figure 5.2 (B) identifies both Dectin-1 Isoform A and Dectin-1 Isoform B were amplified from patient cDNA. In order to determine the presence of any isoform-specific mutations or splice-variants, both Dectin-1 isoforms were separately excised, purified and sent for sequencing.

Two CLR mutants were detected in this cohort, a novel Dectin-2 mutation and a previously identified Mcl mutation.

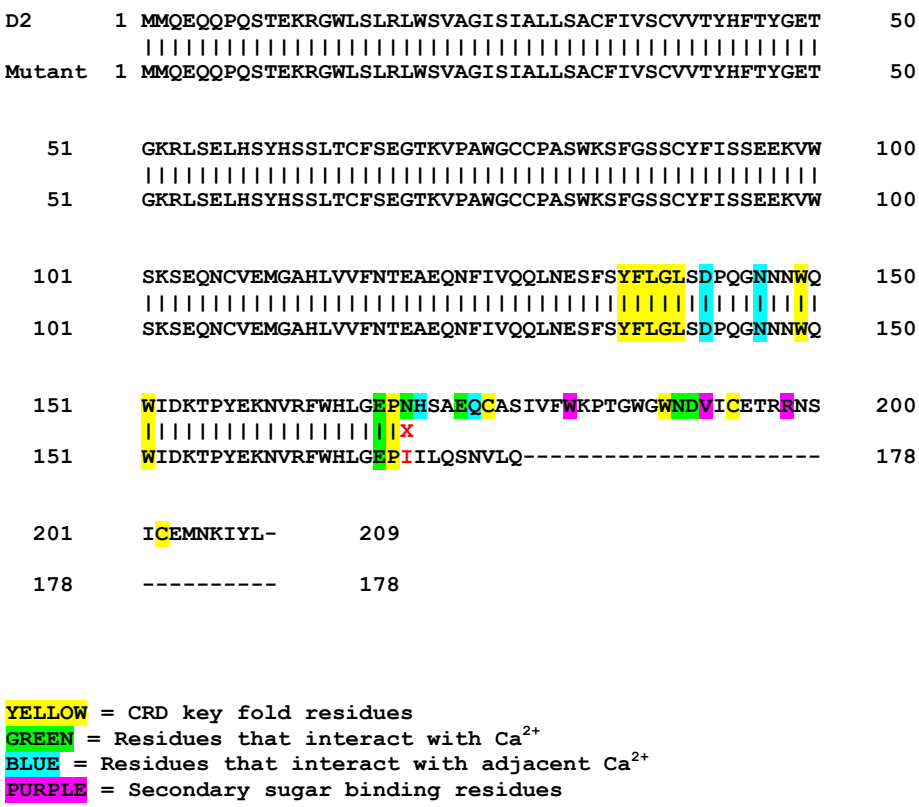

Figure 5.3: Dectin-2 mutant C505X results in an early stop codon and loss of Dectin-2 ligand-recognition domain. Purified CLR PCR product from each patient was sequenced and the presence of CLR mutations determined. Red X indicates mutated residue. Dectin-2 C505X mutant was identified from patient 25. Four Dectin-2 primers were used for complete and thorough gene sequencing coverage. This Dectin-2 mutation was sequenced twice with all four primers. Key residues and domains highlighted in Dectin-2 were attained from [296].

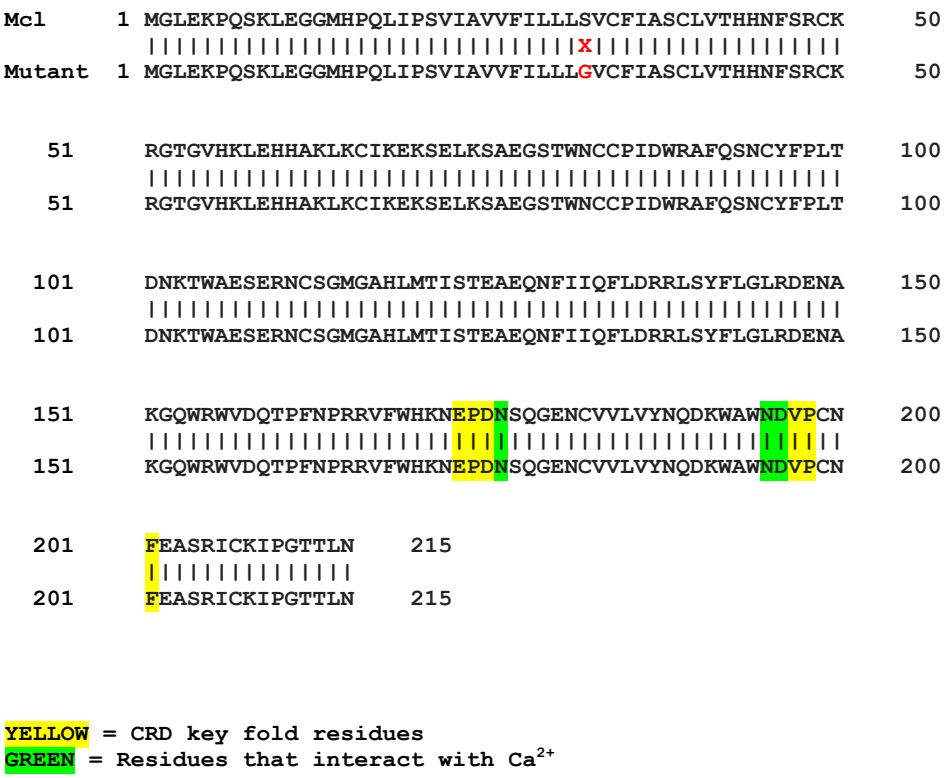

Figure 5.4: Mcl A94G mutant identified in patient populations results in an amino acid substitution from serine to glycine. Purified CLR PCR product from each patient was sequenced and the presence of CLR mutations determined. Red X indicates mutated residue. Mcl A94G mutant was identified from 17 of 42 patients. Four Mcl primers were used for complete and thorough gene sequencing coverage. Key residues and domains highlighted in Mcl were attained from [197].

Having identified CLR mutations and their incidence within the patient cohort, it was next important to determine CLR expression for each patient. This was achieved using Real-Time qPCR analysis of CLR expression. Although CLR mutations have previously been associated with an increased incidence of A.*f*. disease, CLR expression has not been investigated in the same manner [67, 293, 297].

A limited quantity of RNA was extracted from each patient and used to generate cDNA. In order to maximise the use of patient RNA, an experiment was completed comparing the sensitivity of qPCR CLR reactions dependent on the quantity of patient cDNA used. 20ng of cDNA was appropriate for the detection of each CLR gene by qPCR analysis using Taqman qPCR pimer/probe sets.

CLR qPCR reactions on a control sample were included on every 96/384-well qPCR plate used during this study. HPRT expression was measured for every sample and used as the endogenous control. Taken together, a control patient sample and endogenous control (HPRT) in every sample permitted the comparison of all patients CLR gene expression using the ΔΔCt method.

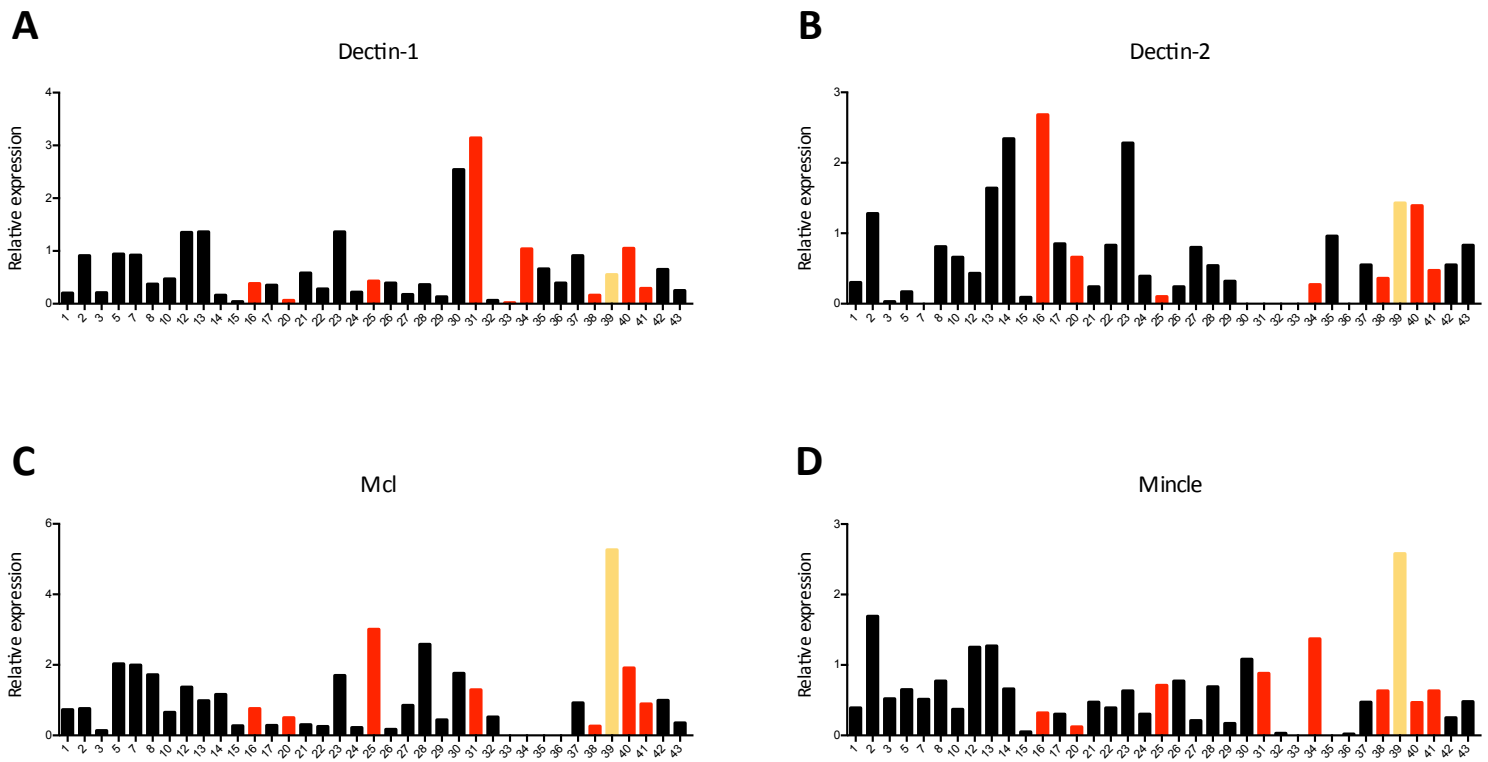

Figure 5.5: Patient CLR expression profiles are highly variable and do not clearly predict A.*f*. disease. Each patient's CLR expression was determined by qPCR using Taqman probes against each CLR. Alongside each patient qPCR reaction, a control sample and HPRT gene was analysed. Data shown from patient samples was calculated using ΔΔCt comparison against control sample and HPRT gene. Each patient CLR sample was assayed in duplicate. Red data points indicate incidence of IA, yellow data points indicate likely incidence of IA.

The results displayed in figure 5.5 highlight the range of CLR expression identified in patients. No clear high or low CLR expression was consistently identified in patients with A.*f*. disease.

Patients enrolled in this study had different types of myeloid cancer and highly variable blood cell counts. White blood cell counts ranged from 0.9 to 16.5 x 10^9 cells/l and neutrophil counts ranged from 0.6 to 14.2 x 10^9 cells/l.

The CLR expression results displayed in figure 5.5 were determined from 20ng cDNA generated from each patient sample. These results did not account for the quantity of cells and cell types present in each patient's blood. Cells that do not express CLRs may have contributed towards patient's CLR expression. Therefore, the results from figure 5.5 were adjusted and normalised against each patient's blood cell count data. Patient's CLR expression was calculated from 20ng cDNA extracted from whole blood and normalised to account for cells present in whole blood able to express CLRs.

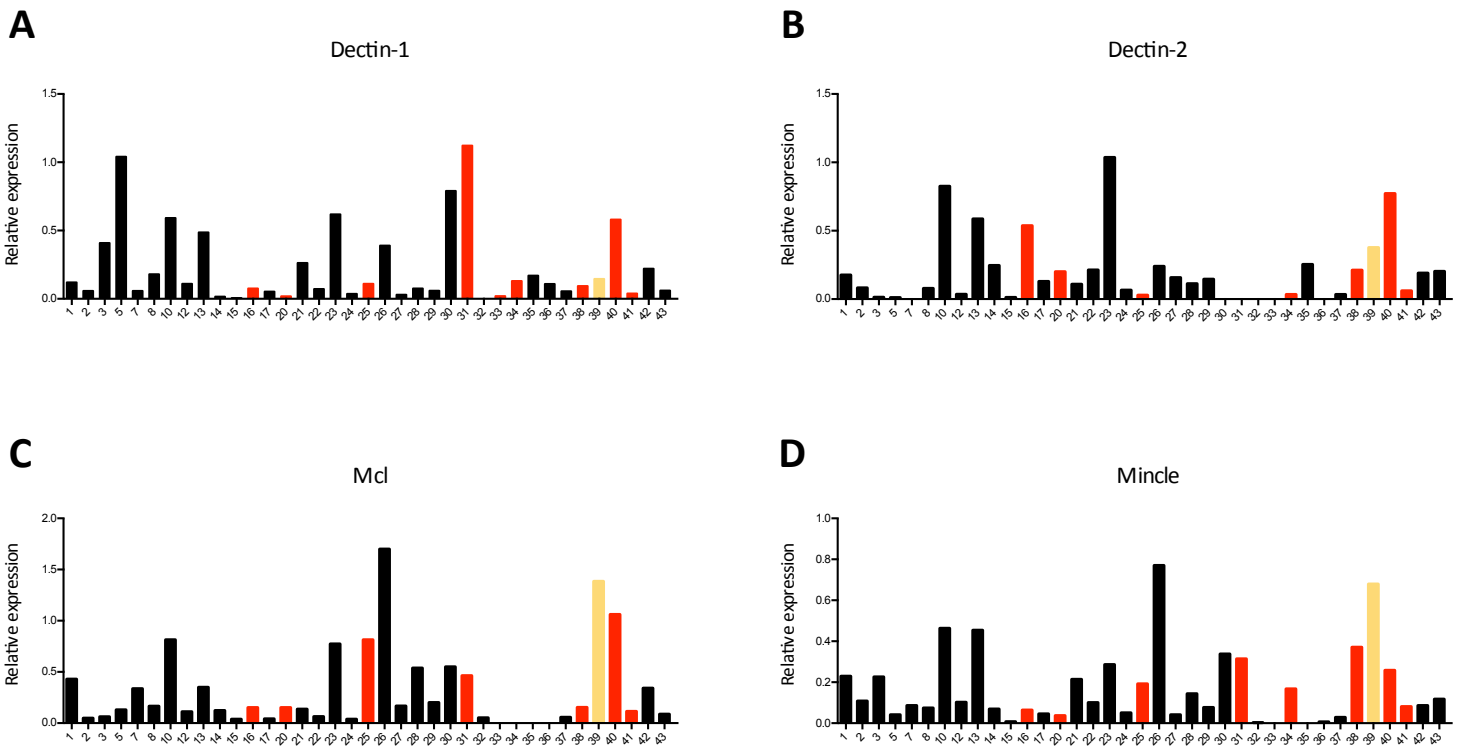

Figure 5.6: Patient CLR expression profiles normalised to patient cell counts are highly variable and do not clearly predict A.*f*. disease. Each patient's CLR expression was determined by qPCR using Taqman probes against each CLR. Alongside each patient qPCR reaction, a control sample and HPRT gene was analysed. Data shown from patient samples was calculated using ΔΔCt comparison against control sample and HPRT gene and was normalised to patient cells that express CLRs using patient's blood cell count results. Each patient CLR sample was assayed in duplicate. Red data points indicate incidence of IA, yellow data points indicate likely incidence of IA.

Figure 5.5 and figure 5.6 suggest there is no clear association between CLR expression and incidence of A.*f*. disease. The impact CLR expression has on the ability of patients to respond to inflammatory stimuli and ultimately their susceptibility to A.*f*. disease will be discussed later in this chapter.

The anti-fungal immune response requires collaboration from a multitude of immune receptors including TLRs and CLRs. Recently, CLR:CLR enhancing collaboration has been identified involving Dectin-1 and Dectin-2 [221]. Patient's CLR expression results provided an opportunity to determine CLR co-expression within this patient cohort. The presence of CLR co-expression may suggest CLR collaboration as was found with Mincle and Mcl [298]. CLR co-expression may also enhance the anti-A.*f*. immune response; therefore, patients with less co-expression may be more susceptible to A.*f*. disease.

In order to identify any CLR co-expression, patient's CLR expression results were plotted on an XY graph.

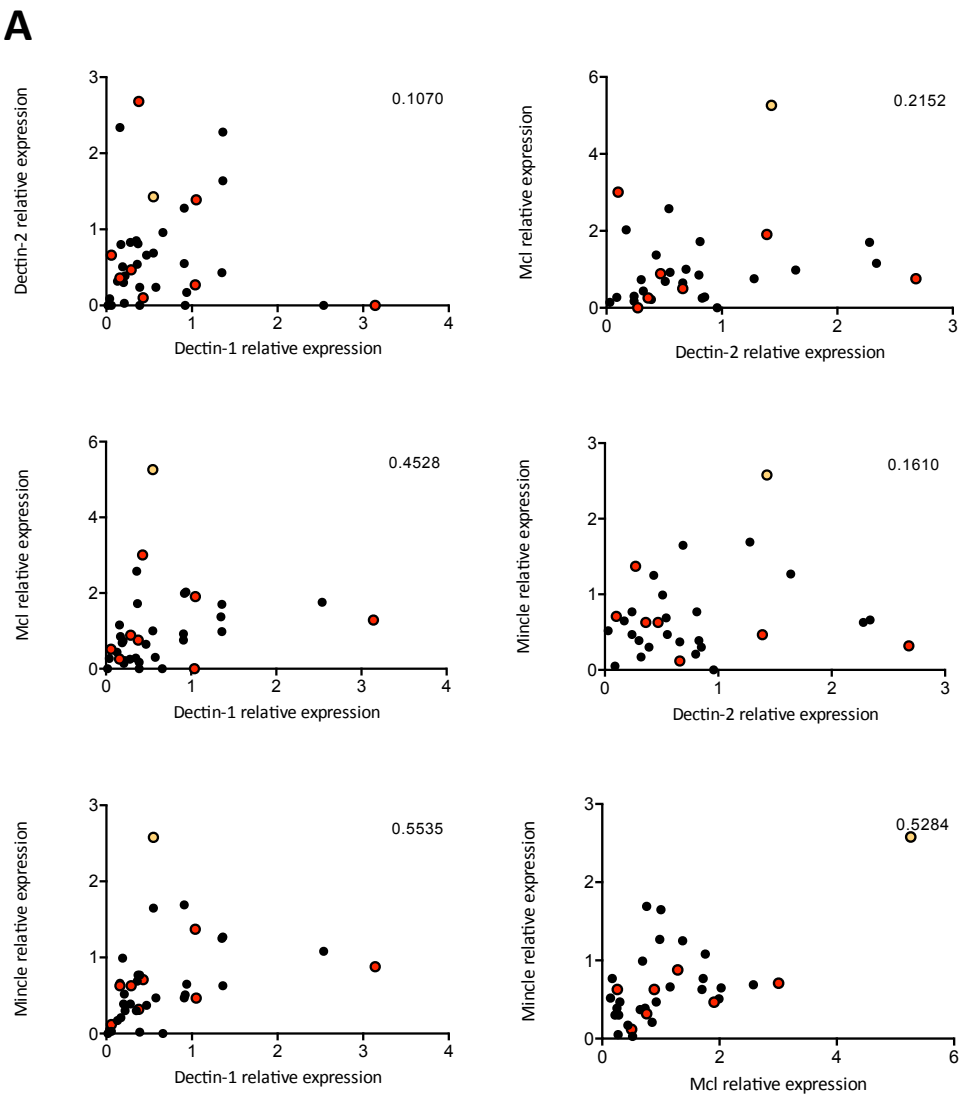

Figure 5.7: Moderate correlation between the expression of Mincle and Dectin-1, and Mincle and Mcl. CLR co-expression does not clearly predict A.*f*. disease. Each patient's CLR expression was determined by qPCR using Taqman probes against each CLR. Alongside each patient qPCR reaction, a control sample and HPRT gene was analysed. Data shown from patient samples was calculated using ΔΔCt comparison against control sample and HPRT gene and was normalised to patient's cells that express CLRs using patient's blood cell count results. A Pearson r test was used to identify statistical significance. Pearson r results were interpreted as > 0.3 negligible, 0.3 to 0.49 low, 0.5 to 0.69 moderate and > 0.7 high [299]. Red data points indicate incidence of IA, yellow data points indicate likely incidence of IA.

Figure 5.7 suggests positive or negative CLR co-expression does not clearly identify patients at risk of developing A.*f*. disease. Although moderate CLR co-expression was identified between Dectin-1 and Mincle, and Mincle and Mcl, IA positive patients were equally distributed within total patient results. Similarly, a lack of CLR co-expression does not clearly identify patients at risk of developing A.*f*. disease.

5.3.2: Determination of patient's functional immune response capabilities

Patients with myeloid cancers are complex and their ability to appropriately respond to pathogen challenge is not well understood. Acute myeloid leukaemia patient's adaptive immune systems recover slowly after chemotherapy. A study showed only two out of ten patients post-chemotherapy generated protective immunity when vaccinated against influenza; this was associated with disrupted B-cell expansion [300]. Furthermore, acute myeloid leukaemia has been demonstrated to disrupt natural killer cell activating receptors reducing the cytotoxic effect of these cells [301]. A similar, slowly recovering immune system has been described in stem-cell transplant patients. Innate immunity is thought to fully recover within months of transplantation but T cell and B cell populations were compromised for years after transplant therapy [302].

Previous studies aiming to elicit risk factors associated with increased A.*f*. disease susceptibility have not investigated patient's functional responses against inflammatory stimuli. Research aiming to identify patients that respond well to immunotherapy has extracted PBMCs and analysed their functional capabilities. However, this was done retrospectively after all patients had received treatment [303, 304]. Stimulating patient's PBMCs *ex vivo* with inflammatory stimuli such as LPS and live A.*f*. may provide insight into how patients respond when challenged with fungal pathogens. This could aid patient stratification according to A.*f*. disease susceptibility.

LPS induces a robust pro-inflammatory response from PBMCs [305]. PBMCs when stimulated with A.*f*.-extracted chitin or live A.*f*. produce pro-inflammatory cytokines

and drive T_H1 immunity [306, 307]. In order to determine the ability of patients to respond against inflammatory and fungal stimuli, PBMCs were extracted and stimulated with LPS or live A.*f*. for 24 hours. ELISA was used to elicit TNF and IL-6 cytokine responses.

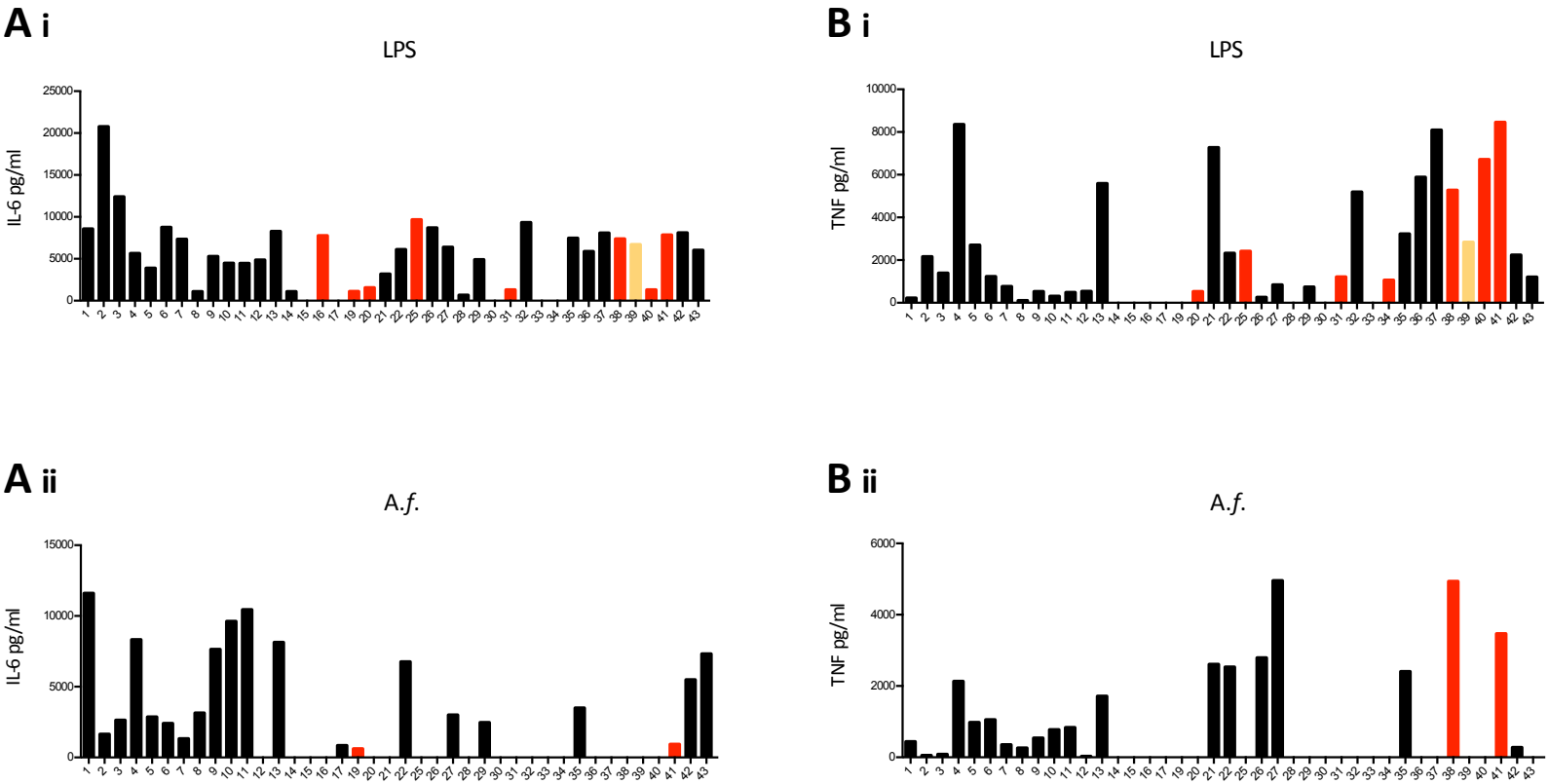

Figure 5.8: IA patients may lack a specific anti-A.*f*. TNF and IL-6 cytokine response. Patient PBMCs were isolated from whole blood and stimulated with **(A i & B i)** 1µg/ml LPS or **(A ii & B ii)** 5x10^6 A.*f*. RC/ml for 24 hours. After stimulation, supernatant was removed and the concentration of TNF and IL-6 determined by ELISA. Red data points indicate incidence of IA, yellow data points indicate likely incidence of IA.

Figure 5.8 shows the majority of patient's PBMCs produce TNF and IL-6 cytokine responses when stimulated with LPS; however, not all patients produce anti-A.*f*. TNF and IL-6 responses. These results suggest IA patients may lack a specific anti-A.*f*. TNF and IL-6 response. Only two of nine patients and two of eight patients generated anti-A.*f*. IL-6 and TNF responses respectively.

Figure 5.8 displays all patient results irrespective of their primary disease. In order to determine whether IA patient's lack of anti-A.*f*. response is linked to their primary disease, patients were separated in AML and SCT groups and the same data displayed. Two of four AML patients produced anti-A.*f*. cytokine responses; therefore, only SCT patient's functional response results were displayed.

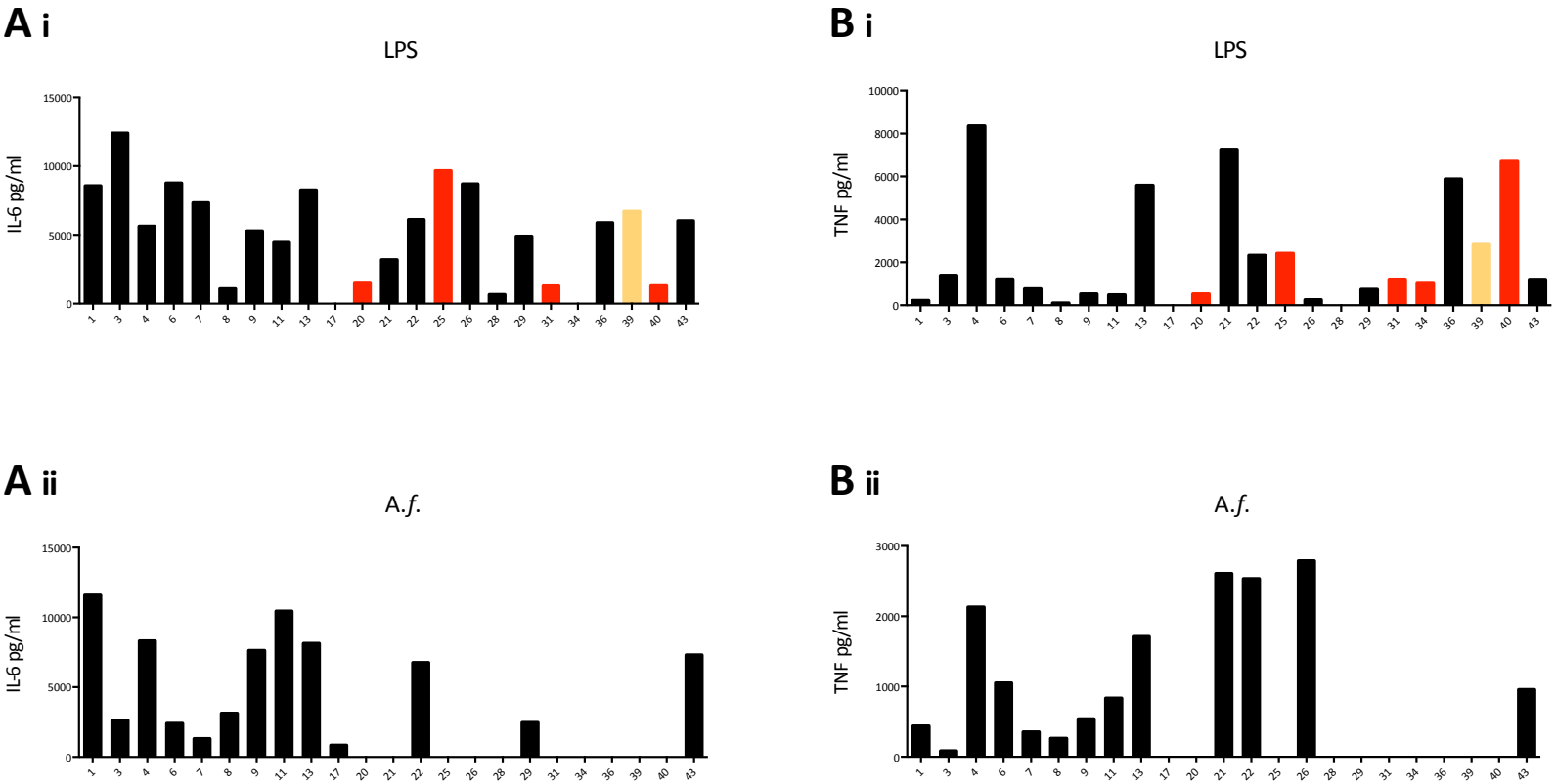

Figure 5.9: SCT IA patients may lack a specific anti-A.*f*. TNF and IL-6 cytokine response. SCT patient PBMCs were isolated from whole blood and stimulated with **(A i & B i)** 1µg/ml LPS or **(A ii & B ii)** $5x10^6$ A.*f*. RC/ml for 24 hours. After stimulation supernatant was removed and the concentration of TNF and IL-6 determined by ELISA. Red data points indicate incidence of IA, yellow data points indicate likely incidence of IA.

Figure 5.9 displays the stark difference in anti-A.*f*. cytokine response between patients who developed A.*f*. disease and patients who did not develop A.*f*. disease. Patients who produced an anti-A.*f*. TNF and IL-6 response did not develop A.*f*. disease. Conversely, the majority of patients who produced an anti-LPS cytokine response but lacked an anti-A.*f*. cytokine response did develop A.*f*. disease. Here, a novel risk factor identifying SCT patients at high risk of developing A.*f*. disease may have been identified.

PBMCs produce robust MIP-1 and KC responses against inflammatory stimuli such as LPS [308, 309]. As the patient PBMC stimulation results had proven so interesting when examining cytokines, MIP-1 and KC chemokines were quantified. Identifying a similar trend in chemokines would only further enhance the power of the potential novel risk factor.

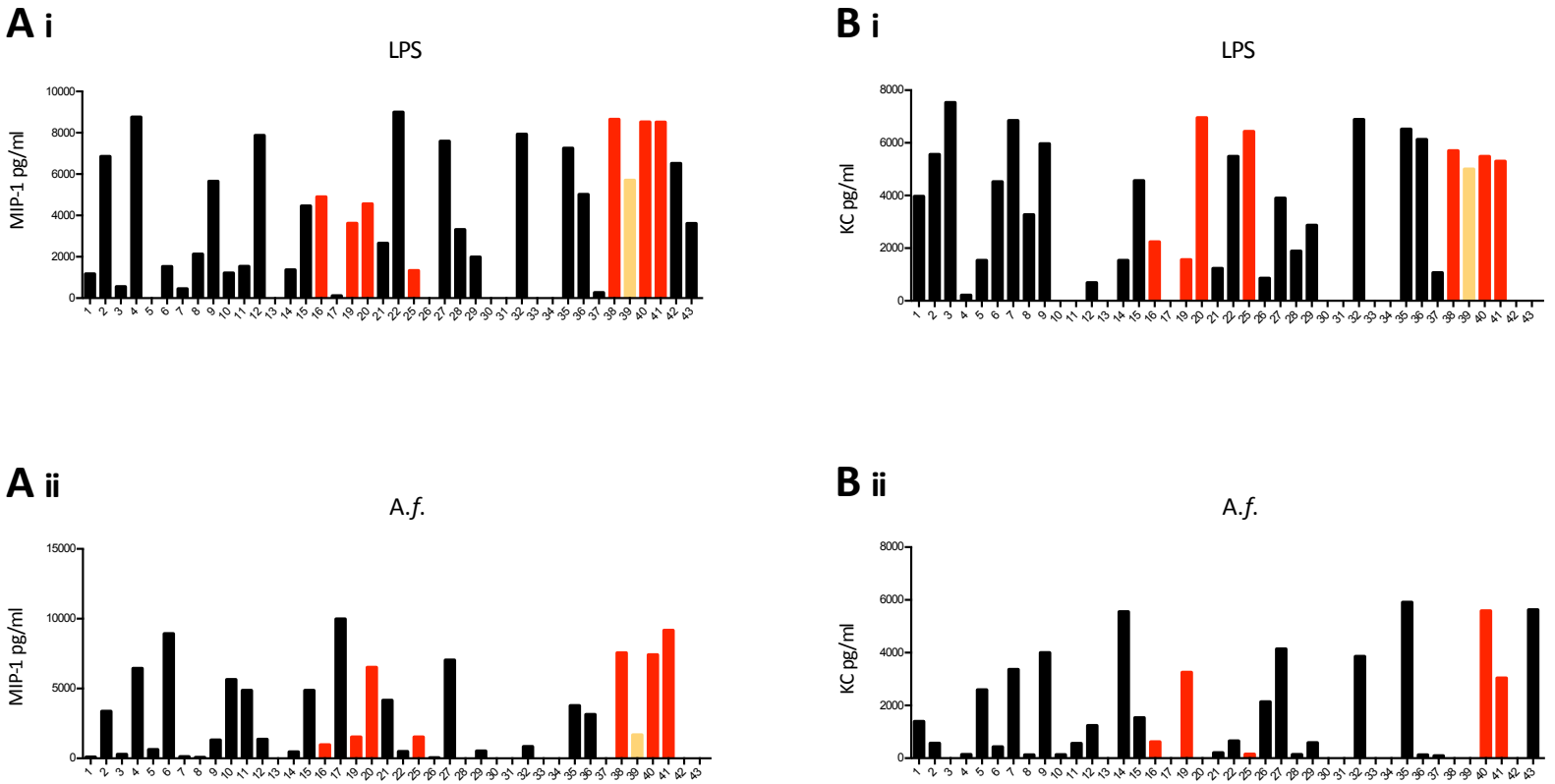

Figure 5.10: The majority of patients generated an anti-A.*f*. chemokine response irrespective of their A.*f*. disease status. Patient PBMCs were isolated from whole blood and stimulated with **(A i & B i)** 1µg/ml LPS or **(A ii & B ii)** 5x10^6 A.*f*. RC/ml for 24 hours. After stimulation, supernatant was removed and the concentration of MIP-1 and KC determined by ELISA. Red data points indicate incidence of IA, yellow data points indicate likely incidence of IA.

5.3.3: Patient stratification system

I have identified patient's CLR status including their CLR expression and the presence of CLR mutations, and I have elicited patient's functional response capabilities. It was next important to determine whether any of these results could be used to stratify patients according to their likelihood of developing A.*f*. disease. The identification of novel risk factors would allow for a personalised medicine approach towards treating A.*f*. disease.

Initially, correlation between CLR expression and incidence of IA was examined. CLR expression was categorised into high or low for each patient. All CLR expression values, after being normalised to patient cell number, were averaged. Patients with CLR expression above the mean were classed as high, patients with CLR expression below the mean were classed as low.

The following results figures contain varying numbers of patients; this is due to a limited quantity of cells and RNA being extracted from patient samples. CLR status and functional response results were not attained from all patients.

Patient group	Parameter	IA	NEF	Odds ratio	95% CI	Significance P value
Total (37)	Low Dectin-1 expression	6/9	18/28	1.111	0.22 to 5.43	1
AML (18)	Low Dectin-1 expression	3/3	7/15	7.933	0.34 to 180.1	0.215
SCT (19)	Low Dectin-1 expression	3/6	11/13	0.181	0.02 to 1.63	0.261
Total (37)	Low Dectin-2 expression	6/9	18/28	1.111	0.22 to 5.53	1
AML (18)	Low Dectin-2 expression	2/3	10/15	1	0.07 to 13.88	1
SCT (19)	Low Dectin-2 expression	4/6	8/13	1.25	0.16 to 9.54	1
Total (37)	Low Mcl expression	5/9	20/28	0.5	0.1 to 2.35	0.43
AML (18)	Low Mcl expression	3/3	10/15	3.667	0.15 to 84.58	0.521
SCT (19)	Low Mcl expression	2/6	10/13	0.15	0.017 to 1.26	0.128
Total (37)	Low Mincle expression	3/9	18/28	0.277	0.05 to 1.358	0.135
AML (18)	Low Mincle expression	1/3	9/15	0.333	0.024 to 4.55	0.558
SCT (19)	Low Mincle expression	2/6	9/13	0.222	0.028 to 1.75	0.319

Figure 5.11: No significant association between CLR expression and incidence of A.*f*. disease. This data was produced from a contingency multivariate statistical analysis of CLR expression against incidence of IA. CLR expression, normalised to each patient's cell counts and relative to a HPRT control, was used for analysis. NEF represents no evidence of fungal disease. Fisher's exact test was used to identify statistical significance. As two variables were examined, statistical significance was set at *p<0.05.

Figure 5.11 displays no significant association between patient's CLR expression status and incidence of A.*f*. disease. However, low Dectin-1 expression and high Mcl expression may increase the risk of developing IA in AML and SCT patients respectively. AML patients with low Dectin-1 expression were 7.9 times more likely to develop A.*f*. disease. SCT patients with low Mcl expression were 6.6 times less likely to develop A.*f*. disease.

I have previously identified two CLR mutants in this cohort, one in Mcl and one in Dectin-2. The Mcl mutation was present in ~40% of patients; the Dectin-2 mutation was only identified in one patient. The patient possessing the Dectin-2 mutation was a proven IA case and did not survive. Unfortunately, as the mutation was only detected in one patient, association between mutated Dectin-2 and incidence of A.*f*. disease is not statistically appropriate.

Association between mutant Mcl and the incidence of IA was examined; the impact mutant Mcl had on Mcl expression was also examined.

Patient group	Parameter	IA	NEF	Odds ratio	95% CI	Significance P value
Total (42)	Mcl A94G mutant	5/10	12/32	1.667	0.39 to 6.97	0.714
AML (19)	Mcl A94G mutant	2/4	5/15	2	0.21 to 18.7	0.603
SCT (23)	Mcl A94G mutant	3/6	7/17	1.429	0.22 to 9.26	1

Patient group	Parameter	Low Mcl expression	High Mcl expression	Odds ratio	95% CI	Significance P value
Total (36)	Mcl A94G mutant	9/24	3/12	1.8	0.38 to 8.45	0.709

Figure 5.12: Mutant Mcl does not significantly impact incidence of IA or Mcl expression. This data was produced from a contingency multivariate statistical analysis of incidence of Mcl mutant against incidence of IA, and incidence of Mcl mutant against Mcl expression. CLR expression normalised to each patient's cell counts and relative to a HPRT control, was used for analysis. NEF represents no evidence of fungal disease. Fisher's exact test was used to identify statistical significance. As two variables were examined, statistical significance was set at *$p<0.05$.

Figure 5.12 displays no significant association between mutant Mcl and the incidence of IA. There is also no association between mutant Mcl and Mcl expression; although, CLR expression was determined at RNA level and so the impact the mutant may have on Mcl cell surface expression cannot be determined.

In figure 5.11 high Mcl expression was loosely associated with an increased risk of IA in SCT patients. Here, mutant Mcl does not alter Mcl expression or the incidence of IA. This may suggest the Mcl mutant identified resulting in an amino acid substitution has little impact on the expression and function of Mcl.

In this small patient study, CLR status alone does not provide any novel and significant risk factors that could be used to stratify patients according to their risk of A.*f*. disease. Next, patient's functional response results were associated with incidence of IA. This would determine whether patient's PBMC stimulation results could be used as an A.*f*. disease risk factor.

Patient group	Parameter	IA	NEF	Odds ratio	95% CI	Significance P value
Total (40)	No A.*f*. TNF response	8/10	11/30	6.909	1.23 to 38.53	***0.0281**
Total (40)	No A.*f*. IL-6 response	8/10	11/30	6.909	1.23 to 38.53	***0.0281**
AML (17)	No A.*f*. TNF response	2/4	6/13	1.167	0.12 to 11	1
AML (17)	No A.*f*. IL-6 response	2/4	7/13	0.857	0.09 to 8.07	1
SCT (23)	No A.*f*. TNF response	6/6	5/17	29.55	1.40 to 622	****0.0046**
SCT (23)	No A.*f*. IL-6 response	6/6	4/17	39	1.81 to 839	****0.0021**
SCT LPS responders (21)	LPS TNF response No A.*f*. TNF response	6/6	3/15	46.63	2.06 to 1043	*****0.0015***

Figure 5.13: Patients who lack an anti-A.*f*. TNF or IL-6 PBMC response are significantly more likely to develop A.*f*. disease. This data was produced from a contingency multivariate statistical analysis of PBMC anti-LPS and anti-A.*f*. cytokine response against incidence of IA. NEF represents no evidence of fungal disease. Fisher's exact test was used to identify statistical significance. Where two variables were examined, statistical significance was set at *p<0.05, **p<0.005; significant values are highlighted bold. Where more than two variables were examined, Bonferroni's correction was applied; significant values are highlighted bold and italic.

Figure 5.13 highlights the significant association between patient's anti-A.*f*. TNF or IL-6 PBMC response and incidence of IA. Here, a novel risk factor identifying patients with an increased likelihood of developing A.*f*. disease has been identified. This risk factor is particularly appropriate for use in SCT patients.

SCT patients are 29.5 times more likely to develop IA if they do not produce an anti-A.*f*. TNF response and 39 times more likely if they do not produce an anti-A.*f*. IL-6 response. Interestingly, if SCT patients produce a response against LPS but not against A.*f*. their risk of developing IA is 46.6 times higher when compared to SCT patients who generated both an anti-LPS and anti-A.*f*. responses. This novel risk factor is not present or significant in the AML patient cohort.

It was important to determine whether patient's lack of anti-A.*f*. response was specific for predicting A.*f*. disease or was a more general indicator of patients responding poorly. Therefore, the incidence of IA and lack of TNF/IL-6 anti-A.*f*. response was associated with mortality in the patient cohort.

Patient group	Parameter	Mortality	Survival	Odds ratio	95% CI	Significance P value
Total (40)	IA	4/15	6/25	1.152	0.26 to 4.99	1
AML (17)	IA	1/6	3/11	0.533	0.04 to 6.65	1
SCT (23)	IA	3/9	3/14	1.833	0.27 to 12.07	0.643
Total (40)	No A.*f*. TNF response	5/15	14/25	0.392	0.10 to 1.49	0.204
Total (40)	No A.*f*. IL-6 response	6/15	13/25	0.615	0.16 to 2.25	0.526
SCT (23)	No A.*f*. TNF response	3/9	8/14	0.375	0.06 to 2.15	0.40
SCT LPS responders (21)	LPS TNF response No A.*f*. TNF response	3/9	8/12	0.25	0.03 to 1.56	0.198

Figure 5.14: No significant association between IA and mortality, and a lack of anti-A.*f*. TNF or IL-6 PBMC response and mortality. This data was produced from a contingency multivariate statistical analysis of IA incidence against incidence of mortality and PBMC anti-LPS and anti-A.*f*. cytokine response against incidence of mortality. NEF represents no evidence of fungal disease. Fisher's exact test was used to identify statistical significance. Where two variables were examined, statistical significance was set at *p<0.05; significant values are highlighted bold. Where more than two variables were examined, Bonferroni's correction was applied; significant values are highlighted bold and italic.

Figure 5.14 demonstrates there is no association between IA and mortality, and no association between lacking an anti-A.*f*. TNF/IL-6 response and mortality. This suggests the results displayed in figure 5.13 relate to a novel and A.*f*. disease specific risk factor. This risk factor does not simply discriminate against patients who are responding poorly and experience higher mortality; this risk factor specifically identifies SCT patients at increased risk of developing IA.

Finally, it was important to use the data displayed in figures 5.11 to 5.14 to generate a model that predicts incidence of A.*f*. disease according to the risk factors identified in this research. The results displayed in the following figures are limited to the patients recruited in this clinical study; therefore the maximum number of patients used to generate IA incidence predictions is 43.

Primary disease + Risk factor	Incidence in Patient cohort	Incidence of IA	Odds ratio	Significance P value
SCT + No A.*f*. TNF response	11/23	6 (54%)	29.55	****0.0046**
SCT + No A.*f*. IL-6 response	10/23	6 (60%)	39	****0.0021**
SCT + LPS TNF/IL-6 response + no A.*f*. TNF/IL-6 response	9/21	6 (66%)	46.63	*****0.0015***
SCT + High Mcl expression	7/19	4 (57.2%)	6.67	0.128
SCT + High Mcl expression + LPS TNF/IL-6 response + no A.*f*. TNF/IL-6 response	5/19	4 (80%)	311.02	*****0.001***
AML + no A.*f*. TNF response	8/17	2 (25%)	1.167	1
AML + no A.*f*. IL-6 response	9/17	2 (22%)	0.857	1
AML + Low Dectin-1 expression	10/18	3 (30%)	7.933	0.215
AML + Low Mcl expression	13/18	3 (23%)	3.667	0.521
AML + Low Dectin-1 expression + Low Mcl expression	9/18	3 (33%)	29.09	0.206

Figure 5.15: An anti-A.*f*. cytokine response and Mcl expression can be used to stratify SCT patients according to their risk of developing A.*f*. infection. Previously identified risk factors were used to stratify patients before the incidence of IA was calculated within this stratified group. Incidence of IA as a percentage relates to the number of IA positive patients stratified by the risk factor parameter. Contingency multivariate statistical analysis of each set of risk factor parameters and their association with IA incidence was used to determine statistical significance. A Chi-squared test was used to identify statistical significance where multiple parameters were associated with IA incidence. Where two variables were examined, statistical significance was set at *p<0.05, **p<0.005; significant values are highlighted bold. Where more than two variables were examined, Bonferroni's correction was applied; significant values are highlighted bold and italic.

The results from figure 5.15 display the incidence of IA within patient groups that were stratified using risk factors from this study. This stratification could be applied to patients as they undergo treatment for haematological malignancies as described in figure 1.4. The presence or absence of risk factors would allow patients to be stratified into high, intermediate and low risk groups' dependent on their risk of developing A.*f*. disease. From this stratification, their anti-fungal diagnosis and treatment regime could be modified accordingly.

The data from figure 5.15 was used to generate a flow diagram clearly defining patients at low, intermediate or high risk of developing A.*f*. disease. Patients were stratified according to the risk factors identified within this research.

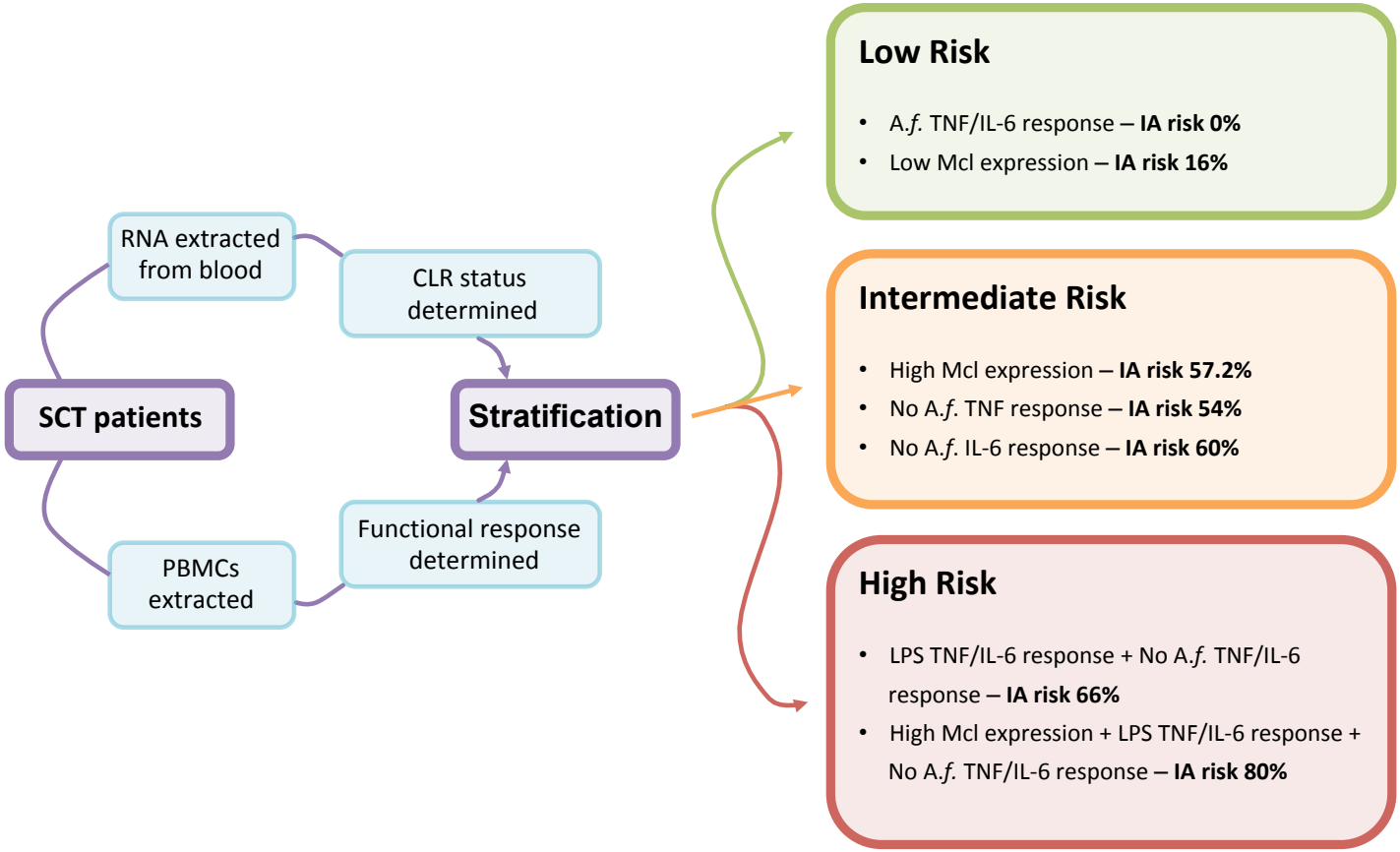

Figure 5.16: System to stratify SCT patients according to risk factors identified within this research. Data collated from figure 5.15 was used to describe risk factors leading patient stratification into low, intermediate and high-risk of A.*f.* disease cohorts.

Figure 5.16 provides the final stratification protocol that can be drawn from this research. These results and protocol could be used to apply a personalised medicine approach to haematology SCT patients at risk of developing A.*f*. disease.

As previously described in figure 1.4, high risk patients may be given prophylactic anti-fungal therapy and their primary disease treatment modulated to reduce the risk of A.*f*. disease. Intermediate risk patients may be given prophylactic anti-fungal therapy but their primary disease treatment prioritised, this cohort may undergo regular fungal infection screening. Low risk patients primary disease may be prioritised without the requirement of prophylactic anti-fungal therapy.

Although the patient cohort was small in size, this study has identified significant novel risk factors associated with an increased susceptibility to A.*f*. disease.

5.4: Discussion

The aims of this research focussed on identifying risk factors associated with an increased susceptibility to A.*f*. disease in haematology patients. The determination of patient's CLR status and their functional immune response capabilities has led to multiple novel risk factors being described. These risk factors can be used to stratify SCT patients according to their risk of developing A.*f*. disease; therefore, driving a personalised medicine approach to anti-fungal therapy.

The requirement for improving current anti-fungal treatment strategies is clear. A.*f*. as a pathogen is responsible for a rapidly increasing disease burden in immune-compromised patients. The prevalence of A.*f*. disease within patients diagnosed with hematologic malignancies is around 10-15%; this high disease prevalence is accompanied by an unacceptably severe mortality rate ranging from 38-80% [7, 40-42]. The incidence of A.*f*. disease in the study centre has been as high as 27%, this study attained A.*f*. incidence of 20.9%.

Current anti-fungal therapeutics are expensive, toxic and highly interactive with other drugs. This often means patient's primary treatments must be modified to allow anti-fungal therapeutics to be administered [56, 57, 60]. Resistance issues are also emerging, rendering front-line anti-fungal therapeutics redundant [58]. These therapeutic insufficiencies, alongside increasing disease burden and high mortality rates highlight the necessity for improvements in anti-fungal therapy. Identifying patients at high risk of developing A.*f*. disease would permit the targeting of anti-fungal therapies; therefore, reducing unnecessarily treated patients, reducing the risk of fungal resistance and reducing the high cost burden associated with anti-fungal therapies.

5.4.1: Determining patients CLR status.

CLRs are crucial during anti-fungal and anti-A.*f*. immune responses. This is highlighted by the increased susceptibility to fungal infection experienced by individuals with defective CARD9 [159]. Recently, mutations in Dectin-1 and DC-SIGN have also been associated with an increased A.*f*. disease susceptibility [67, 292]. Therefore, identifying patient's CLR expression and sequence may have elicited novel risk factors associated with developing A.*f*. disease.

Here, two CLR mutants were identified within the patient cohort, a novel Dectin-2 mutation and Mcl mutation. The Dectin-2 C505X mutant has not been previously described and is a very interesting CLR mutant. The patient with this mutation developed A.*f*. disease and did not survive. Information regarding the cause of death is unavailable and death may or may not have resulted from A.*f*. disease.

Dectin-2 is important during established A.*f*. infection, the CLR recognises larger hyphal morphologies of A.*f*. and generates robust cytokine and chemokine responses driving protective immunity [183, 185]. The mutation in Dectin-2 described in figure 5.3 results in an early stop codon and premature termination of protein translation. This likely severely disrupts the tertiary structure of the CLR and impairs Dectin-2's recognition of A.*f*. [296]. This mutation may be particularly relevant for haematology patients with A.*f*. disease.

Haematology patients experience drastic immune suppression and are at high risk of developing A.*f*. infections [38, 39]. The adaptive immune response recovers slowly after chemotherapy whereas the innate immune response can recover within months [302]. Lacking a crucial CLR such as Dectin-2, involved in the recognition of developed A.*f*. structures, may reduce the capability of patients to generate robust anti-A.*f*. immune responses. If patients are infected with A.*f*. during their treatment, even when their innate immune response recovers they may not be able to appropriately recognise and respond against developed A.*f*. infections.

The mutation identified in 17/43 patient's Mcl gene has been previously described. This missense mutation results in the substitution of serine to glycine at amino acid position 32. Although these two amino acids have different charge, my research suggests this substitution does not impact the expression or function of Mcl.

Figure 5.7 permits the identification of CLR co-expression using patient's CLR expression results displayed in figure 5.6. The requirement for collaborative CLR and TLR responses against A.*f*. infections has been extensively described. This figure highlights moderate correlation between the expression of Dectin-1 and Mincle, and Mincle and Mcl.

Collaborative signalling between Mincle and Mcl has been previously identified. A role for both receptors heterodimerising and enhancing the recognition of carbohydrate and lipid containing molecules has been demonstrated [298]. Research describing Mcl facilitating Mincle expression and signalling provides further evidence of Mincle and Mcl collaboration [310]. However, the functional consequence of Mincle and Mcl engagement during fungal infections has not been described. Patients that developed A.*f*. disease did not possess more or less Mincle and Mcl co-expression when compared to the total patient cohort; therefore, minimal functional conclusions can be drawn from Mincle and Mcl co-expression.

A role for Dectin-1 and Mincle collaborating has not been identified. The two CLRs do appear to be linked as the fungal engagement of Mincle can block Dectin-1 induced anti-fungal T_H1 immunity [157]. However, this research does not demonstrate physical CLR interaction or mention CLR co-expression. Interestingly, Dectin-1 can produce robust responses against mycobacteria but what the CLR recognises on the pathogen is unknown. It is suggested both Dectin-1 and Mincle may be required to recognise and respond against mycobacteria. Both receptors were demonstrated to signal via Syk/CARD9 and generate inflammatory cytokines driving T_H1 and T_H17 immunity upon mycobacterial recognition [311].

No correlation was attained between the expression of Dectin-1 and Dectin-2. The recently described role for Dectin-1 and Dectin-2 enhancing *Tricophyton rubrum* clearance suggests these receptors can collaborate but may not directly impact the others expression [221].

Here, a novel Dectin-2 mutation was identified and the CLR status of 43 patients determined. Although no clear association between CLR expression and incidence of IA was attained, when these results are collated with patient's functional capabilities risk factors aiding in the stratification of patients according to risk of A.*f*. disease may be identified.

5.4.2: Determining patient's functional response capabilities

This research begins to describe a novel risk factor that may identify patients susceptible to A.*f*. disease. Almost all patient's extracted PBMCs generated anti-LPS TNF and IL-6 responses. Interestingly, the majority of patients who did not produce anti-A.*f*. TNF and IL-6 responses developed A.*f*. disease. This trend was not conserved in patient's MIP-1 and KC chemokine responses. The total patient results displayed in figure 5.8 and then narrowed to SCT patients in figure 5.9 highlight the absence of specific anti-A.*f*. cytokine response produced by IA positive SCT patients. Therefore, this potential risk factor may be most appropriate for stratifying SCT patients.

Haematological malignancies and SCT therapy are well known to impair the immune response. However, the explanation for patient's specific lack of anti-A.*f*. cytokine response is not clear, especially when anti-LPS cytokine responses are produced. Why this trend is not conserved in patient's chemokine response is also unknown.

Innate immune responses against LPS require TLR4 and some CD14 signalling and are driven by myeloid immune cells. The immune response against LPS is extremely robust and results in a range of pro-inflammatory cytokines and chemokines being produced [312, 313]. Furthermore, LPS stimulation of PBMCs up-regulates TLR4 expression,

enhancing LPS signalling and cytokine production [314]. Although stem cell transplant therapy impairs the innate immune response, TLRs can still signal post-treatment and are one of the main immune drivers of allograft rejection [315]. Similarly, although chemotherapy and radiotherapy treatments impair the innate immune system, TLRs in the gut can still signal post-treatment, often being linked with gut toxicity and chronic pain [316].

Each patient blood cell count was taken at the same time their functional assays were performed. The blood count data suggests almost all patients possessed some myeloid cells within their blood. This, alongside TLRs sustained impact despite stem cell transplant, chemotherapy or radiotherapy treatment may suggest why the majority of patients generated anti-LPS TNF and IL-6 responses.

The reason underlining patient's specific lack of an anti-A.*f*. response and subsequent enhanced risk of A.*f*. disease is more challenging. A role for CLRs during anti-cancer responses have been described with CLRs expressed on DCs responsible for cancer antigen presentation [317]. However, the presence of CLRs post-stem cell transplant, chemotherapy or radiotherapy has not been clarified. It may be the case that CLR expression is disrupted by these treatments, consequently impairing the anti-fungal immune response without altering patient's LPS response.

In order to generate a robust anti-A.*f*. immune response a complex and multifaceted recognition and signalling sequence must occur. This involves multiple immune cell types and receptors. In contrast the LPS immune response is driven almost exclusively by TLR4 [318]. Patients may produce only anti-LPS cytokine responses, as this immune response requires fewer components and less collaboration. Patients that produce both an anti-LPS and anti-A.*f*. immune response may possess a more intact and better functioning immune system.

The functional PBMC stimulation experiments were completed for 24 hours with LPS and live A.*f*.. These experiments may have primitively, yet accurately reflected what occurred in patients infected with A.*f*.. Patient PBMCs when challenged with LPS

simply had to recognise and respond to the stimulant within 24 hours. However, patient PBMCs when challenged with live A.*f*. had to rapidly recognise and respond against A.*f*. to avoid being killed. If PBMCs did not recognise and respond against A.*f*. no cytokine response would be detected. Therefore, this experiment does not discriminate against anti-A.*f*. cytokine responders or non-responders but stratifies patients according to the ability of their PBMCs to respond against A.*f*. before they were killed. This may be why this assay is so selective for patients highly susceptible to A.*f*. disease.

Finally, an explanation as to why this functional assay stratifies patients according to their anti-A.*f*. cytokine response and not their chemokine response is challenging. PBMCs produce chemokines in much greater quantities than cytokines, especially when stimulated with LPS [319, 320]. Patients susceptible to A.*f*. disease may rapidly produce some chemokines but not cytokines, before their PBMCs are killed by A.*f*..

5.4.3: Patient stratification system

This research has identified multiple novel risk factors that can be used to stratify patients according to their risk of developing A.*f*. disease. These risk factors add to the already described genetic and diagnostic risk factors currently used in healthcare centers to stratify patients [65, 67, 321]. Here, I identify SCT patient's ability to generate an anti-A.*f*. TNF and IL-6 response as a significant risk factor. Furthermore, when patients are stratified according to their Mcl expression and their functional response, as shown in figure 5.16, the incidence of IA goes up to 80%. When used together these parameters represent a novel and significant stratification protocol.

The diagnosis of A.*f*. infections is challenging and relies on the outcome of multiple diagnostic tests including PCR positivity, A.*f*. antibody ELISA and lung scans. Here, this research describes clear and novel risk factors that can be used to stratify high-risk patients and drive a personalised medicine approach. Interestingly, this research also permits the stratification of patients at low risk of developing A.*f*. disease. All patients

that generated anti-A.*f*. TNF and IL-6 responses did not develop A.*f*. disease. This provides a robust strategy to rule out patients at risk of developing A.*f*. disease.

Finally, the experiments undertaken in this research are not impractical to complete on a larger scale and could with some planning, be implemented into the current diagnostic strategy employed in healthcare centers. Before patient's treatment commences, blood could be extracted and used to determine their functional response capabilities and CLR expression status. This is no more intensive than multiple and regular PCR testing, ELISA testing and analysing lung scans.

5.5: Conclusions

The requirement to improve the diagnosis and treatment strategy of A.*f*. infections has been thoroughly discussed in 5.1. The incidence of A.*f*. disease is increasing, mortality is unacceptably high and current therapeutics are toxic, drug interactive, expensive and encountering resistance problems. Therefore, patients are prophylactically treated with anti-fungal therapeutics at the slightest suspicion of A.*f*. disease. This typically results in the modulation of their primary disease therapies and even then, IA is often fatal.

The requirement to stratify patients according to their risk of developing A.*f*. infections is clear. This would allow high-risk patients to be regularly screened and prophylactically treated reducing their risk of A.*f*. disease. Crucially, this would also permit low-risk patients primary disease to be prioritised whilst their A.*f*. disease status was closely monitored.

This research adds multiple novel risk factors to the growing number of genetic, functional and diagnostic risk factors currently used in healthcare centers to stratify patients according to their A.*f*. disease susceptibility.

5.6: Future experiments

The Dectin-2 mutation identified in a patient from this study requires further investigation. This early stop codon mutation likely renders Dectin-2 redundant, which would drastically impair the anti-fungal immune response. The prevalence of this mutation within the population, and patient cohorts at-risk of fungal infection, must be determined. Following this, the mutation must be associated with incidence of fungal disease. This Dectin-2 mutant may increase patient's susceptibility to fungal infection.

The research undertaken within this study was completed using a patient cohort size of 43, of which 10 patients developed A.*f*. disease. Although some of the conclusions drawn from this research were statistically significant, the patient cohort size is small. In order to increase the statistical significance and test the risk factors identified here, more patients could be enrolled. Similar cohorts of patients at-risk of fungal infection could also be retrospectively examined for some of the genetic risk factors identified here.

Chapter 6

General discussion

6.1: Earlier research

C-type lectin receptors comprise a large and diverse family of proteins. CLRs are defined by their possession of a CTLD, a domain that can recognise a multitude of different ligands including carbohydrates, proteins and lipid components [151]. CLRs are predominantly expressed on myeloid cells where their primary function involves pattern recognition. Upon recognition, CLRs drive immune responses against PAMPs, damage associated molecular patterns, and most recently described, tumour associated molecular patterns [317, 322]. CLRs have been demonstrated to drive phagocytic, endocytic, pro-inflammatory and anti-inflammatory responses. This range of CLR-derived responses relies on a complex signalling system comprising of tyrosine-based signals that recruit kinases and phosphatases, and non-tyrosine based signals that typically require coupling to adjacent pathways [323].

Fungal immunity is primarily mediated by CLRs that recognise fungal cell wall carbohydrates acting as PAMPs. Dectin-1 is the best characterised CLR during anti-fungal immune responses [245]. The CLR Dectin-1 recognises β-glucans and is essential for generating protective immune responses against fungal pathogens such as *Candida albicans* [171]. Dectin-2 also plays a crucial role in anti-fungal immunity recognising high mannose structures widely found on fungal cell walls. Dectin-2 is important when generating protective immune responses against *Candida albicans* [180]. The CLR Mincle has a complicated role during anti-fungal immune responses. Mincle was found to be beneficial during *Malassezia* challenge, driving pro-inflammatory cytokine responses [188]. Conversely, the engagement of Mincle by *Fonsecaea monophora* suppressed Dectin-1 protective responses, suggesting a pathogen immune evasion role for Mincle [157]. The anti-fungal capability of Mcl is not well understood. The CLR can mediate immune responses against mycobacterial cord factor and Mcl deficient mice are more susceptible to *Candida albicans* infection [158, 199].

A.*f*. is a complicated pathogen with a severe disease burden. The fungus causes a variety of invasive and allergic type diseases dependent on the host's immune status. Immune suppressed individuals are highly susceptible to invasive A.*f*. infections and

experience unperturbed systemic A.*f*. growth that is associated with an unacceptably high mortality rate [324]. Individuals with compromised immune systems such as those with CF do not experience systemic A.*f*. disease but often struggle with chronic A.*f*. infections in the lung. Persistent A.*f*. infections retained in the lung cause chronic local inflammation; this culminates in tissue scarring and reduced lung capacity [19]. Anti-A.*f*. therapeutics are insufficient at clearing A.*f*. infections and have a range of severe side effects [1, 324].

The anti-A.*f*. immune response likely requires extensive collaboration between PRRs. A.*f*. is a complicated pathogen with multiple morphological states and many immune evasion strategies [128]. Collaboration between CLRs and TLRs has long been understood. Stimulating Dectin-1 and TLR2 with β-glucan and Pam3CSK4 produced a synergistic inflammatory response when compared to stimulating each PRR individually [279]. Immune clearance of *Fonsesaea pedrosoi* was found to require CLR and TLR signalling despite exclusive recognition of the pathogen by a CLR [187]. Recently, CLR:CLR collaboration between Dectin-1 and Dectin-2 was identified. An enhanced response against *Trichophyton rubrum* was demonstrated when both CLRs were engaged; this resulted in reduced fungal burden *in vivo* [221].

Here, I investigated the role of Dectin-1, Dectin-2, Mincle and Mcl during anti-A.*f*. immune responses in immune-compromised, immune-competent and immune-suppressed disease settings.

6.2: CLRs and A.*f*. in the immune-compromised

Individuals with compromised immune systems such as those with CF are susceptible to A.*f*. disease. CF patients typically suffer from repeated lung infections and chronic airway inflammation [19]. The most common cause of death in CF patients is respiratory failure, often resulting from chronic lung infection. A.*f*. is regularly isolated from CF patient respiratory secretions [325]. CF patient's defective mucociliary escalator does not clear A.*f*. that has been inhaled and deposited in the lung;

therefore, the A.*f*. infection persists. Furthermore, the disrupted mucociliary escalator impairs the airway immune response. Recruited, activated immune cells get stuck in mucus and contribute to local inflammation further impairing of the immune response [18]. Poorly challenged A.*f*. exacerbates lung inflammation by providing a persistent stimulus for the defective immune response. However, the underlying reason CF patients are so susceptible to A.*f*. infection and their lack of A.*f*. clearance is not well understood. CLRs drive anti-fungal immunity and their requirement for generating robust immune responses is becoming clear. Here in chapter 3, I identify NE induced cleavage of Dectin-1 and suggest why this may enhance CF patient's susceptibility to A.*f*. infection.

Dectin-1 expressed on alveolar macrophages, monocytes and neutrophils recognises A.*f*. and generates pro-inflammatory cytokine responses. These cell types are present in the CF airway and contribute to the local anti-A.*f*. immune response. Dectin-1 has been demonstrated to bind A.*f*. SC with particularly high affinity, suggesting the receptor is important for early immune responses as conidia are inhaled and begin to germinate [2]. My research demonstrates that NE-induces cleavage of Dectin-1 and therefore likely impairs A.*f*. recognition. I showed that NE-induced cleavage of Dectin-1 resulted in recognition and functional defects in response to zymosan, a β1-3 glucan ligand for Dectin-1. Zymosan has extensively been used as a sterile model of fungal infection [326]. Zymosan engagement of Dectin-1 triggered NFAT activation in macrophages to the same extent that *Candida albicans* stimulation achieved [327]. In the seminal study showing that Dectin-1 KO mice displayed increased susceptibility to *Candida albicans* infection, Dectin-1 KO macrophages were initially stimulated with zymosan to confirm reduced β1-3 glucan recognition [171]. These data suggest zymosan is an useful model of fungal infection/responses and impaired zymosan recognition is often associated with impaired fungal immunity *in vivo*.

Furthermore, the production of cytokines and chemokines such as TNF, IL-6, MIP-1 and KC in response to zymosan or A.*f*. was found to be dependent on Dectin-1 expressed on macrophages [2, 328]. A lack of Dectin-1 engagement reduced the cytokine and chemokine response and increased A.*f*. *in vivo* fungal burden [2]. In

chapter 3, I demonstrate NE-induced cleavage of Dectin-1 and highlight the recognition and functional deficiency resulting from this cleavage event using zymosan and A.*f*.. Losing Dectin-1's anti-A.*f*. impact in the CF airway would likely drastically increase susceptibility to fungal disease. Dectin-1 KOs impact *in vivo* against fungal pathogens has been thoroughly explored with almost all models experiencing significantly increased mortality resulting from impaired anti-fungal responses [171, 173, 174, 329].

My results and the above comparisons with others research suggest the action of NE, present in high concentrations in the CF airway, inducing cleavage of Dectin-1 would drastically reduce A.*f*. recognition and result in an impaired anti-A.*f*. immune response. Poorly challenged A.*f*. would persist in the CF airway and contribute to the local chronic inflammatory setting. This may describe why CF patients have such high A.*f*. disease incidence and suffer from chronic A.*f*. infection. Furthermore, this research not only describes a role for NE inducing Dectin-1 cleavage but also suggests NE may cleave other CLRs important during anti-A.*f*. immune responses [330].

As NE has such a devastating impact when inappropriately regulated in the CF airway, NE-inhibitors are an attractive therapeutic target. Here, my research suggests blocking the action of NE in the CF airway would restore Dectin-1 expression and likely recover the anti-A.*f*. immune response. Dectin-1 generates robust anti-A.*f*. immune responses and is almost exclusively required for clearing early A.*f*. infection [2, 174]. NE-inhibitor therapeutics are a very real possibility with multiple patent applications accepted within the last 8 years [331-334].

6.3: CLRs and A.*f*. in the immune-competent

The majority of research investigating CLRs during A.*f*. infection has been undertaken using immune-competent *in vivo* models. Although this does not provide an accurate representation of what occurs in humans, these models have elicited CLRs impact in other fungal diseases. Previous research has identified a controversial role for Dectin-

1 during *in vivo* fungal challenge. Immune-competent Dectin-1 KO *in vivo* models were used to determine the requirement of Dectin-1 during *Candida albicans* infection [171]. Conversely, research from another lab showed Dectin-1 deficient mice possess the same susceptibility to *Candida albicans* as WT mice. This suggests a lesser role for the CLR or extensive CLR redundancy; however, this reduced Dectin-1 impact was associated with the use of a different *Candida albicans* strain [172, 173]. Blocking Dectin-1 signalling *in vivo* before A.*f*. challenge resulted in significantly impaired cytokine and chemokine production [2]. The production of IL-22 following A.*f*. challenge was found to be dependent on Dectin-1; furthermore, mice lacking IL-22 possessed significantly higher A.*f*. fungal burden [174]. Crucially, Dectin-1 deficient mice were significantly more susceptible to A.*f*. infection, produced impaired cytokine and chemokine responses and experienced increased mortality [100].

Here, my research in chapter 4 aligns with previous work highlighting the impaired anti-A.*f*. cytokine and chemokine response resulting from Dectin-1 KO mice. However, my research suggests this does not translate into an increased susceptibility to A.*f*. infection. The results displayed in chapter 4 indicate this reduced Dectin-1 impact may result from microbiome and/or gender discrepancies between WT and each CLR KO or DKO strain. Several laboratories have demonstrated the immune controlling impact of the microbiome, particularly relevant in lung immunity [262, 263]. There are many examples of microbiome bacteria modulating inflammatory immune responses, often using the ubiquitin system. Iκβ, a crucial signalling component of the NFκβ pathway, can be targeted for degradation by numerous gut bacteria [335-337]. Recently, the influence the microbiome controls over host immunity was clearly demonstrated using *Clostridium difficile*. Adding a single gut bacteria into the microbiome restored bile acid-mediated resistance to the pathogen and cleared infection [281]. Differences in the immune systems of males and females have long been described, with genetic variation and different sex hormones predominantly being responsible [338]. The influence microbiome and gender have during *in vivo* anti-fungal immune responses have not been previously identified. Here, my research suggests both have significant roles controlling host anti-fungal immunity and require further investigation.

The role of Dectin-2 during anti-fungal immune responses is becoming clearer. Dectin-2 deficient mice were more susceptible to *Candida albicans* and *Candida glabrata* infection than WT mice [180, 339]. This was associated with reduced phagocytosis and impaired ROS production [340]. Dectin-2 recognises larger hyphal morphologies of A.*f*. generating cytokines, chemokines and extracellular traps [185]. Although this receptor is likely involved in anti-A.*f*. immunity, limited *in vivo* research has investigated this CLR's role. The impact Mincle has on the anti-A.*f*. *in vivo* immune response is also unclear. Mincle has been shown to have pro-inflammatory and pathogen immune evasion roles during *in vivo* fungal challenge [157, 188]. Here, my research suggests a limited role for Dectin-2 and Mincle influencing the *in vivo* anti-A.*f*. immune response. It appears when the host is immune competent there is enough CLR redundancy to cope with the loss of these CLRs. Dectin-2 and Mincle may have more impact during extensive A.*f*. infections found in immune suppressed patients.

The alveolar macrophage experiments for both these receptors also suggested they had limited impact during anti-A.*f*. immunity. The alveolar macrophage experiments were completed for 24 hours with live A.*f*., this allowed alveolar macrophages to experience all A.*f*. morphologies. Despite this, 24 hours is still an early time-point and A.*f*. growth was not extensive. It may be the case that Mincle and Dectin-2 recognise larger HY morphologies of A.*f*. and possess limited impact on the alveolar macrophage-driven early response. Dectin-1 has been identified as the crucial CLR during early, anti-A.*f*. alveolar macrophage responses [98]. Although I show Dectin-2 and Mincle are expressed on alveolar macrophages, these CLRs may have more anti-A.*f*. impact on cells recruited to combat extensive A.*f*. infection.

My research did identify an interesting result from Mincle Dectin-1 DKO. The alveolar macrophage MD1 DKO cytokine and chemokine response was similar to the reduced response attained from Dectin-1 KO. However, the reduced cytokine and chemokine response observed in Dectin-1 KO mice *in vivo* was recovered when Mincle and Dectin-1 were knocked out together. This again suggests that Mincle has limited impact on alveolar macrophages but may have some role during *in vivo* A.*f*. infection. A.*f*. may engage Mincle on recruited immune cells to evade engagement from other CLRs.

When Mincle is also knocked out alongside Dectin-1, A.*f*. cannot engage Mincle or Dectin-1 and the pathogen is likely recognised by other CLRs. A pathogen evasion role for Mincle engagement has previously been described. Mincle engagement was found to impair Dectin-1 induced IL-12 production blocking T_H1 protective immunity [157]. *Helicobacter pylori* was demonstrated to up-regulate and engage Mincle driving anti-inflammatory immune responses and avoiding clearance [194]. Here, my research aligns with other published results suggesting Mincle not only has a complicated immune role but may be engaged by pathogens to evade protective immunity.

Unfortunately, this chapter of research did not follow my hypothesis, where I expected the anti-A.*f*. response to be significantly reduced in the absence of one or more CLRs. As highlighted in this chapter, the microbiome and sex of the mice impacted results. The differences between WT, CLR KO and CLR DKO mice may be subtle and difficult to extrapolate when mice are otherwise immune competent. The immune competent model used here appears to result in the rapid and robust clearance of A.*f*. before larger hyphae germinate and A.*f*. invades tissues. CLRs likely have clearer roles in immune suppressed models where extensive A.*f*. growth occurs and the different role of each CLR, along with CLR collaboration, is essential for fungal clearance. Immune-competent models may be more appropriate for examining allergic-type A.*f*. disease where chronic A.*f*. exposure results in airway sensitisation rather than this acute infection model where A.*f*. is cleared quickly. The allergic chronic exposure models require mice to be inoculated with A.*f*. multiple times per week for multiple weeks to generate persistent A.*f*. disease [341]. Further study into the role of these CLRs during acute A.*f*. infection in an immune-suppressed model is required.

6.4: CLRs and A.*f*. in the immune-suppressed

A.*f*. is responsible for a significant disease burden in immune suppressed individuals. Patients with neutropenia or patients receiving corticosteroid therapy for graft versus host disease are at significant risk of developing A.*f*. infection [321, 342]. This is associated with a lack of robust anti-A.*f*. immune response and poor fungal clearance.

The CLR-driven anti-A.*f*. immune response during periods of immune suppression is not well understood.

Depleting macrophages and neutrophils in zebra fish attained significantly enhanced susceptibility to A.*f*. disease [343]. In mice, glucocorticoid treatment accelerated the growth rate of A.*f*. *in vivo*; this was associated with an impaired macrophage and neutrophil response [344]. The depletion of neutrophils in mice reduced the required lethal dose of A.*f*. by 1 log $^{(10)}$; however, this research found the immune-suppression regime, mouse strain and A.*f*. strain significantly influenced the *in vivo* anti-A.*f*. response and survival outcome [345]. Despite research demonstrating enhanced *in vivo* susceptibility to A.*f*. following immune suppression, the impact immune suppression has on CLRs and their anti-A.*f*. impact is not understood. Lacking macrophages and neutrophils, significantly impairs the anti-A.*f*. response; however, the definitive impact losing CLRs during A.*f*. challenge has not been thoroughly investigated.

Here, my research in chapter 5 investigates CLR status and functional immune response capability in a cohort of patients at high risk of developing A.*f*. disease. These results were then associated with the incidence of A.*f*. disease. Initially, this research identified the expression of patient's CLRs at haematological malignancy treatment initiation. I demonstrated at this point, patients possessed some myeloid cells and the majority of patients expressed CLRs, although at highly variable expression levels. Due to the small patient cohort size, limited deductions can be attained from this research. However, patient's Dectin-1 expression and Mcl expression were loosely associated with incidence of A.*f*. disease. The Dectin-1 mutation Y238X has been identified to increase susceptibility to A.*f*. disease. This early stop-codon mutation was found to functionally impair anti-A.*f*. cytokine and chemokine responses [292]. My research suggesting Dectin-1 expression impacts A.*f*. susceptibility was therefore expected. So far, Mcl has only been implicated in protective anti-fungal immunity, although the evidence for this is limited. Why patients with high Mcl expression are at greater risk of A.*f*. disease in my model is not clear. This patient cohort is small in size and the impact Mcl expression has may have not been detected.

My research also identified a novel Dectin-2 mutation that results in an early stop codon and loss of CRD. One patient was homozygous for this novel CLR mutation. This patient did not produce an anti-A.*f*. cytokine and chemokine response and developed a lethal A.*f*. infection. This mutation may have similar impact to the Dectin-1 Y238X early stop codon mutation that was associated with an increased susceptibility to A.*f*. disease. Dectin-1 Y238X resulted in an impaired anti-A.*f*. cytokine and chemokine response likely due to the loss of A.*f*. recognition [292]. Multiple mutations in Dectin-1 and DC-SIGN have been associated with an increased susceptibility to A.*f*. disease [67, 346]. The Dectin-2 mutant may provide a novel risk factor identifying patients susceptible to A.*f*. disease; this mutation requires further investigation.

This research also determined the ability of patient's to generate functional anti-fungal immune responses during periods of immune-suppression. Interestingly, lacking a specific anti-A.*f*. cytokine response was identified as a novel risk factor that could be used to stratify patients according to their A.*f*. disease susceptibility. The anti-A.*f*. response is complex and likely requires CLR and TLR collaboration, and multiple components; where as the anti-LPS response is almost exclusively driven by TLR4 [318]. Patients who generated anti-A.*f*. cytokine and chemokine responses may have more intact and capable immune systems able to generate protective immune responses. Patients that only generated anti-LPS responses may lack key anti-fungal immune components and are therefore more susceptible to A.*f*. disease. In this research I have only identified patients CLR expression at RNA level and sequenced CLR exon regions. It is possible that CLR protein expression deficiencies, CLR intron mutations, CLR splice deficiencies or CLR signalling deficiencies may be present in this cohort, however due to limited sample size these properties have not been examined. These aspects of each patient's CLR status may provide further insight as to why patients susceptible to A.*f*. disease lack a specific anti-A.*f*. cytokine response. Here, in a small patient cohort I have identified a combination of novel risk factors that can be used to stratify patients according to their A.*f*. disease susceptibility. Further study in a larger patient cohort is warranted to thoroughly test the ability of these risk factors to successfully stratify patients.

6.5: Conclusions

Understanding the individual and collaborative role of CLRs during the complex anti-A.*f*. immune response may allow the generation of novel therapeutics that enhance the CLR-driven anti-A.*f*. immune response. The exogenous administration of TLR ligands restored impaired PRR co-stimulation and enhanced clearance of *Fonsecaea perdrosoi* [187]. In a similar mechanism, exogenously administering ligands that restore or enhance CLR collaboration may generate more robust anti-A.*f*. immunity.

This research describes a clear role for NE inducing Dectin-1 cleavage and impairing the anti-A.*f*. immune response. This is particularly relevant for CF patients who experience a severe A.*f*. disease burden and possess high concentrations of NE within their airway. Blocking the action of NE in the CF airway, alongside the administration of therapeutics that enhances the CLR-driven anti-A.*f*. response may reduce CF patient's A.*f*. morbidity and mortality. This research also identifies novel risk factors that can be used to stratify patients according to their susceptibility to A.*f*. infection. Determining patient's CLR status and functional immune response capability upon initiation of their primary disease treatment would allow the stratification of patients at high risk of A.*f*. disease. Therefore, a personalised medicine approach could be implemented and the empirical prophylactic use of inadequate anti-fungal therapeutics reduced.

Chapter 7

Appendix

Table 7.1: Cell media used in this research

Media	Quantity/ Concentration	Constituent	Company
BMDM		DMEM	LifeTechnologies
	10%	Fetal bovine serum	LifeTechnologies
	5%	Horse serum	LifeTechnologies
	2mM	L-glutamine	LifeTechnologies
	1%	Penicillin Streptomycin	LifeTechnologies
	25mM	HEPES	LifeTechnologies
	10ng/ml final	M-CSF	Peprotech
Alveolar macrophage		IMDM	LifeTechnologies
Neutrophil/ Monocyte		RPMI 1640	LifeTechnologies
	10%	Fetal bovine serum	LifeTechnologies
	1%	Penicillin Streptomycin	LifeTechnologies
NIH-3T3		DMEM	LifeTechnologies
	10%	Fetal bovine serum	LifeTechnologies
	2mM	L-glutamine	LifeTechnologies
	1%	Penicillin Streptomycin	LifeTechnologies
For selection	0.5mg/ml final	G418	LifeTechnologies
Ecopack		DMEM	LifeTechnologies
	10%	Fetal bovine serum	LifeTechnologies
FACS buffer		PBS	LifeTechnologies
	0.1%	Bovine serum albumin	Sigma
	0.05%	Sodium azide	Sigma
NE assay buffer		PBS	LifeTechnologies
	0.1%	Bovine serum albumin	Sigma
	5mM	EDTA	Fisher Scientific
PBMC		RPMI 1640	LifeTechnologies
	10%	Fetal bovine serum	LifeTechnologies
	2%	Human serum	Sigma
	10mM	L-glutamine	LifeTechnologies
	10mM	Sodium pyruvate	LifeTechnologies
	100µg/ml final	Gentamicin	LifeTechnologies

Table 7.2: Antibodies used in this research

Antibody	Fluorophore	Species	Final concentration	Clone	Company
CD11b	APC-Cy7	Mouse	2µg/ml	M1/70	BioLegend
CD11b	PerCP-Cy5.5	Mouse	4µg/ml	M1/70	BioLegend
CD11c	PE-Cy7	Mouse	2µg/ml	N418	BioLegend
F4/80	PB	Mouse	4µg/ml	BM8	BioLegend
Ly6G	PE	Mouse	4µg/ml	1A8	BioLegend
Dectin-1	APC	Mouse	2µg/ml	MCA228	Bio-Rad
Dectin-2	Biotin	Mouse	4µg/ml	ILE4	Homemade
Mincle	Biotin	Mouse	4µg/ml	4A9	Homemade
Streptavidin	PE		4µg/ml		BioLegend

Table 7.3: ELISA kits used in this research

ELISA target	Species	Product	Company
TNF	Mouse	14-7423-68A	eBioscience
IL-6	Mouse	14-7061-68	eBioscience
Mip-1	Mouse	DuoSet DY450	R & D Systems
Mip-2	Mouse	DuoSet DY452	R & D Systems
KC	Mouse	DuoSet DY453	R & D Systems
TNF	Human	DuoSet DY210	R & D Systems
IL-6	Human	DuoSet DY206	R & D Systems
Mip-1	Human	DuoSet DY270	R & D Systems
KC	Human	DuoSet DY275	R & D Systems

Table 7.4: qPCR probes used in this research

qPCR Probe target	Species	Product	Company
HPRT	Human	02800695 m1	ThermoFisher
Dectin-1	Human	00224028 m1	ThermoFisher
Dectin-2	Human	01073951 m1	ThermoFisher
Mcl	Human	01073582 m1	ThermoFisher
Mincle	Human	00372017 m1	ThermoFisher
A.*f*. 18S rRNA	A.*f*.	Custom probe GenBank accession reference AB008401	ThermoFisher

Figure 7.5: CLR sequences and PCR primers used in this research

A) Human Dectin-1

atggaatatcatcctgatttagaaaatttggatgaagatggatatactcaattacacttcgact
ctcaaagcaataccaggatagctgttgtttcagagaaaggatcgtgtgctgcatctcctccttg
gcgcctcattgctgtaattttgggaatcctatgcttggtaatactggtgatagctgtggtcctg
ggtaccatgggggttctttccagcccttgtcctcctaattggattatatatgagaagagctgtt
atctattcagcatgtcactaaattcctgggatggaagtaaaagacaatgctggcaactgggctc
taatctcctaaagatagacagctcaaatgaattgggatttatagtaaaacaagtgtcttcccaa
cctgataattcattttggataggcctttctcggccccagactgaggtaccatggctctgggagg
atggatcaacattctcttctaacttatttcagatcagaaccacagctacccaagaaaacccatc
tccaaattgtgtatggattcacgtgtcagtcatttatgaccaactgtgtagtgtgccctcatat
agtatttgtgagaagaagttttcaatgtaa

Forward Primer 1	atggaatatcatcctgatttagaaa
Forward Primer 2	ttcagcatgtcactaaattcc
Reverse Primer 1	ttacattgaaaacttcttctcacaa
Reverse Primer 2	aggagattagagcccagttg
C203G Forward Primer	ggtcctgggtaccatgggtatttggagatccaatt
Reverse Primer	aattggatctccaaatacccatggtacccaggacc
T311G Forward Primer	catctttagaagacagtgggactcctaccaaagctgt
Reverse Primer	acagctttggtaggagtcccactgtcttctaaagatg
C326G Forward Primer	gtgactcctaccaaaggtgtcaaaaccacaggg
Reverse Primer	ccctgtggttttgacacctttggtaggagtcac

B) Human Dectin-2

atgatgcaagagcagcaacctcaaagtacagagaaaagaggctggttgtccctgagactctggt
ctgtggctgggatttccattgcactcctcagtgcttgcttcattgtgagctgtgtagtaactta
ccattttacatatggtgaaactggcaaaaggctgtctgaactacactcatatcattcaagtctc
acctgcttcagtgaagggacaaaggtgccagcctggggatgttgcccagcttcttggaagtcat
ttggttccagttgctacttcatttccagtgaagagaaggtttggtctaagagtgagcagaactg
tgttgagatgggagcacatttggttgtgttcaacacagaagcagagcagaatttcattgtccag
cagctgaatgagtcattttcttattttctggggctttcagacccacaaggtaataataattggc
aatggattgataagacaccttatgagaaaaatgtcagattttggcacctaggtgagcccaatca
ttctgcagagcaatgtgcttcaatagtcttctggaaacctacaggatggggctggaatgatgtt
atctgtgaaactagaaggaattcaatatgtgagatgaataagatttacctatga

Forward Primer 1	atgatgcaagagcagcaa
Forward Primer 2	cccagcttcttggaagtca
Reverse Primer 1	tcataggtaaatcttattcatctcacat
Reverse Primer 2	actcattcagctgctggac

C) Human Mcl

atggggctagaaaaacctcaaagtaaactggaaggaggcatgcatccccagctgataccttcgg
ttattgctgtagttttcatcttacttctcagtgtctgttttattgcaagttgtttggtgactca
tcacaacttttcacgctgtaagagaggcacaggagtgcacaagttagagcaccatgcaaagctc
aaatgcatcaaagagaaatcagaactgaaaagtgctgaagggagcacctggaactgttgtccta
ttgactggagagccttccagtccaactgctattttcctcttactgacaacaagacgtgggctga
gagtgaaaggaactgttcagggatgggggcccatctgatgaccatcagcacggaagctgagcag
aactttattattcagtttctggatagacggctttcctatttccttggacttagagatgagaatg
ccaaaggtcagtggcgttgggtggaccagacgccatttaacccacgcagagtattctggcataa
gaatgaacccgacaactctcagggagaaaactgtgttgttcttgtttataaccaagataaatgg
gcctggaatgatgttccttgtaactttgaagcaagtaggatttgtaaaatacctggaacaacat
tgaactag

Forward Primer 1	atggggctagaaaaacctca
Forward Primer 2	acaagacgtgggctgaga
Reverse Primer 1	ctagttcaatgttgttccaggtattt
Reverse Primer 2	ccactgacctttggcatt

D) Human Mincle

atgaattcatctaaatcatctgaaacacaatgcacagagagaggatgcttctcttcccaaatgt
tcttatggactgttgctgggatccccatcctatttctcagtgcctgtttcatcaccagatgtgt
tgtgacatttcgcatctttcaaacctgtgatgagaaaaagtttcagctacctgagaatttcaca
gagctctcctgctacaattatggatcaggttcagtcaagaattgttgtccattgaactgggaat
attttcaatccagctgctacttcttttctactgacaccatttcctgggcgttaagtttaaagaa
ctgctcagccatgggggctcacctggtggttatcaactcacaggaggagcaggaattcctttcc
tacaagaaacctaaaatgagagagttttttattggactgtcagaccaggttgtcgagggtcagt
ggcaatgggtggacggcacacctttgacaaagtctctgagcttctgggatgtaggggagcccaa
caacatagctaccctggaggactgtgccaccatgagagactcttcaaacccaaggcaaaattgg
aatgatgtaacctgtttcctcaattattttcggatttgtgaaatggtaggaataaatcctttga
acaaaggaaaatctctttaa

Forward Primer 1	atgaattcatctaaatcatctgaaac
Forward Primer 2	accatttcctgggcgtta
Reverse Primer 1	ttaaagagattttcctttgttcaaa
Reverse Primer 2	tcctgctcctcctgtgag

Figure 7.6: Animal distress scoring system used in this research

ANIMAL DISTRESS SCORING SHEET Aspergillus challenge 15/05/17
(Adapted from Wolfensohn and Lloyd, 1998)

Exp ID	Completed by	Time	Date

1. APPEARANCE
Normal
General lack of grooming
Coat starring, ocular and nasal discharging
Piloerection, hunched posture

2. FOOD AND WATER INTAKE
Normal
5% weight loss
Upto 15% weight loss
Over 15% weight loss

3. NATURAL BEHAVIOUR
Normal respiratory rate and pattern
Slight changes, increased rate only
Increased rate with abdominal breathing
Decreased rate with marked abdominal breating

4. PROVOKED BEHAVIOUR
Normal
Minor depression or exaggerated response
Moderate change in expected behaviour
Reacts violently, or very weak and precomatose

5. SCORE ADJUSTMENT
If you have scored 3 more than once add 1 point per 3 score

6. TOTAL

JUDGEMENT

0-3	Normal
4-8	Monitor Carefully (daily)
9-12	Observe regularly
>13	Kill by schedule 1

COMMENTS: 0-3 = Normal; 4-8 = Monitor Carefully; 9-12 = Provide relief where possible, observe regularly, seek advice as appropriate from NACWO and/or NVS; >13 = Kill by schedule 1 method. Humane-end-point is reached at 20% loss of body weight.

ADDITIONAL COMMENTS: Actual severity: Mild – score 0-4 with up to 15% weight loss; Moderate – score >5 and/or >15% weight loss; Severe – moribund or found dead

ID												
1. 0 1 2 3												
2. 0 1 2 3												
3. 0 1 2 3												
4. 0 1 2 3												
5. 2-4												
6. 0-16												
-20% mass												

Additional examination												
Completed by			**Time**									

Bibliography

1. Latge, J.P., *Aspergillus fumigatus and aspergillosis.* Clinical Microbiology Reviews, 1999. **12**(2): p. 310-+.
2. Steele, C., et al., *The beta-glucan receptor dectin-1 recognizes specific morphologies of Aspergillus fumigatus.* Plos Pathogens, 2005. **1**(4): p. 323-334.
3. Schrettl, M., et al., *Distinct roles for intra- and extracellular siderophores during Aspergillus fumigatus infection.* Plos Pathogens, 2007. **3**(9): p. 1195-1207.
4. Dagenais, T.R.T. and N.P. Keller, *Pathogenesis of Aspergillus fumigatus in Invasive Aspergillosis.* Clinical Microbiology Reviews, 2009. **22**(3): p. 447-465.
5. Chazalet, V., et al., *Molecular typing of environmental and patient isolates of Aspergillus fumigatus from various hospital settings.* J Clin Microbiol, 1998. **36**(6): p. 1494-500.
6. O'Gorman, C.M., H.T. Fuller, and P.S. Dyer, *Discovery of a sexual cycle in the opportunistic fungal pathogen Aspergillus fumigatus.* Nature, 2009. **457**(7228): p. 471-U5.
7. Marr, K.A., et al., *Invasive aspergillosis in allogeneic stem cell transplant recipients: changes in epidemiology and risk factors.* Blood, 2002. **100**(13): p. 4358-4366.
8. Girmenia, C., et al., *Prophylaxis and treatment of invasive fungal diseases in allogeneic stem cell transplantation: results of a consensus process by Gruppo Italiano Trapianto di Midollo Osseo (GITMO).* Clin Infect Dis, 2009. **49**(8): p. 1226-36.
9. Palmer, L.B., H.E. Greenberg, and M.J. Schiff, *Corticosteroid treatment as a risk factor for invasive aspergillosis in patients with lung disease.* Thorax, 1991. **46**(1): p. 15-20.
10. Kamai, Y., et al., *Interactions of Aspergillus fumigatus with vascular endothelial cells.* Medical Mycology, 2006. **44**: p. S115-S117.
11. Kamai, Y., et al., *Polarized response of endothelial cells to invasion by Aspergillus fumigatus.* Cellular Microbiology, 2009. **11**(1): p. 170-182.
12. Culpitt, S.V., et al., *Impaired inhibition by dexamethasone of cytokine release by alveolar macrophages from patients with chronic obstructive pulmonary disease.* Am J Respir Crit Care Med, 2003. **167**(1): p. 24-31.
13. Fitzpatrick, A.M., et al., *Alveolar macrophage phagocytosis is impaired in children with poorly controlled asthma.* J Allergy Clin Immunol, 2008. **121**(6): p. 1372-1378.e3.
14. John, M., et al., *Inhaled corticosteroids increase interleukin-10 but reduce macrophage inflammatory protein-1alpha, granulocyte-macrophage colony-stimulating factor, and interferon-gamma release from alveolar macrophages in asthma.* Am J Respir Crit Care Med, 1998. **157**(1): p. 256-62.
15. Hirsch, G., et al., *Neutrophils Are Not Less Sensitive Than Other Blood Leukocytes to the Genomic Effects of Glucocorticoids.* PLOS ONE, 2012. **7**(9): p. e44606.
16. Schleimer, R.P., et al., *An assessment of the effects of glucocorticoids on degranulation, chemotaxis, binding to vascular endothelium and formation of leukotriene B4 by purified human neutrophils.* J Pharmacol Exp Ther, 1989. **250**(2): p. 598-605.
17. Schleimer, R.P., *Glucocorticoids suppress inflammation but spare innate immune responses in airway epithelium.* Proc Am Thorac Soc, 2004. **1**(3): p. 222-30.
18. Ratner, D. and C. Mueller, *Immune responses in cystic fibrosis: are they intrinsically defective?* Am J Respir Cell Mol Biol, 2012. **46**(6): p. 715-22.
19. King, J., S.F. Brunel, and A. Warris, *Aspergillus infections in cystic fibrosis.* J Infect, 2016. **72 Suppl**: p. S50-5.
20. Cheng, S.H., et al., *DEFECTIVE INTRACELLULAR-TRANSPORT AND PROCESSING OF CFTR IS THE MOLECULAR-BASIS OF MOST CYSTIC-FIBROSIS.* Cell, 1990. **63**(4): p. 827-834.
21. Engelhardt, J.F., et al., *Submucosal glands are the predominant site of CFTR expression in the human bronchus.* Nature Genetics, 1992. **2**: p. 240.

22. Welsh, M.J. and A.E. Smith, *Molecular mechanisms of CFTR chloride channel dysfunction in cystic fibrosis.* Cell, 1993. **73**(7): p. 1251-1254.
23. Frizzell, R.A., G. Rechkemmer, and R.L. Shoemaker, *ALTERED REGULATION OF AIRWAY EPITHELIAL-CELL CHLORIDE CHANNELS IN CYSTIC-FIBROSIS.* Science, 1986. **233**(4763): p. 558-560.
24. Bonfield, T.L., et al., *Inflammatory cytokines in cystic fibrosis lungs.* Am J Respir Crit Care Med, 1995. **152**(6 Pt 1): p. 2111-8.
25. Downey, D.G., S.C. Bell, and J.S. Elborn, *Neutrophils in cystic fibrosis.* Thorax, 2009. **64**(1): p. 81-88.
26. Lyczak, J.B., C.L. Cannon, and G.B. Pier, *Lung Infections Associated with Cystic Fibrosis.* Clinical Microbiology Reviews, 2002. **15**(2): p. 194-222.
27. Twigg, M.S., et al., *The Role of Serine Proteases and Antiproteases in the Cystic Fibrosis Lung.* Mediators Inflamm, 2015. **2015**: p. 293053.
28. Chmiel, J.F., M. Berger, and M.W. Konstan, *The role of inflammation in the pathophysiology of CF lung disease.* Clin Rev Allergy Immunol, 2002. **23**(1): p. 5-27.
29. Rohm, M., et al., *NADPH oxidase promotes neutrophil extracellular trap formation in pulmonary aspergillosis.* Infect Immun, 2014. **82**(5): p. 1766-77.
30. Koller, D.Y., R. Urbanek, and M. Gotz, *Increased degranulation of eosinophil and neutrophil granulocytes in cystic fibrosis.* Am J Respir Crit Care Med, 1995. **152**(2): p. 629-33.
31. Taggart, C., et al., *Increased elastase release by CF neutrophils is mediated by tumor necrosis factor-alpha and interleukin-8.* Am J Physiol Lung Cell Mol Physiol, 2000. **278**(1): p. L33-41.
32. Benabid, R., et al., *Neutrophil Elastase Modulates Cytokine Expression: CONTRIBUTION TO HOST DEFENSE AGAINST PSEUDOMONAS AERUGINOSA-INDUCED PNEUMONIA.* The Journal of Biological Chemistry, 2012. **287**(42): p. 34883-34894.
33. Lopez-Boado, Y.S., et al., *Neutrophil serine proteinases cleave bacterial flagellin, abrogating its host response-inducing activity.* J Immunol, 2004. **172**(1): p. 509-15.
34. McGreal, E.P., et al., *Inactivation of IL-6 and soluble IL-6 receptor by neutrophil derived serine proteases in cystic fibrosis.* Biochim Biophys Acta, 2010. **1802**(7-8): p. 649-58.
35. van den Berg, C.W., et al., *Mechanism of neutrophil dysfunction: neutrophil serine proteases cleave and inactivate the C5a receptor.* J Immunol, 2014. **192**(4): p. 1787-95.
36. Tosi, M.F., H. Zakem, and M. Berger, *Neutrophil elastase cleaves C3bi on opsonized pseudomonas as well as CR1 on neutrophils to create a functionally important opsonin receptor mismatch.* J Clin Invest, 1990. **86**(1): p. 300-8.
37. Zen, K., et al., *Cleavage of the CD11b extracellular domain by the leukocyte serprocidins is critical for neutrophil detachment during chemotaxis.* Blood, 2011. **117**(18): p. 4885-94.
38. Marr, K.A., T. Patterson, and D. Denning, *Aspergillosis. Pathogenesis, clinical manifestations, and therapy.* Infect Dis Clin North Am, 2002. **16**(4): p. 875-94, vi.
39. Chandrasekar, P.H., G. Alangaden, and E. Manavathu, *Aspergillus: an increasing problem in tertiary care hospitals?* Clin Infect Dis, 2000. **30**(6): p. 984-5.
40. Pagano, L., et al., *The epidemiology of fungal infections in patients with hematologic malignancies: the SEIFEM-2004 study.* Haematologica, 2006. **91**(8): p. 1068-1075.
41. Martino, R., et al., *Invasive fungal infections after allogeneic peripheral blood stem cell transplantation: incidence and risk factors in 395 patients.* Br J Haematol, 2002. **116**(2): p. 475-82.
42. Morgan, J., et al., *Incidence of invasive aspergillosis following hematopoietic stem cell and solid organ transplantation: interim results of a prospective multicenter surveillance program.* Medical Mycology, 2005. **43**(Supplement 1): p. S49-S58.

43. Denning, D.W., *Invasive aspergillosis.* Clin Infect Dis, 1998. **26**(4): p. 781-803; quiz 804-5.
44. Alexander, B.D., *Prophylaxis of invasive mycoses in solid organ transplantation.* Curr Opin Infect Dis, 2002. **15**(6): p. 583-9.
45. Minari, A., et al., *The incidence of invasive aspergillosis among solid organ transplant recipients and implications for prophylaxis in lung transplants.* Transpl Infect Dis, 2002. **4**(4): p. 195-200.
46. el-Dahr, J.M., et al., *Development of immune responses to Aspergillus at an early age in children with cystic fibrosis.* Am J Respir Crit Care Med, 1994. **150**(6 Pt 1): p. 1513-8.
47. Maturu, V.N. and R. Agarwal, *Prevalence of Aspergillus sensitization and allergic bronchopulmonary aspergillosis in cystic fibrosis: systematic review and meta-analysis.* Clin Exp Allergy, 2015. **45**(12): p. 1765-78.
48. Baxter, C.G., et al., *Novel immunologic classification of aspergillosis in adult cystic fibrosis.* J Allergy Clin Immunol, 2013. **132**(3): p. 560-566.e10.
49. Lee, J.Y., et al., *Impact of previous invasive pulmonary aspergillosis on the outcome of allogeneic hematopoietic stem cell transplantation.* The Korean Journal of Hematology, 2012. **47**(4): p. 255-259.
50. Singh, N. and D.L. Paterson, *Aspergillus Infections in Transplant Recipients.* Clinical Microbiology Reviews, 2005. **18**(1): p. 44-69.
51. Fukuda, T., et al., *Risks and outcomes of invasive fungal infections in recipients of allogeneic hematopoietic stem cell transplants after nonmyeloablative conditioning.* Blood, 2003. **102**(3): p. 827-33.
52. Singh, N. and S. Husain, *Aspergillus infections after lung transplantation: clinical differences in type of transplant and implications for management.* J Heart Lung Transplant, 2003. **22**(3): p. 258-66.
53. Fortun, J., et al., *Risk factors for invasive aspergillosis in liver transplant recipients.* Liver Transpl, 2002. **8**(11): p. 1065-70.
54. Montoya, J.G., et al., *Invasive aspergillosis in the setting of cardiac transplantation.* Clin Infect Dis, 2003. **37 Suppl 3**: p. S281-92.
55. Altiparmak, M.R., et al., *Systemic fungal infections after renal transplantation.* Scand J Infect Dis, 2002. **34**(4): p. 284-8.
56. Cornely, O.A., et al., *Liposomal Amphotericin B as Initial Therapy for Invasive Mold Infection: A Randomized Trial Comparing a High–Loading Dose Regimen with Standard Dosing (AmBiLoad Trial).* Clinical Infectious Diseases, 2007. **44**(10): p. 1289-1297.
57. Herbrecht, R., et al., *Voriconazole versus amphotericin B for primary therapy of invasive aspergillosis.* N Engl J Med, 2002. **347**(6): p. 408-15.
58. Ghannoum, M.A. and D.M. Kuhn, *Voriconazole -- better chances for patients with invasive mycoses.* Eur J Med Res, 2002. **7**(5): p. 242-56.
59. Johnson, L.B. and C.A. Kauffman, *Voriconazole: a new triazole antifungal agent.* Clin Infect Dis, 2003. **36**(5): p. 630-7.
60. Kikuchi, T., et al., *Variable magnitude of drug interaction between oral voriconazole and cyclosporine A in recipients of allogeneic hematopoietic stem cell transplantation.* Clin Transplant, 2012. **26**(5): p. E544-8.
61. Karthaus, M., *Prophylaxis and treatment of invasive aspergillosis with voriconazole, posaconazole and caspofungin - review of the literature.* European Journal of Medical Research, 2011. **16**(4): p. 145-152.
62. Park, S.Y., J.-A. Yoon, and S.-H. Kim, *Voriconazole-refractory invasive aspergillosis.* The Korean Journal of Internal Medicine, 2017. **32**(5): p. 805-812.

63. Hellinger, W.C., et al., *Risk stratification and targeted antifungal prophylaxis for prevention of aspergillosis and other invasive mold infections after liver transplantation.* Liver Transpl, 2005. **11**(6): p. 656-62.
64. Garcia-Vidal, C., et al., *Epidemiology of invasive mold infections in allogeneic stem cell transplant recipients: biological risk factors for infection according to time after transplantation.* Clin Infect Dis, 2008. **47**(8): p. 1041-50.
65. Barnes, P.D. and K.A. Marr, *Risks, diagnosis and outcomes of invasive fungal infections in haematopoietic stem cell transplant recipients.* Br J Haematol, 2007. **139**(4): p. 519-31.
66. Martino, R., et al., *Lower respiratory tract respiratory virus infections increase the risk of invasive aspergillosis after a reduced-intensity allogeneic hematopoietic SCT.* Bone Marrow Transplant, 2009. **44**(11): p. 749-56.
67. White, P.L., C. Parr, and R.A. Barnes, *Predicting Invasive Aspergillosis in Hematology Patients by Combining Clinical and Genetic Risk Factors with Early Diagnostic Biomarkers.* J Clin Microbiol, 2018. **56**(1).
68. Chang, Y.C., et al., *THTA, a thermotolerance gene of Aspergillus fumigatus.* Fungal Genet Biol, 2004. **41**(9): p. 888-96.
69. Hohl, T.M. and M. Feldmesser, *Aspergillus fumigatus: principles of pathogenesis and host defense.* Eukaryot Cell, 2007. **6**(11): p. 1953-63.
70. Paris, S., et al., *Conidial Hydrophobins of Aspergillus fumigatus.* Applied and Environmental Microbiology, 2003. **69**(3): p. 1581-1588.
71. Warwas, M.L., et al., *Structure and role of sialic acids on the surface of Aspergillus fumigatus conidiospores.* Glycobiology, 2007. **17**(4): p. 401-10.
72. Wasylnka, J.A. and M.M. Moore, *Adhesion of Aspergillus species to extracellular matrix proteins: evidence for involvement of negatively charged carbohydrates on the conidial surface.* Infect Immun, 2000. **68**(6): p. 3377-84.
73. Latge, J.P., et al., *Specific molecular features in the organization and biosynthesis of the cell wall of Aspergillus fumigatus.* Med Mycol, 2005. **43 Suppl 1**: p. S15-22.
74. Maubon, D., et al., *AGS3, an alpha(1-3)glucan synthase gene family member of Aspergillus fumigatus, modulates mycelium growth in the lung of experimentally infected mice.* Fungal Genet Biol, 2006. **43**(5): p. 366-75.
75. Li, H., et al., *Glycosylphosphatidylinositol (GPI) anchor is required in Aspergillus fumigatus for morphogenesis and virulence.* Mol Microbiol, 2007. **64**(4): p. 1014-27.
76. Romano, J., et al., *Disruption of the Aspergillus fumigatus ECM33 homologue results in rapid conidial germination, antifungal resistance and hypervirulence.* Microbiology, 2006. **152**(Pt 7): p. 1919-28.
77. Schleimer, R.P., et al., *Epithelium: at the interface of innate and adaptive immune responses.* J Allergy Clin Immunol, 2007. **120**(6): p. 1279-84.
78. Ganesan, S., A.T. Comstock, and U.S. Sajjan, *Barrier function of airway tract epithelium.* Tissue Barriers, 2013. **1**(4): p. e24997.
79. Allen, M.J., D.R. Voelker, and R.J. Mason, *Interactions of surfactant proteins A and D with Saccharomyces cerevisiae and Aspergillus fumigatus.* Infect Immun, 2001. **69**(4): p. 2037-44.
80. Madan, T., et al., *Binding of pulmonary surfactant proteins A and D to Aspergillus fumigatus conidia enhances phagocytosis and killing by human neutrophils and alveolar macrophages.* Infect Immun, 1997. **65**(8): p. 3171-9.
81. Dumestre-Perard, C., et al., *Aspergillus conidia activate the complement by the mannan-binding lectin C2 bypass mechanism.* J Immunol, 2008. **181**(10): p. 7100-5.
82. Kaur, S., et al., *Protective role of mannan-binding lectin in a murine model of invasive pulmonary aspergillosis.* Clinical and Experimental Immunology, 2007. **148**(2): p. 382-389.

83. Filler, S.G. and D.C. Sheppard, *Fungal invasion of normally non-phagocytic host cells.* PLoS Pathog, 2006. **2**(12): p. e129.
84. Paris, S., et al., *Internalization of Aspergillus fumigatus conidia by epithelial and endothelial cells.* Infect Immun, 1997. **65**(4): p. 1510-4.
85. Kauffman, H.F., et al., *Protease-dependent activation of epithelial cells by fungal allergens leads to morphologic changes and cytokine production.* J Allergy Clin Immunol, 2000. **105**(6 Pt 1): p. 1185-93.
86. Kogan, T.V., et al., *Involvement of secreted Aspergillus fumigatus proteases in disruption of the actin fiber cytoskeleton and loss of focal adhesion sites in infected A549 lung pneumocytes.* J Infect Dis, 2004. **189**(11): p. 1965-73.
87. Ibrahim-Granet, O., et al., *Phagocytosis and intracellular fate of Aspergillus fumigatus conidia in alveolar macrophages.* Infect Immun, 2003. **71**(2): p. 891-903.
88. Philippe, B., et al., *Killing of Aspergillus fumigatus by alveolar macrophages is mediated by reactive oxidant intermediates.* Infect Immun, 2003. **71**(6): p. 3034-42.
89. Jahn, B., et al., *Isolation and characterization of a pigmentless-conidium mutant of Aspergillus fumigatus with altered conidial surface and reduced virulence.* Infect Immun, 1997. **65**(12): p. 5110-7.
90. Langfelder, K., et al., *Biosynthesis of fungal melanins and their importance for human pathogenic fungi.* Fungal Genetics and Biology, 2003. **38**(2): p. 143-158.
91. Cenci, E., et al., *Impaired antifungal effector activity but not inflammatory cell recruitment in interleukin-6-deficient mice with invasive pulmonary aspergillosis.* Journal of Infectious Diseases, 2001. **184**(5): p. 610-617.
92. Mehrad, B., R.M. Strieter, and T.J. Standiford, *Role of TNF-alpha in pulmonary host defense in murine invasive aspergillosis.* Journal of Immunology, 1999. **162**(3): p. 1633-1640.
93. Morrison, B.E., et al., *Chemokine-mediated recruitment of NK cells is a critical host defense mechanism in invasive aspergillosis.* Journal of Clinical Investigation, 2003. **112**(12): p. 1862-1870.
94. Phadke, A.P. and B. Mehrad, *Cytokines in host defense against Aspergillus: recent advances.* Medical Mycology, 2005. **43**: p. S173-S176.
95. Netea, M.G., et al., *Aspergillus fumigatus evades immune recognition during germination through loss of toll-like receptor-4-mediated signal transduction.* Journal of Infectious Diseases, 2003. **188**(2): p. 320-326.
96. Balloy, V., et al., *Involvement of toll-like receptor 2 in experimental invasive pulmonary aspergillosis.* Infection and Immunity, 2005. **73**(9): p. 5420-5425.
97. Bellocchio, S., et al., *The contribution of the Toll-like/IL-1 receptor superfamily to innate and adaptive immunity to fungal pathogens in vivo.* Journal of Immunology, 2004. **172**(5): p. 3059-3069.
98. Gersuk, G.M., et al., *Dectin-1 and TLRs permit macrophages to distinguish between different Aspergillus fumigatus cellular states.* Journal of Immunology, 2006. **176**(6): p. 3717-3724.
99. Hohl, T.M., et al., *Aspergillus fumigatus triggers inflammatory responses by stage-specific beta-glucan display.* Plos Pathogens, 2005. **1**(3): p. 232-240.
100. Werner, J.L., et al., *Requisite Role for the Dectin-1 β-Glucan Receptor in Pulmonary Defense against Aspergillus fumigatus.* The Journal of Immunology, 2009. **182**(8): p. 4938-4946.
101. Bellocchio, S., et al., *TLRs govern neutrophil activity in aspergillosis.* Journal of Immunology, 2004. **173**(12): p. 7406-7415.
102. Kennedy, A.D., et al., *Dectin-1 promotes fungicidal activity of human neutrophils.* European Journal of Immunology, 2007. **37**(2): p. 467-478.

103. van Bruggen, R., et al., *Complement receptor 3, not Dectin-1, is the major receptor on human neutrophils for beta-glucan-bearing particles.* Mol Immunol, 2009. **47**(2-3): p. 575-81.
104. van de Vijver, E., T.K. van den Berg, and T.W. Kuijpers, *Leukocyte adhesion deficiencies.* Hematol Oncol Clin North Am, 2013. **27**(1): p. 101-16, viii.
105. Diamond, R.D. and R.A. Clark, *DAMAGE TO ASPERGILLUS-FUMIGATUS AND RHIZOPUS-ORYZAE HYPHAE BY OXIDATIVE AND NON-OXIDATIVE MICROBICIDAL PRODUCTS OF HUMAN-NEUTROPHILS INVITRO.* Infection and Immunity, 1982. **38**(2): p. 487-495.
106. Levitz, S.M. and T.P. Farrell, *HUMAN NEUTROPHIL DEGRANULATION STIMULATED BY ASPERGILLUS-FUMIGATUS.* Journal of Leukocyte Biology, 1990. **47**(2): p. 170-175.
107. Gazendam, R.P., et al., *Human Neutrophils Use Different Mechanisms To Kill Aspergillus fumigatus Conidia and Hyphae: Evidence from Phagocyte Defects.* J Immunol, 2016. **196**(3): p. 1272-83.
108. Rex, J.H., et al., *NORMAL AND DEFICIENT NEUTROPHILS CAN COOPERATE TO DAMAGE ASPERGILLUS-FUMIGATUS HYPHAE.* Journal of Infectious Diseases, 1990. **162**(2): p. 523-528.
109. Nauseef, W.M., *How human neutrophils kill and degrade microbes: an integrated view.* Immunological Reviews, 2007. **219**: p. 88-102.
110. Fuchs, T.A., et al., *Novel cell death program leads to neutrophil extracellular traps.* J Cell Biol, 2007. **176**(2): p. 231-41.
111. Bruns, S., et al., *Production of extracellular traps against Aspergillus fumigatus in vitro and in infected lung tissue is dependent on invading neutrophils and influenced by hydrophobin RodA.* PLoS Pathog, 2010. **6**(4): p. e1000873.
112. Bonnett, C.R., et al., *Early neutrophil recruitment and aggregation in the murine lung inhibit germination of Aspergillus fumigatus Conidia.* Infect Immun, 2006. **74**(12): p. 6528-39.
113. Krappmann, S., et al., *The Aspergillus fumigatus transcriptional activator CpcA contributes significantly to the virulence of this fungal pathogen.* Molecular Microbiology, 2004. **52**(3): p. 785-799.
114. Haas, H., et al., *Characterization of the Aspergillus nidulans transporters for the siderophores enterobactin and triacetylfusarinine C.* Biochemical Journal, 2003. **371**: p. 505-513.
115. Cramer, R.A., A. Rivera, and T.M. Hohl, *Immune responses against Aspergillus fumigatus: what have we learned?* Current opinion in infectious diseases, 2011. **24**(4): p. 315-322.
116. Lewis, R.E., et al., *Frequency and species distribution of gliotoxin-producing Aspergillus isolates recovered from patients at a tertiary-care cancer center.* Journal of Clinical Microbiology, 2005. **43**(12): p. 6120-6122.
117. Reeves, E.P., et al., *Correlation between gliotoxin production and virulence of Aspergillus fumigatus in Galleria mellonella.* Mycopathologia, 2004. **158**(1): p. 73-79.
118. Eichner, R.D., et al., *GLIOTOXIN CAUSES OXIDATIVE DAMAGE TO PLASMID AND CELLULAR DNA.* Journal of Biological Chemistry, 1988. **263**(8): p. 3772-3777.
119. Eichner, R.D., et al., *THE EFFECT OF GLIOTOXIN UPON MACROPHAGE FUNCTION.* International Journal of Immunopharmacology, 1986. **8**(7): p. 789-797.
120. Niide, O., et al., *Fungal metabolite gliotoxin blocks mast cell activation by a calcium- and superoxide-dependent mechanism: Implications for immuno suppressive activities.* Clinical Immunology, 2006. **118**(1): p. 108-116.
121. Stanzani, M., et al., *Aspergillus fumigatus suppresses the human ceflular immune response via ghotoxin-mediated apoptosis of monocytes.* Blood, 2005. **105**(6): p. 2258-2265.

122. Yamada, A., T. Kataoka, and K. Nagai, *The fungal metabolite gliotoxin: immunosuppressive activity on CTL-mediated cytotoxicity.* Immunology Letters, 2000. **71**(1): p. 27-32.
123. Bok, J.W., et al., *GliZ, a transcriptional regulator of gliotoxin biosynthesis, contributes to Aspergillus fumigatus virulence.* Infection and Immunity, 2006. **74**(12): p. 6761-6768.
124. Cramer, R.A., et al., *Disruption of a nonribosomal peptide synthetase in Aspergillus fumigatus eliminates gliotoxin production.* Eukaryotic Cell, 2006. **5**(6): p. 972-980.
125. Kupfahl, C., et al., *Deletion of the gliP gene of Aspergillus fumigatus results in loss of gliotoxin production but has no effect on virulence of the fungus in a low-dose mouse infection model.* Molecular Microbiology, 2006. **62**(1): p. 292-302.
126. Sugui, J.A., et al., *Gliotoxin is a virulence factor of Aspergillus fumigatus: gliP deletion attenuates virulence in mice Immunosuppressed with hydrocortisone.* Eukaryotic Cell, 2007. **6**(9): p. 1562-1569.
127. Spikes, S., et al., *Gliotoxin production in Aspergillus fumigatus contributes to host-specific differences in virulence.* Journal of Infectious Diseases, 2008. **197**(3): p. 479-486.
128. Heinekamp, T., et al., *Interference of Aspergillus fumigatus with the immune response.* Semin Immunopathol, 2015. **37**(2): p. 141-52.
129. Chaudhary, N., J.F. Staab, and K.A. Marr, *Healthy Human T-Cell Responses to Aspergillus fumigatus Antigens.* PLOS ONE, 2010. **5**(2): p. e9036.
130. Serbina, N.V., et al., *Distinct responses of human monocyte subsets to Aspergillus fumigatus conidia.* J Immunol, 2009. **183**(4): p. 2678-87.
131. Hohl, T.M., et al., *Inflammatory monocytes facilitate adaptive CD4 T cell responses during respiratory fungal infection.* Cell Host Microbe, 2009. **6**(5): p. 470-81.
132. Cenci, E., et al., *Th1 and Th2 cytokines in mice with invasive aspergillosis.* Infection and Immunity, 1997. **65**(2): p. 564-570.
133. Hebart, H., et al., *Analysis of T-cell responses to Aspergillus fumigatus antigens in healthy individuals and patients with hematologic malignancies.* Blood, 2002. **100**(13): p. 4521-8.
134. Murdock, B.J., et al., *Coevolution of TH1, TH2, and TH17 responses during repeated pulmonary exposure to Aspergillus fumigatus conidia.* Infect Immun, 2011. **79**(1): p. 125-35.
135. Rivera, A., et al., *Dectin-1 diversifies Aspergillus fumigatus–specific T cell responses by inhibiting T helper type 1 CD4 T cell differentiation.* The Journal of Experimental Medicine, 2011. **208**(2): p. 369-381.
136. Yamasaki, S., et al., *Mincle is an ITAM-coupled activating receptor that senses damaged cells.* Nature Immunology, 2008. **9**(10): p. 1179-1188.
137. Plato, A., S.E. Hardison, and G.D. Brown, *Pattern recognition receptors in antifungal immunity.* Semin Immunopathol, 2015. **37**(2): p. 97-106.
138. Li, Z.Z., et al., *Role of NOD2 in regulating the immune response to Aspergillus fumigatus.* Inflamm Res, 2012. **61**(6): p. 643-8.
139. Jaeger, M., et al., *The RIG-I-like helicase receptor MDA5 (IFIH1) is involved in the host defense against Candida infections.* Eur J Clin Microbiol Infect Dis, 2015. **34**(5): p. 963-974.
140. von Bernuth, H., et al., *Pyogenic bacterial infections in humans with MyD88 deficiency.* Science, 2008. **321**(5889): p. 691-6.
141. Netea, M.G., et al., *Variable recognition of Candida albicans strains by TLR4 and lectin recognition receptors.* Med Mycol, 2010. **48**(7): p. 897-903.
142. Brown, G.D., *Innate Antifungal Immunity: The Key Role of Phagocytes.* Annual Review of Immunology, 2011. **29**(1): p. 1-21.

143. Bourgeois, C., et al., *Conventional dendritic cells mount a type I IFN response against Candida spp. requiring novel phagosomal TLR7-mediated IFN-beta signaling.* J Immunol, 2011. **186**(5): p. 3104-12.
144. Gil, M.L. and D. Gozalbo, *Role of Toll-like receptors in systemic Candida albicans infections.* Front Biosci (Landmark Ed), 2009. **14**: p. 570-82.
145. Luisa Gil, M., et al., *Role of Toll-like receptors in systemic Candida albicans infections.* Front Biosci (Landmark Ed), 2016. **21**: p. 278-302.
146. Netea, M.G., et al., *Recognition of fungal pathogens by Toll-like receptors.* Eur J Clin Microbiol Infect Dis, 2004. **23**(9): p. 672-6.
147. Meier, A., et al., *Toll-like receptor (TLR) 2 and TLR4 are essential for Aspergillus-induced activation of murine macrophages.* Cellular Microbiology, 2003. **5**(8): p. 561-570.
148. Netea, M.G., et al., *An integrated model of the recognition of Candida albicans by the innate immune system.* Nat Rev Microbiol, 2008. **6**(1): p. 67-78.
149. Zhong, Y., A. Kinio, and M. Saleh, *Functions of NOD-Like Receptors in Human Diseases.* Front Immunol, 2013. **4**: p. 333.
150. Tomalka, J., et al., *A Novel Role for the NLRC4 Inflammasome in Mucosal Defenses against the Fungal Pathogen Candida albicans.* PLOS Pathogens, 2011. **7**(12): p. e1002379.
151. Zelensky, A.N. and J.E. Gready, *The C-type lectin-like domain superfamily.* Febs Journal, 2005. **272**(24): p. 6179-6217.
152. Geijtenbeek, T.B.H., et al., *Self- and nonself-recognition by C-type lectins on dendritic cells.* Annual Review of Immunology, 2004. **22**: p. 33-54.
153. Drickamer, K., *C-type lectin-like domains.* Current Opinion in Structural Biology, 1999. **9**(5): p. 585-590.
154. Takahashi, K., et al., *The mannose-binding lectin: a prototypic pattern recognition molecule.* Current Opinion in Immunology, 2006. **18**(1): p. 16-23.
155. Drummond, R.A., et al., *The role of Syk/CARD9 coupled C-type lectins in antifungal immunity.* Eur J Immunol, 2011. **41**(2): p. 276-81.
156. Strasser, D., et al., *Syk kinase-coupled C-type lectin receptors engage protein kinase C-sigma to elicit Card9 adaptor-mediated innate immunity.* Immunity, 2012. **36**(1): p. 32-42.
157. Wevers, B.A., et al., *Fungal Engagement of the C-Type Lectin Mincle Suppresses Dectin-1-Induced Antifungal Immunity.* Cell Host & Microbe, 2014. **15**(4): p. 494-505.
158. Miyake, Y., et al., *C-type Lectin MCL Is an FcR gamma-Coupled Receptor that Mediates the Adjuvanticity of Mycobacterial Cord Factor.* Immunity, 2013. **38**(5): p. 1050-1062.
159. Glocker, E.O., et al., *A homozygous CARD9 mutation in a family with susceptibility to fungal infections.* N Engl J Med, 2009. **361**(18): p. 1727-35.
160. Brown, G.D., *Dectin-1: a signalling non-TLR pattern-recognition receptor.* Nature Reviews Immunology, 2006. **6**(1): p. 33-43.
161. Heinsbroek, S.E.M., et al., *Expression of Functionally Different Dectin-1 Isoforms by Murine Macrophages.* The Journal of Immunology, 2006. **176**(9): p. 5513.
162. Palma, A.S., et al., *Ligands for the beta-glucan receptor, Dectin-1, assigned using "designer" microarrays of oligosaccharide probes (neoglycolipids) generated from glucan polysaccharides. (vol 281, pg 5771, 2006).* Journal of Biological Chemistry, 2006. **281**(34): p. 24999-24999.
163. Brown, J., et al., *Structure of the fungal β-glucan-binding immune receptor dectin-1: Implications for function.* Protein Science : A Publication of the Protein Society, 2007. **16**(6): p. 1042-1052.
164. Goodridge, H.S., et al., *Activation of the innate immune receptor Dectin-1 upon formation of a 'phagocytic synapse'.* Nature, 2011. **472**(7344): p. 471-5.

165. Rogers, N.C., et al., *Syk-Dependent Cytokine Induction by Dectin-1 Reveals a Novel Pattern Recognition Pathway for C Type Lectins.* Immunity, 2005. **22**(4): p. 507-517.
166. Deng, Z., et al., *Tyrosine phosphatase SHP-2 mediates C-type lectin receptor-induced activation of the kinase Syk and anti-fungal TH17 responses.* Nat Immunol, 2015. **16**(6): p. 642-52.
167. Gross, O., et al., *Card9 controls a non-TLR signalling pathway for innate anti-fungal immunity.* Nature, 2006. **442**(7103): p. 651-656.
168. Lemoine, S., et al., *Dectin-1 activation unlocks IL12A expression and reveals the TH1 potency of neonatal dendritic cells.* J Allergy Clin Immunol, 2015. **136**(5): p. 1355-68.e1-15.
169. del Fresno, C., et al., *Interferon-beta production via Dectin-1-Syk-IRF5 signaling in dendritic cells is crucial for immunity to C. albicans.* Immunity, 2013. **38**(6): p. 1176-86.
170. LeibundGut-Landmann, S., et al., *Syk- and CARD9-dependent coupling of innate immunity to the induction of T helper cells that produce interleukin 17.* Nature Immunology, 2007. **8**(6): p. 630-638.
171. Taylor, P.R., et al., *Dectin-1 is required for beta-glucan recognition and control of fungal infection.* Nature Immunology, 2007. **8**(1): p. 31-38.
172. Saijo, S., et al., *Dectin-1 is required for host defense against Pneumocystis carinii but not against Candida albicans.* Nature Immunology, 2007. **8**(1): p. 39-46.
173. Marakalala, M.J., et al., *Differential Adaptation of Candida albicans In Vivo Modulates Immune Recognition by Dectin-1.* PLOS Pathogens, 2013. **9**(4): p. e1003315.
174. Gessner, M.A., et al., *Dectin-1-Dependent Interleukin-22 Contributes to Early Innate Lung Defense against Aspergillus fumigatus.* Infection and Immunity, 2012. **80**(1): p. 410-417.
175. Graham, L.M. and G.D. Brown, *The Dectin-2 family of C-type lectins in immunity and homeostasis.* Cytokine, 2009. **48**(1-2): p. 148-155.
176. Taylor, P.R., et al., *Dectin-2 is predominantly myeloid restricted and exhibits unique activation-dependent expression on maturing inflammatory monocytes elicited in vivo.* European Journal of Immunology, 2005. **35**(7): p. 2163-2174.
177. Gavino, A.C.P., et al., *Identification and expression profiling of a human C-type lectin, structurally homologous to mouse dectin-2.* Experimental Dermatology, 2005. **14**(4): p. 281-288.
178. Sun, H., et al., *Dectin-2 is predominately macrophage restricted and exhibits conspicuous expression during Aspergillus fumigatus invasion in human lung.* Cell Immunol, 2013. **284**(1-2): p. 60-7.
179. Sato, K., et al., *Dectin-2 is a pattern recognition receptor for fungi that couples with the Fc receptor gamma chain to induce innate immune responses.* Journal of Biological Chemistry, 2006. **281**(50): p. 38854-38866.
180. Saijo, S., et al., *Dectin-2 recognition of alpha-mannans and induction of Th17 cell differentiation is essential for host defense against Candida albicans.* Immunity, 2010. **32**(5): p. 681-91.
181. Ritter, M., et al., *Schistosoma mansoni triggers Dectin-2, which activates the Nlrp3 inflammasome and alters adaptive immune responses.* Proc Natl Acad Sci U S A, 2010. **107**(47): p. 20459-64.
182. Gringhuis, S.I., et al., *Selective C-Rel Activation via Malt1 Controls Anti-Fungal T-H-17 Immunity by Dectin-1 and Dectin-2.* Plos Pathogens, 2011. **7**(1): p. 11.
183. McGreal, E.P., et al., *The carbohydrate-recognition domain of Dectin-2 is a C-type lectin with specificity for high mannose.* Glycobiology, 2006. **16**(5): p. 422-430.
184. Parsons, M.W., et al., *Dectin-2 Regulates the Effector Phase of House Dust Mite-Elicited Pulmonary Inflammation Independently from Its Role in Sensitization.* Journal of Immunology, 2014. **192**(4): p. 1361-1371.

185. Loures, F.V., et al., *Recognition of Aspergillus fumigatus Hyphae by Human Plasmacytoid Dendritic Cells Is Mediated by Dectin-2 and Results in Formation of Extracellular Traps.* PLOS Pathogens, 2015. **11**(2): p. e1004643.
186. Bi, L., et al., *CARD9 mediates dectin-2-induced IkappaBalpha kinase ubiquitination leading to activation of NF-kappaB in response to stimulation by the hyphal form of Candida albicans.* J Biol Chem, 2010. **285**(34): p. 25969-77.
187. Sousa, M.D., et al., *Restoration of Pattern Recognition Receptor Costimulation to Treat Chromoblastomycosis, a Chronic Fungal Infection of the Skin.* Cell Host & Microbe, 2011. **9**(5): p. 436-443.
188. Yamasaki, S., et al., *C-type lectin Mincle is an activating receptor for pathogenic fungus, Malassezia.* Proceedings of the National Academy of Sciences of the United States of America, 2009. **106**(6): p. 1897-1902.
189. Ishikawa, E., et al., *Direct recognition of the mycobacterial glycolipid, trehalose dimycolate, by C-type lectin Mincle.* J Exp Med, 2009. **206**(13): p. 2879-88.
190. Wells, C.A., et al., *The macrophage-inducible C-type lectin, Mincle, is an essential component of the innate immune response to Candida albicans.* Journal of Immunology, 2008. **180**(11): p. 7404-7413.
191. Zhao, G., et al., *The role of Mincle in innate immune to fungal keratitis.* J Infect Dev Ctries, 2017. **11**(1): p. 89-97.
192. Behler, F., et al., *Role of Mincle in alveolar macrophage-dependent innate immunity against mycobacterial infections in mice.* J Immunol, 2012. **189**(6): p. 3121-9.
193. Heitmann, L., et al., *TGF-beta-responsive myeloid cells suppress type 2 immunity and emphysematous pathology after hookworm infection.* Am J Pathol, 2012. **181**(3): p. 897-906.
194. Devi, S., E. Rajakumara, and N. Ahmed, *Induction of Mincle by Helicobacter pylori and consequent anti-inflammatory signaling denote a bacterial survival strategy.* Scientific Reports, 2015. **5**: p. 13.
195. Graham, L.M., et al., *The C-type Lectin Receptor CLECSF8 (CLEC4D) Is Expressed by Myeloid Cells and Triggers Cellular Activation through Syk Kinase.* Journal of Biological Chemistry, 2012. **287**(31): p. 25964-25974.
196. Yamasaki, S., *Signaling while eating: MCL is coupled with Mincle.* European Journal of Immunology, 2013. **43**(12): p. 3156-3158.
197. Furukawa, A., et al., *Structural analysis for glycolipid recognition by the C-type lectins Mincle and MCL.* Proceedings of the National Academy of Sciences of the United States of America, 2013. **110**(43): p. 17438-17443.
198. Lobato-Pascual, A., et al., *Mincle, the receptor for mycobacterial cord factor, forms a functional receptor complex with MCL and Fc epsilon RI-gamma.* European Journal of Immunology, 2013. **43**(12): p. 3167-3174.
199. Zhu, L.L., et al., *C-type lectin receptors Dectin-3 and Dectin-2 form a heterodimeric pattern-recognition receptor for host defense against fungal infection.* Immunity, 2013. **39**(2): p. 324-34.
200. Wilson, G.J., et al., *The C-Type Lectin Receptor CLECSF8/CLEC4D Is a Key Component of Anti-Mycobacterial Immunity.* Cell Host & Microbe, 2015. **17**(2): p. 252-259.
201. Blander, J.M. and R. Medzhitov, *Regulation of phagosome maturation by signals from Toll-like receptors.* Science, 2004. **304**(5673): p. 1014-1018.
202. Marr, K.A., et al., *Differential role of MyD88 in macrophage-mediated responses to opportunistic fungal pathogens.* Infect Immun, 2003. **71**(9): p. 5280-6.
203. Bonifacino, J.S. and E.C. Dell'Angelica, *Molecular bases for the recognition of tyrosine-based sorting signals.* Journal of Cell Biology, 1999. **145**(5): p. 923-926.

204. Mahnke, K., et al., *The dendritic cell receptor for endocytosis, DEC-205, can recycle and enhance antigen presentation via major histocompatibility complex class II-positive lysosomal compartments.* Journal of Cell Biology, 2000. **151**(3): p. 673-683.
205. Herre, J., et al., *Dectin-1 uses novel mechanisms for yeast phagocytosis in macrophages.* Blood, 2004. **104**(13): p. 4038-4045.
206. Underhill, D.M., et al., *Dectin-1 activates Syk tyrosine kinase in a dynamic subset of macrophages for reactive oxygen production.* Blood, 2005. **106**(7): p. 2543-2550.
207. Kerrigan, A.M. and G.D. Brown, *C-type lectins and phagocytosis.* Immunobiology, 2009. **214**(7): p. 562-75.
208. Sanjuan, M.A., et al., *Toll-like receptor signalling in macrophages links the autophagy pathway to phagocytosis.* Nature, 2007. **450**(7173): p. 1253-7.
209. Balestrieri, B., et al., *Group V secretory phospholipase A2 modulates phagosome maturation and regulates the innate immune response against Candida albicans.* J Immunol, 2009. **182**(8): p. 4891-8.
210. Engering, A., et al., *The dendritic cell-specific adhesion receptor DC-SIGN internalizes antigen for presentation to T cells.* Journal of Immunology, 2002. **168**(5): p. 2118-2126.
211. Tacken, P.J., R. Torensma, and C.G. Figdor, *Targeting antigens to dendritic cells in vivo.* Immunobiology, 2006. **211**(6-8): p. 599-608.
212. Vautier, S., D.M. MacCallum, and G.D. Brown, *C-type lectin receptors and cytokines in fungal immunity.* Cytokine, 2012. **58**(1): p. 89-99.
213. Netea, M.G., et al., *Increased susceptibility of TNF-alpha lymphotoxin-alpha double knockout mice to systemic candidiasis through impaired recruitment of neutrophils and phagocytosis of Candida albicans.* J Immunol, 1999. **163**(3): p. 1498-505.
214. Sambatakou, H., et al., *Cytokine profiling of pulmonary aspergillosis.* International Journal of Immunogenetics, 2006. **33**(4): p. 297-302.
215. Vazquez-Torres, A. and E. Balish, *Macrophages in resistance to candidiasis.* Microbiol Mol Biol Rev, 1997. **61**(2): p. 170-92.
216. Silva, P.M., S. Gonçalves, and N.C. Santos, *Defensins: antifungal lessons from eukaryotes.* Frontiers in Microbiology, 2014. **5**: p. 97.
217. Kawai, T. and S. Akira, *Toll-like receptors and their crosstalk with other innate receptors in infection and immunity.* Immunity, 2011. **34**(5): p. 637-50.
218. Gantner, B.N., et al., *Collaborative induction of inflammatory responses by dectin-1 and Toll-like receptor 2.* J Exp Med, 2003. **197**(9): p. 1107-17.
219. Gringhuis, S.I., et al., *C-type lectin DC-SIGN modulates Toll-like receptor signaling via Raf-1 kinase-dependent acetylation of transcription factor NF-kappaB.* Immunity, 2007. **26**(5): p. 605-16.
220. Empey, K.M., M. Hollifield, and B.A. Garvy, *Exogenous heat-killed Escherichia coli improves alveolar macrophage activity and reduces Pneumocystis carinii lung burden in infant mice.* Infect Immun, 2007. **75**(7): p. 3382-93.
221. Yoshikawa, F.S., et al., *Dectin-1 and Dectin-2 promote control of the fungal pathogen Trichophyton rubrum independently of IL-17 and adaptive immunity in experimental deep dermatophytosis.* 2016(1753-4267 (Electronic)).
222. Brown, G.D., et al., *Hidden killers: human fungal infections.* Sci Transl Med, 2012. **4**(165): p. 165rv13.
223. Hays, S., et al., *Structural changes to airway smooth muscle in cystic fibrosis.* Thorax, 2005. **60**(3): p. 226-228.
224. Mayer-Hamblett, N., et al., *Association between pulmonary function and sputum biomarkers in cystic fibrosis.* Am J Respir Crit Care Med, 2007. **175**(8): p. 822-8.
225. Belaaouaj, A., et al., *Mice lacking neutrophil elastase reveal impaired host defense against gram negative bacterial sepsis.* Nature Medicine, 1998. **4**(5): p. 615-618.

226. Pham, C.T.N., *Neutrophil serine proteases: specific regulators of inflammation.* Nature Reviews Immunology, 2006. **6**(7): p. 541-550.
227. Taylor, P.R., et al., *The beta-glucan receptor, dectin-1, is predominantly expressed on the, surface of cells of the monocyte/macrophage and neutrophil lineages.* Journal of Immunology, 2002. **169**(7): p. 3876-3882.
228. Fischer, M., et al., *Isoform localization of Dectin-1 regulates the signaling quality of anti-fungal immunity.* Eur J Immunol, 2017. **47**(5): p. 848-859.
229. Yokota, K., et al., *Identification of a human homologue of the dendritic cell-associated C-type lectin-1, dectin-1.* Gene, 2001. **272**(1-2): p. 51-60.
230. Helenius, A. and M. Aebi, *Roles of N-linked glycans in the endoplasmic reticulum.* Annu Rev Biochem, 2004. **73**: p. 1019-49.
231. Willment, J.A., et al., *The human beta-glucan receptor is widely expressed and functionally equivalent to murine Dectin-1 on primary cells.* Eur J Immunol, 2005. **35**(5): p. 1539-47.
232. Greene, C.M., et al., *TLR-induced inflammation in cystic fibrosis and non-cystic fibrosis airway epithelial cells.* J Immunol, 2005. **174**(3): p. 1638-46.
233. Bruscia, E.M. and T.L. Bonfield, *Cystic Fibrosis Lung Immunity: The Role of the Macrophage.* J Innate Immun, 2016. **8**(6): p. 550-563.
234. Fimmel, A.L. and U. Norris, *The F1F0-ATPase of Escherichia coli. The substitution of glycine by valine at position 29 in the c-subunit affects function but not assembly.* Biochim Biophys Acta, 1989. **986**(2): p. 257-62.
235. Javadpour, M.M., et al., *Helix packing in polytopic membrane proteins: Role of glycine in transmembrane helix association.* Biophysical Journal, 1999. **77**(3): p. 1609-1618.
236. Dennehy, K.M., et al., *Syk kinase is required for collaborative cytokine production induced through Dectin-1 and Toll-like receptors.* European Journal of Immunology, 2008. **38**(2): p. 500-506.
237. Faro-Trindade, I., et al., *Characterisation of Innate Fungal Recognition in the Lung.* PLOS ONE, 2012. **7**(4): p. e35675.
238. Simonin-Le Jeune, K., et al., *Impaired functions of macrophage from cystic fibrosis patients: CD11b, TLR-5 decrease and sCD14, inflammatory cytokines increase.* PLoS One, 2013. **8**(9): p. e75667.
239. Branzk, N., et al., *Neutrophils sense microbe size and selectively release neutrophil extracellular traps in response to large pathogens.* Nature Immunology, 2014. **15**: p. 1017.
240. Bonfim, C.V., R.L. Mamoni, and M.H. Blotta, *TLR-2, TLR-4 and dectin-1 expression in human monocytes and neutrophils stimulated by Paracoccidioides brasiliensis.* Med Mycol, 2009. **47**(7): p. 722-33.
241. del Fresno, C., et al., *Monocytes from cystic fibrosis patients are locked in an LPS tolerance state: down-regulation of TREM-1 as putative underlying mechanism.* PLoS One, 2008. **3**(7): p. e2667.
242. Placzek, S., et al., *BRENDA in 2017: new perspectives and new tools in BRENDA.* Nucleic Acids Research, 2017. **45**(Database issue): p. D380-D388.
243. Sinha, S., et al., *Primary structure of human neutrophil elastase.* Proc Natl Acad Sci U S A, 1987. **84**(8): p. 2228-32.
244. Boxio, R., et al., *Neutrophil elastase cleaves epithelial cadherin in acutely injured lung epithelium.* Respiratory Research, 2016. **17**(1): p. 129.
245. Hardison, S.E. and G.D. Brown, *C-type Lectin Receptors Orchestrate Anti-Fungal Immunity.* Nature immunology, 2012. **13**(9): p. 817-822.
246. Dillon, S., et al., *Yeast zymosan, a stimulus for TLR2 and dectin-1, induces regulatory antigen-presenting cells and immunological tolerance.* Journal of Clinical Investigation, 2006. **116**(4): p. 916-928.

247. Pasare, C. and R. Medzhitov, *Toll-like receptors: linking innate and adaptive immunity.* Microbes Infect, 2004. **6**(15): p. 1382-7.
248. Wang, F., et al., *Innate and adaptive immune response to chronic pulmonary infection of hyphae of Aspergillus fumigatus in a new murine model.* J Med Microbiol, 2017. **66**(10): p. 1400-1408.
249. Stuehler, C., et al., *Cross-protective TH1 immunity against Aspergillus fumigatus and Candida albicans.* Blood, 2011. **117**(22): p. 5881-91.
250. Bhatia, S., et al., *Rapid Host Defense against Aspergillus fumigatus Involves Alveolar Macrophages with a Predominance of Alternatively Activated Phenotype.* Plos One, 2011. **6**(1): p. 15.
251. Sheppard, D.C., et al., *Comparison of three methodologies for the determination of pulmonary fungal burden in experimental murine aspergillosis.* Clinical Microbiology and Infection, 2006. **12**(4): p. 376-380.
252. Mattila, P.E., et al., *Dectin-1 Fc targeting of Aspergillus fiumigatus beta-glucans augments innate defense against invasive pulmonary aspergillosis.* Antimicrobial Agents and Chemotherapy, 2008. **52**(3): p. 1171-1172.
253. Khot, P.D., et al., *Development and optimization of quantitative PCR for the diagnosis of invasive aspergillosis with bronchoalveolar lavage fluid.* BMC Infectious Diseases, 2008. **8**: p. 73-73.
254. Sheppard, D.C., et al., *Standardization of an experimental murine model of invasive pulmonary aspergillosis.* Antimicrobial Agents and Chemotherapy, 2006. **50**(10): p. 3501-3503.
255. White, P.L., et al., *Critical stages of extracting DNA from Aspergillus fumigatus in whole-blood specimens.* J Clin Microbiol, 2010. **48**(10): p. 3753-5.
256. Griffiths, L.J., et al., *Comparison of DNA extraction methods for Aspergillus fumigatus using real-time PCR.* J Med Microbiol, 2006. **55**(Pt 9): p. 1187-91.
257. Leite, G.M., N. Magan, and Á. Medina, *Comparison of different bead-beating RNA extraction strategies: An optimized method for filamentous fungi.* Journal of Microbiological Methods, 2012. **88**(3): p. 413-418.
258. Bowman, J.C., et al., *Quantitative PCR assay to measure Aspergillus fumigatus burden in a murine model of disseminated aspergillosis: demonstration of efficacy of caspofungin acetate.* Antimicrob Agents Chemother, 2001. **45**(12): p. 3474-81.
259. Bozza, S., et al., *Dendritic cells transport conidia and hyphae of Aspergillus fumigatus from the airways to the draining lymph nodes and initiate disparate Th responses to the fungus.* Journal of Immunology, 2002. **168**(3): p. 1362-1371.
260. Lilly, L.M., et al., *The β-Glucan Receptor Dectin-1 Promotes Lung Immunopathology during Fungal Allergy via IL-22.* The Journal of Immunology, 2012. **189**(7): p. 3653.
261. Graham, G.J., *D6 and the atypical chemokine receptor family: novel regulators of immune and inflammatory processes.* Eur J Immunol, 2009. **39**(2): p. 342-51.
262. Belkaid, Y. and T. Hand, *Role of the Microbiota in Immunity and inflammation.* Cell, 2014. **157**(1): p. 121-41.
263. Belkaid, Y. and O.J. Harrison, *Homeostatic Immunity and the Microbiota.* Immunity, 2017. **46**(4): p. 562-576.
264. Lloyd, C.M. and B.J. Marsland, *Lung Homeostasis: Influence of Age, Microbes, and the Immune System.* Immunity, 2017. **46**(4): p. 549-561.
265. Brinkman, B.M., et al., *Gut microbiota affects sensitivity to acute DSS-induced colitis independently of host genotype.* Inflamm Bowel Dis, 2013. **19**(12): p. 2560-7.
266. Laukens, D., et al., *Heterogeneity of the gut microbiome in mice: guidelines for optimizing experimental design.* FEMS Microbiol Rev, 2016. **40**(1): p. 117-32.
267. Cai, K.C., et al., *Age and sex differences in immune response following LPS treatment in mice.* Brain, Behavior, and Immunity, 2016. **58**(Supplement C): p. 327-337.

268. Klein, S.L., I. Marriott, and E.N. Fish, *Sex-based differences in immune function and responses to vaccination.* Transactions of the Royal Society of Tropical Medicine and Hygiene, 2015. **109**(1): p. 9-15.
269. Scotland, R.S., et al., *Sex differences in resident immune cell phenotype underlie more efficient acute inflammatory responses in female mice.* Blood, 2011. **118**(22): p. 5918-5927.
270. Klein, S.L. and K.L. Flanagan, *Sex differences in immune responses.* 2016. **16**: p. 626.
271. Matsumoto, M., et al., *A novel LPS-inducible C-type lectin is a transcriptional target of NF-IL6 in macrophages.* 1999(0022-1767 (Print)).
272. Flornes, L.M., et al., *Identification of lectin-like receptors expressed by antigen presenting cells and neutrophils and their mapping to a novel gene complex.* 2004 (0093-7711 (Print)).
273. Misharin, A.V., et al., *Flow Cytometric Analysis of Macrophages and Dendritic Cell Subsets in the Mouse Lung.* American Journal of Respiratory Cell and Molecular Biology, 2013. **49**(4): p. 503-510.
274. Clarke, D.L., et al., *Dectin-2 sensing of house dust mite is critical for the initiation of airway inflammation.* Mucosal Immunol, 2014. **7**(3): p. 558-67.
275. Kottom, T.J., et al., *Dectin-2 Is a C-Type Lectin Receptor that Recognizes Pneumocystis and Participates in Innate Immune Responses.* Am J Respir Cell Mol Biol, 2018. **58**(2): p. 232-240.
276. Johnson, G.B., G.J. Brunn, and J.L. Platt, *Cutting edge: An endogenous pathway to systemic inflammatory response syndrome (SIRS)-Like reactions through toll-like receptor 4.* Journal of Immunology, 2004. **172**(1): p. 20-24.
277. Spellberg, B., et al., *Mice with disseminated candidiasis die of progressive sepsis.* Journal of Infectious Diseases, 2005. **192**(2): p. 336-343.
278. Tanaka, R.J., et al., *In silico modeling of spore inhalation reveals fungal persistence following low dose exposure.* Scientific Reports, 2015. **5**: p. 13958.
279. Ferwerda, G., et al., *Dectin-1 synergizes with TLR2 and TLR4 for cytokine production in human primary monocytes and macrophages.* Cell Microbiol, 2008. **10**(10): p. 2058-66.
280. Loures, F.V., et al., *TLR-4 cooperates with Dectin-1 and mannose receptor to expand Th17 and Tc17 cells induced by Paracoccidioides brasiliensis stimulated dendritic cells.* Frontiers in Microbiology, 2015. **6**: p. 261.
281. Buffie, C.G., et al., *Precision microbiome reconstitution restores bile acid mediated resistance to Clostridium difficile.* Nature, 2015. **517**(7533): p. 205-208.
282. Rochereau, N., et al., *Dectin-1 Is Essential for Reverse Transcytosis of Glycosylated SIgA-Antigen Complexes by Intestinal M Cells.* Plos Biology, 2013. **11**(9): p. 18.
283. Lamprinaki, D., et al., *LC3-Associated Phagocytosis Is Required for Dentric Cell to Inflammatory Cytokine Response to Gut Commensal Yeast Saccharomyces Cerevisiae.* Frontiers in Immunology, 2017. **8**: p. 12.
284. Lortholary, O., et al., *Influence of gender and age on course of infection and cytokine responses in mice with disseminated Cryptococcus neoformans infection.* Clin Microbiol Infect, 2002. **8**(1): p. 31-7.
285. Cornillet, A., et al., *Comparison of Epidemiological, Clinical, and Biological Features of Invasive Aspergillosis in Neutropenic and Nonneutropenic Patients: A 6-Year Survey.* Clinical Infectious Diseases, 2006. **43**(5): p. 577-584.
286. Arvanitis, M. and E. Mylonakis, *Diagnosis of invasive aspergillosis: recent developments and ongoing challenges.* (1365-2362 (Electronic)).
287. Barnes, R.A., et al., *Prevention and diagnosis of invasive fungal disease in high-risk patients within an integrative care pathway.* J Infect, 2013. **67**(3): p. 206-14.

288. Morrissey, C.O., et al., *Galactomannan and PCR versus culture and histology for directing use of antifungal treatment for invasive aspergillosis in high-risk haematology patients: a randomised controlled trial.* Lancet Infect Dis, 2013. **13**(6): p. 519-28.
289. Aguado, J.M., et al., *Serum galactomannan versus a combination of galactomannan and polymerase chain reaction-based Aspergillus DNA detection for early therapy of invasive aspergillosis in high-risk hematological patients: a randomized controlled trial.* Clin Infect Dis, 2015. **60**(3): p. 405-14.
290. Leonardelli, F., et al., *Aspergillus fumigatus Intrinsic Fluconazole Resistance Is Due to the Naturally Occurring T301I Substitution in Cyp51Ap.* (1098-6596 (Electronic)).
291. Ferwerda, B., et al., *Human dectin-1 deficiency and mucocutaneous fungal infections.* (1533-4406 (Electronic)).
292. Cunha, C., et al., *Dectin-1 Y238X polymorphism associates with susceptibility to invasive aspergillosis in hematopoietic transplantation through impairment of both recipient- and donor-dependent mechanisms of antifungal immunity.* (1528-0020 (Electronic)).
293. Chai, L.Y.A., et al., *The Y238X Stop Codon Polymorphism in the Human β-Glucan Receptor Dectin-1 and Susceptibility to Invasive Aspergillosis.* The Journal of Infectious Diseases, 2011. **203**(5): p. 736-743.
294. De Pauw, B., et al., *Revised Definitions of Invasive Fungal Disease from the European Organization for Research and Treatment of Cancer/Invasive Fungal Infections Cooperative Group and the National Institute of Allergy and Infectious Diseases Mycoses Study Group (EORTC/MSG) Consensus Group.* Clinical infectious diseases : an official publication of the Infectious Diseases Society of America, 2008. **46**(12): p. 1813-1821.
295. Skrypina, N.A., et al., *Total RNA suitable for molecular biology analysis.* (0168-1656 (Print)).
296. Feinberg, H., et al., *Mechanism of pathogen recognition by human dectin-2.* J Biol Chem, 2017. **292**(32): p. 13402-13414.
297. Rosentul, D.C., et al., *Genetic Variation in the Dectin-1/CARD9 Recognition Pathway and Susceptibility to Candidemia.* The Journal of Infectious Diseases, 2011. **204**(7): p. 1138-1145.
298. Richardson, M.B. and S.J. Williams, *MCL and Mincle: C-Type Lectin Receptors That Sense Damaged Self and Pathogen-Associated Molecular Patterns.* Frontiers in Immunology, 2014. **5**: p. 288.
299. Mukaka, M.M., *A guide to appropriate use of Correlation coefficient in medical research.* Malawi Medical Journal : The Journal of Medical Association of Malawi, 2012. **24**(3): p. 69-71.
300. Goswami, M., et al., *Impaired B cell immunity in acute myeloid leukemia patients after chemotherapy*. J Transl Med, 2017. **15**(1): p. 155.
301. Khaznadar, Z., et al., *Acute myeloid leukemia impairs natural killer cells through the formation of a deficient cytotoxic immunological synapse.* Eur J Immunol, 2014. **44**(10): p. 3068-80.
302. Williams, K.M. and R.E. Gress, *Immune reconstitution and implications for immunotherapy following haematopoietic stem cell transplantation.* Best practice & research. Clinical haematology, 2008. **21**(3): p. 579-596.
303. Goswami, S., S. Basu, and P. Sharma, *A potential biomarker for anti-PD-1 immunotherapy.* Nat Med, 2018. **24**(2): p. 123-124.
304. Masucci, G.V., et al., *Validation of biomarkers to predict response to immunotherapy in cancer: Volume I — pre-analytical and analytical validation.* Journal for ImmunoTherapy of Cancer, 2016. **4**(1): p. 76.

305. Jansky, L., P. Reymanova, and J. Kopecky, *Dynamics of cytokine production in human peripheral blood mononuclear cells stimulated by LPS or infected by Borrelia.* Physiol Res, 2003. **52**(6): p. 593-8.
306. Becker, K.L., et al., *Aspergillus Cell Wall Chitin Induces Anti- and Proinflammatory Cytokines in Human PBMCs via the Fc-γ Receptor/Syk/PI3K Pathway.* mBio, 2016. **7**(3): p. e01823-15.
307. Chai, L.Y.A., et al., *Anti-Aspergillus human host defence relies on type 1 T helper (Th1), rather than type 17 T helper (Th17), cellular immunity.* Immunology, 2010. **130**(1): p. 46-54.
308. Muhl, H. and C.A. Dinarello, *Macrophage inflammatory protein-1 alpha production in lipopolysaccharide-stimulated human adherent blood mononuclear cells is inhibited by the nitric oxide synthase inhibitor N(G)-monomethyl-L-arginine.* J Immunol, 1997. **159**(10): p. 5063-9.
309. Eggesbo, J.B., et al., *LPS-induced release of EGF, GM-CSF, GRO alpha, LIF, MIP-1 alpha and PDGF-AB in PBMC from persons with high or low levels of HDL lipoprotein.* Cytokine, 1995. **7**(6): p. 562-7.
310. Miyake, Y., O.H. Masatsugu, and S. Yamasaki, *C-Type Lectin Receptor MCL Facilitates Mincle Expression and Signaling through Complex Formation.* J Immunol, 2015. **194**(11): p. 5366-74.
311. Marakalala, M.J., L.M. Graham, and G.D. Brown, *The Role of Syk/CARD9-Coupled C-Type Lectin Receptors in Immunity to Mycobacterium tuberculosis Infections.* Clinical and Developmental Immunology, 2010. **2010**.
312. Alexander, C. and E.T. Rietschel, *Bacterial lipopolysaccharides and innate immunity.* J Endotoxin Res, 2001. **7**(3): p. 167-202.
313. Rosadini, C.V. and J.C. Kagan, *Early innate immune responses to bacterial LPS.* Curr Opin Immunol, 2017. **44**: p. 14-19.
314. Riordan, S.M., et al., *Peripheral blood mononuclear cell expression of toll-like receptors and relation to cytokine levels in cirrhosis.* Hepatology, 2003. **37**(5): p. 1154-64.
315. Alegre, M.-L., D.R. Goldstein, and A.S. Chong, *Toll-like receptor signaling in transplantation.* Current opinion in organ transplantation, 2008. **13**(4): p. 358-365.
316. Gibson, R.J., et al., *Chemotherapy-induced gut toxicity and pain: involvement of TLRs.* Support Care Cancer, 2016. **24**(5): p. 2251-2258.
317. Yan, H., et al., *Targeting C-Type Lectin Receptors for Cancer Immunity.* Frontiers in Immunology, 2015. **6**: p. 408.
318. Lu, Y.C., W.C. Yeh, and P.S. Ohashi, *LPS/TLR4 signal transduction pathway.* Cytokine, 2008. **42**(2): p. 145-151.
319. Krakauer, T., *Stimulant-Dependent Modulation of Cytokines and Chemokines by Airway Epithelial Cells: Cross Talk between Pulmonary Epithelial and Peripheral Blood Mononuclear Cells.* Clinical and Diagnostic Laboratory Immunology, 2002. **9**(1): p. 126-131.
320. Foreback, J.L., et al., *Blood mononuclear cell production of TNF-alpha and IL-8: engagement of different signal transduction pathways including the p42 MAP kinase pathway.* J Leukoc Biol, 1998. **64**(1): p. 124-33.
321. Baddley, J.W., *Clinical risk factors for invasive aspergillosis.* Med Mycol, 2011. **49 Suppl 1**: p. S7-s12.
322. Hoving, J.C., G.J. Wilson, and G.D. Brown, *Signalling C-Type lectin receptors, microbial recognition and immunity.* Cellular Microbiology, 2014. **16**(2): p. 185-194.
323. Kerrigan, A.M. and G.D. Brown, *Syk-coupled C-type lectins in immunity.* Trends in Immunology, 2011. **32**(4): p. 151-156.
324. Kousha, M., R. Tadi, and A.O. Soubani, *Pulmonary aspergillosis: a clinical review.* Eur Respir Rev, 2011. **20**(121): p. 156-74.

325. Pihet, M., et al., *Occurrence and relevance of filamentous fungi in respiratory secretions of patients with cystic fibrosis — a review.* Medical Mycology, 2009. **47**(4): p. 387-397.
326. Brown, G.D., et al., *Dectin-1 is a major beta-glucan receptor on macrophages.* J Exp Med, 2002. **196**(3): p. 407-12.
327. Goodridge, H.S., R.M. Simmons, and D.M. Underhill, *Dectin-1 Stimulation by Candida albicans Yeast or Zymosan Triggers NFAT Activation in Macrophages and Dendritic Cells.* The Journal of Immunology, 2007. **178**(5): p. 3107.
328. Underhill, D.M., *Macrophage recognition of zymosan particles.* J Endotoxin Res, 2003. **9**(3): p. 176-80.
329. Saijo, S. and Y. Iwakura, *Dectin-1 and Dectin-2 in innate immunity against fungi.* International Immunology, 2011. **23**(8): p. 467-472.
330. Griffiths, J.S., et al., *Differential susceptibility of Dectin-1 isoforms to functional inactivation by neutrophil and fungal proteases.* The FASEB Journal, 2018: p. fj.201701145R.
331. Tsai, Y.F. and T.L. Hwang, *Neutrophil elastase inhibitors: a patent review and potential applications for inflammatory lung diseases (2010 - 2014).* Expert Opin Ther Pat, 2015. **25**(10): p. 1145-58.
332. von Nussbaum, F. and V.M.J. Li, *Neutrophil elastase inhibitors for the treatment of (cardio)pulmonary diseases: Into clinical testing with pre-adaptive pharmacophores.* Bioorganic & Medicinal Chemistry Letters, 2015. **25**(20): p. 4370-4381.
333. Tsai, Y.-F., et al., *Sirtinol Inhibits Neutrophil Elastase Activity and Attenuates Lipopolysaccharide-Mediated Acute Lung Injury in Mice.* Scientific Reports, 2015. **5**: p. 8347.
334. Polverino, E., et al., *The Role of Neutrophil Elastase Inhibitors in Lung Diseases.* CHEST, 2017. **152**(2): p. 249-262.
335. Rytkonen, A. and D.W. Holden, *Bacterial interference of ubiquitination and deubiquitination.* Cell Host Microbe, 2007. **1**(1): p. 13-22.
336. Neish, A.S., et al., *Prokaryotic regulation of epithelial responses by inhibition of IkappaB-alpha ubiquitination.* Science, 2000. **289**(5484): p. 1560-3.
337. Neish, A.S., *Mucosal immunity and the microbiome.* Ann Am Thorac Soc, 2014. **11 Suppl 1**: p. S28-32.
338. Fransen, F., et al., *The Impact of Gut Microbiota on Gender-Specific Differences in Immunity.* Frontiers in Immunology, 2017. **8**: p. 754.
339. Ifrim, D.C., et al., *Role of Dectin-2 for host defense against systemic infection with Candida glabrata.* Infect Immun, 2014. **82**(3): p. 1064-73.
340. Ifrim, D.C., et al., *The Role of Dectin-2 for Host Defense Against Disseminated Candidiasis.* Journal of Interferon & Cytokine Research, 2016. **36**(4): p. 267-276.
341. Yamashita, Y., et al., *Carbohydrates expressed on Aspergillus fumigatus induce in vivo allergic Th2-type response.* Clin Exp Allergy, 2002. **32**(5): p. 776-82.
342. Muhlemann, K., et al., *Risk factors for invasive aspergillosis in neutropenic patients with hematologic malignancies.* Leukemia, 2005. **19**(4): p. 545-50.
343. Knox, B.P., et al., *Distinct Innate Immune Phagocyte Responses to Aspergillus fumigatus Conidia and Hyphae in Zebrafish Larvae.* Eukaryotic Cell, 2014. **13**(10): p. 1266-1277.
344. Lionakis, M.S. and D.P. Kontoyiannis, *Glucocorticoids and invasive fungal infections.* The Lancet, 2003. **362**(9398): p. 1828-1838.
345. Stephens-Romero, S.D., A.J. Mednick, and M. Feldmesser, *The pathogenesis of fatal outcome in murine pulmonary aspergillosis depends on the neutrophil depletion strategy.* Infect Immun, 2005. **73**(1): p. 114-25.

346. Fischer, M., et al., *Polymorphisms of Dectin-1 and TLR2 Predispose to Invasive Fungal Disease in Patients with Acute Myeloid Leukemia.* PLoS One, 2016. **11**(3): p. e0150632.